SYNTHESIS OF 1,2,4-TRIAZOLES AND THEIR RUTHENIUM BIS-BIPYRIDYL COMPLEXES.

Ph.D. Thesis

Donal Hughes BSc.

Dublin City University
School of Chemical Sciences

November 1999

Under the supervision of
Dr P. James
and
Prof. J.G. Vos

Acknowledgements

What a team we had International class In the front row we had Jay When he was propped well he was awesome Sometimes collapsed (scrums) in pressure situations Kenny was our hooker, not afraid to get in low and forage Number three was Fayner, who made some famous breaks on his own late in the game In the second row we had height There was Lomu-like Farmer Win, lose or draw Farmer talked a great game His optimism lifted the whole team Partnered ably by Mikey, who really blossomed when he trimmed his mane At number eight was the young lad Keither Came in at half time but gelled straight away Still playing Impossible to knock, legend has it he even slept standing up (in the Porterhouse) Shiny was scrum half Prone to injury but when fit, could kick like a mule Often however, when it looked like Shiny was going to score in the corner, he was penalised for excessive talking Dave, at outhalf was well known for his outrageous tactics Even when he spilled the ball he somehow managed to retrieve the situation Magpie in the centre had a habit of fleeing the pitch at the first sign of danger Shiny always came to the rescue and quelled the flames Burner was a committed centre also but unfortunately got a transfer early in the game Guv was rock solid at full back Well known for deft flicks, had a habit of drifting in and out of the game Banned for life for use of illegal growth promoters Mike, the winger always stood out He was the only man on the team who insisted on wearing a woolly jumper over his jersey, but was a commentator's dream with his red flowing locks So there I was on the other wing, privileged to play with these players Though there were times we were covered in filth, getting red cards, or missing obvious scores, to each other we were all one thing Winners

I wish to thank all of the technical staff of the DCU team, especially Mick, Damien, Veronica, Anne, Maurice, Shane and Ambrose Thanks also to the team managers Paraic James and Jan Vos Thanks to the Vos team for letting me train with them Then there were the mentors Josh Howarth and John Gallagher often came on with the stretcher and Frances and Christine who brought on the magic water bottle when I was dazed Thanks to the physio team, the Hughes family They gave me a solid gameplan Time and again they picked me up when I was down, helped me recover from injury and pumped in the kind of financial aid that's critical these days Thanks to Woody who plays for Queens for all his help

Thanks most especially, to the head cheerleader, my wife Deirdre and her young apprentice Naoise I love you both with all my heart

Declaration

I hereby certify that this material, which I now submit for assessment on the program of study leading to the award of Doctor of Philosophy is entirely my own work and has not been taken from the work of others save and to the extent that such work has been cited and acknowledged within the text of my work

Signed 

ID No 95970746

Date

Abstract

On foot of the success of the ruthenium tris-bipyridine complex as a complex capable of catalysing reactions which can convert solar energy into electrical energy, much work has been done to synthesize alternative ligands for use with ruthenium in an effort to increase stability. 1,2,4-triazoles have, for a number of years, been synthesised with a view to acting as ligands in these ruthenium complexes. These complexes are vital pieces in the puzzle that will ultimately result in the development of successful artificial photosynthetic systems.

While previous work has concentrated on investigation of electrochemical and photophysical properties of ruthenium complexes, this work concerns the synthesis of new 1,2,4-triazole ligands and their complexes. These triazoles have been carefully pre-designed with the aim of being successful ligands in the search for the more efficient electrochemical devices.

The thesis follows the logical thought process of the organic experimentalist. The initial challenge was not only to synthesise a heretofore-unknown ligand, but to also develop a synthetic procedure, which can be routinely followed, enabling the facile production of high yields of analogous ligands.

The first chapter introduces the problem, which must be investigated. The reader is then introduced to the people and the research behind 1,2,4-triazole synthesis aswell as the synthetic methods used. The next logical step in the process was to produce model compounds. This has the practical advantage of giving the researcher experience in the reactions required in the synthesis. It allows reaction methods to be compared and the possible pitfalls established at an early stage. During model synthesis, one of the stages of triazole synthesis, namely amidrazone formation, produced a bipyridyl dihydrazide molecule from which we obtained a never before reported crystal structure. Along with successful model compound synthesis, a thorough spectroscopic investigation of the 1,2,4-triazoles by ^{1}H-NMR is described.

Chapter two describes the synthesis of larger 1,2,4-triazole containing molecules most of which comprise two 1,2,4-traizole moieties encased in a heteroaromatic system Research carried out into these ligands is discussed and the synthetic methods used evaluated The experimental section of chapter two describes the synthesis of a number of new 1,2,4-triazole ligands, termed the "target ligands" of the research Extensive ^{1}H-NMR and microanalytical data is provided to confirm the punty of the ligands X-ray crystal structures of all but one of the ligands have been obtained, all of which are new and the publication of which is keenly awaited

Chapter three takes the research a stage further by incorporating the "target ligands" into ruthenium complexes The issue of the removal of methyl ether protecting groups is discussed and solved All of the target ligands were successfully complexed Detailed ^{1}H-NMR analysis is provided for all the complexes and a deuterated bis-bipyridyl version of each of the complexes prepared and spectroscopically compared The X-ray crystal structure of one complex gives a superb illustration of the spatial make-up of these rarely reported molecules Chapter three also contains an organic experimentalist's introduction to the electrochemistry involved and a cursory investigation of each complex is provided Ground and excited state absorption and emission results are presented, among others

Chapter four aims to put the thesis into perspective from a practical point of view For all the experimental work, descriptions of solvent and chemical preparation, equipment and instrumentation used is provided The aim of the thesis is to have, in this work, a bench-top manual of triazole production to serve as a clear and simple guide to aid researchers in furthering 1,2,4-triazole synthesis toward the goal of the ultimate "target molecule"

Abbreviations

λ	Wavelength
δ	Chemical shift
ACN	Acetonitrile
bipy	2,2'-bipyridyl
COSY	COrrelated SpectroscopY
DCM	Dichloromethane
DMAC	Dimethylacetamide
DMF	Dimethylformamide
DMSO	Dimethylsulfoxide
Et	Ethyl group
EtOH	Ethanol
FID	Free Induction Decay
HMPA	Hexamethylphosphoramide
IR	Infra Red
LC	Ligand Centered
MC	Metal Centered
Me	Methyl group
MeOH	Methanol
MLCT	Metal to Ligand Charge Transfer
Mol	Mole
NMP	*N*-methylpyrollidine
NMR	Nuclear Magnetic Resonance
Ph	Phenyl
THF	Tetrahydrofuran
TLC	Thin Layer Chromatography
TMS	Trimethylsilane
UV/vis	Ultraviolet/Visible

1. Introduction to 1,2,4-Triazoles: Synthesis of Model Compounds

1.1 GENERAL INTRODUCTION

On foot of the success of the ruthenium tris-bipyridine complex as a complex capable of catalysing reactions which can convert solar energy into electrical energy, much work has been done to synthesize alternative ligands for use with ruthenium in an effort to increase stability 1,2,4-triazoles have, for a number of years, been synthesised with a view to acting as ligands in these ruthenium complexes These complexes are vital pieces in the puzzle that will ultimately result in the development of successful artificial photosynthetic systems

While previous work has concentrated on investigation of electrochemical and photophysical properties of ruthenium complexes, this work concerns the synthesis of new 1,2,4-triazole ligands and their complexes These triazoles have been carefully pre-designed with the aim of being successful ligands in the search for the more efficient electrochemical devices

This chapter introduces 1,2,4-triazoles and their synthesis Mono- and bis-triazoles were formed as model compounds We look at amidrazone formation and investigate the by-products of this reaction Acylamidrazones formed from amidrazone reaction with acid chlorides are the precursors of triazoles Acylamidrazones are cyclysed to triazoles at differing rates depending on substitution Oxadiazoles can also be formed from acylamidrazones by varying reaction conditions Spectral characteristics of triazoles, oxadiazoles and their pre-cursors are presented

In chapter two, tailored mono- and bis-triazole ligands are described using the practical knowledge obtained in chapter one The ligands all contained a 2,5-dihydroxybenzene central ring protected as its methoxy ether Crystal structures of these ligands are described H-bonding effects can be seen in the packing structures of the ligands, one of which is visually very striking

Again spectral detail of the ligands and their precursors is presented A broad range of reactions are used to form the target triazole These include reaction of a nitrile with hydrazine hydrate, a saponification, protecting hydroxyl groups as ethers using methyl iodide, acid chloride formation with phosphorous pentachloride, reaction of acid chloride and amidrazone and finally cyclization of acylamidrazone to triazoles All of these reactions have been incorporated into a general triazole synthesis

The protected ligands are then incorporated into ruthenium complexes The issue of the removal of methyl ether protecting groups is solved using boron tribromide A general procedure for this reaction is described All of the target ligands were successfully complexed Detailed ^{1}H-NMR analysis is provided for all the complexes and a deuterated bis-bipyridyl version of each of the complexes prepared and spectroscopically compared The X-ray crystal structure of one complex is discussed and compared to the free ligand structure Ground and excited state absorption and emission spectra are discussed for selected complexes
The final chapter contains descriptions of solvent and chemical preparation, equipment and instrumentation used

1.1.1 Introduction

This chapter introduces the synthesis of 1,2,4-triazoles and charts their development from the late 19th century to today The mechanisms employed by the early chemists are compared with those in use today Several different synthetic routes to triazoles found in the literature are discussed along with the merits of each By-products of triazole synthesis are also addressed This chapter deals mainly with mono-triazoles, chapter three deals in detail with the synthesis of larger triazoles A number of model triazoles were synthesized and are described in detail in section 1 2 An in-depth spectral analysis of these models is provided

1.1.2 Early Triazole Formation

One of the first methods used for the synthesis of 3,5-disubstituted-1,2,4-triazoles involved the thermal condensation of an acid hydrazide with an amide[1], to form the diphenyl-triazole **(4)** as shown in Scheme [1 1]

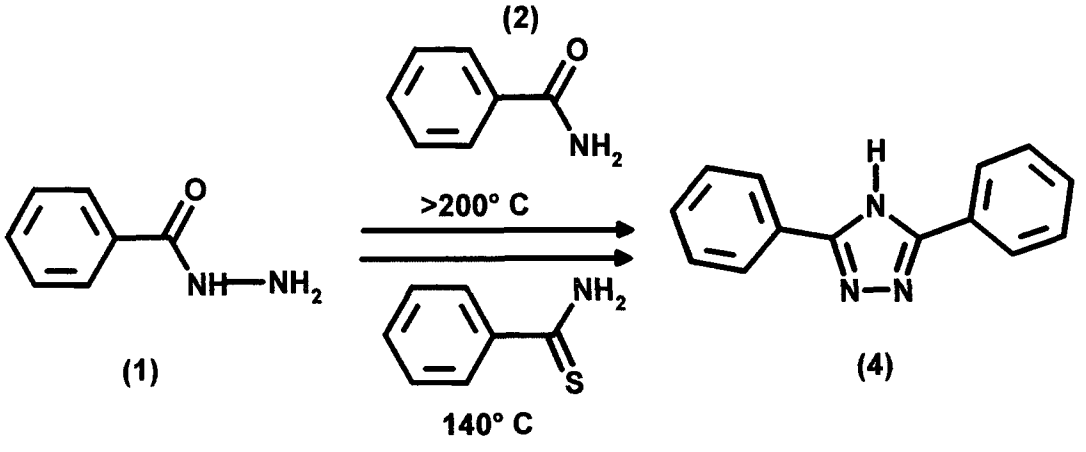

Scheme [1.1]

This reaction, called the Pellizari reaction, had the disadvantage however of the production of mixtures of triazoles, presumably by transamination reactions between the hydrazide and the amide due to the high reaction temperatures employed in the reaction[2,3]

Higher yields of triazoles (e g **(4)**) were obtained in the reaction of aryl thioamides, (e g **(3)**), with aryl hydrazides (e g **(1)**)[4 5 6], also shown in Scheme [1 1] These reactions occurred at lower temperatures

In the early years of this century, Stolle[7] worked on developing methods of disubstituted triazole formation He succeeded in forming 3,5-dimethyl-triazole **(6)** in low yields by the reaction of the 5-diacylhydrazine **(5)** with ammonia at high temperature in the presence of calcium chloride (drying agent) as shown in Scheme [1 2]

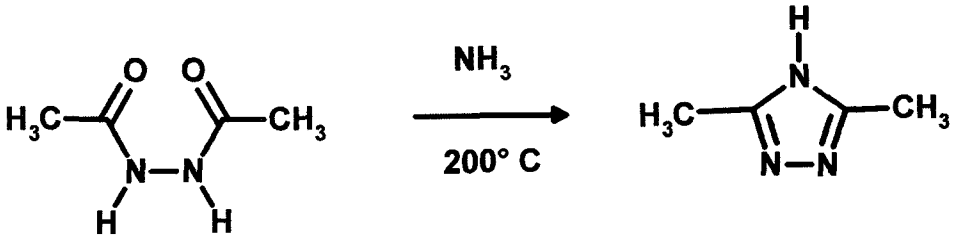

(5) (6)

Scheme [1.2]

Higher yields of triazoles (e g **(7)** and **(8)**) were soon being obtained by the use of higher temperatures, and excess ammonium chloride, as in Scheme [1 3]

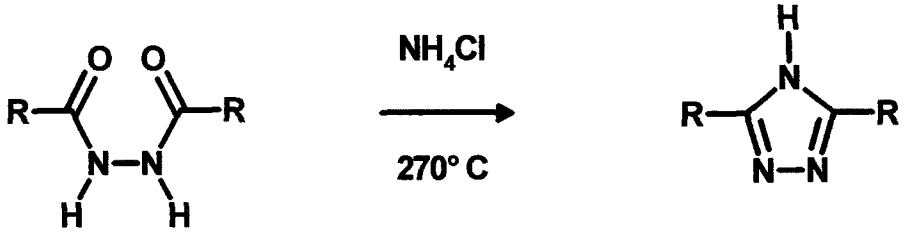

(7) R = 4-C_5H_4N

(8) R = 2-C_5H_4N

Scheme [1.3]

3,5-diphenyl-1,2,4-triazole **(4)** was also synthesized by the same method as Scheme [1 3] This technique was superseded by the method of initially forming the dihydrazide chloride instead of the diacylhydrazide Stolle synthesized the triazole **(11)**[8] by firstly heating dimethoxybenzoyl-hydrazine **(9)** with PCl_5 under dry conditions The dichloride product **(10)** was then cyclized to the triazole **(11)** by heating to 150°C with an ammonia saturated alcohol solution

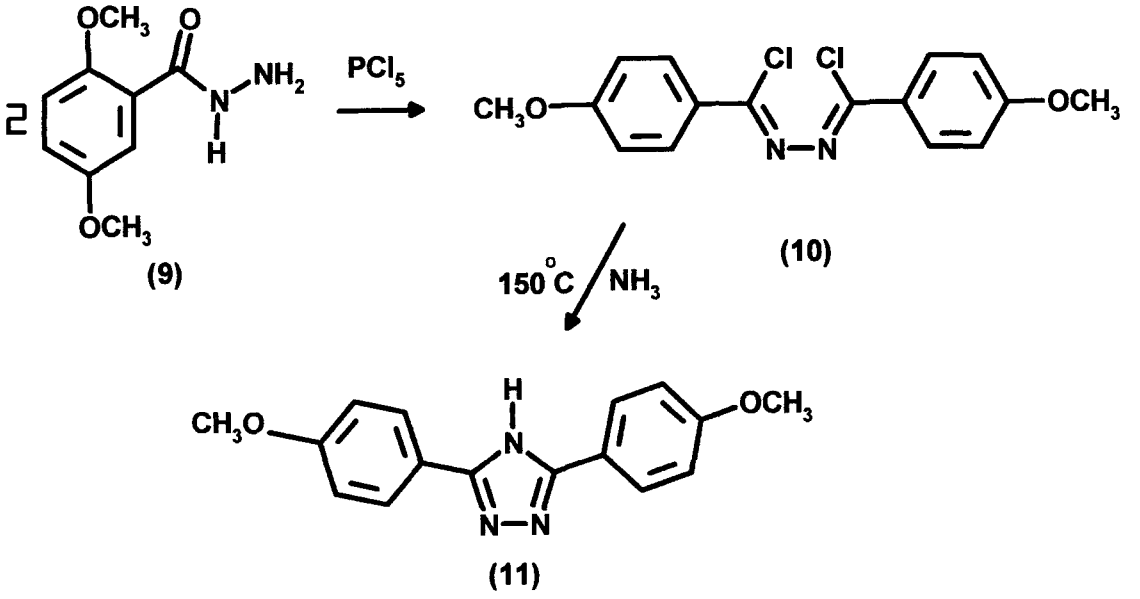

Scheme [1.4]

Though these early condensation reactions produced the desired 1,2,4 - triazoles as reaction products, they often only did so in small yield and produced side products This is, of course, only to be expected when one takes into account the high temperatures used in these reactions

Thus, it was somewhat of a breakthrough in these types of condensations when it was discovered that an aryl nitrile reacted with aryl sulfonate salts of aryl hydrazides in equimolar amounts at 200°C to give 3,5-diaryl-1,2,4-triazoles in good yields[3] A number of molecules synthesized using this method are shown in Scheme [1 5]

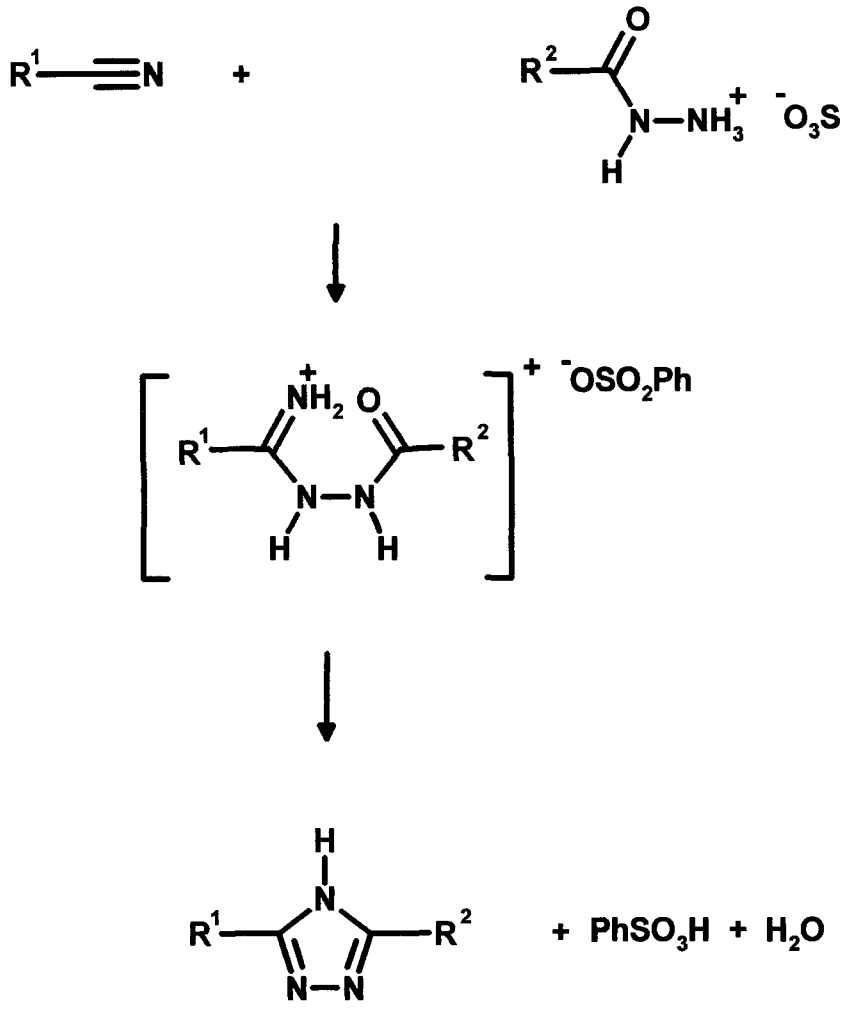

(4) R^1 = Ph, R^2 = Ph

(12) R^1 = Ph, R^2 = *p*-C_6H_4–Me

(13) R^1 = Ph, R^2 = *o*-C_6H_4–Me

(14) R^1 = Ph, R^2 = α-$C_{10}H_7$

(15) R^1 = Ph, R^2 = *p*-C_6H_4–NO_2

(16) R^1 = *p*-C_6H_4–NO_2, R^2 = Ph

(17) R^1 = *p*-C_6H_4–NO_2, R^2 = CH_2–Ph

(18) R^1 = *p*-C_6H_4–NO_2, R^2 = *p*-C_6H_4–NO_2

(19) R^1 = *p*-C_6H_4–NO_2, R^2 = α-$C_{10}H_7$

(20) R^1 = α-C_5H_4N, R^2 = Ph

(21) R^1 = α-C_5H_4N R^2 = p-C_6H_4–Me

Scheme [1.5]

As can be seen in Scheme [1.5] a key feature in the production of triazoles is the use of molecules with available nitrile groups as starting materials. In order to assemble the desired triazole, the nitrile groups are subjected to attack from nucleophiles. Benzene sulphonic acid promotes the nucleophilic attack of the amide on the nitrile group by stabilising the intermediate formed. The ensuing ring closure reaction resulted in higher yields of the desired triazoles. The intermediate in the reaction, shown in brackets, called an acylamidrazone, was thought to form and then dehydrate readily to produce the triazole. The reaction has the added advantage of being a one pot process, operable without the use of a solvent.

A similar procedure used in the production of fluoro-aromatic substituted heterocyclic compounds. 3,5-Disubstituted-1,2,4-triazoles[9] were synthesized by the reaction of a nitrile and a hydrazide in the presence of an acid. Preferred acids were sulphonic acids such as benzene and toluene sulphonic acid; other acids used included phosphoric acid and benzene phosphoric acid.

Indeed this method was also used to prepare 5-phenyl-3-(2-pyridyl)-1,2,4-triazole **(20)**, a molecule used as a model in our work and the formation of which by an alternative method is described in Section 1.2.

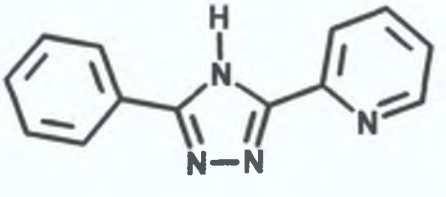

(20)

Potts reacted phenyl cyanide and α-picolin-hydrazide benzenesuphonate at 200°C for 3 hours to form the triazole[2]. As mentioned earlier, Potts encountered the problem of obtaining mixtures of triazoles when carrying out these reactions and offered a rational explanation for the occurrence. The

reaction in question was the formation of 3-alkyl-5-aryl-1,2,4-triazoles from aromatic cyanides and hydrazide benzenesulphonates of aliphatic acids

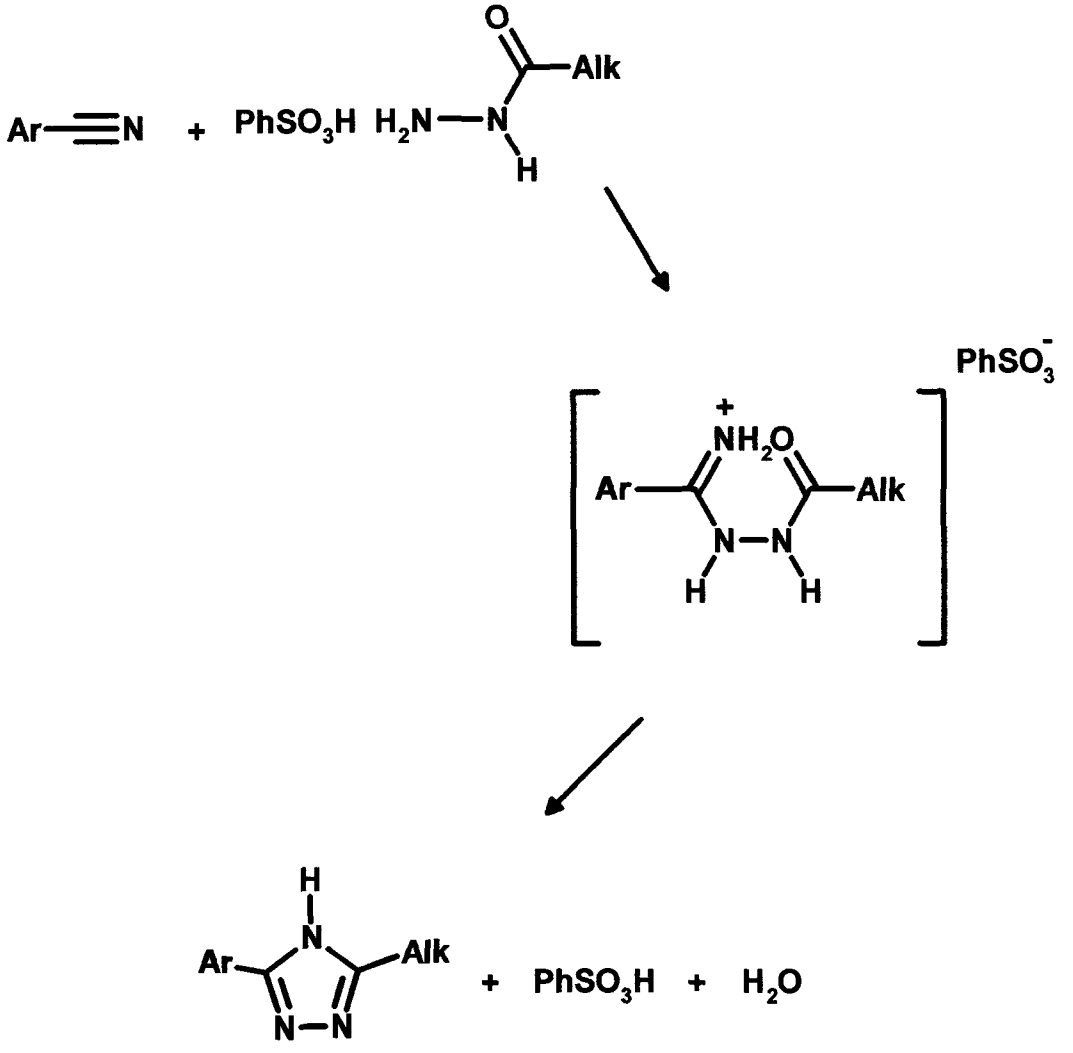

Scheme [1.6]

Along with the desired product a 3,5-diaryl triazole was also produced, the aryl groups corresponding to the aromatic cyanide used, as shown in scheme [1 6]

The unwanted by product may be formed in either of two ways

(a) by reaction of the aromatic cyanide with some intermediate product or

(b) by a similar condensation between products derived from the initial reactants

When *o*-toluyl cyanide was reacted with hydrazide benzenesulphonates of alphatic acids *o*-toluamide was isolated This may have occurred by hydration of the *o*-toluyl cyanide, the necessary water coming from the ring closure[10 11,12] (to the desired triazole) which occurs simultaneously Under these conditions cyanides are known to give amides readily[13 14]

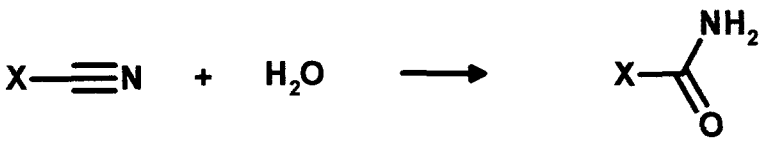

Amide

Scheme [1.7]

The amide formed can then take part in a transamination[15,16]

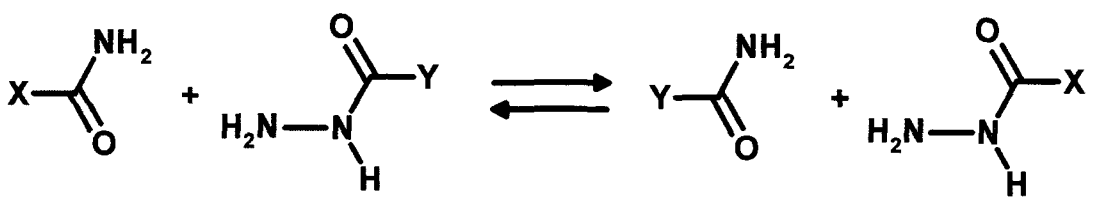

Amide **Hydrazide**

Scheme [1.8]

A transamination in general may occur where the nucleophile is the conjugate base of a primary amine, NH_2 can be a leaving group In this case

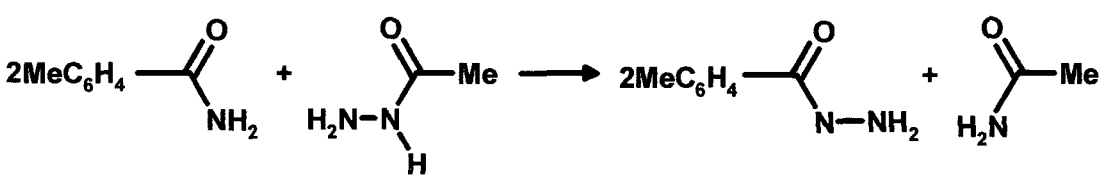

Scheme [1.9]

The reaction of the product of this reaction with the aryl cyanide or amide leads to the 3,5-diaryl-1,2,4-triazole[2] 3,5-dialkyl triazoles could not be formed in good yields using this method

Weidinger and Kranz introduced a further advancement in the use of the benzenesulfonic acid salt of the hydrazide in triazole formation, which saw the free acid hydrazide being employed Using this method dialkyl, diaryl, 3-alkyl-5-aryl-1,2,4-triazoles, 3-amino-5-phenyl-1,2,4-triazole and ditriazoles[17] were obtained An excess of the nitrile was heated with the acid hydrazide in a bomb at 200°C to give the triazolic product

Scheme [1 10] below illustrates the formation of 3-hydroxy-5-phenyl-1,2,4-triazole **(22)**

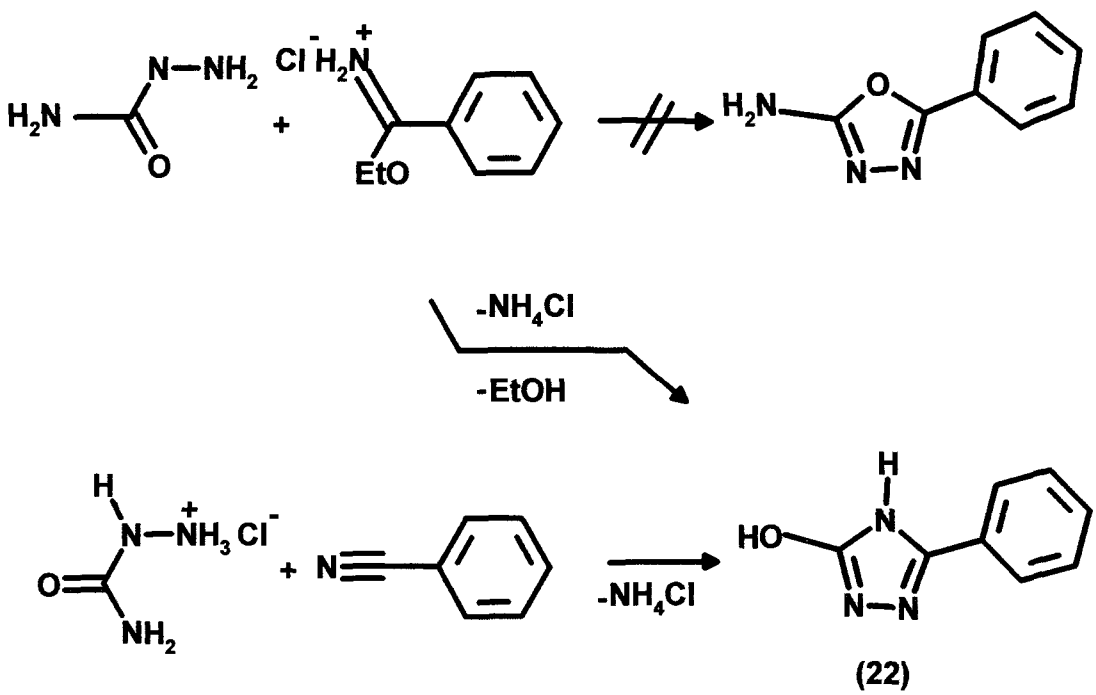

Scheme [1.10]

The expected 1,3,4 oxadiazole was not formed in the above reaction Instead **(22)** was formed with the simultaneous reduction of the ketone group With the formation of **(22)** using the lower reaction in scheme [1 10] an even simpler method for triazole formation had been achieved

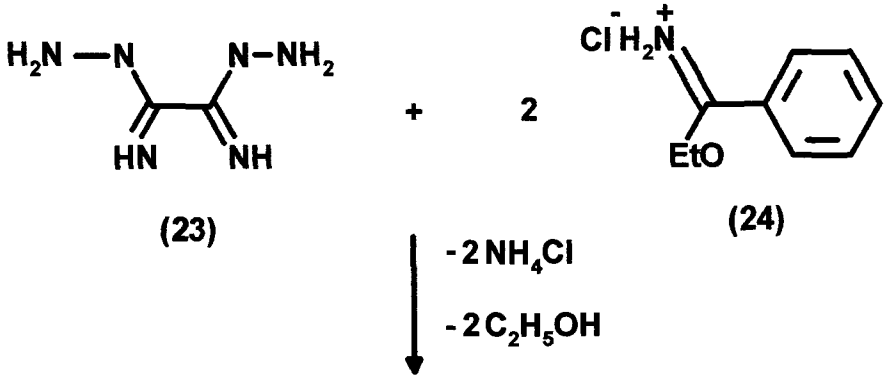

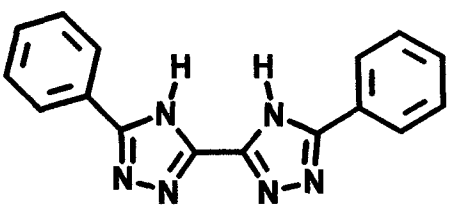

(25)

Scheme [1.11]

The ditriazole **(25)** in Scheme [1.11] was formed by the reaction of the di-amidrazone **(23)** and the iminoether hydrochloride **(24)** Unlike previous reactions that proceeded through an intermediate acylamidrazone and then formed the triazole through the elimination of water, these reactions eliminate ammonium chloride as the triazole ring forms

Weidinger and Kranz also reported a method of synthesizing symmetric disubstituted 1,2,4-triazoles[18] starting with the corresponding nitrile and sulphur trioxide[19] The 4,6-diaryl-1,2,3,5-oxathiadiazine 2,2-dioxide produced was treated with hydrazine (or a substituted hydrazide) in 5% alkali to give symmetrical 3,5-diaryl-1,2,4-triazoles readily The reaction and reported products are shown in Scheme [1 12]

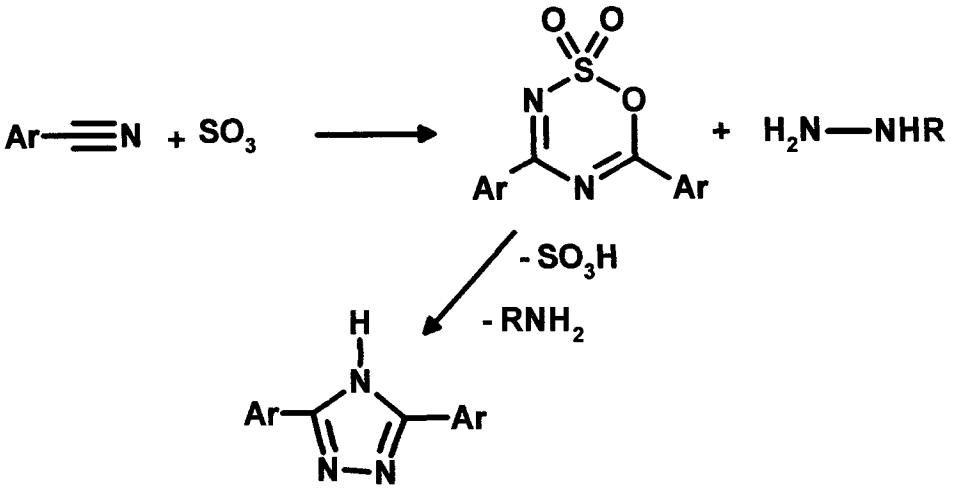

(26) Ar = *m*-CH_3–C_6H_4, R = H

(27) Ar = C_6H_5, R = H

(28) Ar = C_6H_5, R = $CONH_2$

(29) Ar = C_6H_5, R = COC_6H_5

(30) Ar = C_6H_5, R = $C(NH)NH_2$

(31) Ar = C_6H_5, R = $C(NH)C(NH)NHNH_2$

(32) Ar = C_6H_5, R = $CSNH_2$

Scheme [1.12]

The use of amidrazones in triazole synthesis was to become the most common method for their preparation

1.1.3 Triazoles from Direct Cyclization of Amidrazones

The direct cyclization of amidrazones to form 3,5-disubstituted-1,2,4-triazoles (e g **(35)**) can be achieved by heating the amidrazone **(33)** in an excess of acetic or propionic anhydride[20] Initially the *N*-acylated triazole **(34)** was formed which was easily hydrolysed in hot water to give **(35)** in Scheme [1 13]

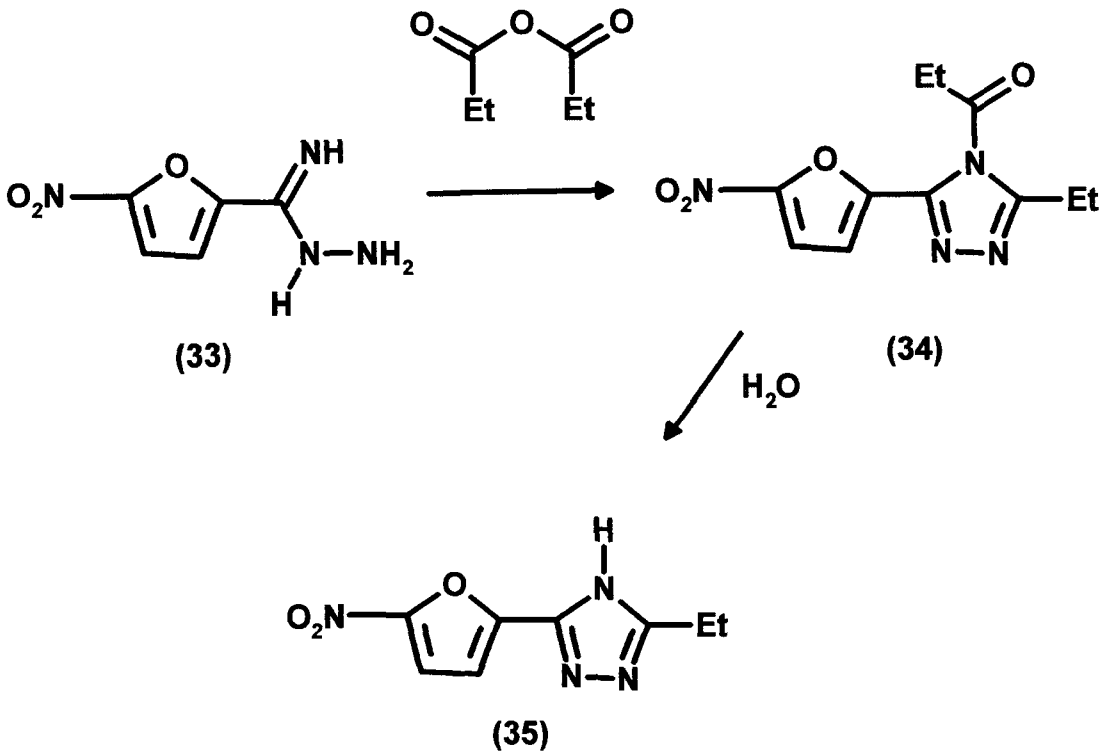

Scheme [1.13]

The acetic anhydride reaction has also been used for the production of potential anti-tuberculosis compounds Vereschagina and co-workers[21] formed an amidrazone from the reaction of the corresponding nitrile with hydrogen sulfide in pyridine solution in the presence of triethylamine base, followed by reaction with hydrazine hydrate The amidrazone when boiled for 2 hours with acetic anhydride, followed by removal of most of the acetic acid and addition of water, precipitated the 1,2,4-triazole **(36)** shown in Scheme [1 14]

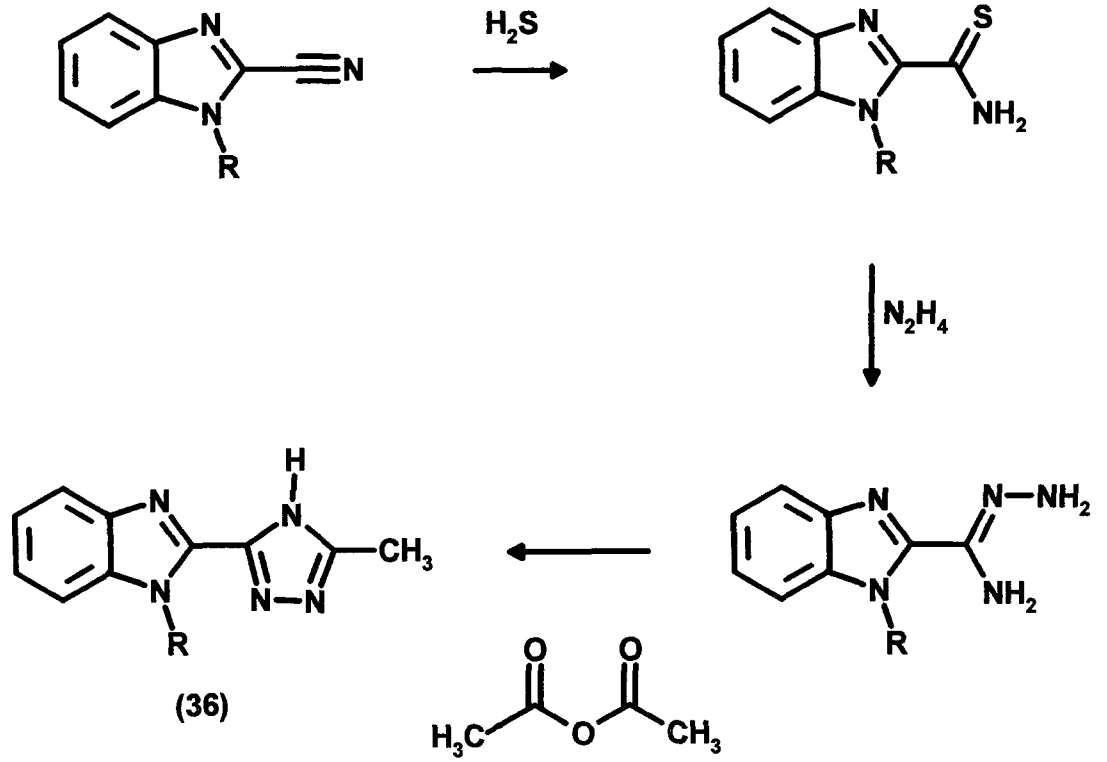

Scheme [1.14]

Reaction of the amidrazone **(37)**, however, with acetic acid and a small amount of nitric acid[22] gave a mixture of both the corresponding triazole **(39)** and oxadiazole **(38)** as illustrated in scheme [1 15]

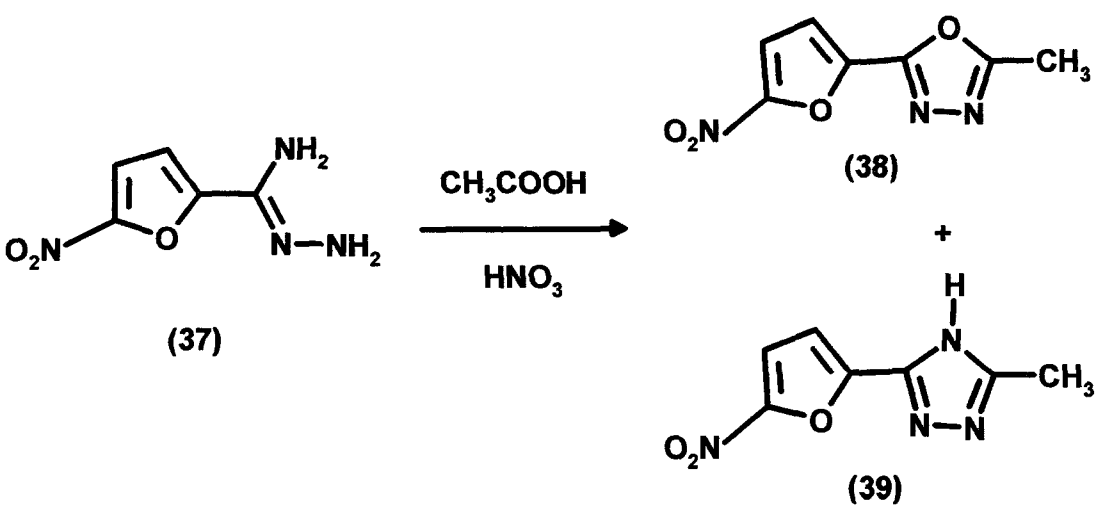

Scheme [1.15]

A less common synthetic route involved the reaction of an amidrazone e g **(40)** and an orthoester to produce 3-aminomethyl disubstituted 1,2,4-triazoles[23,24,25] The formation of alkyl-aryl **(41)** and aryl-aryl triazoles **(42)** as shown below was carried out

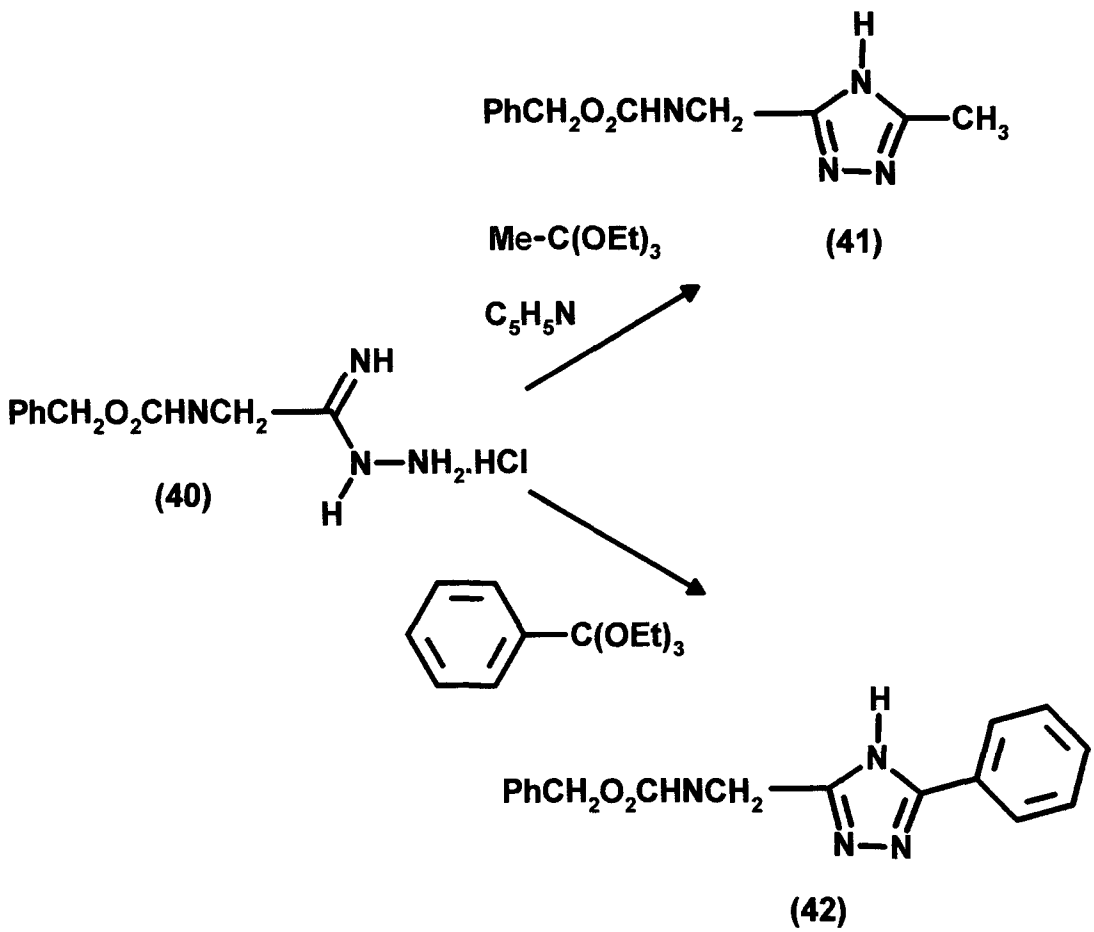

Scheme [1.16]

3-aminomethyl-5-aryl disubstituted triazole **(42)** was also synthesized by an interesting alternative method[26] The benzylidene derivative **(43)** was formed from an iminoether hydrochloride reacting with a substituted hydrazine The triazole **(42)** was then formed by oxidative ring closure with palladium[27,] in refluxing mesitylene

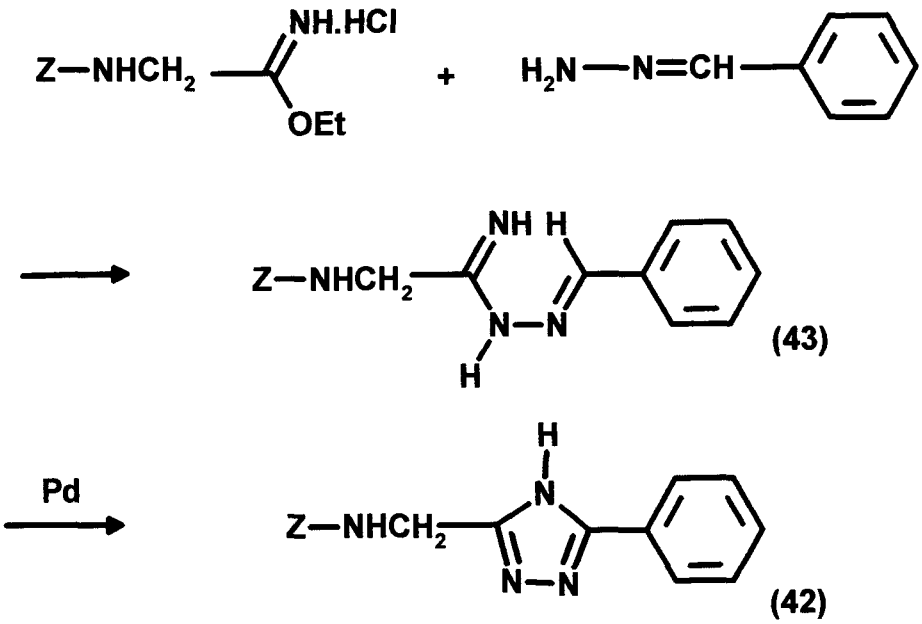

$Z = CO_2CH_2Ph$

Scheme [1.17]

This reaction is thought to proceed via triazoline intermediate formation

Frank Case reported the reaction of phenyl picolinamide hydrazone with a number of aldehydes such as benzaldehyde to form 3-aminomethyl-5-aryl disubstituted triazoles After heating the triazoline in Scheme [1 18] with 10% palladium on charcoal in decahydronaphthalene dehydrogenation afforded the corresponding 1,2,4-triazoles **(44)**,**(20)**,**(45)** and **(8)** [28]

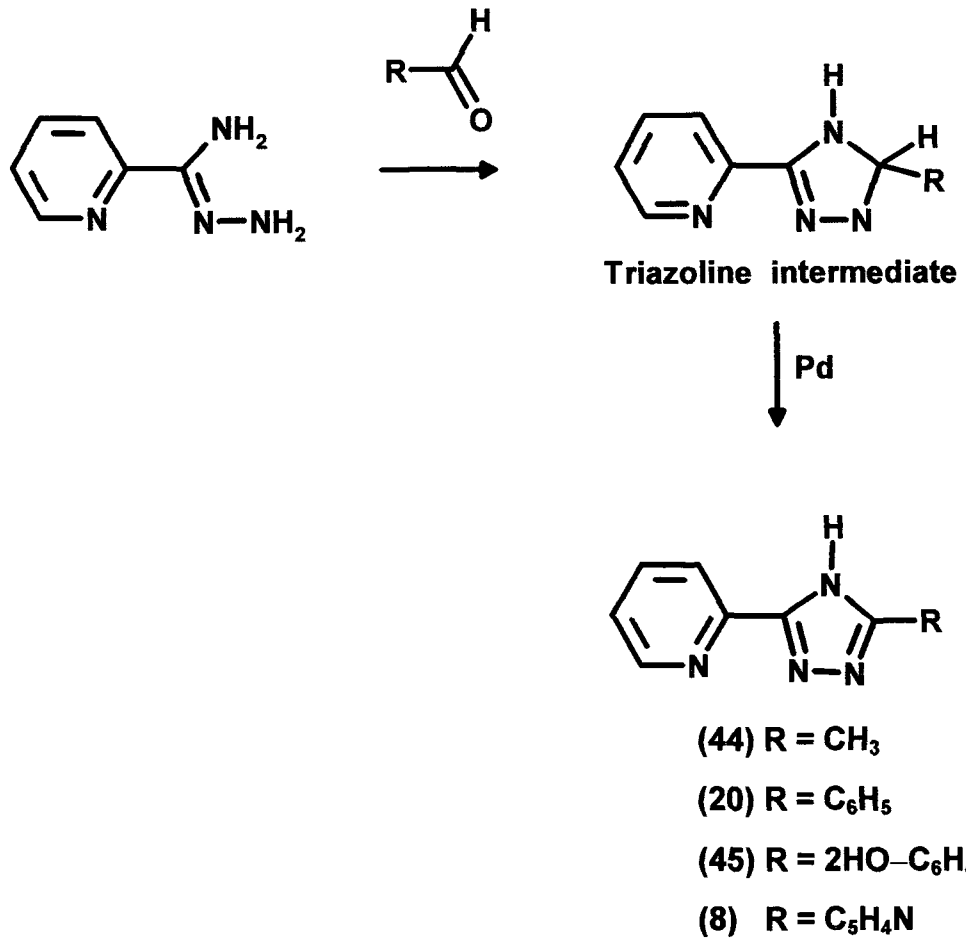

(44) R = CH_3

(20) R = C_6H_5

(45) R = 2HO–C_6H_4

(8) R = C_5H_4N

Scheme [1.18]

Baccheti reacted 1-(α-chlorobenzylidene)-(2-ethoxycarbonyl) hydrazine **(46)** with benzamidine to form a similar amidrazone intermediate en-route to forming the 3,5-disubstituted-1,2,4-triazole **(4)**[29] as shown in Scheme [1 19]

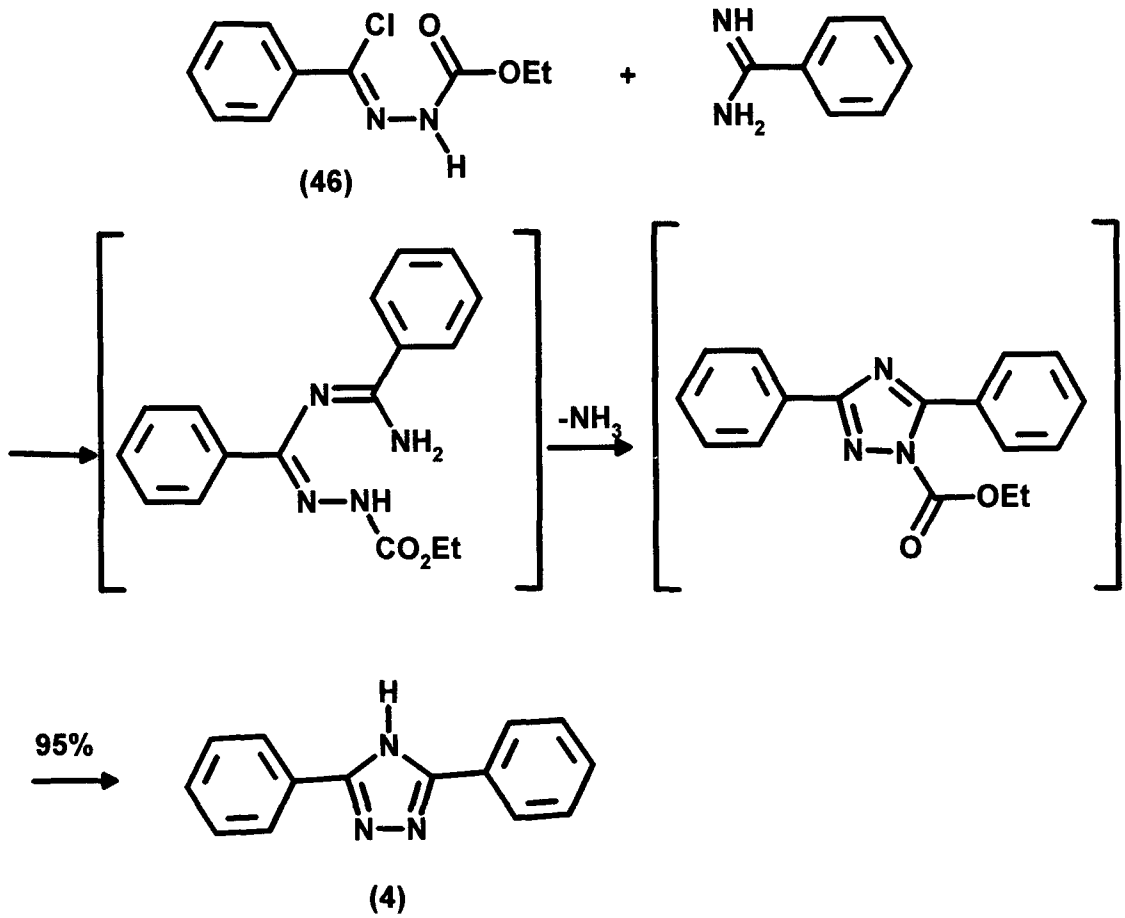

(4)

Scheme [1.19]

Also, 1,2,4-triazoles[30] can be formed from 1,2-bis-(imidoyl) hydrazine by refluxing in formic acid to affect the cyclization The dichlorodifluoro iminoether reacted with hydrazine hydrate with stirring to produce the bis-imidoyl hydrazine **(47)** as in Scheme [1 20] A molecule of ammonia is eliminated as the cyclization occurs to form **(48)**

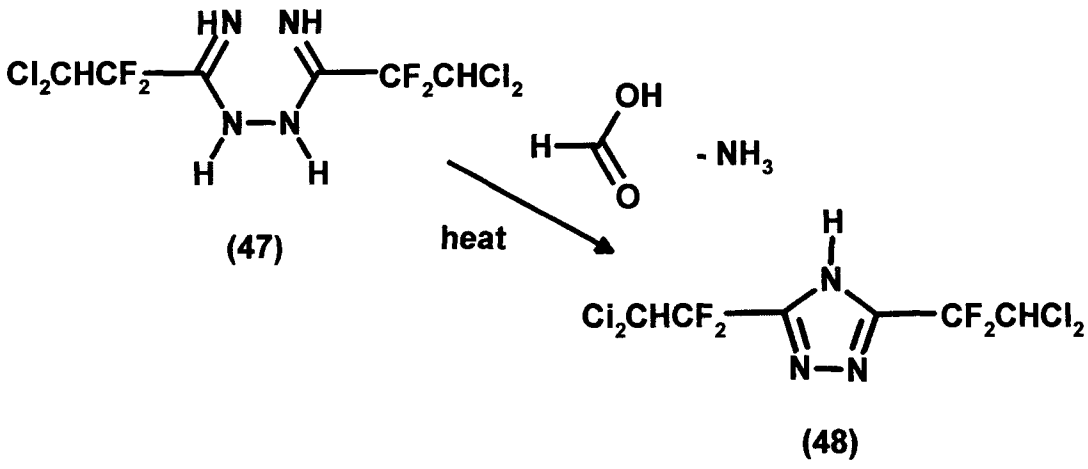

Scheme [1.20]

1.1.4 1,2,4-Triazoles from Iminoethers and Hydrazides

Postovskii and Vereshchagina[31] developed one of the best methods for the production of 3,5-diaryl-1,2,4-triazoles in good yields The triazoles were obtained by the reaction of an iminoether with an acid hydrazide via the acylamidrazone intermediate

In general

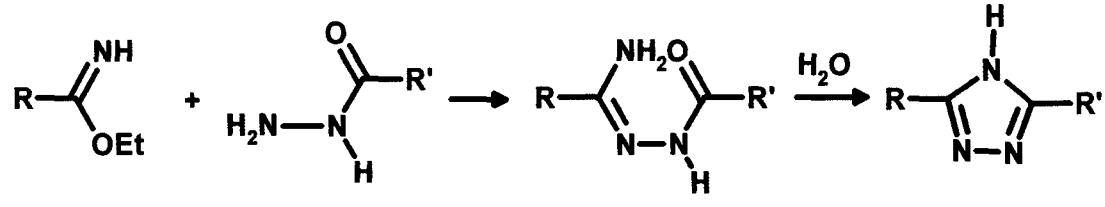

(6) R = CH_3	**$R^1 = CH_3$**	**(20) R = C_6H_5**	**$R^1 = C_5H_4N$**
(49) R = CH_3	**$R^1 = C_6H_5$**	**(53) R = $C_6H_5CH_2$**	**$R^1 = CH_3$**
(50) R = CH_3	**$R^1 = C_6H_5CH_2$**	**(54) R = $C_6H_5CH_2$**	**$R^1 = C_5H_4N$**
(51) R = CH_3	**$R^1 = C_5H_4N$**	**(55) R = $C_6H_5CH_2$**	**$R^1 = C_9H_6N$**
(4) R = C_6H_5	**$R^1 = C_6H_5$**	**(56) R = $C_6H_5CH_2$**	**$R^1 = H$**
(52) R = C_6H_5	**$R^1 = C_6H_5CH_2$**	**(27) R = C_6H_5**	**$R^1 = H$**

Scheme [1.21]

In theory, each disubstituted triazole could be obtained by two routes, as shown in Scheme [1 22]

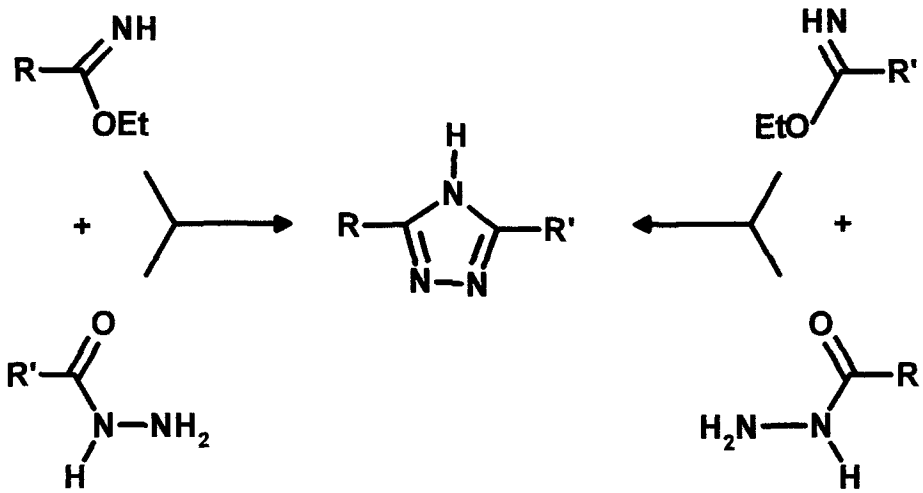

Scheme [1.22]

Thus this method has the advantage that from two different iminoethers and two hydrazides, it is possible to choose the most convenient route for the synthesis

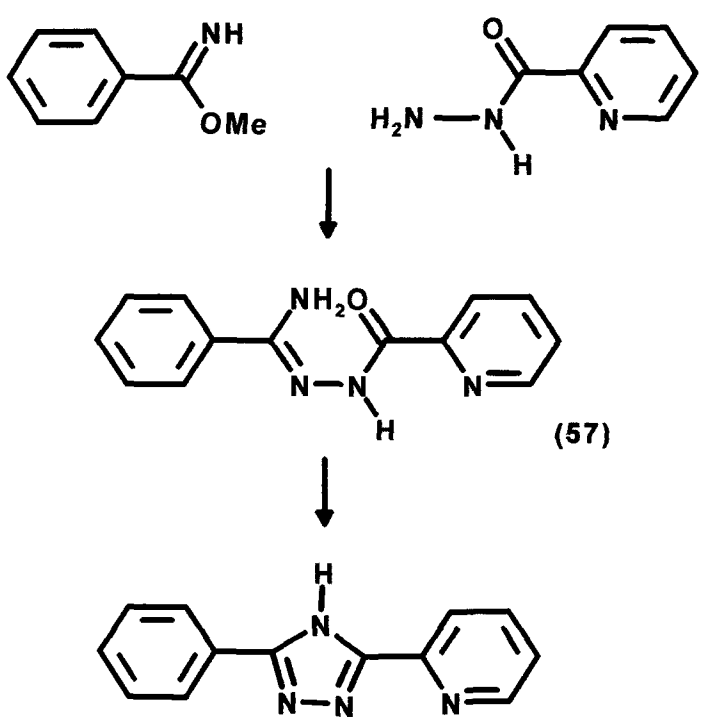

(57)

(20)

Scheme [1.23]

In the synthesis of 3-(2-pyridyl)-5-phenyl-1,2,4-triazole[31] **(20)** shown in scheme [1 23] above, the iminoether hydrochloride was firstly converted to its free form by stirring with sodium hydroxide dissolved in anhydrous alcohol The precipitated mineral salt was then removed by filtration and the filtrate was refluxed with the hydrazide Unlike other reactions, which are presumed to proceed through an acylamidrazone intermediate that is never isolated, here the acylamidrazone **(57)** is obtained and recrystallized before further reaction The corresponding triazoles were then formed by immersion in a high boiling alloy (known as Woods' alloy) and heated to 5-10°C above the melting point until the evolution of water bubbles ceased

Gol'din et al synthesized diakyl triazoles[32] using the iminoether/hydrazide route The formation of bis-triazoles is also reported

For example, the formation of **(6)** in Scheme [1 24]

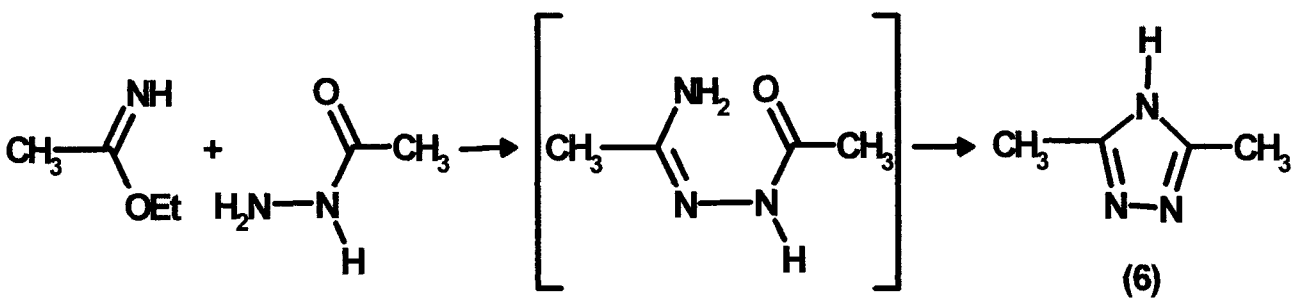

Scheme [1.24]

Intramolecular cyclization with elimination of water to form the corresponding 1,2,4-triazoles occurred readily for mono-triazoles, but heating the precursor acylamidrazone e g **(58)** to 200°C was required for the production of bis-triazoles such as **(59)** shown in Scheme [1 25]

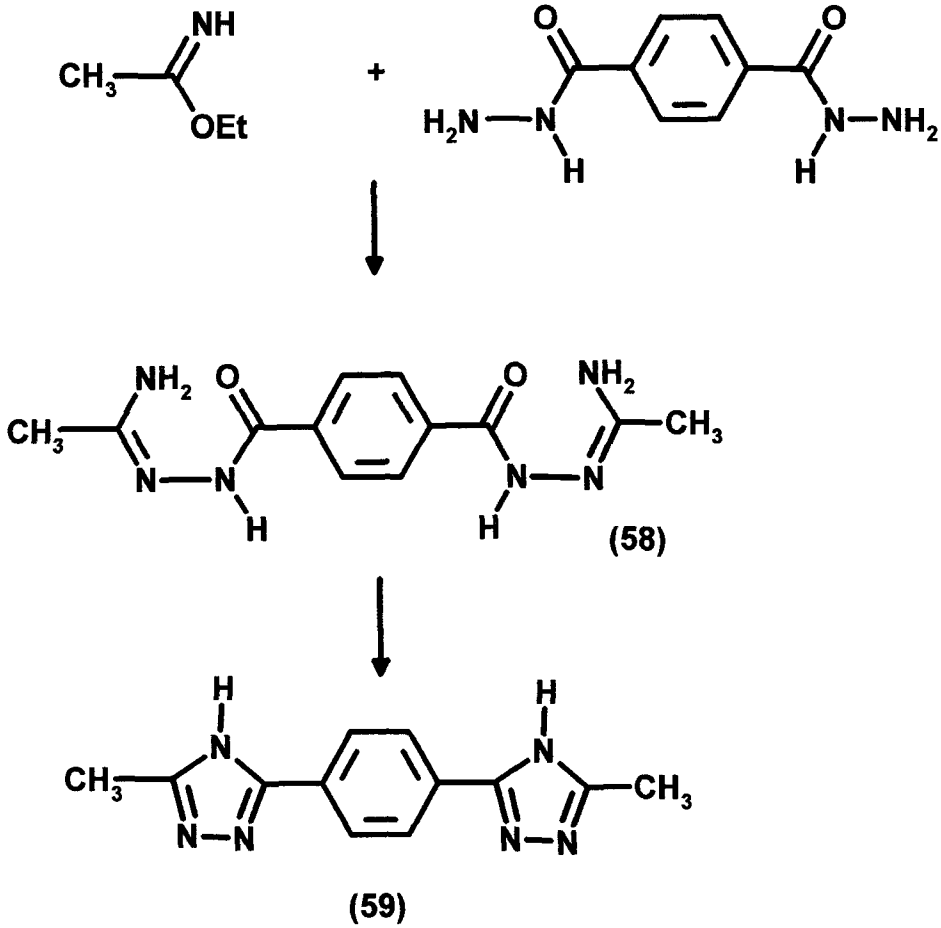

(58)

(59)

Scheme [1.25]

Mono-triazoles dissolved in ethanol and chloroform but bis-triazoles were noted as having limited solubility even in solvents such as pyridine, dimethyl sulphoxide and dimethylformamide The mono-triazoles were also readily vacuum sublimed whilst bis-triazoles were high-melting compounds Triazoles containing long chain alkyl groups[33] were readily formed by reaction of an alkyl amidrazone with a long chain acid halide Alkyl-aryl triazoles have been synthesized by Browne, in particular 1,2,4-triazoles-3-carbaldehydes which are thought to exist in the hemiaminal form in the solid state[34]

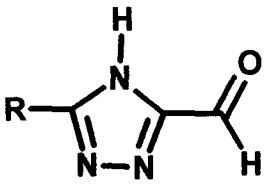

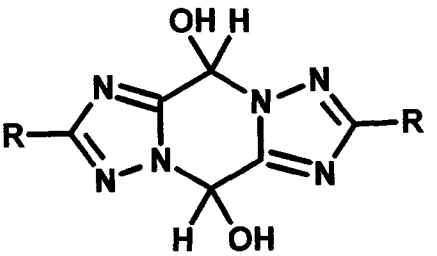

1,2,3-triazole-3-carbaldehyde **Hemiaminal**

The method of formation of the triazoles is through the iminoether-hydrazide reaction

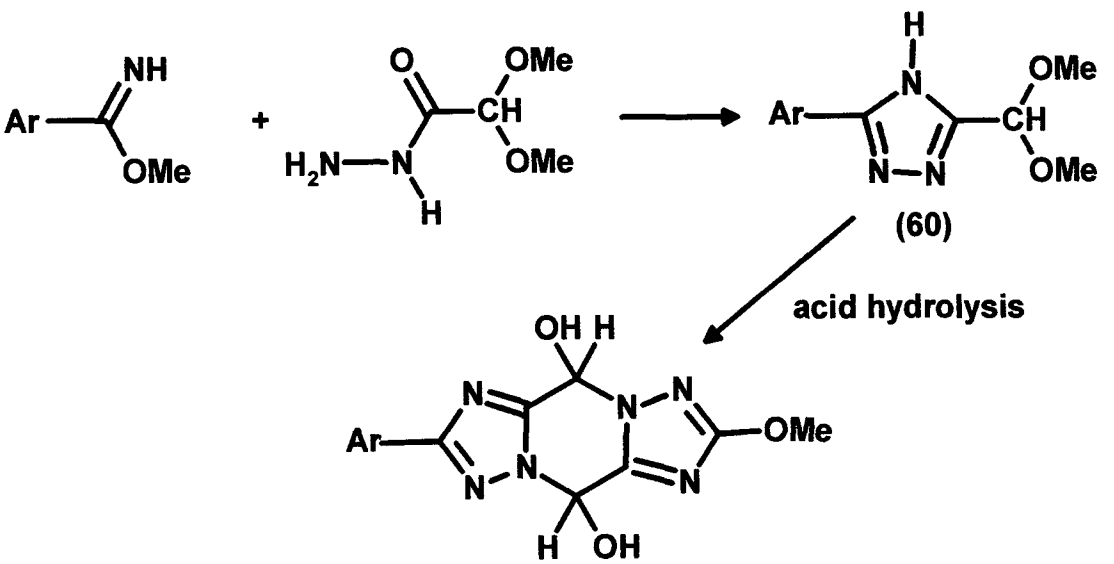

(60)

acid hydrolysis

(61)

Scheme [1.26]

The hemiaminal **(61)** was then obtained by acid hydrolysis of the triazole **(60)** Thermal dehydration of acylamidrazones either with a high boiling solvent or in a melt is the method of choice for the formation of 3,5-disubstituted triazoles containing alkyl-aryl and alkyl-heteroaryl moieties[35,36,37]

1.1.5 Triazoles From 3-Acylamidrazones

Thus far we have seen reactions leading to triazole formation involving 1-acylamidrazones 3-Acylamidrazones can also be cyclized in 2 N HCl to give 3-5-diaryl and 3-alkyl-5-aryl-1,2,4-triazoles[38] The starting point for this reaction is with an iminoether or its corresponding hydrochloride salt as seen in Scheme [1 27]

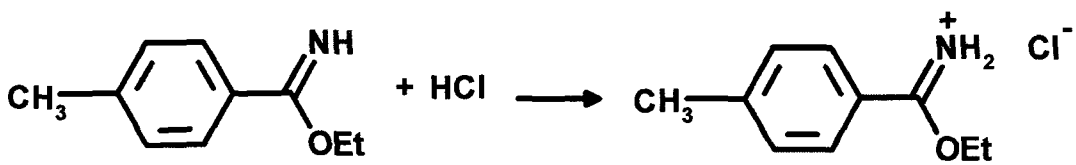

Scheme [1.27]

The first step in the reaction as shown in Scheme [1 28] is the reaction of the iminoether (hydrochloride) with an acid chloride The subsequent reaction of the product with hydrazine gives the 3-acylamidrazone which undergoes ring closure to the disubstituted triazole in the presence of acid

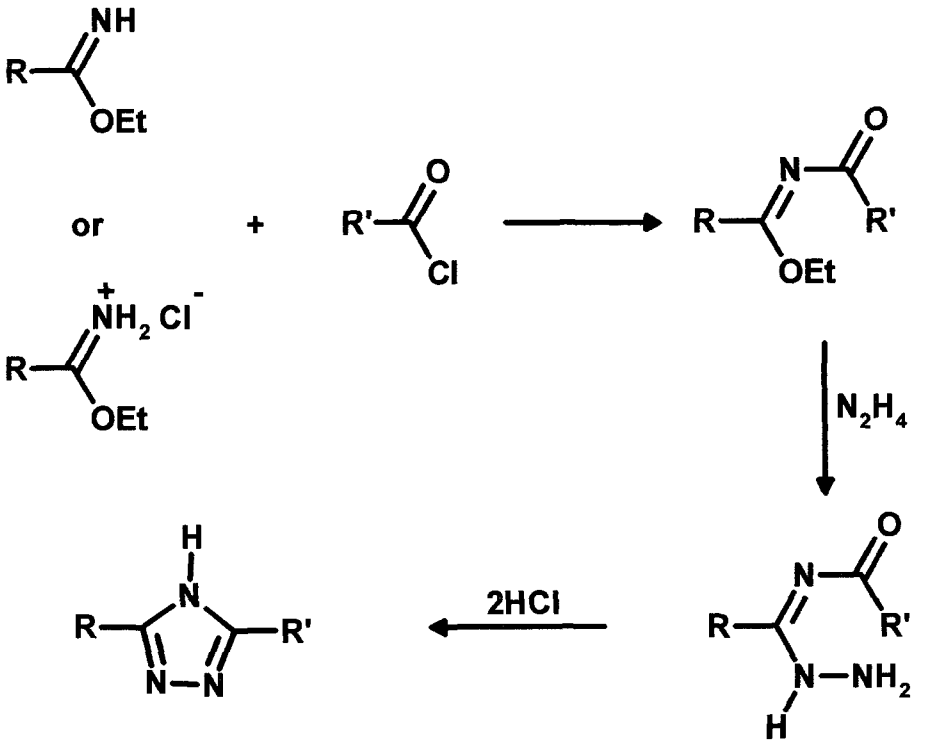

(49) R = C_6H_5 $R^1 = CH_3$

(62) R = C_6H_5 $R^1 = C_2H_5$

(4) R = C_6H_5 $R^1 = C_6H_5$

(63) R = *p*-CH_3-C_6H_5 $R^1 = CH_3$

(64) R = *p*-CH_3-C_6H_5 $R^1 = C_6H_5$

(65) R = *p*-CH_3-C_6H_5 $R^1 = C_6H_5CH_2$

Scheme [1.28]

3,5-Diphenyl-1,2,4-triazole **(4)** was formed in a similar way to that described above by Fujimori and co-workers who reacted α-benzoyliminio benzyl-cyanide with hydrazine[39] The reaction that proceeds through the 3-acylamidrazone seems to be caused by an elimination of the cyano group when attacked by the nucleophilic amine group of hydrazine The α-benzoyl-iminobenzyl cyanide was initially formed by the oxidation of α-benzamidobenzyl cyanide[40] using thionyl chloride in pyridine[41,42,43 44]

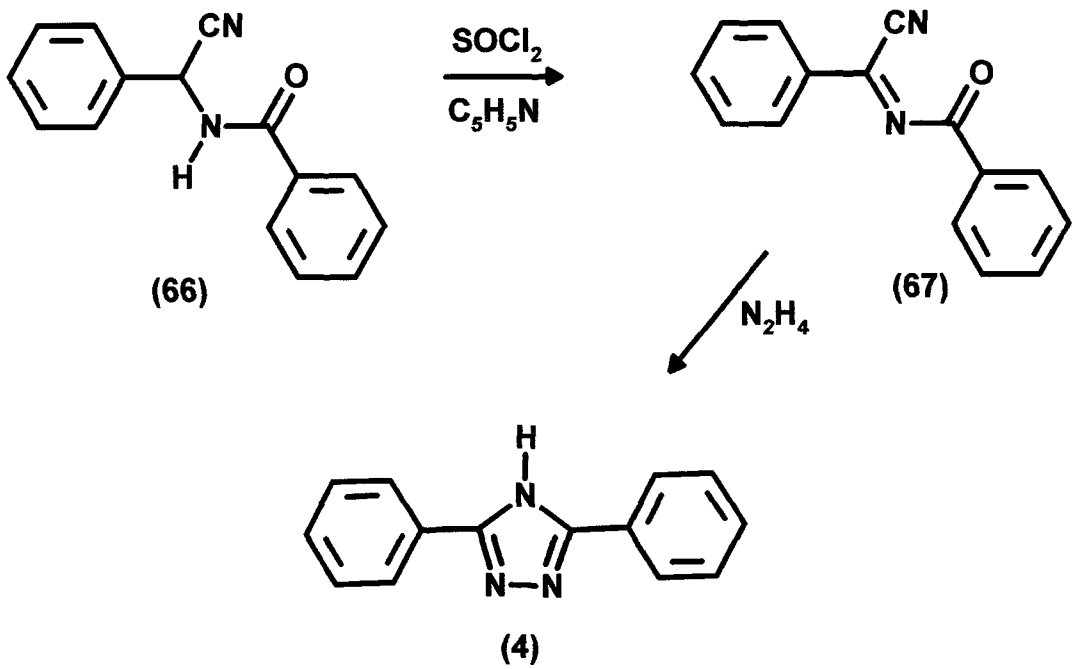

Scheme [1.29]

The acylimino cyanide has three carbon atom sites at which nucleophiles can potentially attack Reaction with a substituted hydrazine e g phenyl hydrazine **(68)** or a hydroxylamine e g "hydroxylamine"**(69)**, bifunctional nucleophilic reagents, leads to a 1,2,4 triazole **(70)** or an oxadiazole **(71)** respectively[45] as shown in Scheme [1 30]

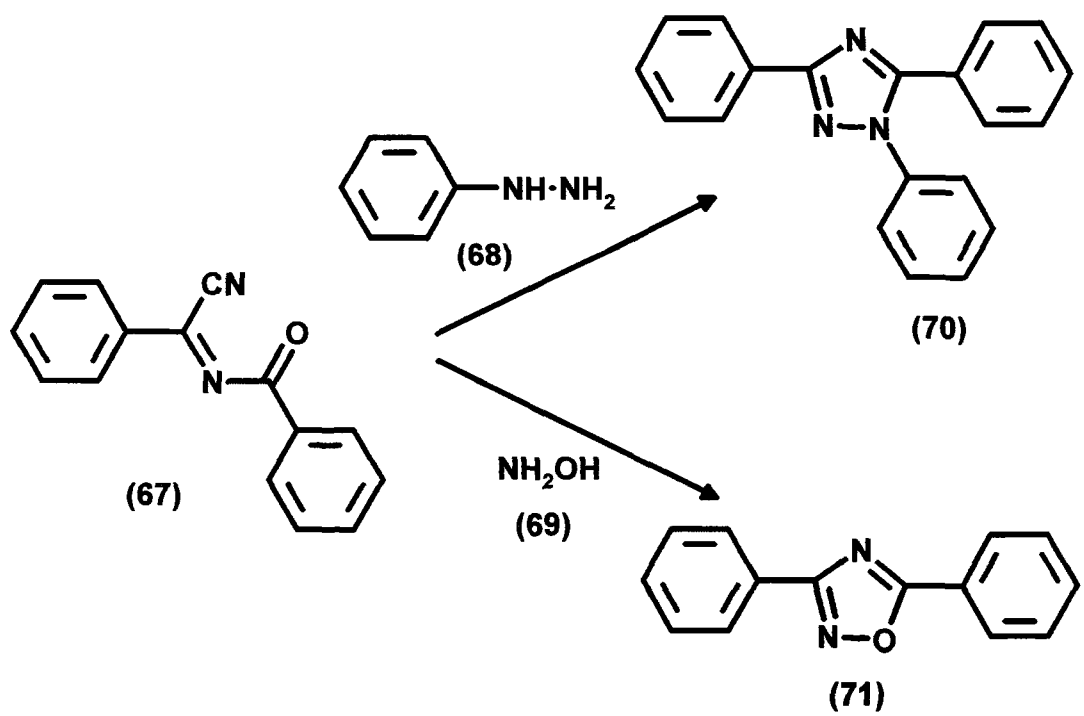

Scheme [1.30]

1,3-Benzoxazines e g **(72)** have been converted to 1,2,4-triazoles e g **(73)** by their reaction with hydrazine[46], as in Scheme [1 31] This reaction is also thought to proceed via the 3-acylamidrazone intermediate

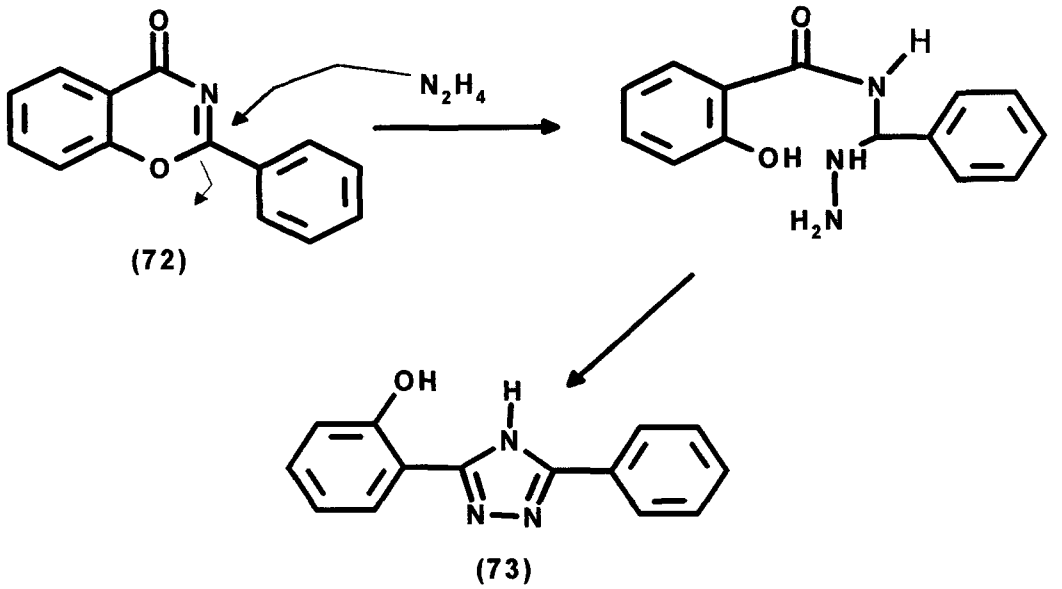

(72)

(73)

Scheme [1.31]

The reaction also occurs when the ring carbonyl group is replaced by a thio-group In both reactions this group is eliminated as H_2O or H_2S respectively when ring closure occurs The initial ring opening reaction involving hydrazine is known by the term hydrazinolysis

Another example of a hydrazinolysis is the formation of triazoles in good yields from 2-oxazolin-4-ones[47] The reaction of acyl-isocyanates with diazomethane has been used to prepare substituted 2-oxazolin-4-ones[48] Once formed, the oxazolinones were very unstable and were treated immediately with hydrazine hydrate to produce the corresponding 3-hydroxymethyl-1,2,4-triazoles[49] as shown in scheme [1 32]

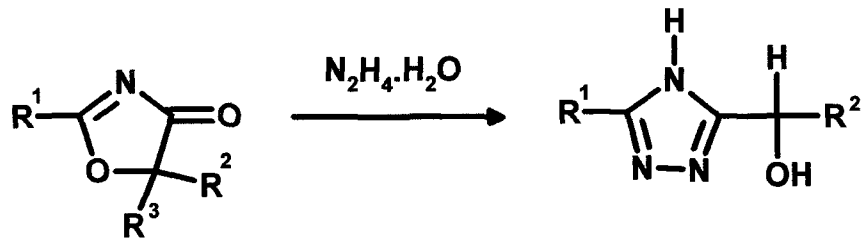

Oxazolinone		→	Triazole	
R^1 = Ph	$R^2 = R^3$ = H	→	(74) R^1 = Ph	R^2 = H
R^1 = EtO–C_6H_4	$R^2 = R^3$ = H	→	(75) R^1 = EtO–C_6H_4	R^2 = H
R^1 = *p*-Cl–C_6H_4	$R^2 = R^3$ = H	→	(76) R^1 = *p*-Cl–C_6H_4	R^2 = H
$R^1 = R^2$ = Ph	R^3 = H	→	(77) R^1 = Ph	R^2 = Ph

Scheme [1.32]

Nucleophilic attack by the hydrazine molecule occurs at the C-1 position of **(78)** causing the ring to open, forming an intermediate 3-acylamidrazone **(79)** This is rapidly followed by the ring closure with loss of H_2O to form the product triazole **(80)** as in Scheme [1 33]

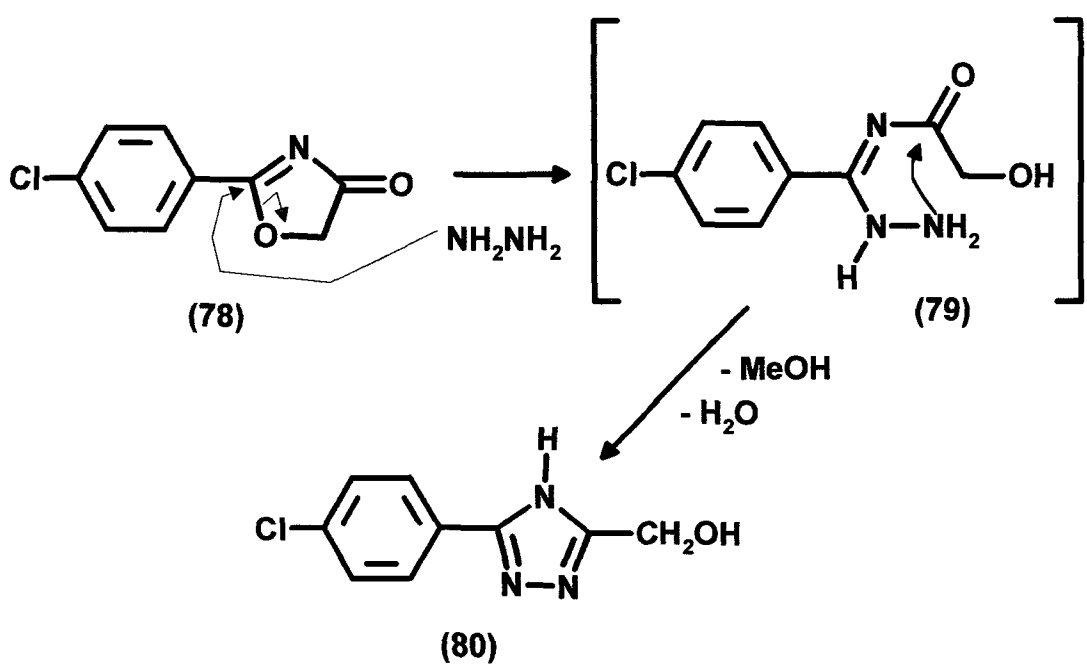

(78) (79) (80)

Scheme [1.33]

1.1.6 Triazoles from Other Methods of Theoretical Interest

The Chichibabin reaction[50,51] has also been used to form 3,5-diaryl triazoles from aryl azines[52] This type of reaction involves the amination of a pyridine or other heterocyclic nitrogen compound with alkali metal amides[53,54,55] For instance in Scheme [1 34]

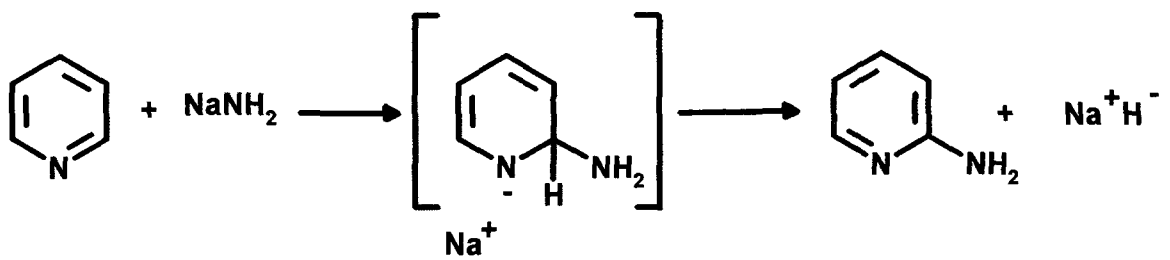

Scheme [1.34]

Applying the same theory to the aryl azine with attack at the 2-position leads to the triazole **(81)** as in scheme [1 35]

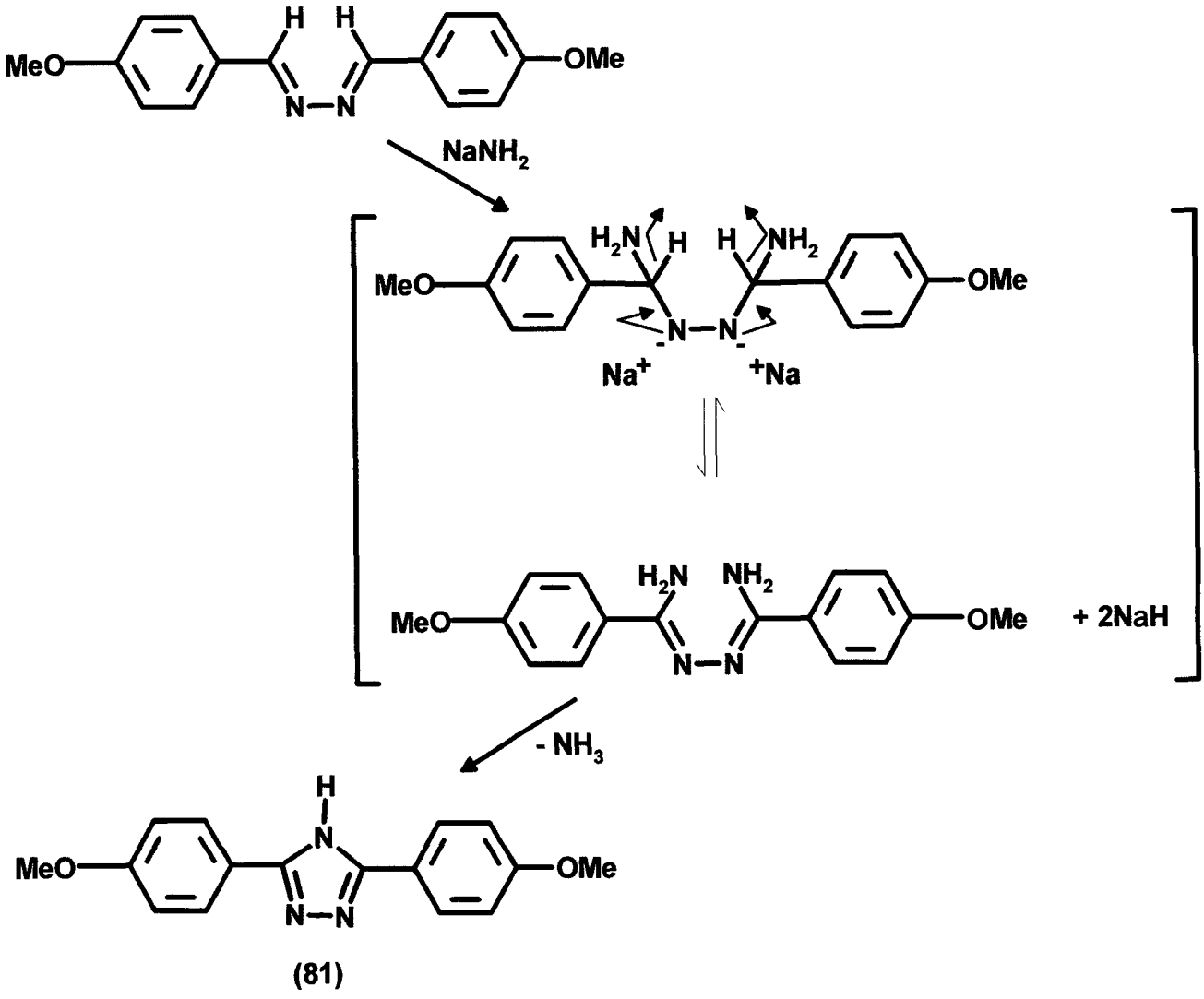

Scheme [1.35]

Oxidative dimerization via copper containing intermediates[56,57] has been reported to produce triazoles in high yields[58] The process involves the initial formation of sodium amidines, obtained by treatment of benzonitrile with sodium amide The amidines were then treated with a molar amount of anhydrous $CuCl_2$ in dimethoxymethane at 20°C The mixture was then heated to 85°C while a stream of oxygen[59] was passed through it The diazabutadiene-1,4-diamine intermediate rapidly loses a molecule of ammonia[60] to form the disubstituted triazole **(4)** in 74% yield in Scheme [1 36]

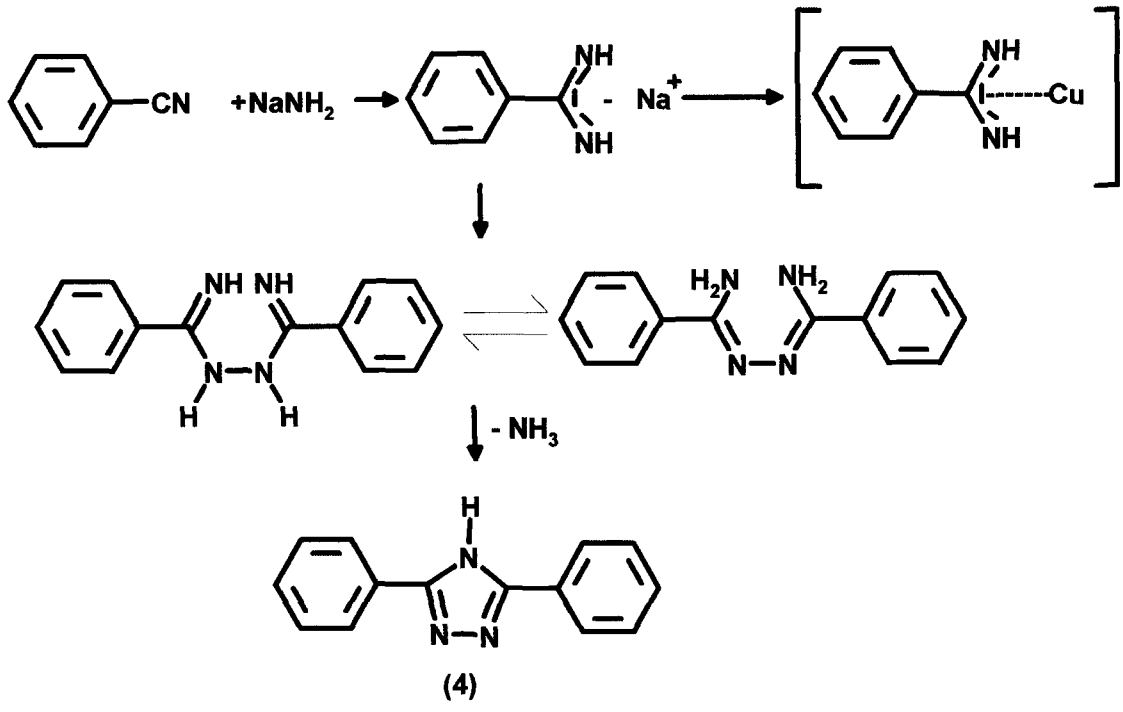

(4)

Scheme [1.36]

Aryl azines similar to those described in the Chichibabin reaction also react with strong bases such as potassium *t*-butoxide (in boiling toluene over 40 hours) in the absence of oxygen to produce 3,5-disubstituted-1,2,4-triazoles[61] The suggested mechanism in this case in Scheme [1 37] involves an elimination reaction of an aryl azine to form a nitrile and an imine

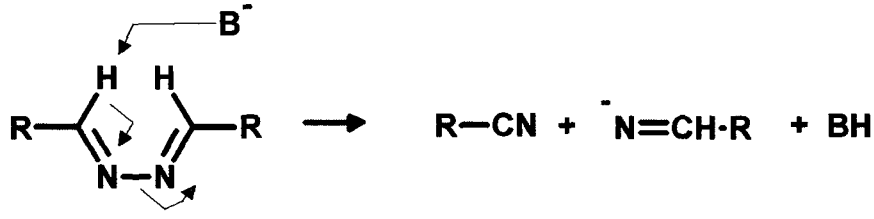

Scheme [1.37]

Labelling experiments were used to show that this nitrile can react with the unchanged aryl azine starting material to form the triazole product

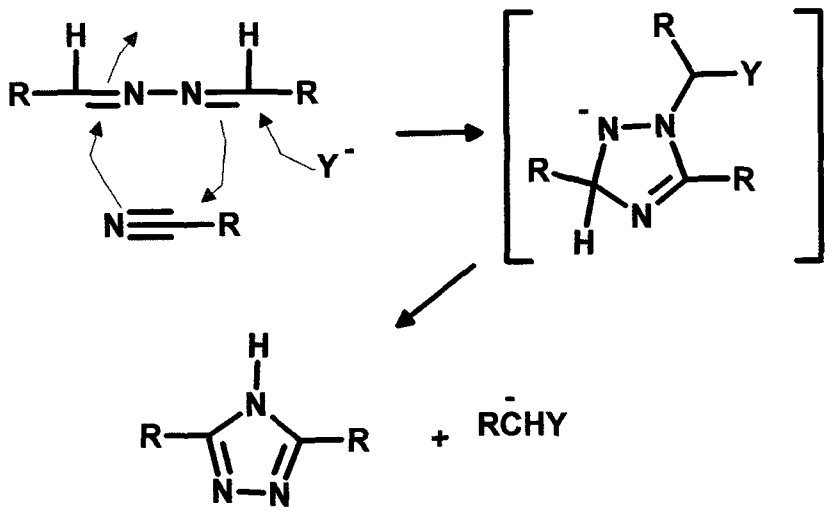

Scheme [1.38]

The nucleophile (Y^- in Scheme [1 38]) in this case may be either the anion $RCH{=}N^-$ or $RC^-{=}N{-}N{=}CHR$, either of which would provide good leaving groups for susequent elimination

An unusual route to the formation of 3,5-diaryl-1,2,4-triazoles involves using the reactive power of silyl azides[62,63,64] This method has proved useful for forming unsymmetrical (and symmetrical, example 4) 3,5-disubstituted-1,2,4-triazoles[65,66] In general aromatic cyanides were reacted with trimethyl silyl azide (or diphenyl-diazidosilane and $AlCl_3$) to form the silylated tetrazole A ring opening of the tetrazole then occurs with loss of N_2 e g from **(82)** in Scheme [1 39] This is followed by reaction of the 1,3-dipole **(83)** with a second molecule of benzyl nitrile This results in the formation of the silylated triazole **(84)** which can be hydrolysed easily to produce the disubstituted triazole **(4)** as shown in Scheme [1 39]

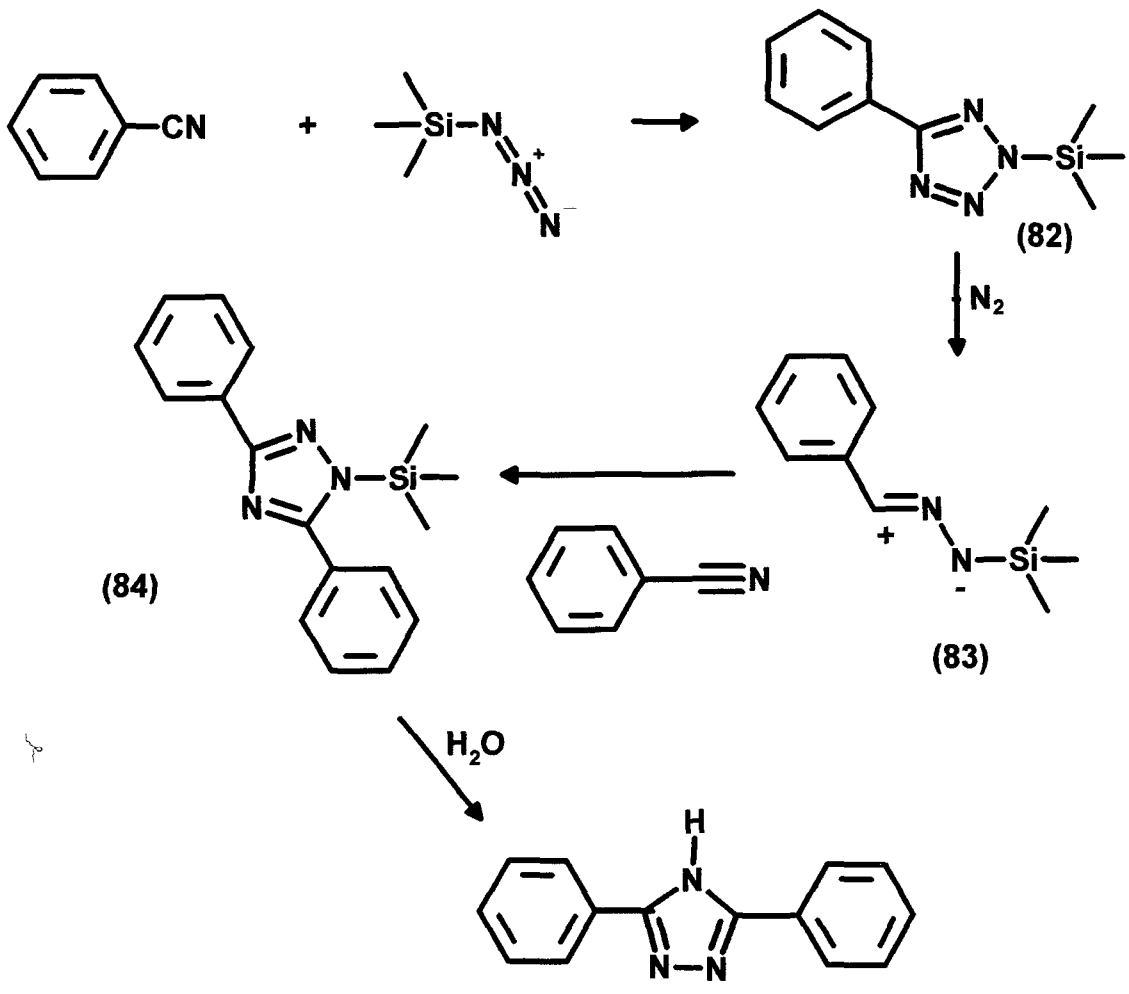

Scheme [1.39]

A similar ring opening of 5-Phenyl tetrazole[67,68] **(85)** when heated to high temperatures[69] (164°C in mesitylene) undergoes a thermolysis reaction expelling N_2 to form a 1,3-dipolar ring opened product **(86)**[70]

Reaction of **(86)** with an aryl nitrile as described previously produced the disubstituted triazole **(4)** However dimerisation reactions also occurred forming the dihydrotetrazine **(87)** and subsequently the amino-triazole **(88)**[71], which could be subsequently converted to **(4)** as shown in Scheme [1 40]

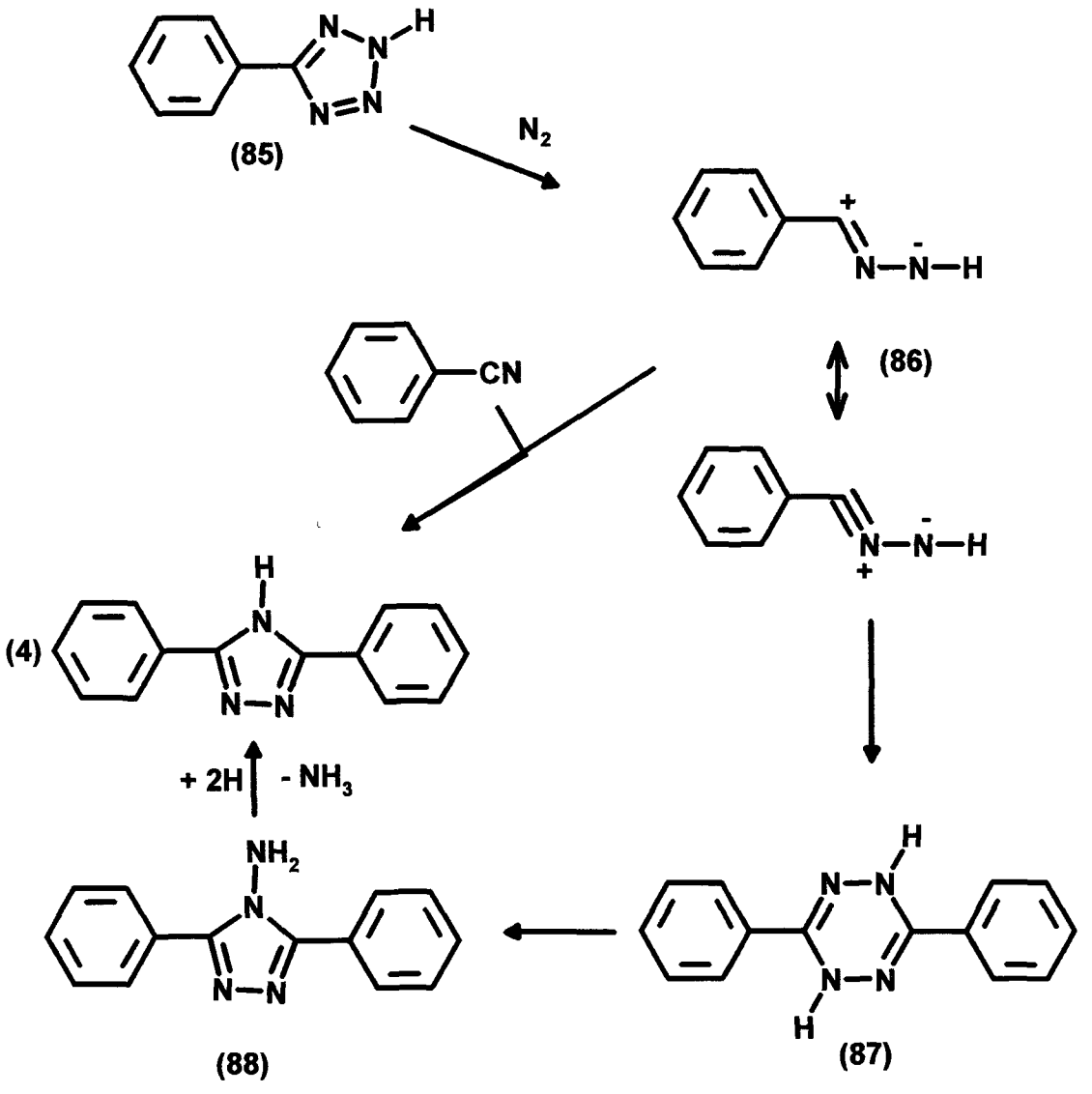

Scheme [1.40]

Conversion of the dihydrotetrazine **(87)** to the triazole **(4)** may be achieved directly by reaction with Zn in acetic acid[72] forming the diazabutadiene-1,4-diamine **(89)** which eliminates ammonia to form **(4)**

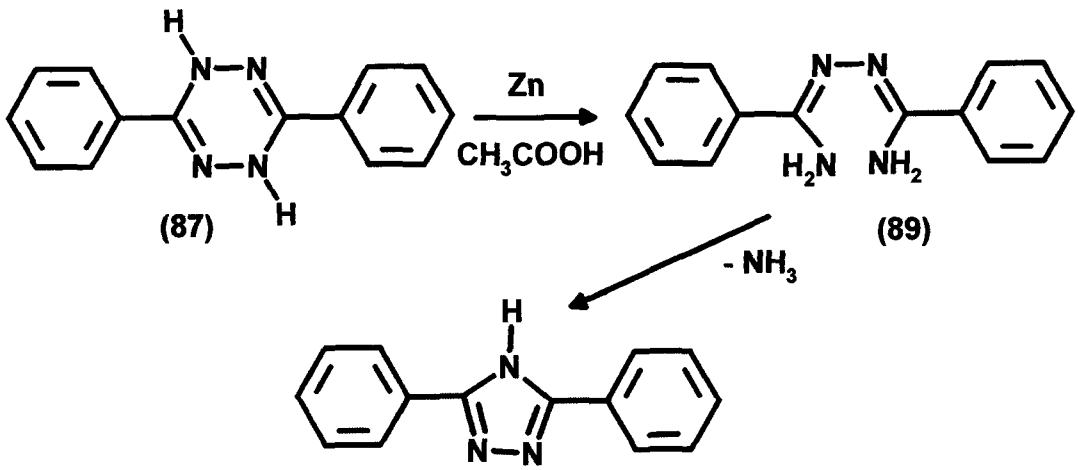

Scheme [1.41]

The 4-amino triazole **(88)** can easily be formed from the dihydrotetrazine **(87)** by the addition of acid[72,73,74] The reaction proceeds via the nitrilium ion

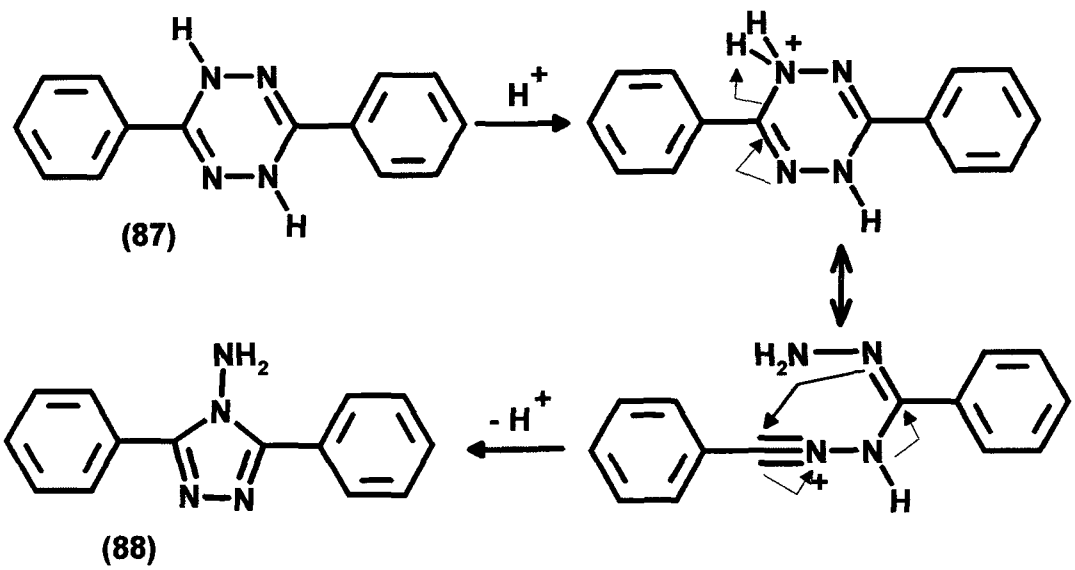

Scheme [1.42]

Thus disubstituted triazole formation reactions often involve the formation of symmetric diamines, hydrazines, tetrazines and 4-amino triazoles as side products of the desired reaction The conversion of these side products to the desired triazole is often facile (See section 1 2)

1.1.7 Self Condensation of Amidrazones

Perfluoroacetimidoyl hydrazine **(89b)**[75] underwent conversion to 1,2-bis(perfluoroacetimidoyl)hydrazine **(90)** over a period of time at 20°C A self condensation occurs with the elimination of hydrazine Heating the bis-hydrazine hydrochloride in a sealed tube at 140°C afforded ring closure to the disubstituted triazole **(91)**[76]

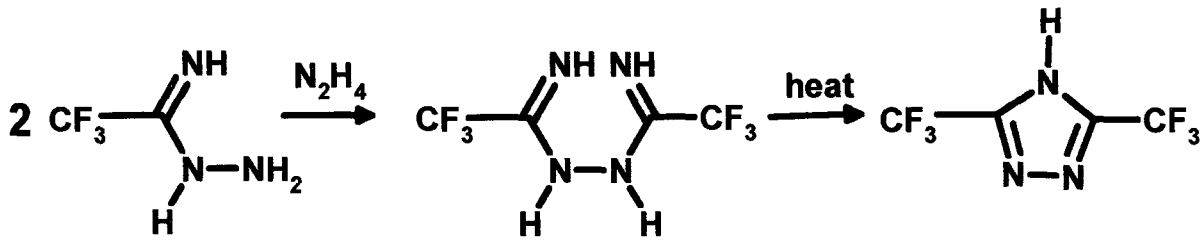

(89b) **(90)** **(91)**

Scheme [1.43]

3,5-Diphenyl-1,2,4-triazole **(4)** was also formed via the diazabutadiene-1,4-diamine by another method[77]

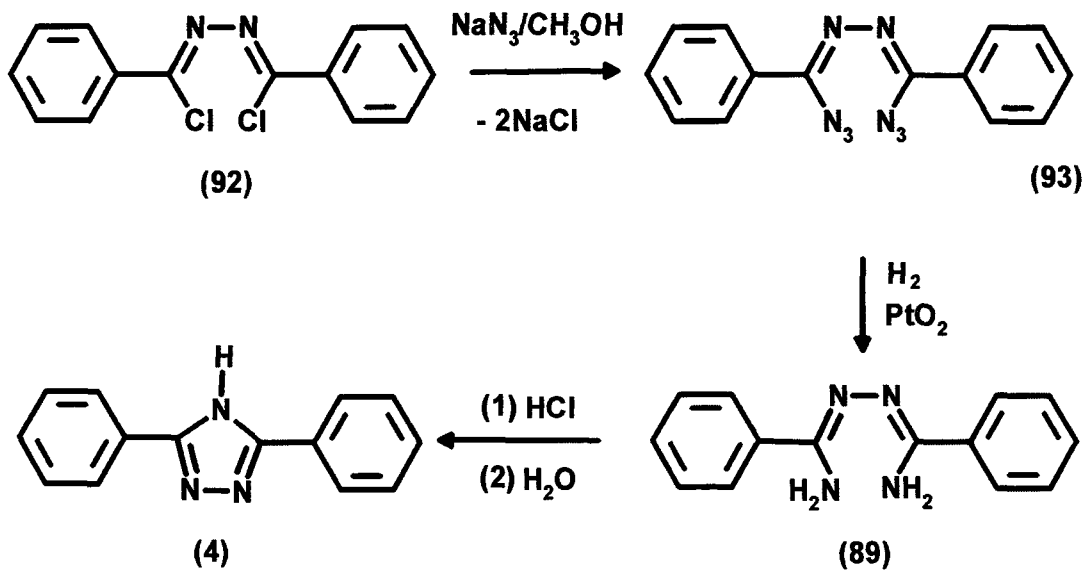

(92) **(93)** **(4)** **(89)**

Scheme [1.44]

The dibenzhydrazide dichloride **(92)** was firstly treated with sodium azide in methanol[78] which easily produced the diazide **(93)** with the loss of two NaCl molecules A reduction of the diazide with PtO_2 in the presence of H_2 produced the diamine[79] The ring closure step involves treatment of the diamine with acid This step ensures 1,2,4-triazole formation and is followed by addition of water to hydrolyse the amino-triazole causing the ammonia group to be cleaved as seen before

1,3-disubstituted nitrile imines generated from the aryl hydrazones of acyl halides by the action of triethylamine, react with hydrazones of aromatic aldehydes to form 2-arylidene-4-arylhydrazidines[80] as per Scheme [1 45]

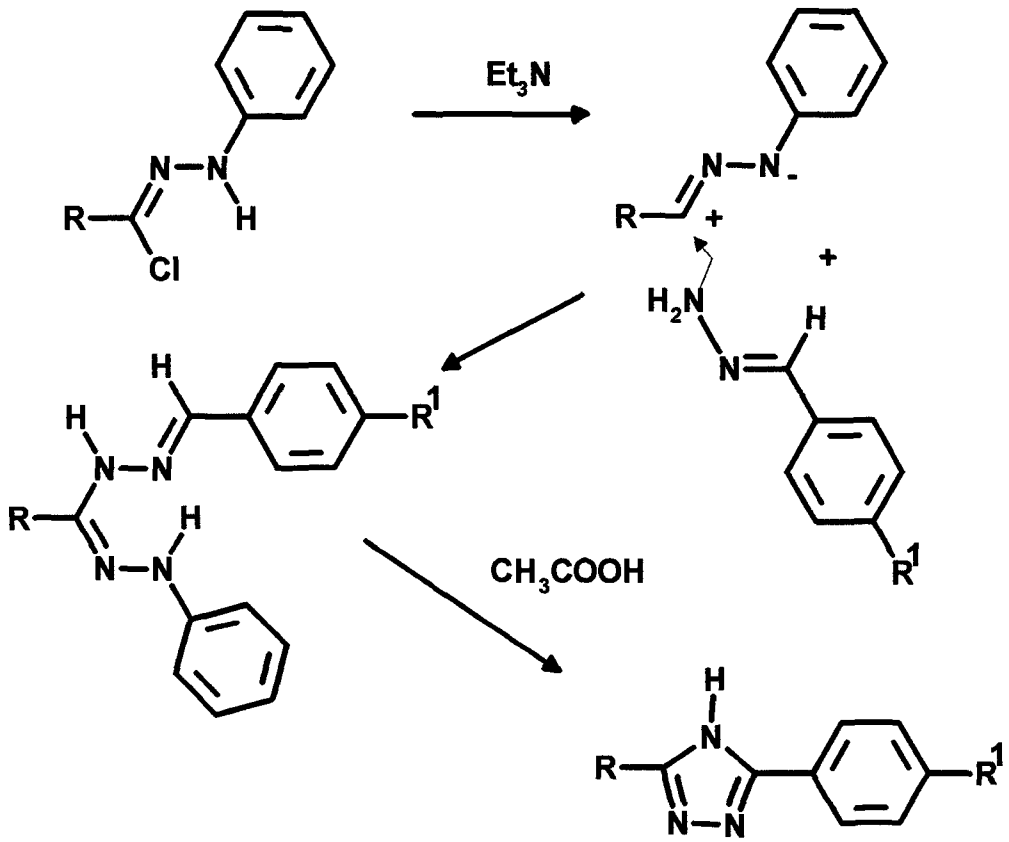

(4) R = Ph **R^1 = H**

(16) R = Ph **R^1 = 4-NO_2**

(94) R = 4Br-C_6H_4 **R^1 = H**

Scheme [1.45]

These dihydrazidines were converted to 1,2,4-triazoles in very high yields by refluxing in acetic acid For example in the synthesis of **(16)** in Scheme [1 46] the mechanism of the reaction may involve the initial formation of a dihydrotetrazine **(95)** This then rearranges to the 4-amino triazole **(96)** before eliminating 4-nitroaniline to give the 3,5-disubstituted triazole **(16)**

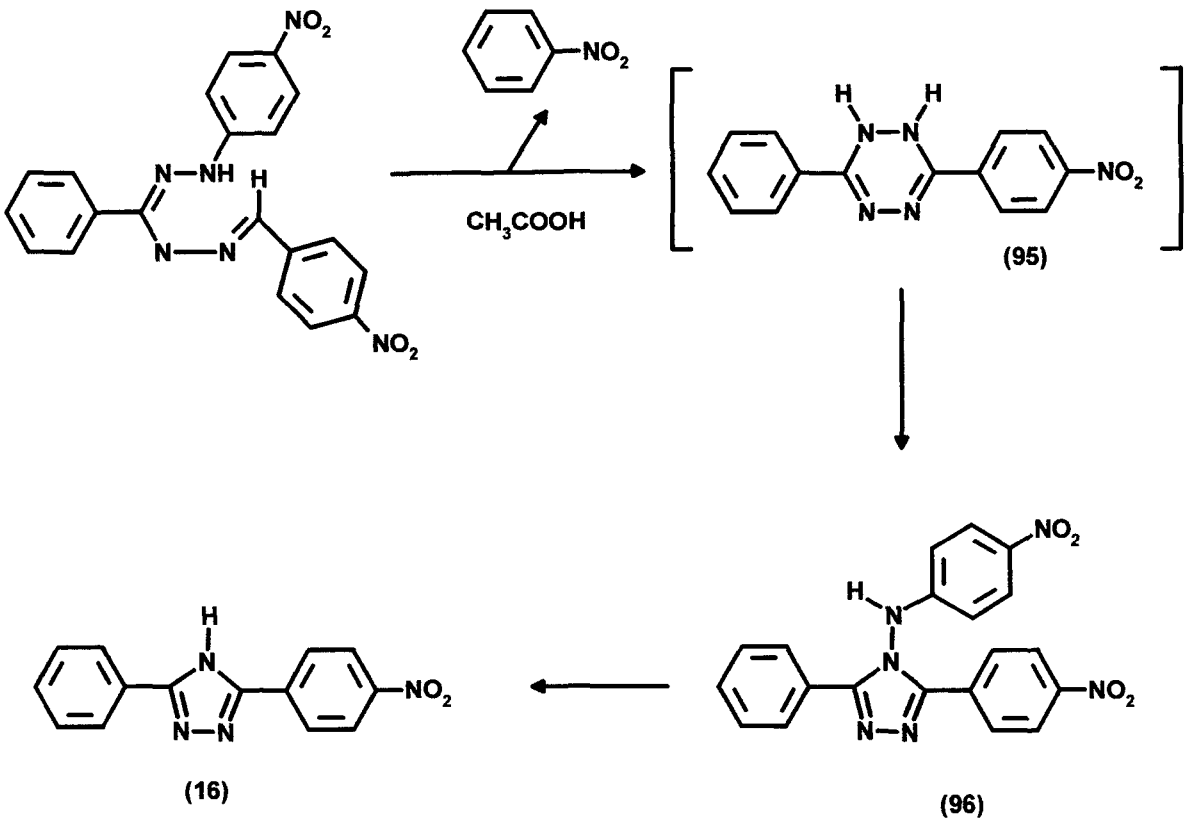

Scheme [1.46]

1.1.8 By-products of Triazole Preparation.

The cyclization of acylamidrazones in solution under basic conditions gives exclusively triazoles The basic conditions favour the elimination of a molecule of H_2O during the ring closure However, under acidic conditions the elimination of a molecule of ammonia occurs with the formation of an oxadiazole

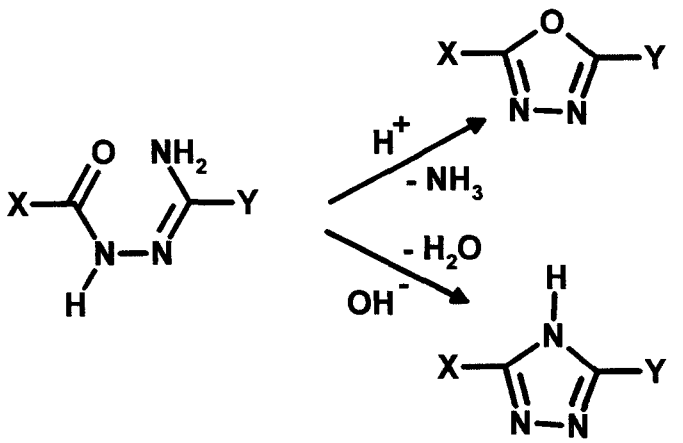

Scheme [1.47]

Eilingsfeld[81] investigated this cyclization reaction in some detail The reaction he used was the following (Scheme [1 48])

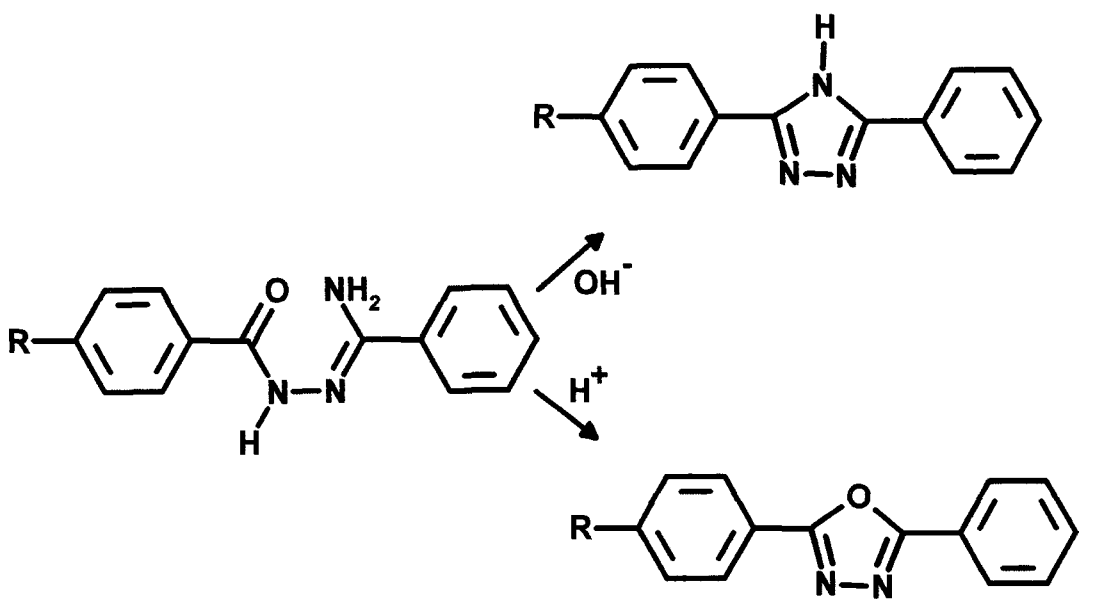

Scheme [1.48]

Three different R groups were used in order to see what effect, if any, they would have on the reaction

(a) R = an electron withdrawing group $-NO_2$,

(b) R =H,

(c) R = $-OCH_3$, an electron donating substituent

The cylization reaction was then carried out on the three acylamidrazones in reaction media varying from neutral through weakly acidic or basic and strongly acidic or basic Different combinations of *N*-methylpyrrolidine (NMP) and acetic acid provided neutral, weakly acidic and weakly basic conditions Acetic acid alone provided a more acidic medium and dichloroacetic acid, used alone produced an even more strongly acidic medium *N*-methylpyrrolidine used alone ensured a basic medium and a more strongly basic medium was achieved using pyridine The results are shown in Fig [1 1]

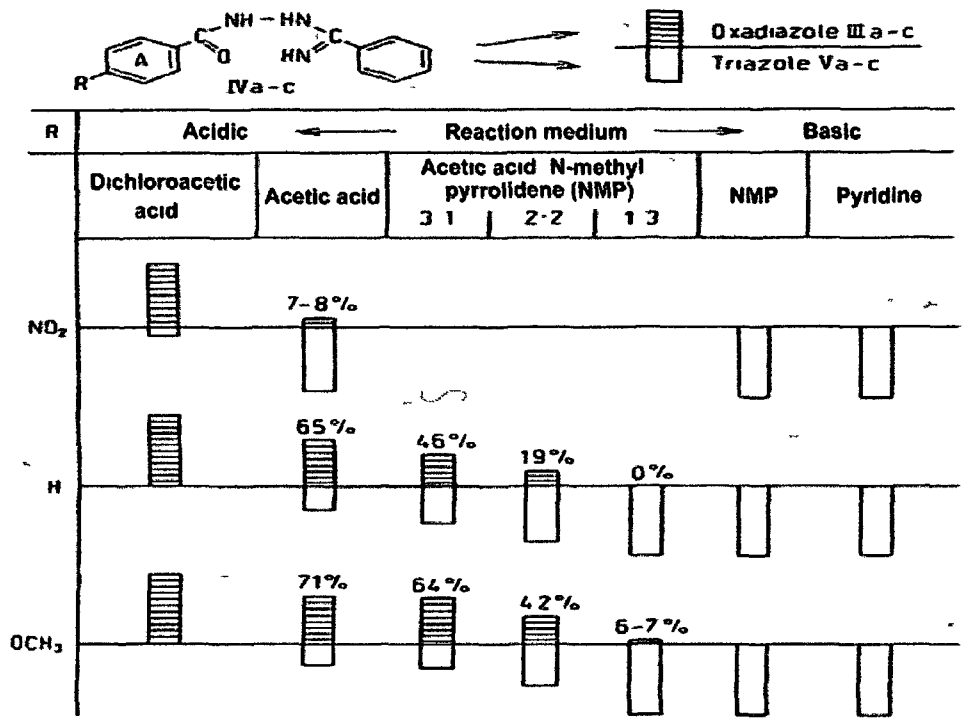

Fig. [1.1]

Where R=H, the ring closure occured in base regardless of strength of pH to give only 3,5-diphenyl-1,2,4-triazole In acetic acid, 65% oxadiazole was formed and in strongly acidic conditions only the oxadiazole was produced The presence of an electron withdrawing group, NO_2 on the ring in the *para*-position to the carbonyl group reduces the formation of oxadiazole in acetic acid from 65% to about 8% The NO_2 group effectively draws electron density away from the carbonyl group making that carbon more susceptible

to attack from the amine group. In a strongly acidic medium the effect of the electron withdrawing group is more or less negated with 90% oxadiazole production. On the other hand, when R is an electron donating group such as $-OCH_3$, oxadiazole formation is promoted. The presence of the methoxy group ensures more electron density around the carbonyl group which in turn promotes the carbonyl oxygen to attack as a nucleophile and close the ring to form an oxadiazole with the expulsion of ammonia. In acetic acid 71% oxadiazole is formed and in dichloroacetic acid the only product is oxadiazole.

Even when the N of the acylamidrazone is substituted, oxadiazole formation can occur in the presence of acid. In the case shown in Scheme [1.49], oxadiazole formation leads to the production of aniline.

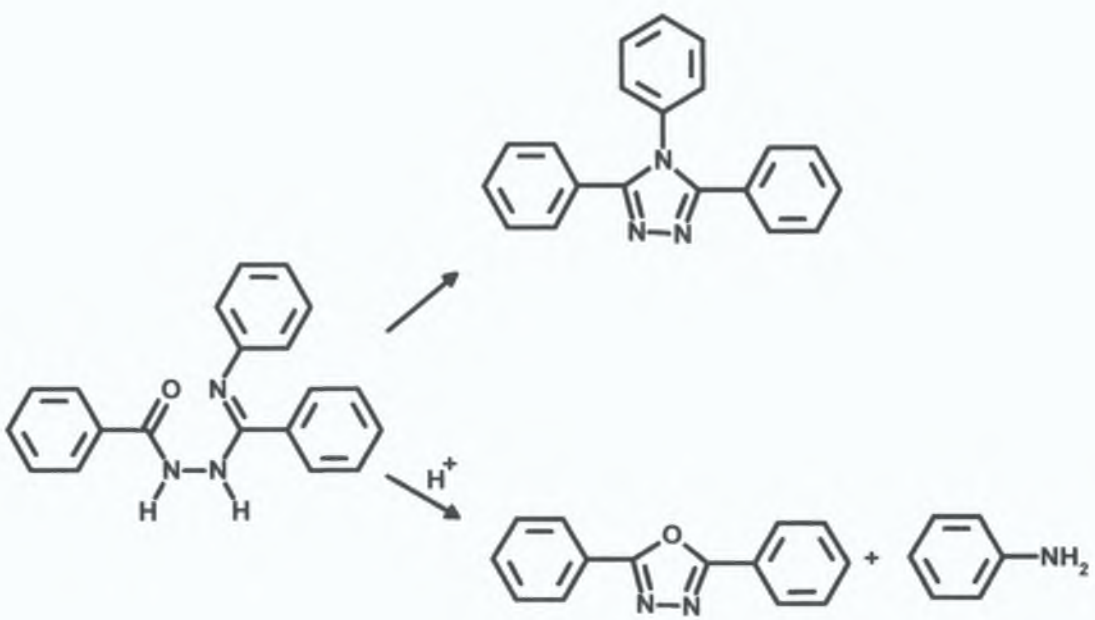

Scheme [1.49]

As we have seen, triazole preparation is often carried out via the preparation of an amidrazone. Geldard and Lions carried out an investigation on the by-products of this amidrazone reaction[82]. When 2-cyanopyridine and hydrazine hydrate are heated together under reflux as in Scheme [1.50], the product

was 3,6-di(2-pyridyl)-1,2-dihydro-1,2,4,5-tetrazine[83] **(97)** The reaction proceeds through the pyridine amidrazone (also known as picolinamhydrazone) intermediate which is isolable if the reaction is carried out at low temperatures This dihydrotetrazine can be rearranged to form the 3,5-di(2-pyridyl)-4-amino-1,2,4-triazole **(98)** In order to achieve this the dihydrotetrazine was suspended in aqueous 2 N HCl then boiled for 10 minutes On cooling and adding base, the amino-1,2,4-triazole precipitates

This amino triazole **(98)** can then, in turn, be converted to bi-pyridyl triazole **(8)** by dissolving the amino triazole in boiling nitric acid, cooling to 0°C, then adding aqueous sodium nitrite solution After stirring for 15 minutes and boiling for a further 5 minutes the bipyridyl triazole **(8)** precipitated on addition of 3 N ammonium hydroxide solution

The dihydrotetrazine **(97)**, has also been shown on treatment with nitrous acid to give one of two products depending on the pH of the reaction medium In most weakly acidic solutions[83] nitrous acid (or nitric acid with Raney Ni) oxidizes the dihydrotetrazine to 3,5-di(2-pyridyl)-1,2,4,5-tetrazine **(99)** In acidic media, nitrous acid converts the dihydrotetrazine to 2,5-di-(2-pyridyl)-1,3,4-oxadiazole **(100)** The reaction involved firstly dissolving the dihydrotetrazine in hot aqueous 2 N HCl then cooling to 0°C Then a solution of sodium nitrite in water was slowly added giving the solution a slightly purple colour The solution was boiled until colourless and made basic with sodium hydroxide The oxadiazole **(100)** could then be extracted from the reaction mixture into ether

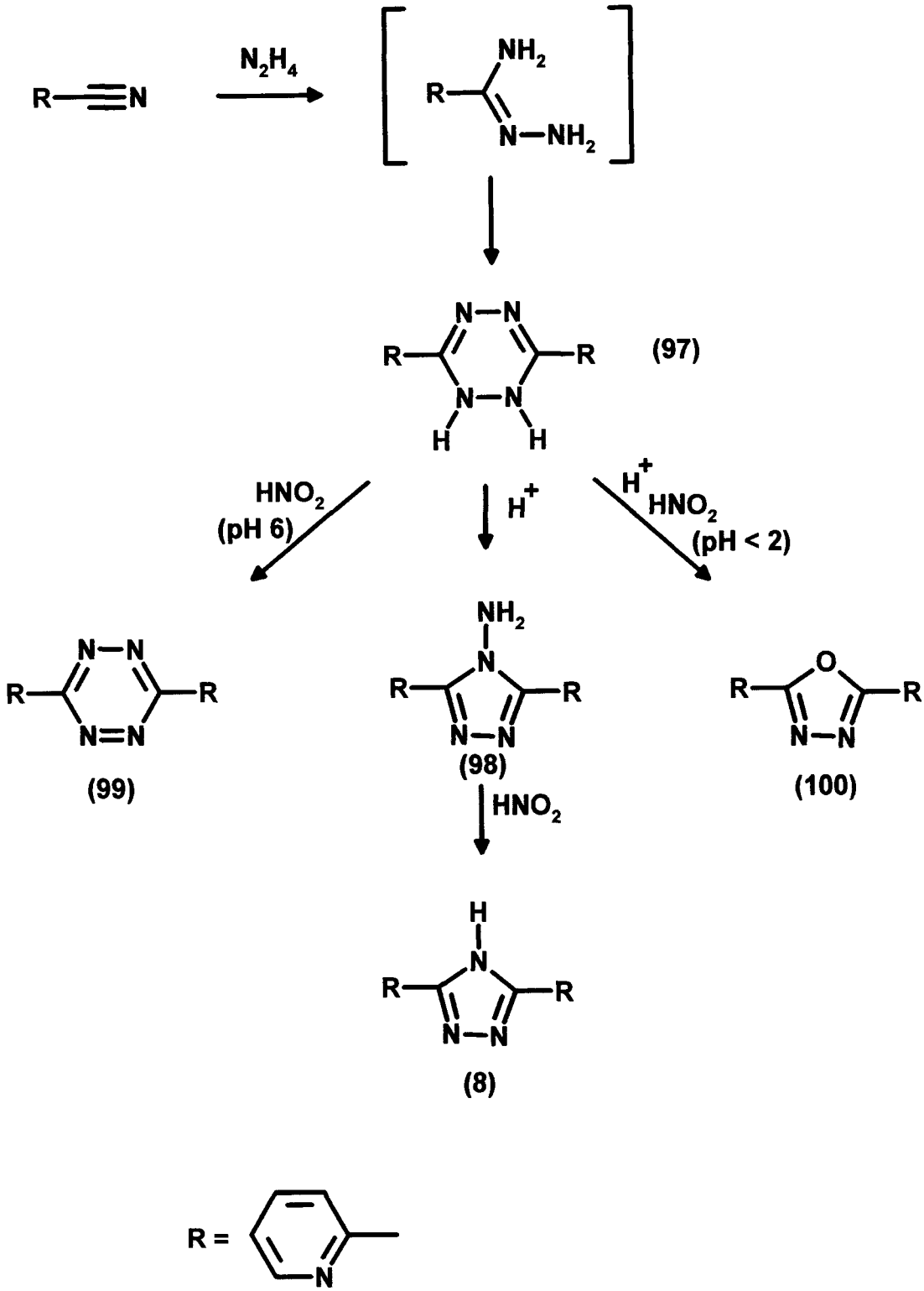

Scheme [1.50]

The conversion of the dihydrotetrazine **(97)** to the amino-triazole **(98)** and the oxadiazole **(100)**, both achieved by the action of acid, is thought to proceed via a common pathway[82]

We have already described that nitrous acid attack on the aminotriazole **(98)** results in the formation of bipyridyl-1,2,4-triazole **(8)** Thus we can say that during formation of the oxadiazole **(100)** the dihydrotetrazine **(97)** does not rearrange to the aminotriazole **(98)** A suggested mechanism is shown below

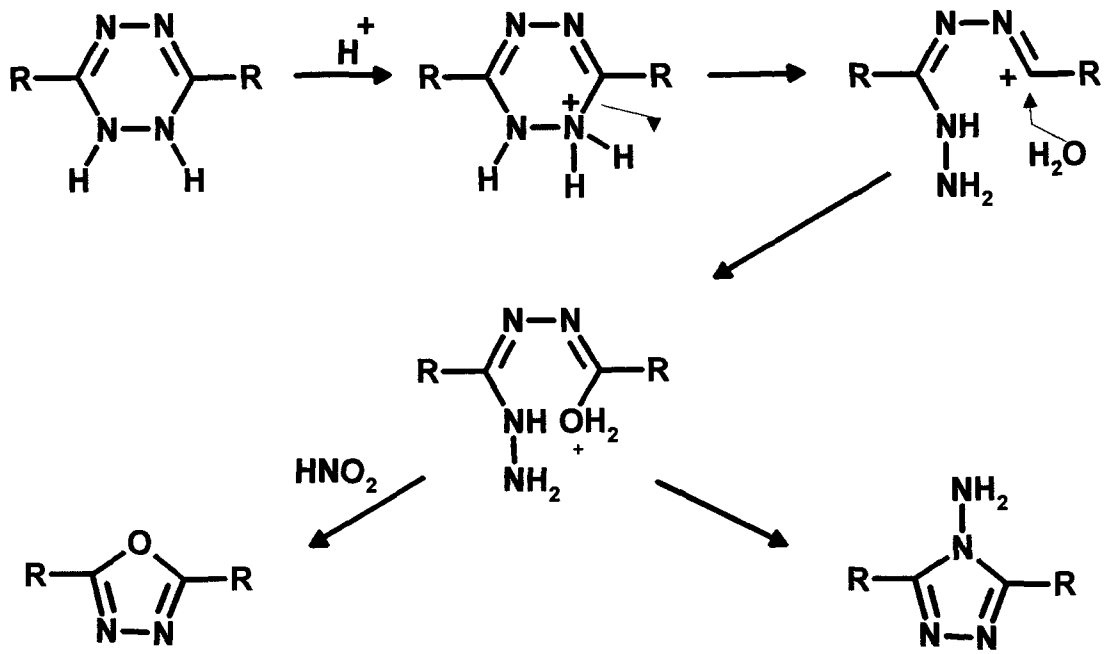

Scheme [1.51]

The dihydrotetrazines shown in Scheme [1 52] were formed by reaction of the amidinium chloride and hydrazine hydrate at reflux temperature[84] The addition of water to the cooled solution yielded the dihydrotetrazines

Preparation of the amino triazoles[85] from the dihydrotetrazines was achieved in this case by initially dissolving the dihydrotetrazines in dry methanol then passing dry HCl into the solution After 24 hours at 0°C the aminotriazoles were obtained on removal of the solvent by rotary evaporation The 4-aminotriazole, when treated with sodium nitrite then converts to the 4-H-triazoles.

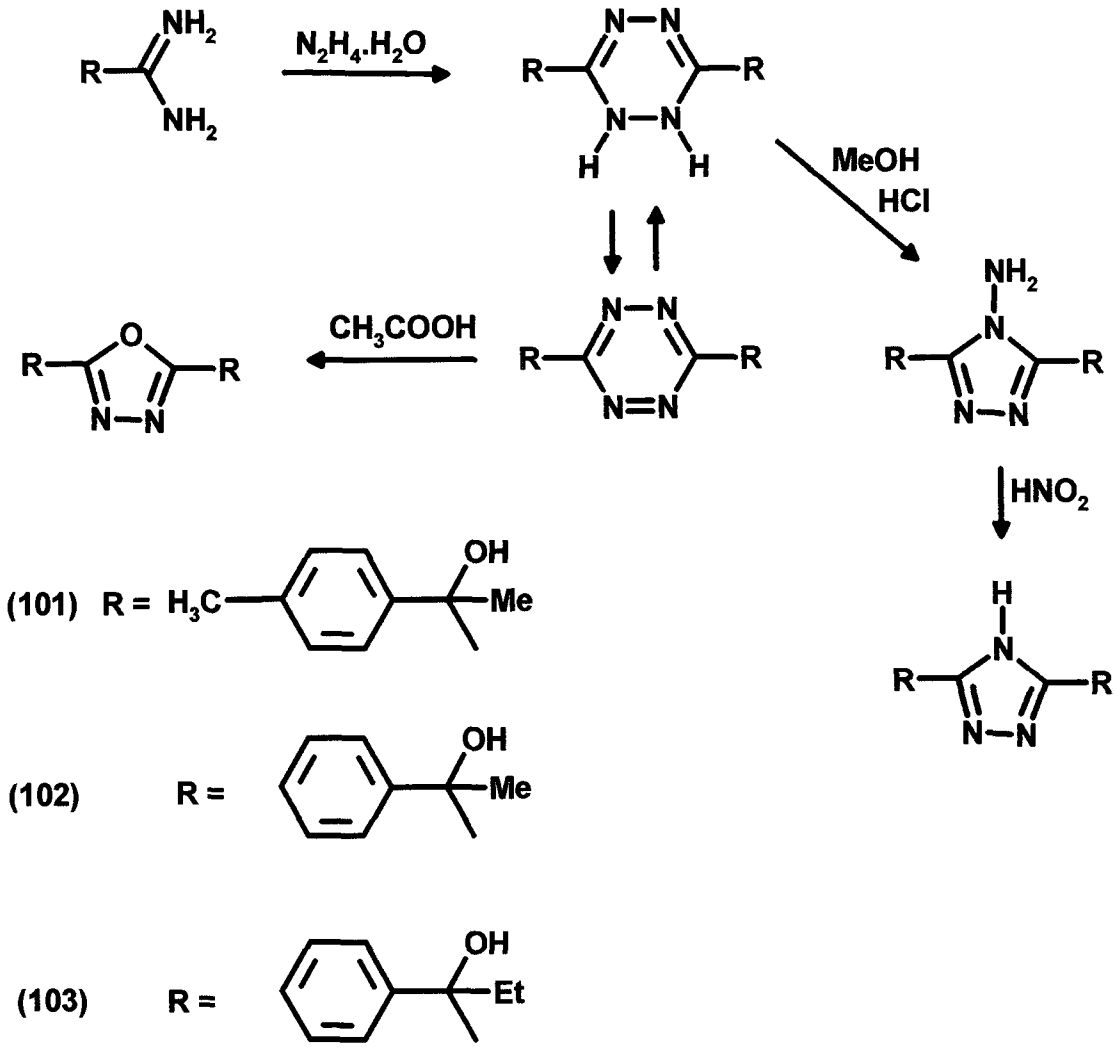

Scheme [1.52]

The dihydrotetrazines shown in Scheme [1 52] were again shown to form tetrazines by oxidation with nitrous acid However if the tetrazines were mixed with solid sodium dithionite[86,87,88] in aqueous ethanol until the red colour of the tetrazines disappeared, addition of water caused the dihydrotetrazines to be reformed In the previous reaction oxadiazole formation was achieved by heating the dihydrotetrazine in acidic media with nitrous acid Interestingly the oxadiazole in this case was formed from the tetrazine To the tetrazine was added peracetic acid buffered to p*H* 5 with sodium acetate and the mixture stirred at 50–60°C On disappearance of the red colour and addition of water the 1,3,4-oxadiazole was obtained

The formation of 3,6-di(2-pyridyl)-1,2-dihydro-1,2,4,5-tetrazine **(97)** by the reaction of cyanopyridine and hydrazine hydrate, posed two important questions, unanswered by Geldard and Lions[82]. It was not clear whether the molecule existed in the 1,2-dihydro form or as the 1,4-dihydro-*s*-tetrazine and secondly whether the pyridine N-atoms are *syn*- or *anti*- with respect to one other. The elucidation of the crystal structure by Caira *et al* [89](shown below) helped answer these questions.

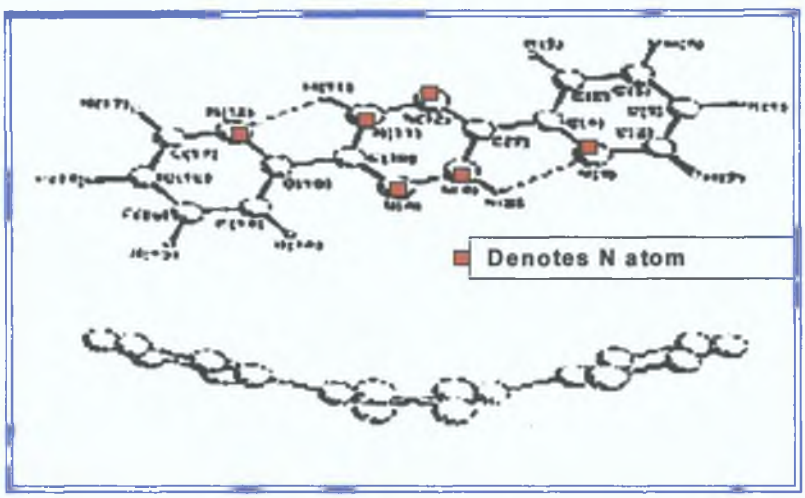

Fig. [1.2]: Molecular structure of 3,6-di(2-pyridyl)-1,2-dihydro-1,2,4,5-tetrazine (top) and edge-on view of the molecule (bottom) with H atoms omitted for clarity; as published by Caira *et al*[89].

From the structure[89] shown in Fig. [1.2], it can be seen that the molecule in the solid state exists in the 1,4-dihydro form with the pyridine N-atoms in the *anti*- configuration.

1.2 RESULTS AND DISCUSSION

1.2.1 Assessment of amidrazone preparation.

The preparation of hydrazidines of the general formula $RC(=NH)NH_2$ known throughout this work as "amidrazones" is a central step to the formation of triazoles Amidrazones can be formed by the action of hydrazine on a thioamide[90] or an imidoether[91]

In these reactions the thioamide or the imidoether need firstly be prepared from the corresponding nitrile Conversion of the nitrile to either of these forms allows easier attack by the hydrazine However, in the case of cyanopyridine and cyanopyrazine the amidrazones can be formed directly by the action of hydrazine on the nitrile As opposed to the reaction carried out by Geldard and Lions[82] involving cyanopyridine and hydrazine, this reaction is carried out at 20–40°C in ethanol over a period of approximately 12 h The amidrazone **(104)** when formed often precipitates as needles from the ethanol or precipitation can be easily induced by placing in a freezer overnight or by seeding Seeding with a tiny crystal of the product has been seen to produce spectacular crystal growth in seconds

While the yields from this reaction are ordinarily quantitative, invariably a small amount of the desired amidrazone remains in the mother liquor after work-up In co-operation with an undergraduate exchange student, Ms Nieves Payan[92], we investigated what other products, if any, would be obtained if the contents of the mother liquor were kept stirring over a period of time in the original reaction vessel

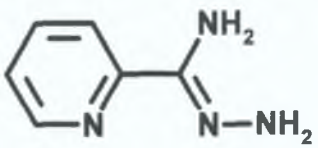

(104)

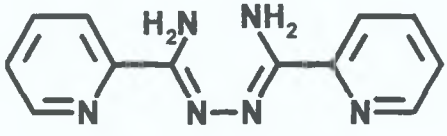

(105)

After approximately seven days stirring at room temperature a new product was detected by TLC and soon after precipitated from the solution. The bright yellow crystals obtained by filtration were found to be the 1,2-bis-imidoyl hydrazine **(105).** Ms Payan established the molecular structure of the crystal by X-ray crystallography with the help of Dr. Conor Long in DCU. (see Figs. 1.7 and 1.8). Approximately seven days later, another precipitate, this time bright orange crystals were seen to precipitate from the mother liquor. Again these were removed and analyzed. One suspected that this product was the corresponding dihydrotetrazine **(97)** described previously by Caira et al[89]. Questions such as: could this be the 1,2-dihydrotetrazine form, or was it the 1,4-form already described by Caira were very valid. It was even possible that this molecule was the tetrazine molecule with the protons removed. Ms Payan investigated the structure of the molecule by X-ray crystallography (again with the crystallographic work being carried out by Dr. Long) and found it to be that already reported by Caira, the 1,4-dihyro-tetrazine molecule shown in fig.1.2. Interestingly, while this crystal structure has been published in the literature, the X-ray crystal structure of the bis-hydrazine **(105)** has not been reported. These results are thus of some importance in deducing the pattern of by-product formation in the amidrazone reaction. Note: It was requested by Ms Payans research supervisor, Prof. Vos, that the above mentioned crystal structures obtained by Ms Payan be included in this thesis.

We have discussed the work carried out by Geldard and Lions[82] with respect to the by-products obtained in the 2-pyridyl amidrazone **(104)** synthesis. It is very apparent (in practise) in the synthetic laboratory that the amount of heat applied to a reaction involving **(104)** determines the type of product or

products obtained In general carrying out a reaction using **(104)** at room temperature is the best method of ensuring the reaction proceeds in the desired way If a small amount of heat is needed to drive the reaction, then the chance of self condensation of **(104)** increases, often resulting in the formation of tetrazines and dihydrazines If **(104)** is heated to high temperatures (approx 200°C) in a melt or a high boiling solvent one can expect one of the many by-products of the reaction to be bipyridyl-1,2,4-triazole **(8)**

An established old method for the production of bi-pyridyl triazole involved initially refluxing cyanopyridine and sodium methoxide for 1 h Hydrazine was then added and again reflux continued The methanol solvent must then be replaced with a high boiling solvent such as ethylene glycol to complete the reaction The initial addition of sodium methoxide leads to the formation of an iminoether, for example that shown below

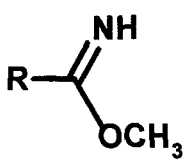

The addition of hydrazine causes some of the iminoether molecules to form amidrazone molecules, which can then react with unchanged iminoether molecules to give the diamine product as in Scheme [1 53]

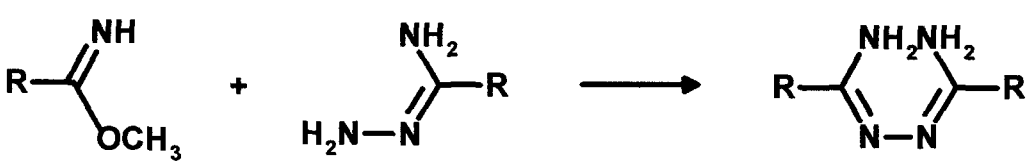

Scheme [1.53]

Heating causes the ring closure reaction with elimination of ammonia Hage's[93] method of bipyridyl triazole **(8)** formation involved initially forming a tetrazine, which was subsequently converted to the corresponding 4-amino

triazole **(98)** and finally to **(8)** using standard methods as shown in Scheme [1 54] The method of heating 2-pyridyl amidrazone **(104)** described above has the problems of by-product formation and of only being useful for simple symmetric triazole synthesis

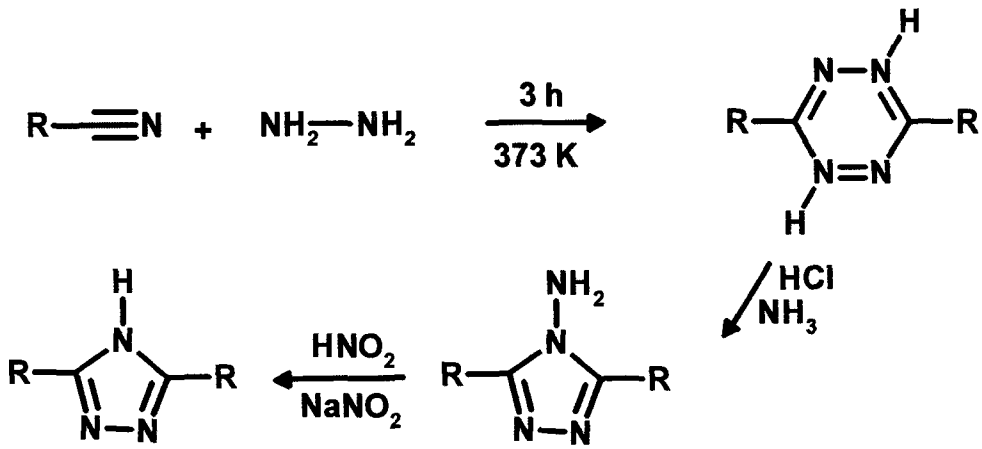

Scheme [1.53]

Following the procedures described by Hergenrother (which will be discussed and referenced in chapter 2) were found to be the best overall synthetic procedure for triazole production Only by using relatively low temperatures when reacting amidrazones with acid chlorides and having the ability to isolate the acylamidrazone formed can one control the formation of the finished triazole

The initial investigation of this report had a number of aims

1 To establish the best possible procedure for the production of the "target" triazole
2 To identify the pitfalls associated with the reaction, i e the areas where yields are not as expected or the reasons for by-product production
3 To form a number of mono- and bis- triazoles by our chosen reaction method to serve as model compounds to validate our final "target" synthesis

4 To become familiar with the spectroscopic techniques best suited to the analysis of these triazoles

1.2.2 Model Compound Formation.

Having reviewed the formation of amidrazones attention was focused on the reaction of 2-pyridyl amidrazone **(104)** and benzoyl chloride The reaction proceeded to the acylamidrazone **(110)** as shown below

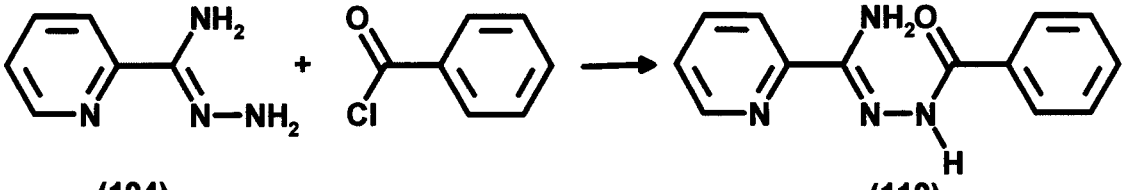

(104) **(110)**

Scheme [1.55]

The danger of dimerisation of the amidrazone can easily be monitored in this case by NMR, due to benzyl and pyridyl peaks appearing at different chemical shifts on the spectrum The addition was found to be best carried in dry DCM, a low boiling solvent Heating the product **(110)** to a temperature slightly above its melting point (~220°C) in the absence of solvent shown in scheme [1 56], in a boiling tube under vacuum caused formation of the corresponding oxadiazole **(111)** to form

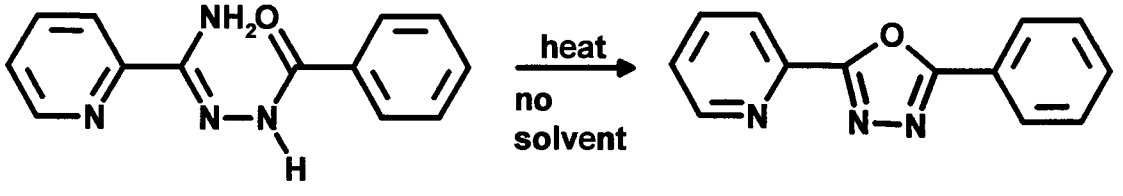

(110) **(111)**

Scheme [1.56]

This simple method produced fine white crystals of **(111)**, which crystallized in a cooler part of the tube Removal was facile using a spatula, no solvent had been involved However, heating the triazole in a high boiling solvent such as ethylene glycol resulted in the formation of the corresponding 1,2,4-triazole One of the disadvantages of using this solvent however is that its excellent solvating properties often result in low yields of product being obtained The addition of acetone to the ethylene glycol solution often aids in further product precipitation Another method of increasing yields involves reducing the volume of solvent, which with ethylene glycol is tedious and in many cases the prolonged heating required destroys the product

The merits of the use of ethylene glycol far outweigh the disadvantages, however Acylamidrazones and triazoles, especially those containing aryl- or hetero-aryl substituents are notorious for their inability to dissolve in common organic solvents Ethylene glycol dissolves acylamidrazones at high temperatures allowing them to cyclize with prolonged heating On cooling, the solvating power of the solvent is such that in general only the triazole precipitates from the solution Given that we have described the many by-products that can form during the synthesis, this selective precipitation of the triazole is very helpful

The cyclization reaction itself is a somewhat subjective operation in that the time required for the heating of an acylamidrazone in ethylene glycol until the triazole is formed varies dramatically A few points to note based on experience of the reaction may be useful

1 In general the larger the molecule (i e the higher the molecular mass) to be cyclized, the longer the heating time required
2 Carrying out a purification of the acylamidrazone immediately before the reaction results in shorter heating times being required This purification can often be achieved by heating the acylamidrazone in DMSO If the

acylamidrazone dissolves in this solvent with heating, a recrystallization can be carried out If the acylamidrazone does not dissolve, stirring in hot DMSO often serves to dissolve unwanted impurities leaving the pure product as a solid

3 As cyclization takes place, a colour change can be observed in the reaction vessel This is difficult to see in the clear solution but experience shows that the reaction is complete when the solution turns a slightly darker colour

4 Termination of the reaction soon after the colour change is observed resulted in the highest yields of triazoles being formed Heating longer than necessary results in lower yields probably because of by-product formation

An interfacial method was used to form the acylamidrazone described above Benzoyl chloride in chloroform was added rapidly to a vigorously stirred solution of pyridine amidrazone **(104)** and sodium carbonate in water The yellow solid acylamidrazone began to precipitate immediately

The alternative method of acylamidrazone **(110)** production involved the addition of benzoyl chloride in DCM to the amidrazone in DCM While the product is seen to precipitate immediately, continued stirring after addition is often required to bring reaction to completion and maximize yields
Having successfully produced these mono-triazoles we then focussed on the synthesis of bis-triazoles Terephthaloyl dichloride **(106)** was reacted with pyridine amidrazone **(104)** to firstly produce the acylamidrazone **(107)** which was then cyclized to form either the corresponding triazole **(108)** or oxadiazole **(109)** as in scheme [1 57] If the cyclization is carried out in ethylene glycol, only the triazole will precipitate from the solution avoiding mixtures Similarly only the oxadiazole is obtained on heating the acylamidrazone in a sublimation tube in the absence of a solvent

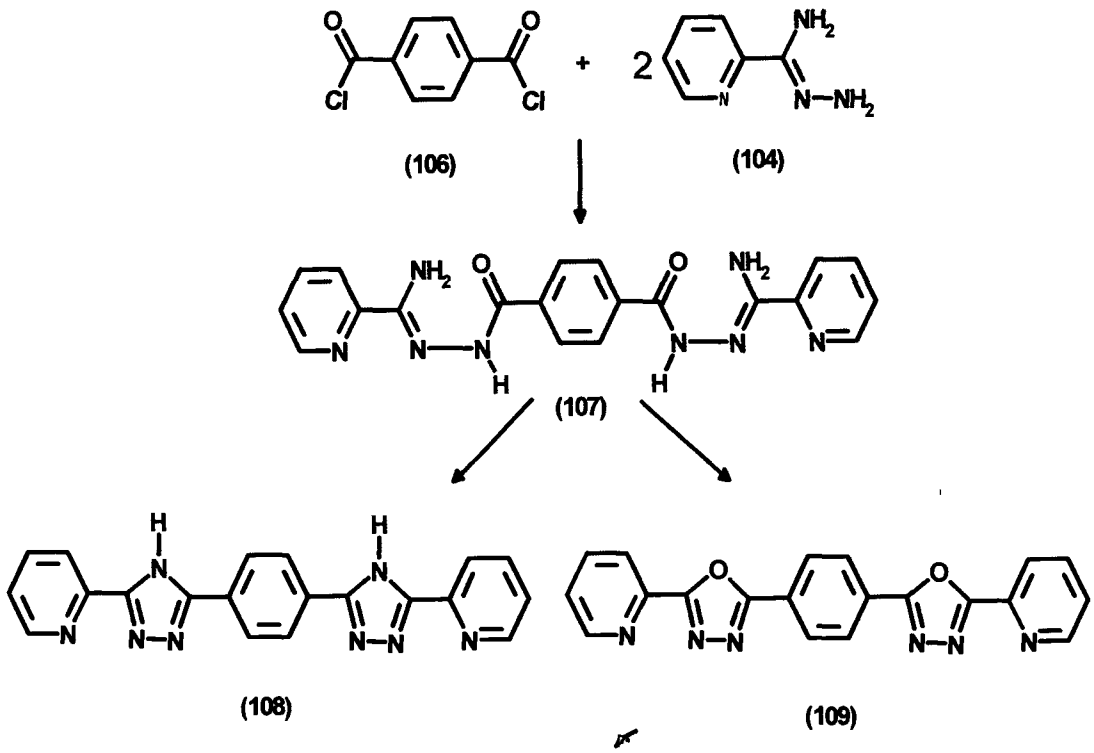

Scheme [1.57]

The bis-triazole **(108)** was formed in high yield using the same general procedure as described for mono-triazoles The milky yellow acylamidrazone **(107)** isloated in the reaction was a larger sized molecule to any previously prepared models and as such exhibited different properties
Whilst DCM was the solvent of choice for earlier model formation it was not suitable in this case Dry DMAC was also tested as a possible solvent but was not practically useful Dry THF however was found to be perfectly suited to this reaction The acid chloride and the amidrazone were soluble in THF while the acylamidrazone was not THF was adopted as the solvent of choice for all further large acylamidrazone preparation

One work-up procedural change is needed when THF is the solvent Whereas in general water is added to the reaction vessel at the end of the reaction to dissolve unwanted sodium carbonate and unreacted starting materials, when THF is used the solvent must firstly be completely removed by vacuum filtration before the product is stirred in water to dissolve

impurities. When THF and water mix in the reaction vessel the resultant solvent mixture can be extremely difficult to filter and dry.

In a similar experiment to that just described isophthaloyl and phthaloyl dichloride (which are similar to the diacid chloride **(106)** except that the acid chloride groups are *ortho*- to each other in one case and *meta*- to each other in the other) were reacted with pyridine amidrazone **(104)**. No acylamidrazones were formed in either case. This may be due to the sterically unfavourable situation which would exist in the product. Acylamidrazones were always well dried before further reaction. An effective method of drying uses phosphorous pentoxide as drying agent in a Kugelrohr oven at 90°C under vacuum.

1.2.3 ^{1}H-NMR Analysis of Model Ligands.

The elucidation of acylamidrazones and triazoles has been carried out throughout this work by extensive use of ^{1}H-NMR spectroscopy and 2-D experiments. ^{13}C experiments were carried out where possible but such is the nature of acylamidrazones and triazoles that dissolution problems in deuterated solvents often hindered this technique. Since only 1.1% of naturally occurring carbon consists of ^{13}C the sensitivity is much lower. Fourier transform NMR and signal averaging is essential for the detection of ^{13}C, but even so, these experiments require up to ten times the sample quantity that a ^{1}H- NMR would require. While it is possible to get small quantities of acylamidrazones and triazoles to dissolve in DMSO-d^{6} (the best NMR solvent for these compounds) larger amounts precipitate from solution very quickly making ^{13}C analysis very difficult.

COSY is a two dimensional NMR experiment that produces a map rather than a spectrum. In the H,H-COSY experiment both axes correspond to proton chemical shifts. The central map contains contours which represent intensity. The idea of a two-dimensional experiment is to identify nuclei that are

engaged in some kind of interaction by mapping out their inter-relationships directly.

Examination of the COSY of the model acylamidrazone **(110),** shown in Fig. 1.4, shows that there are two types of peak: those peaks running along the diagonal of the spectrum which have the same shift in each frequency dimension and others known as cross-peaks which have different shifts in each dimension. These cross-peaks provide the interaction information in the spectrum. Along the axis of the COSY is the one dimensional proton spectrum of the sample. This axis serves as a reference from which assignments are made. Each multiplet has a corresponding signal along the diagonal of the central map. The arrow in the top left hand corner of the spectrum points to the contour of the most upfield doublet. By then following the arrows across one finds signals that are coupled to the starting contour in square patterns.Thus if the assignment of one reference is known, then by orienteering a path through the spin system by systematically examining each contour along the diagonal and its corresponding cross-peaks one can easily identify related peaks.

As can be seen in some of the more complicated COSY's presented in this work it is possible to identify signals of coupling partners even when they are hidden in complex multiplet patterns in the normal ^{1}H-NMR spectrum. A crowded spectrum often produces a well resolved COSY with easily identifiable cross-peaks because it makes use of the large mapping area available. Finally a COSY experiment takes a relatively short time and the problem of precipitation of samples is not as much an encumbrance as with other time consuming experiments.

1-Phenyl-4-(pyridin-2-yl)-acylamidrazone **(110)** shown here with pyridine and phenyl protons numbered, served as a model compound to aid in establishing the expected chemical shift pattern of such proton signals in the NMR spectrum.

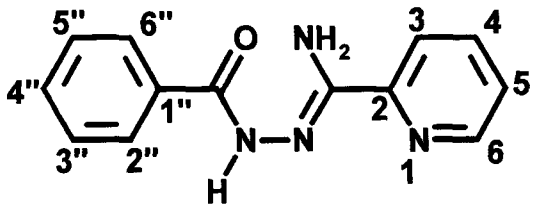

(110)

The ^{1}H-NMR spectrum shown below shows two broad singlets shifted downfield and a number of aromatic multiplets in the 7 5–9 ppm region of the spectrum The broad singlet at 11 54 ppm corresponds to the –NH proton This proton lies in an area where there is a strong anisotropic effect (i e molecules in close proximity spatially, experience a deshielding effect) from the nearby carbonyl group which has a deshielding effect on the proton nucleus resulting in their appearance this far downfield The $-NH_2$ protons also appear downfield at 10 18 ppm They are affected to a lesser extent by the deshielding effects of its neighbours Hydrogen bonding of the $-NH_2$ protons to the nearby carbonyl group may also contribute to its downfield shift The broad appearance of peaks denoting protons bound to N atoms is a characteristic feature of such protons One of the reasons attributed to this broadening is chemical "exchange" effects which can occur between N–H and water in the solvent Protons bonded to nitrogen or oxygen can exchange with water in a solvent This exchange can have the effect of "pulling" the shifts of acidic protons to lower chemical shifts and if exchange does not occur quickly enough for complete averaging, resonances involved may be broadened This exchange is effected by changes in solvent and the amount of dissolved water therein, temperature changes and purity of the sample and solvent

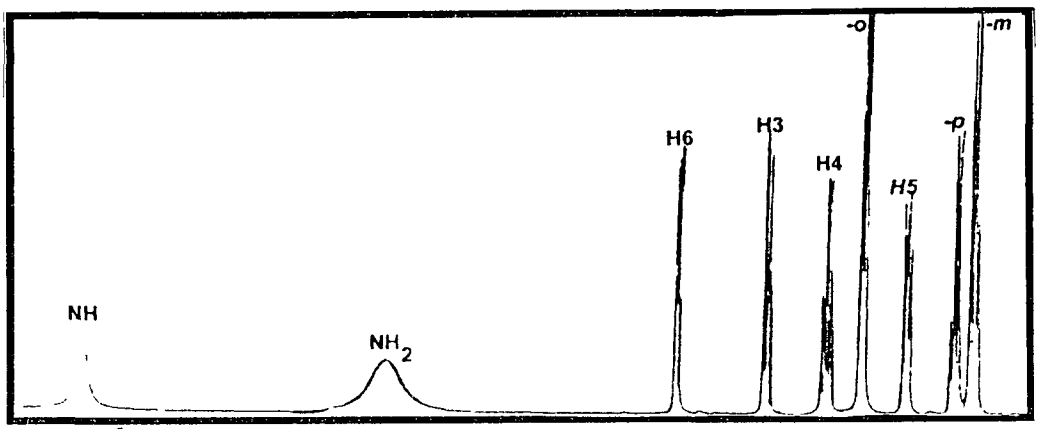

Fig. [1.3]: ^{1}H-NMR spectrum of model acylamidrazone **(110).** Solvent DMSO-d^6

*No scale is available for the above spectrum (due to a plotter error)

In the case of acylamidrazones and triazoles, the most useful solvent for their dissolution is DMSO-d^6 Heating is often required to dissolve samples in the solvent This, coupled to the fact that DMSO boils at a relatively high temperature (compared to H_2O) mean that NMR experiments of this nature may be carried out at higher temperatures than normal This heat contributes to greater molecular vibration within the sample helping to reduce broadening effects

Switching attention to the aromatic region of the spectrum it is important to elucidate the general chemical shifts of the phenyl and pyridyl protons of the acylamidrazone In this case a COSY experiment is useful The COSY map for this molecule is shown in fig 1 4 The furthest downfield doublet corresponds to a pyridyl proton, which is seen to couple to three other protons It is reasonable to assign this doublet to H^6, the proton two bonds away from the more electronegative (and more deshielding) N atom of the pyridine ring Using the cross-peaks of the COSY, H^5, which is coupled to H^6, can be identified as the furthest upfield pyridyl proton at 7 84 ppm by the intensity of its contours on the map This is denoted by two "x" marks on the COSY shown In this way the four pyridyl peaks are assigned starting from the furthest downfield and moving up as H^6 (doublet), H^3 (doublet), H^4 (multiplet), H^5 (multiplet) The phenyl peaks can be assigned in the same way A line of symmetry is present along the molecules central aromatic ring

causing $H^{2'}$ and $H^{6'}$ (the protons in the *ortho-* position) to be equivalent as are $H^{3'}$ and $H^{5'}$ (the protons in the *meta-* position). The inductive effect of the carbonyl group causes $H^{2'}$ and $H^{6'}$ peaks to be shifted downfield. The anomalous nature of π-electrons circulating in response to the applied magnetic field results in $H^{4'}$ (the *–para* proton) appearing more deshielded than $H^{3'}$ and $H^{5'}$.

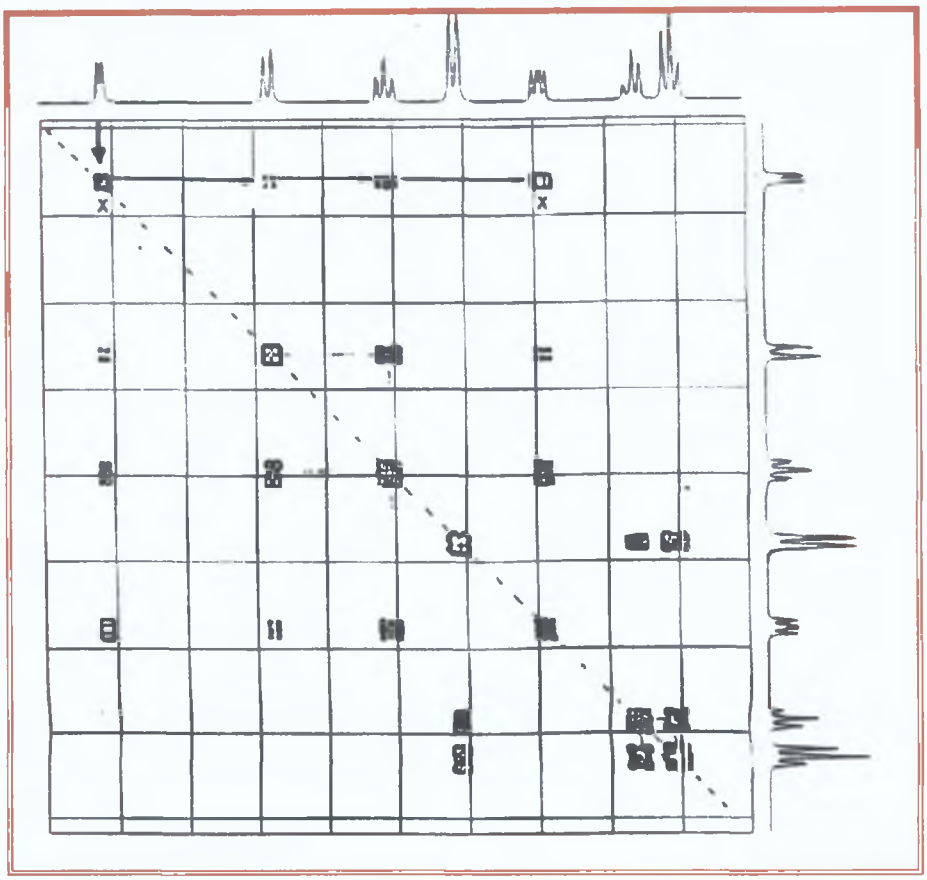

Fig. [1.4]: COSY spectrum of model acylamidrazone **(110)***.

*No scale was printed on the COSY above.

One dimensional ^{1}H-NMR spectroscopy, in most cases provides enough information in terms of chemical shift, integration and splitting to allow peak and structure assignment. The COSY spectrum is a valuable tool in the elucidation of unfamiliar spectra, in cases where peak splitting cannot be seen (peak averaging occurs) and in instances where complex peak patterns need to be elucidated.

Thermal cyclization of **(110)** results in the formation of 3(pyridin-2-yl)-5-phenyl-1,2,4-triazole **(20)**. The N–H proton signal of the protonated triazole is observed at 14.82 ppm. This proton is not localized and tautomeric forms of this triazole do exist. X-ray crystallography studies carried out on triazoles show that the position of the proton on the triazole ring varies and is unpredictable. From an NMR point of view, it suffices to say this delocalization of the triazole proton coupled with the rapid exchange of the proton leads to the characteristic appearance of much broadened triazolic N–H proton signals at very low fields. The spectrum shown below is typical of a disubstituted 1,2,4-triazole.

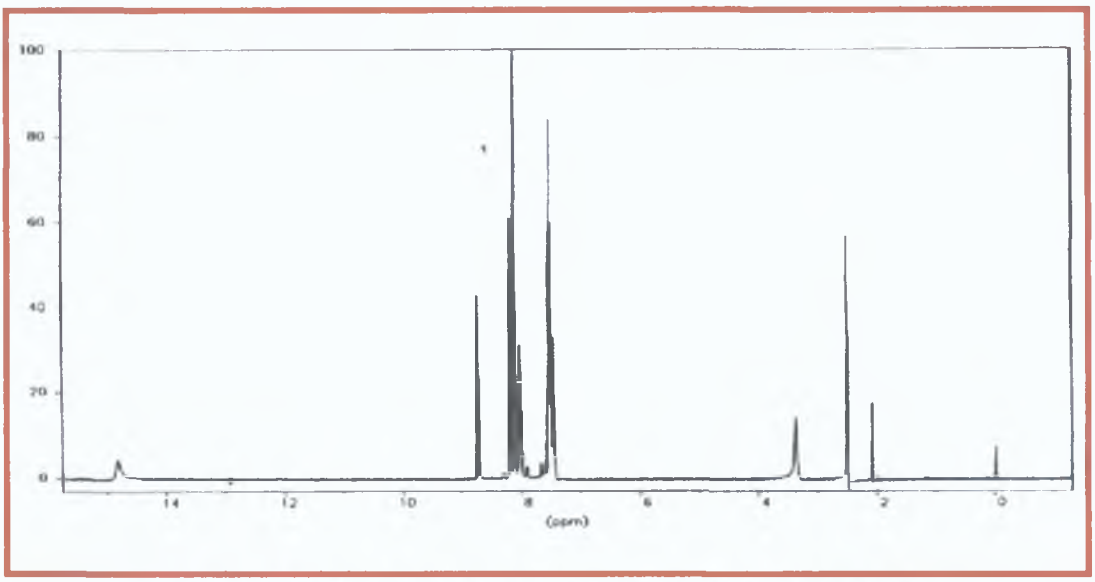

Fig. [1.5]: ^{1}H-NMR of model triazole **(20)**. DMSO-d^{6}

Comparing the ^{1}H- NMR spectrum of 3(pyridin-2-yl)-5-phenyl 1,2,4-triazole **(20)** and its corresponding 1,3,4-oxadizole **(111)**, the oxadiazole ring seems to have an overall more inductive effect than the triazole.

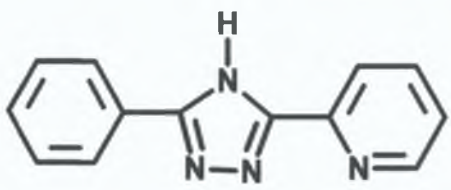

(20)

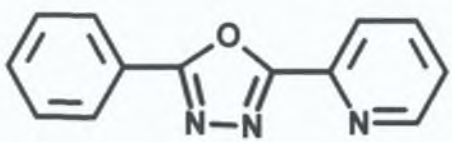

(111)

It appears to act as a sink for electron density, effectively deshielding the pyridine- and to an extent the phenyl ring on either side The phenyl signals are all shifted downfield while the H^3 signal of the pyridine is also pulled downfield possibly due to intra- and inter-molecular H-bonding with the ring oxygen

Having obtained the general knowledge required to assign acylamidrazone and triazole spectra the ^{1}H-NMR spectrum of the acylamidrazone, 1,4-bis(acyl-pyridin-2-yl-amidrazone)-benzene **(107)** was studied The spectrum differs from that of 1-phenyl-4-pyridin-2-yl acylamidrazone **(110)** in a number of respects, most notable of which is that **(107)** is symmetrical around the central benzene As such, only one of each symmetrical set of protons is seen This symmetry causes the protons of the central benzene to be equivalent and appear in the spectrum as a singlet The N–H peak has shifted upfield from 11 55 ppm to 10 36 ppm The benzene peak signal is also shifted upfield as are the pyridine peaks The $-NH_2$ signal which appeared in the smaller acylamidrazone **(110)** at 10 18 ppm now appears at 8 05 ppm A very significant upfield shift has occurred One can only postulate that the reason for this deviation is that the $-NH_2$ in this case is not as deshielded by H-bonding as in the earlier case or that chemical exchange effects which may have previously caused the $-NH_2$ signal to be brought downfield, in this case are not prevalent

Shown below are the spectra of the acylamidrazone **(107)** and its corresponding triazole **(108)** The spectrum of the triazole has very similar chemical shift values to those of 1-phenyl-4-(pyridin-2-yl)-1,2,4-triazole **(20)** shown earlier

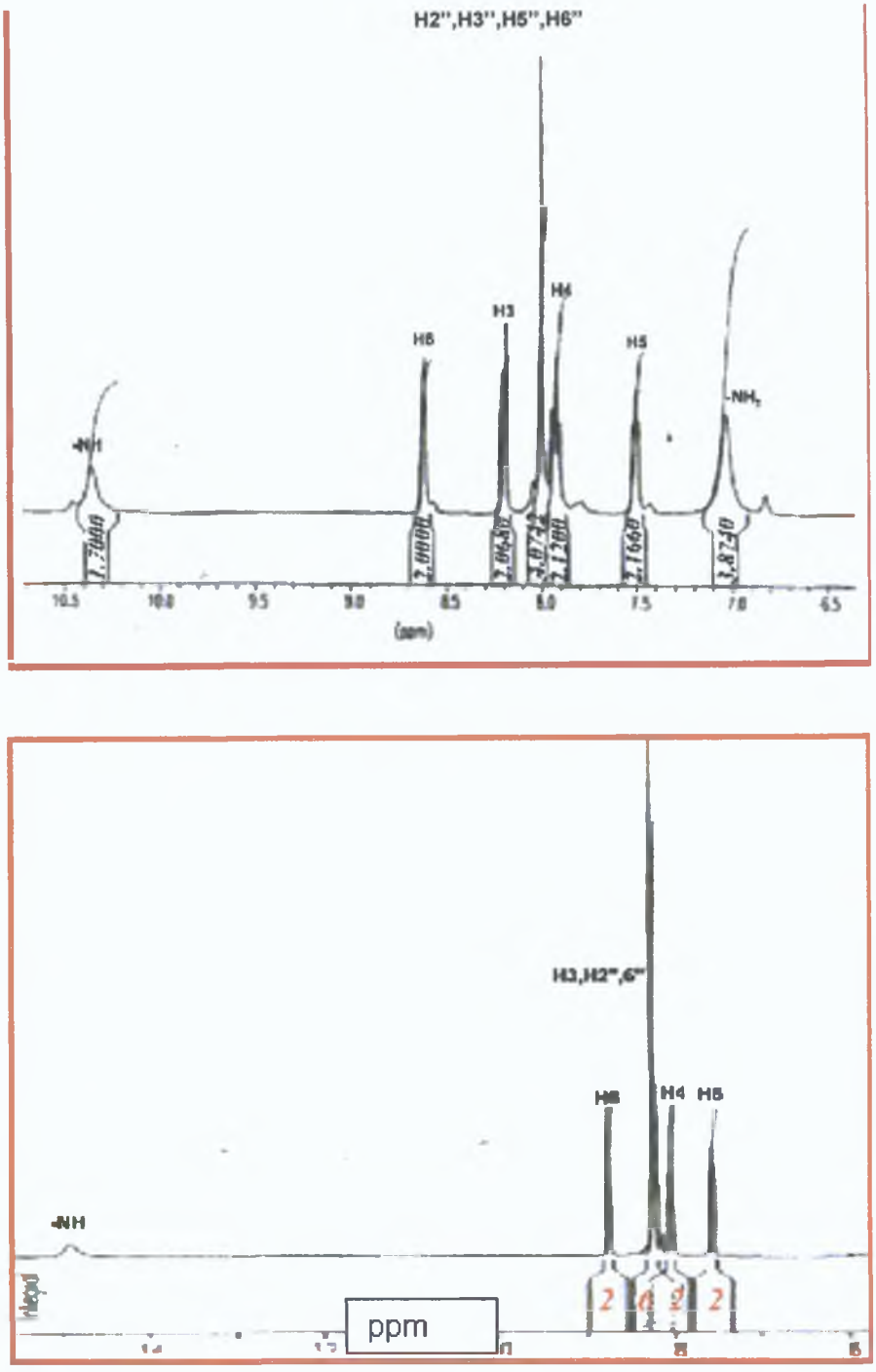

Fig. [1.6]: ^{1}H-NMR spectra of model acylamidrazone **(107)** (top) and triazole **(108)** (bottom).

1.2.4 Description of X-ray Structures.

1.2.4.1 Bi-2-pyridyl-bis-imidoylhydrazine. $C_{12}H_{12}N_6$ (105)

Note This crystal structure was obtained by Ms Nieves Payan[92], with the help of crystallographer Dr Conor Long (DCU) Note It was requested by Ms Payans research supervisor, Prof Vos, that this crystal structure be included in this thesis

Fig [1 7] shows a crystal structure of the molecule with atomic numbering shown Bond distances and angles are presented in Table [1 1] A complete list of distances, angles and further data can be found in the appendix The arrangement of the molecules in the unit cell is presented in Fig [1 8] The crystal used for analysis had dimensions 0 5x0 6x0 5 mm and was formed by slow recrystallization from an ethanol solution The crystal was found to be orthorhombic with space group *Pcab*

Bond distances (*Angstroms*)			
Bond	**Dist.**	**Bond**	**Dist.**
N(1)–C(1)	1 338(2)	C(1)–C(6)	1 490(2)
N(1)–C(5)	1 341(2)	C(2)–C(3)	1 377(2)
N(2)–C(6)	1 347(2)	C(3)–C(4)	1 372(3)
N(3)–C(6)	1 299(2)	C(4)–C(5)	1 363(3)
N(3)–N(4)	1 406(2)	C(7)–C(8)	1 485(2)
N(4)–C(7)	1 303(2)	C(8)–C(9)	1 385(2)
N(5)–C(7)	1 348(2)	C(9)–C(10)	1 374(2)
N(6)–C(8)	1 339(2)	C(10)–C(11)	1 364(3)
N(6)–C(12)	1 341(2)	C(11)–C(12)	1 366(3)
C(1)–C(2)	1 386(2)		

Table [1.1]: (a) Bond distances for $C_{12}H_{12}N_6$ **(105)**

Bond angles (deg.)			
Atoms	**Angle**	**Atoms**	**Angle**
C(1)–N(1)–C(5)	116.6(2)	N(3)–C(6)–C(1)	117.71(13)
C(6)–N(3)–N(4)	111.46(11)	N(2)–C(6)–C(1)	116.40(14)
C(7)–N(4)–N(3)	111.82(11)	N(4)–C(7)–N(5)	125.16(13)
C(8)–N(6)–C(12)	116.9(2)	N(4)–C(7)–C(8)	116.86(13)
N(1)–C(1)–C(2)	122.64(14)	N(5)–C(7)–C(8)	117.98(13)
N(1)–C(1)–C(6)	115.27(14)	N(6)–C(8)–C(9)	122.49(14)
C(2)–C(1)–C(6)	122.08(13)	N(6)–C(8)–C(7)	116.22(13)
C(3)–C(2)–C(1)	119.1(2)	C(9)–C(8)–C(7)	121.29(13)
C(4)–C(3)–C(2)	118.6(2)	C(10)–C(9)–C(8)	119.1(2)
C(5)–C(4)–C(3)	118.7(2)	C(11)–C(10)–C(9)	118.8(2)
N(1)–C(5)–C(4)	124.3(2)	C(10)–C(11)–C(12)	119.1(2)
N(3)–C(6)–N(2)	125.89(14)	N(6)–C(12)–C(11)	123.7(2)

Table [1.1]: (b) Bond angles for $C_{12}H_{12}N_6$ **(105)**.

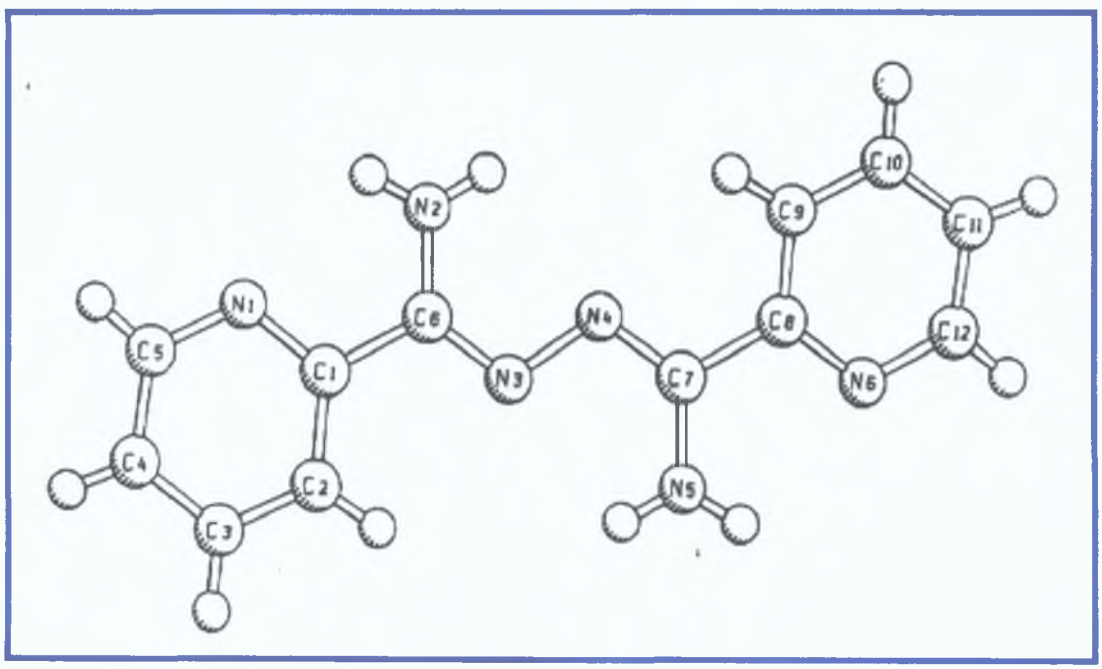

Fig [1.7]: X-ray structure of $C_{12}H_{12}N_6$ (105) with atomic numbering shown.

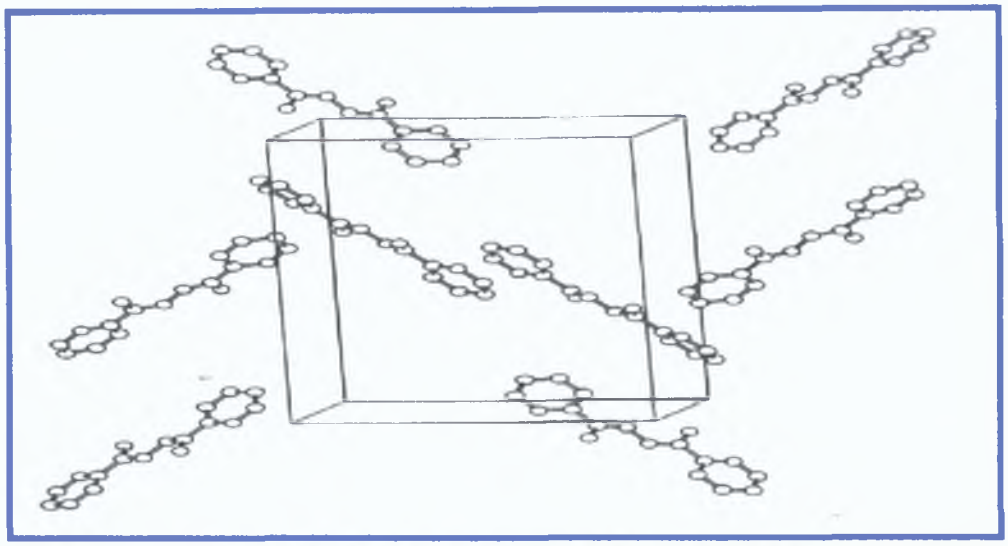

Fig [1.8]: Packing picture of $C_{12}H_{12}N_6$ (105)

1.2.4.2 3,6-bis-pyridin-2-yl-1,4-dihydrotetrazine $C_{12}H_{10}N_6$ (97).

Note: This crystal structure was obtained by Ms Nieves Payan[92], with the help of crystallographer Dr. Conor Long (DCU). Note: It was requested by Ms Payans research supervisor, Prof. Vos, that this crystal structure be included in this thesis.

This 1,4-dihydrotetrazine crystal **(97)** was originally reported by Caira et al[89]. Bond distances and angles are listed in table[1.2]. Also listed in the table are the related results reported by Caira[89].

	Bond distances (*Angstroms*)			Bond distances (*Angstroms*)	
Bond	**Dist**	**Ref** [93]	**Bond**	**Dist.**	**Ref** [93]
C(1)–C(2)	1 382	1 39	N(1)–C(1)	1 332	1 33
C(1)–C(6)	1 484	1 47	N(1)–C(5)	1 341	1 34
C(2)–C(3)	1 366	1 38	N(2)–C(6)	1 274	1 28
C(3)–C(4)	1 369	1 37	N(2)–N(3)	1 431	1 43
C(4)–C(5)	1 367	1 37	N(3)–C(7)	1 396	1 40
C(7)–C(8)	1 471	1 46	N(4)–C(7)	1 285	1 29
C(8)–C(9)	1 377	1 39	N(4)–N(5)	1 424	1 42
C(9)–C(10)	1 369	1 37	N(5)–C(6)	1 396	1 42
C(10)–C(11)	1 381	1 38	N(6)–C(12)	1 339	1 33
C(11)–C(12)	1 364	1 38	N(6)–C(8)	1 342	1 35

Table [1.2]: (a) Bond distances (top) for $C_{12}H_{10}N_6$ **(97).**

	Bond angles (*deg*)			Bond angles (*deg*)	
Atoms	**Angle**	**Ref** [93]	**Atoms**	**Angle**	**1 2.4 2 1 ef** [93]
C(1)–N(1)–C(5)	117 0	117 4	N(2)–C(6)–N(5)	121 4	120 1
C(6)–N(2)–N(3)	110 4	111 4	N(2)–C(6)–C(1)	119 9	119 6
C(7)–N(3)–N(2)	113 2	113 9	N(5)–C(6)–C(1)	118 7	119 6
C(7)–N(4)–N(5)	111 4	111 9	N(4)–C(7)–N(3)	119 9	119 9
C(6)–N(5)–N(4)	113 2	113 9	N(4)–C(7)–C(8)	121 0	121 4
C(12)–N(6)–C(8)	116 8	118 3	N(3)–C(7)–C(8)	119 2	118 7
N(1)–C(1)–C(2)	122 6	122 6	N(6)–C(8)–C(9)	122 6	121 6
N(1)–C(1)–C(6)	115 6	115 6	N(6)–C(8)–C(7)	114 8	115 9
C(2)–C(1)–C(6)	121 8	121 9	C(9)–C(8)–C(7)	122 6	122 6
C(3)–C(2)–C(1)	119 0	118 4	C(10)–C(9)–C(8)	119 5	119 2
C(2)–C(3)–C(4)	119 4	119 8	C(9)–C(10)–C(11)	118 7	119 7
C(5)–C(4)–C(3)	118 2	117 9	C(12)–C(11)–C(10)	118 3	118 0
N(1)–C(5)–C(4)	123 8	123 9	N(6)–C(12)–C(11)	124 2	123 3

Table [1.2]: (b) Bond angles (bottom) for $C_{12}H_{10}N_6$ **(97)**

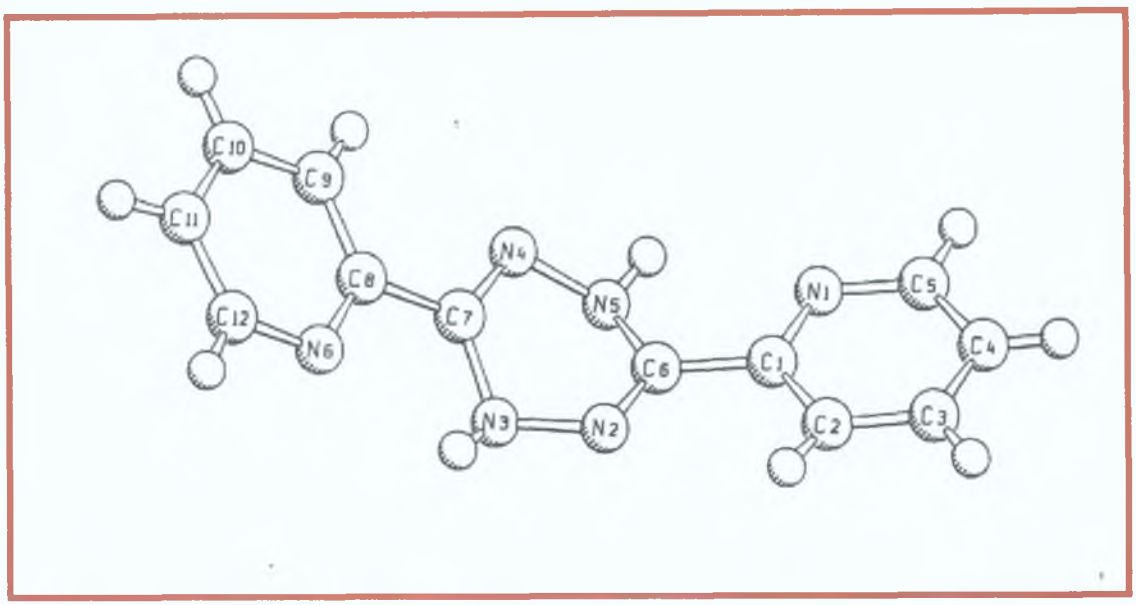

Fig [1.9]: X-ray structure of $C_{12}H_{10}N_6$ (97). with atomic numbering shown.

1.3 EXPERIMENTAL

^{1}H-NMR note: Coupling constants are provided where splitting was clearly seen in the spectra. In cases where broadening of peaks was seen, accurate coupling constants could not be obtained.

1.3.1 2-pyridine amidrazone ($C_6H_8N_4$)[31] (104)

To a stirred mixture of 2-cyanopyridine, 78.10 g (0.75 mol), in 150 ml ethanol at 25°C, was slowly added 36.4 ml (0.75 mol, d=1.032) of hydrazine hydrate. The reaction temperature was brought up to 40°C and maintained overnight. On cooling, pink needles were obtained which were dried under vacuum and washed with 100 ml ether (5 ml petroleum ether may need to be added or crystallization induced by the addition of one seeding crystal). The amidrazone was recrystallized twice from toluene. Fine white crystals of amidrazone were dried under vacuum and stored under N_2 in the freezer: yield, 94 g (0.69 mol), 92%. Mp=67°C.

^{1}H NMR ($CDCl_3$) (δ,ppm, J, Hz) 8.50(1H, d, 2.16); 8.00(1H, d, 1.00); 7.67(1H, t, 1.48); 7.24(1H, d,); 5.35(2H, s); 4.68(2H, s).

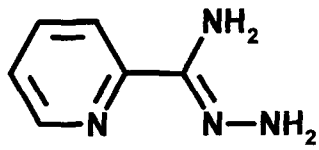

(104)

1.3.2 1,4-bis(pyridin-2-yl)azabutadiene-1,4-diamine($C_{12}H_{12}N_6$) (105).

These products were obtained from the mother liquor of the above amidrazone reaction, in small amounts, when left stirring over a period of approximately 21 days at room temperature The 1,4-bis(pyridin-2-yl)azabutadiene-1,4-diamine crystals were the first to emerge from solution as yellow needles The needles were filtered and washed with diethyl ether The absence of any minor peaks in the NMR analysis on the crystals was taken to be a sign of their purity Mp=98°C

^{1}H NMR ($CDCl_3$) (δ,ppm) 8 58 (1H, d), 8 36 (1H, d), 7 76 (1H, t), 7 34(1H, t), 6 37(s, 2H) (The X-ray crystal structure of this molecule is presented in the results and discussion section)

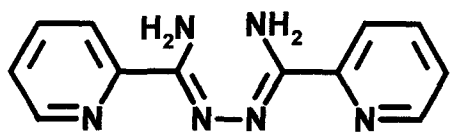

(105)

1.3.3 Dihydro-3,6-bis(pyridin-2-yl)-1,2,4,5-tetrazine($C_{12}H_{10}N_6$) (97).

On removal of the 1,4-bis(pyridin-2-yl)azabutadiene-1,4-diamine crystals, the mother liquor of the 2-pyridyl amidrazone reaction (1 4 1) was again stirred at room temperature After 48 h, more precipitate was seen in the reaction vessel This solid was filtered and washed with ether TLC analysis of the product in pet ether ethyl acetete (1 4) mobile phase showed the presence of two product spots, one of these corresponding to 1,4-bis(pyridin-2-yl)azabutadiene-1,4-diamine **(105)** The other spot was isolated with flash

chromatography, using the same mobile phase, and identified by NMR and X-ray crystallography (see results and discussion) as being dihydro-3,6-bis(pyridin-2-yl)-1,2,4,5-tetrazine **(97)** Mp=93°C

^{1}H NMR ($CDCl_3$) (δ,ppm) 8 99 (1H, s), 8 63 (1H, d), 7 96 (1H, d), 7 92 (1H t), 7 52 (1H, t)

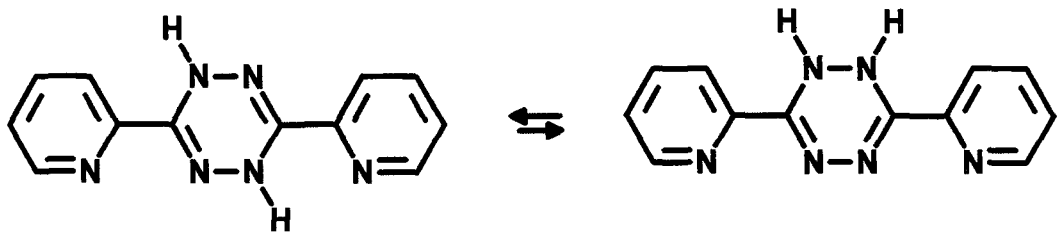

(97)

Geldard and Lions[86] identified these products previously and the crystal structure of the dihydrotetrazine has also appeared in the literature[89] Ms Nieves Payan[92] also isolated these products and in cooperation with this work we have investigated the X-ray crystal structures of the previously published dihydrotetrazine **(97)** and the as yet unpublished azabutadiene **(105)** product

1.3.4 2-pyrazine amidrazone ($C_5H_7N_5$) (111a).

The pyrazine analogue of the above amidrazone was similarly prepared using pyrazine carbonitrile instead of 2-cyanopyridine (1 4 1) yield, 95 g (0 96 mol), 93% m p =57°C

^{1}H NMR ($CDCl_3$) (δ,ppm , J, Hz) 8 98(1H, d, 2 16), 8 53(1H, d, 1 00), 7 88(1H, m, 1 48), 6 04(2H, s), 5 63(2H, s)

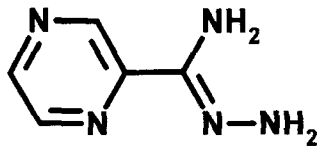

(111a)

1.3.5 1,4-Bis(pyridin-2-yl)-4-acylamidrazone($C_{11}H_{11}N_5O$) (112).

Picolinic acid, 2 26 g (0 02 mol) was added to freshly distilled thionyl chloride (14 5 ml, 0 2 mol) slowly through a dropping funnel The reaction was then arranged for reflux and heated at reflux temperature for 2 h The reaction had by then taken on a red colour characteristic of the acid chloride Unreacted thionyl chloride was removed by distillation at reduced pressure leaving a dark red product, the acid chloride yield, 1 84 g (0 014 mol), 69%

A mixture of 2 45 g (0 018 mol) of 2-picolinamhydrazone (amidrazone) and 1 91 g, (0 018 mol) sodium carbonate were stirred in 20 ml dry DMF at 0°C A solution of 1 84 g (0 014 mol) of picolinoyl chloride in 20 ml dry DMF was added over a period of 30 min through a dropping funnel The reaction mixture was then stirred at room temperature for 12 h after which time a brown solid had precipitated from solution This solid was separated by filtration, decolourised with charcoal and recrystallized from ethanol The bipyridylacylamidrazone **(112)** was used without characterization yield 0 23 g (9 x 10^{-4} mol), 6% Mp=187°C (Low yield attributed to impurity of picolinoyl chloride)

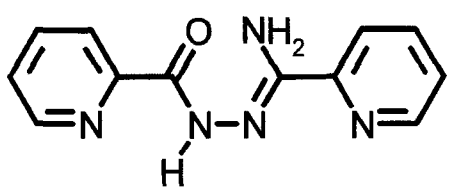

(112)

1.3.6 3,5-Bis(pyridin-2-yl)-1,2,4-triazole($C_{12}H_9N_5$) (8).

0 23 g (9 x 10^{-4} mol) of **112** was dissolved in 30 ml ethylene glycol (b p 196°C) and maintained at reflux temperature for 2 h The solvent was then removed by distillation at reduced pressure leaving a brown palpituous mass Methanol (5 ml) and water (2 ml) were added causing a brown solid to form This solid was removed by filtration, washed with ethanol, dried *in vacuo* over P_2O_5 and characterised by NMR yield, 0 089 g (4 x 10^{-4} mol), 44%
m p >200°C ^{1}H NMR (dmso-d^6) (δ,ppm , J, Hz) 14 63(1H,s), 8 71(1H, d, J=4 6), 8 16(1H, d, J=7 4), 7 99(1H, t, J=7 4), 7 51(1H, t, J=7 5)

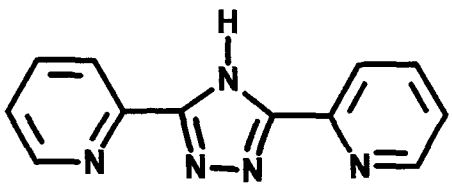

(8)

1.3.7 1-(pyridin-2-yl)-4-phenyl-acylamidrazone($C_{13}H_{12}N_4O$) (110).

Method One: A solution of 4 12 ml (0 036 mol) benzoyl chloride (d = 1 211) in 20 ml dry DCM was added slowly to a stirred solution of 5 g (0 036 mol) of amidrazone in 20 ml dry DCM A yellowish product precipitated immediately, dried and recrystallized from ethanol This fine solid was characterized by NMR as the desired acylamidrazone **(110)** yield, 6 22 g (0 03 mol), 83%

Method Two: A solution of 5 16 g (0 07 mol) of benzoyl chloride in 30 ml dry DCM was added rapidly to a vigorously stirred solution of 5 g (0 07 mol) amidrazone and 3 86 g (0 07 mol) sodium carbonate in 100 ml water A yellow solid began to precipitate immediately The reaction mixture was stirred for 10 min and filtered The product acylamidrazone was characterised by NMR after drying under vacuum at 80°C over P_2O_5 yield, 11 6 g (0 05 mol), 71%

^{1}H NMR (dmso-d^{6}) (δ,ppm, J,Hz) 11 54(1H, broad s, –NH), 10 18(2H, broad s, –NH_2), 8 88(1H, d, J=3 68, H6), 8 48(1H, d, J=9 24, H3), 8 21(1H, t, J=7 4, H4), 8 04(2H, d, J=7 4, H2",H6"), 7 84(1H, t, H5), 7 63(1H, t, J=7 4, H4"), 7 54(2H, t, J=7 4, H3",H5")

^{13}C NMR (δ, ppm) 165 62, 160 62, 150 16, 143 02, 138 56, 132 46, 131 65, 128 90, 128 43, 128 26, 124 09 m p 173°C

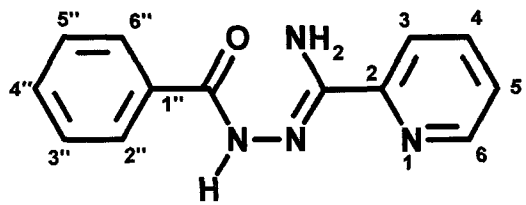

(110)

1.3.8 3'-(Pyridin-2-yl)-5'-phenyl-1,2,4-triazole($C_{13}H_{10}N_4$) (20).

4 g (0 017 mol) of 3-pyridyl-5-phenyl-acylamidrazone and 40 ml ethylene glycol were stirred in a round bottom flask On heating the solid dissolved completely leaving a clear yellow solution The solution was maintained at reflux temperature for 2 h until it appeared clear brown The solvent was reduced to a volume of 5 ml by distillation under reduced pressure A solid which precipitated over the following 48 h, was filtered and washed with ethanol and acetone, then dried *in vacuo* over P_2O_5 at 100°C Pale brown crystals of the product 3-pyridin-2-yl-5-phenyl-1,2,4-triazole **(20)** were characterised by NMR yield, 0 8 g (3 6 x 10^{-3} mol) 21 18 %

^{1}H NMR (dmso-d^{6}) (δ,ppm, J,Hz) 14 82(1H, s, –NH), 8 72(1H, d, J=4 6, H6), 8 17(1H, d, J=8 33, H3), 8 09(2H, d, H2",H6"), 8 00(1H, t, H4), 7 5(4H, m, H3",H5", H4", H5) m p >200°C

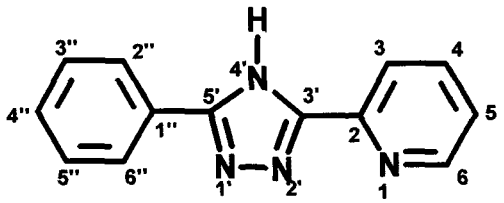

(20)

1.3.9 2-Phenyl-5-(pyridin-2-yl)-1,3,4-oxadiazole($C_{13}H_9N_3O$) (111).

0 5 g (2 1 x 10^{-3} mol) of 3-pyridyl-5-phenyl-acylamidrazone was placed in a sublimation tube and a vacuum applied The tube was then immersed in a preheated oil bath at 180°C Over the following 2 5 h a white crystalline solid formed a layer on the part of the tube not immersed in the oil bath This solid was removed and characterised by NMR as 2-pyridin-2-yl-5-phenyl-1,3,4-oxadiazole **(111)** yield 30 mg (1 35 x 10^{-4} mol), 6% m p 186°C

^{1}H NMR (dmso-d^6) (δ, ppm, J,Hz) 8 81(1H, d, J=4 63), 8 27(1H, d, J=7 4), 8 12(3H, m), 7 67(4H, m) ^{13}C NMR (δ, ppm) 164 69, 163 60, 152 5, 150 38, 142 7, 137 96, 132 32, 129 57, 126 82, 126 50, 123 23, 123 15 C,H,N Analysis $C_{13}H_9N_3O$ (% Theory/Found) C(69 9/ 68 2), H(4 0/4 0), N(18 8,18 9)

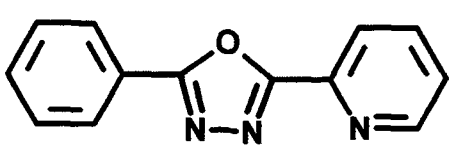

(111)

1.3.10 1'',4''-Bis(acyl-[pyridin-2-yl]-amidrazone)-benzene($C_{20}H_{18}N_8O_2$) (107).

4 g (0 03 mol) of 2-pyridinyl amidrazone and 1 56 g (0 015 mol) sodium carbonate were stirred in 30 ml dry THF while cooling in an ice bath A

solution of 3 g (0 015 mol) of terephthaloyl dichloride in 30 ml dry THF was added to the reaction mixture slowly through a dropping funnel A yellow solid formed immediately The reaction mixture was stirred overnight then poured onto ice water The yellow solid formed was removed by filtration through a sintered funnel, washed with water, then acetone The product acylamidrazone was recrystallised from DMSO washed with acetone and dried *in vacuo* over P_2O_5 at 100°C overnight and characterised by NMR yield, 4 g (0 01 mol), 33 33% m p >200°C

^{1}H NMR (dmso-d^6) (δ, ppm, J,Hz) 10 36(2H, broad s, –**NH**), 8 63(2H, d, J=5 55, **H6**), 8 20(2H, d, J=7 4, **H3**), 8 01(4H, s, **Phenyl-H**), 7 93(2H, t, **H4**), 7 51(2H, t, **H5**), 7 04(4H, broad s, –**NH$_2$**)

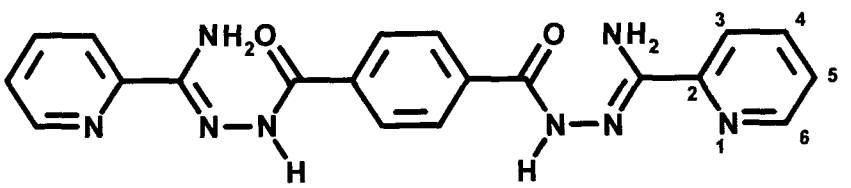

(107)

1.3.11 1,4-bis-(5-pyridin-2-yl-1,2,4triazol-3-yl)-benzene. ($C_{20}H_{14}N_8$)[20] (108)

2 g (5 x 10^{-3} mol) of 1,4-bis(acyl-pyridin-2-yl amidrazone)-benzene in 30 ml ethylene glycol were heated at reflux temperature on a heating mantle for 3 h until the solution changed from clear yellow to a clear brown colour The volume of ethylene glycol was reduced to 10 ml by distillation and the flask allowed to stand until a precipitate emerged The pale brown solid precipitate was washed several times with acetone and impurities removed by stirring in hot DMSO followed by filtration
The resultant 1,2,4-triazole **(108)** was characterised by NMR and microanalysis yield, 0 77 g (2 1 x 10^{-3} mol), 42 % m p >200°C

^{1}H NMR (dmso-d^6) (δ, ppm, J,Hz) 14 91(2H, s, –NH), 8 75(2H, d, J=3 7, H6), 8 25(4H, broad s, Phenyl-H), 8 22(2H, d, J=7 4, H3), 8 04(2H, t, J=7 4, H4),

7 57(2H, t, J=7 4, H5) ^{13}C NMR (δ,ppm) 150 42, 141 71, 137 88, 127 43, 126 81, 126 42, 125 09, 123 22, 121 52 C,H,N Analysis $C_{20}H_{14}N_8$ $1H_2O$(% Theory/Found) C(65 2/65 2), H(3 3/3 5), N(22 8/26 8)

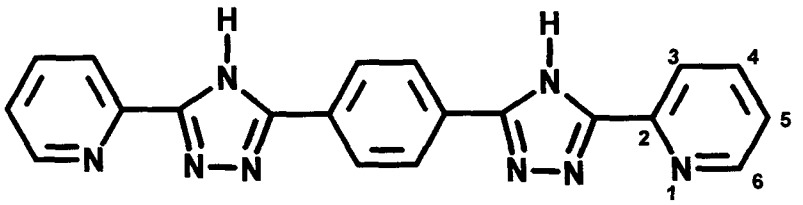

(108)

1.4 CONCLUSIONS

We have shown in this chapter the potential for triazole formation by the initial reaction of amidrazones and acid chlorides to form acylamidrazones which can then be heated to form triazoles via a condensation reaction Our literature survey has shown this to be the method of choice for triazole synthesis although other synthetic methods have also been reviewed Of these other synthetic routes, acylamidrazone formation from the reaction of iminoethers and hydrazides is also a commonly used reaction

Early triazole synthesis relied greatly on the use of heat to form triazoles This resulted in unwanted by-product formation This is still a problem to some extent at present We have shown that amidrazones tend to form tetrazines and diamines easily when heated We have also seen that acylamidrazones with alkyl (or non-aromatic) substituents tend to be less stable and proceed quickly to the triazole form We have shown that under certain reaction conditions oxadiazoles can also be formed from acylamidrazones with heating However advances in solvent use has made triazole formation more controllable

From a spectroscopic view we have seen that ^{1}H-NMR is a very important structure elucidation tool in these syntheses ^{13}C-NMR is impractical because of the solubility problems of the compounds involved COSY experiments help greatly in distinguishing aromatic protons and establishing coupling patterns of these protons Characteristic peaks have been noted such as the broad $-NH_2$ and –NH signals of acylamidrazones and the characteristic downfield –NH peak of triazoles

1.5 REFERENCES

[1] G Pellizari, *Gazz Chim Ital*, **41**, 20, (1911)

[2] D R Liljegren, K T Potts, *J Chem Soc*, 518, (1961)

[3] K T Potts, *J Chem Soc*, 3461, (1954)

[4] D Libman, R Slack, *J Chem Soc*, 2253, (1956)

[5] M Pesson, S Dupin, *Bull Soc Chim Fr*, 1364, (1962)

[6] P Dubus, B Decroix, *C R Acad Sci Ser C*, **278**, 61, (1974)

[7] R Stolle, *Berichte*, **32**, 797, (1899)

[8] R Stolle, A Bambach, *J Prakt Chem*, **74**, 23, (1906)

[9] E R Lynch, W Cummings, *British Patent*, 1, 096, 600

[10] M R Atkinson, J B Polya, *J Chem Soc*, 3323, (1954)

[11] M R Atkinson, J B Polya, *J Am Chem Soc*, **75**, 1471, (1953)

[12] A Pinner, *Berichte*, **27**, 997, (1894)

[13] M C Kilpatrick, *J Am Chem Soc*, **69**, 42, (1947)

[14] P L de Benneville, Levesque, Exner, Herts, *J Org Chem*, **21**, 1072, (1956)

[15] G Pellizari, *Gazz Chim Ital*, **41**, 20, (1911)

[16] E Hoggarth, *J Chem Soc*, 1164, (1949)

[17] H Weidinger, J Kranz, *Chem Ber*, 1065, (1963)

[18] H Weidinger, J Kranz, *Berichte*, **96**, 2071, (1963)

[19] P Eitner, *Ber Dtsch Chem Ges* , **25**, 462, (1892)

[20] I Hirao, Y Kato, H Tateishi, *Bull Chem Soc Jpn* , **45**, 208, (1972)

[21] N N Vereshchagina, G S Melkozerova, N N Frolova, A V Bebrin, I Y Postovskii, *Khin Farm Zh (Engl Ed)*, **7**, 350, (1973)

[22] A A Korshak, E A Parkes, J B Polya, M R Atkinson, *J Chem Soc* , 4508, (1954)

[23] P Westermann, H Paul, G Hilgetag, *Berichte*, **97**, 528, (1964)

[24] I Y Postovskii, N N Vereschagina, *J allg Chem (russ)*, **29**, 2139, (1959)

[25] I Y Postovskii, N N Vereschagina, *Chem Abs* , **54**, 9898, (1960)

[26] P Westermann, H Paul, G Hilgetag, *Berichte*, **99**, 1111, (1966)

[27] D C Remy, U S Patent No 3,115,498, (1963)

[28] F H Case, *J Heterocyclic Chem*, **7**, 1001, (1970)

[29] T Baccheti, *Gazz Chim Ital* , **91**, 866, (1961)

[30] H Rochling, G Hoerlein, *Justus Liebigs Ann Chem*, 504, (1974)

[31] I Y Postovskii, N N Vereshchagina, *J Gen Chem URSS Engl Trans* , **29**, 2105, (1959)

[32] G S Gol'din, M V Maksakova, V G Poddubnyi, A N Kol'tsova, A V Kisin, V N Torochesnikov, A A Simonova, *Zh Obsch Khim* , **44**, 113, (1974)

[33] T Kauffmann, *Chem Ber* , 3436, (1964)

[34] E J Browne, *Aust J Chem* , **24**, 393, (1971)

[35] E J Browne, *Aust J Chem* , **24**, 2389, (1971)

[36] E J Browne, J B Polya, *J Chem Soc* C, 1056, (1969)

[37] H E Kuenzel, G D Wolf, F Bentz, *Makromol Chem* , **130**, 103, (1969)

[38] B G Baccar, F Mathis, *C R Acad Sci Paris*, **261**, 174, (1965)

[39] M Fujimori, E Haruki, E Imoto, *Bull Chem Soc Jpn* , **41**, 1372, (1968)

[40] R Ruggeri, G Rigoli, *Gazz Chim Ital* , **54**, 555, (1924)

[41] H Takimoto, L Krbechek, *J Org Chem* , **27**, 4688, (1962)

[42] K A Pollart, H J Harwood, *J Org Chem* , **27**, 4444, (1962)

[43] S Patai, F Bergmann, *J Am Chem Soc* , **72**, 1035, (1950)

[44] W B Bromwell, L C King, *J Am Chem Soc* , **71**, 2926, (1949)

[45] M Fujimori, E Haruki, E Imoto, *Bull Chem Soc Jpn* , **41**, 1372, (1968)

[46] A Mustafa, A E A A Hassan, *J Am Chem Soc* **79**, 3846, (1957)

[47] E J Browne, E E Nunn, J B Polya, *J Chem Soc C*, 1515, (1970)

[48] J C Sheehan, P T Izzo, *J Am Chem Soc* , **74**, 4059, (1949)

[49] E J Browne, E E Nunn, J B Polya, *J Chem Soc C*, 1515, (1970)

[50] A E Tschitschibabin, O A Siede, *J Obst Chimii*, **46**, 1216, (1914)

[51] A E Tschitschibabin, R A Konowalowa, *Ber Dtsch Chem Ges* , **54**, 814, (1921)

[52] A Spassov, E Golovinsky, *Chem Ber* **98**, 932, (1965)

[53] J March, Advanced Organic Chemistry, 4th ed , Wiley, New York, 1992, p 688

[54] A Spassov, S Robev, *Ber Akad Wiss UdSSR*, **95**, 559, (1954)

[55] A Spassov, S Robev, *Ber Akad Wiss UdSSR*, **95**, 817, (1954)

[56] T Kauffmann, W Sahm, *Angew Chem* , **79**, 101, (1967)

[57] T Kauffmann, W Sahm, *Angew Chem Int Ed Engl* , **6**, 85, (1967)

[58] T Kauffmann, J Albrecht, D Berger, J Legler, *Angew Chem Int Ed Engl* , **6**, 633, (1967)

[59] C Glasner, *Justus Liebigs Ann Chem* , **154**, 159, (1870)

[60] A Pinner, *Justus Liebigs Ann Chem* , **297**, 228, (1897)

[61] Boyle, Grundon, Scott J Chem Soc Perkin Trans vol 1 1976, p 207

[62] L Birkofer, P Wegner, *Chem Ber* , **99**, 2512, (1966)

[63] E Zbiral, K Kischa, *Tetrahedron Lett* , 1167, (1969)

[64] L Birkofer, F Muller, W Kaiser, *Tetrahedron Lett* , 2781, (1967)

[65] E Ettenhuber, K Ruhlmann, *Chem Ber* , **101**, 743, (1968)

[66] S S Washburne, W R Peterson Jnr , *J Organomet Chem* , **21**, 427, (1970)

[67] R Huisgen, J Sauer, H J Sturm, J H Markgraf, *Chem Ber* , **93**, 2106, (1960)

[68] R Huisgen, J Sauer, H J Sturm, *Tetrahedron*, **11**, 241, (1960)

[69] W Lossen, C Lossen , *Justus Liebigs Ann Chem* , **263**, 101, (1891)

[70] R Huisgen, J Sauer, *Justus Liebigs Ann Chem* , **654**, 146, (1962)

[71] A Werner, H Buss, *Ber Dtsch Chem Ges* , **27**, 2193, (1894)

[72] A Pinner, *Justus Liebigs Ann Chem* , **297**, 221, (1897)

[73] R Stolle, *J Prakt Chem* , **75**[2], 416, (1907)

[74] H Franzen, F Kraft, *J Prakt Chem* , **84**[2], 122, (1911)

[75] H C Brown, D Pilipovich, *J Am Chem Soc* , **82**, 4700, (1960)

[76] H Brown, C R Wetzel, *J Org Chem* **30**, 3729, (1965)

[77] H Behringer, H J Fischer, *Berichte*, 2547, (1962)

[78] R Stolle, A Netz, *Ber Dtsch Chem Ges* , **55**, 1297, (1922)

[79] A Darapsky, *J Prakt Chem* , 97[2], 194, (1918)

[80] B I Buzykın, G D Lezhnına, Y P Kıtaev, *Zh Org Khım Engl Ed* , **2**, 1066, (1975)

[81] H Eılıngsfeld, *Chem Ber* , **98**, 1308, (1965)

[82] J F Geldard, F Lıons, *J Org Chem* , **30**, 1318, (1965)

[83] F Dallacker, *Monatsch* , **91**, 294, (1960)

[84] D G Nıelson, S Mahmood, K M Watson *J Chem Soc Perkın Trans 1*, 335, (1973)

[85] V P Wystrach, ın R C Elderfield (Ed), Heterocyclıc Compounds, vol 8, Wıley, New York, 1967, p 105

[86] J L Fahey, P A Foster, D G Nıelson, K M Watson, J L Brokenshıre, D A V Peters, *J Chem Soc C*, 719, (1970)

[87] R A Bowıe, M D Gardner, D G Nıelson, K M Watson, S Mahmood, V Rıdd, *J Chem Soc Perkın Trans 1*, 2395, (1972)

[88] P Truıtt, L T Creagh, *J Org Chem*, **28**, 1910, (1963)

[89] M R Caıra, R G F Gıles, L Nassımbenı, G M Sheldrıck, R G Hazell, *Acta Crystallogr B*, 32, 1467, (1976)

[90] W Van der Burg, *Rec Trav Chım* , **74**, 257, (1955)

[91] D Lıbman, R Slack, *J Chem Soc* , 2253, (1956)

[92] N Perez-Payan, Research Report, Dublın Cıty Unıversıty, 1995

[93] R Hage, Ruthenıum and Osmıum Complexes Contaınıng Trıazole Lıgands, Ph D Thesıs, Leıden Unıversıty, 1991

2. Introduction to Large Triazoles:

Synthesis of Target 1,2,4-Triazoles

2.1 INTRODUCTION

Ligands discussed in this chapter

Note Triazoles are shown here as being N4 protonated for clarity HL1/HL3 are N1 protonated as will be seen in crystal structures

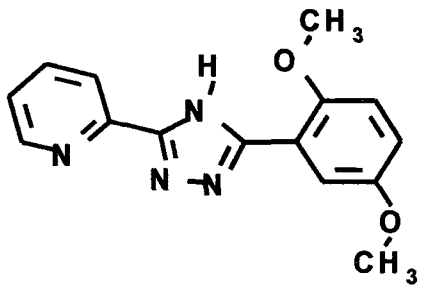

HL1

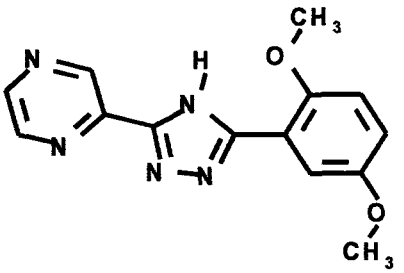

HL2

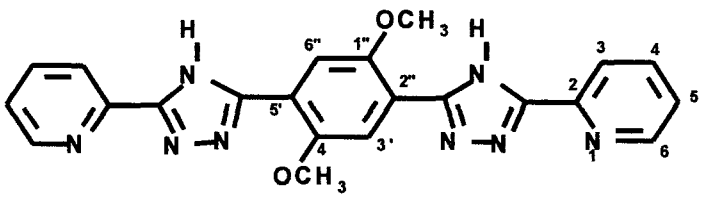

H_2L3

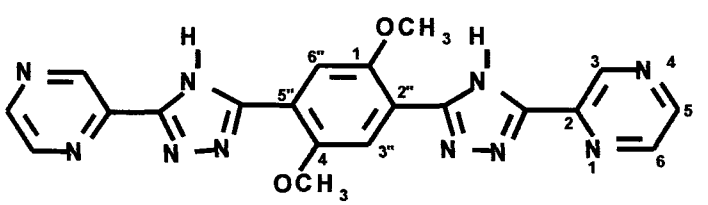

H_2L4

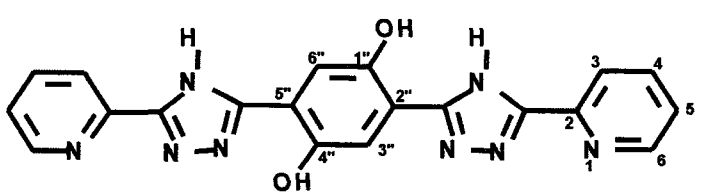

H_2L7

HL1= 1,4-dimethoxyphenyl-5-pyndin-2-yl-1,2,4-triazole
HL2= 1,4-dimethoxyphenyl-5-pyrazin-2-yl-1,2,4-triazole
H_2L3= 1,4-bis(5-pyridin-2-yl-1,2,4-triazol-3-yl)-2,5-dimethoxybenzene)
H_2L4= 1,4-bis(5-pyrazin-2-yl-1,2,4-triazol-3-yl)-2,5-dimethoxybenzene)
H_2L7= 1,4-bis(5-pyridin-2-yl-1,2,4-triazol-3-yl)-2,5-dihydroxybenzene)

In 1969, Hergenrother[1] reported the formation of 1,2,4-triazoles and 1,3,4-oxadiazoles from acylhydrazidines[2,3,4,5] (or acylamidrazones, as they are more commonly known) Hergenrother, as part of an investigation into the reaction conditions necessary for polymer formation[6] realised the potential to produce pyridyl-triazoles through the reaction of amidrazones and acid chlorides, a reaction previously carried out by Saga and Shono[7] Carrying out the reactions shown below in Schemes [2 1], [2 2] and [2 3], he made a number of observations and offered guidelines on how best to maximize yields

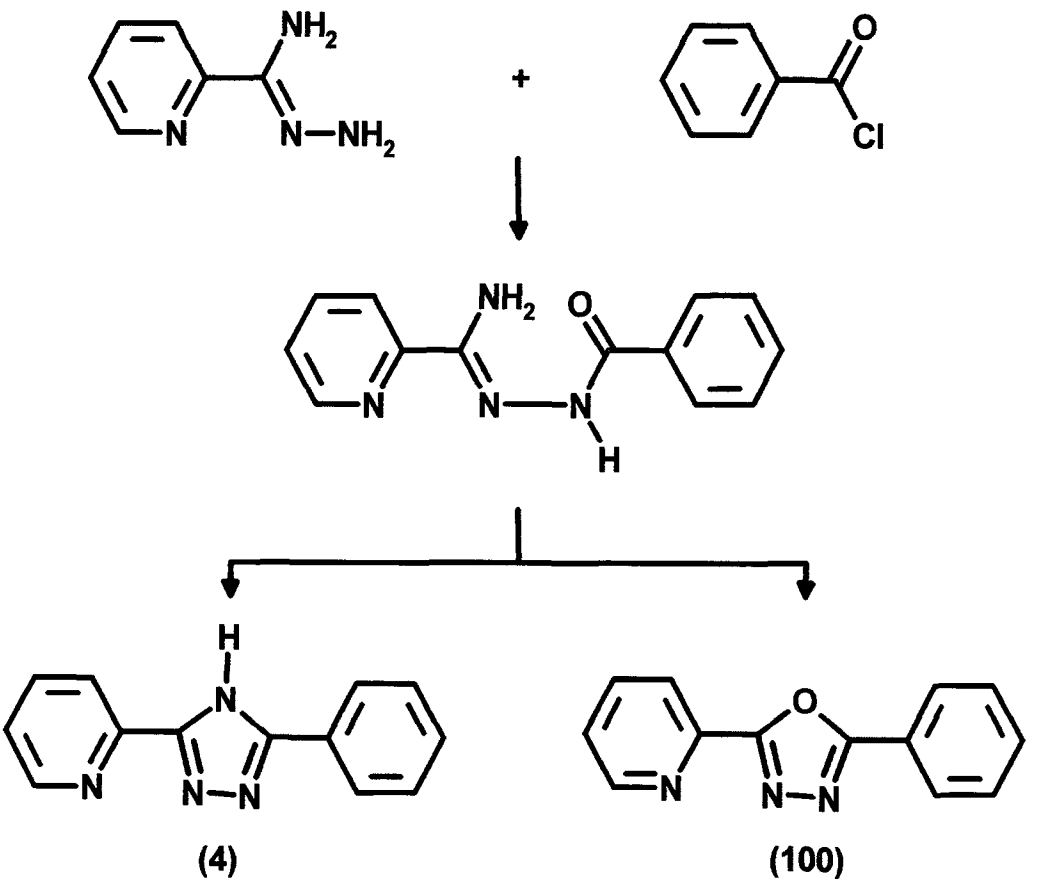

(4) (100)

Scheme [2.1]

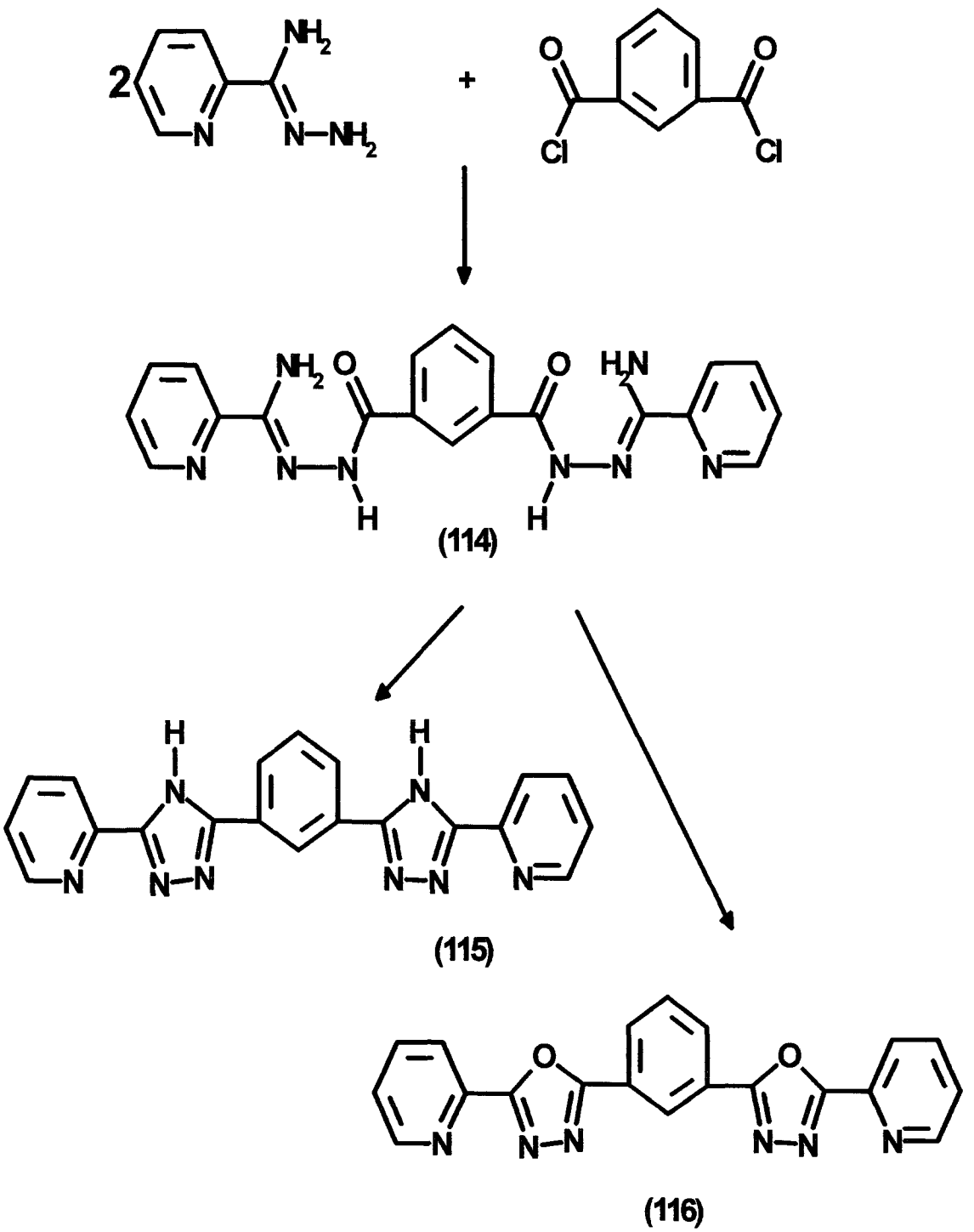
2
NH2
N
N–NH2
+
O
O
Cl
Cl
NH2
O
O
H2N
N
N–N
H
N–N
N
H
(114)
H
N
N
N–N
N–N
N
N
(115)
O
O
N
N–N
N–N
N
(116)

Scheme [2.2]

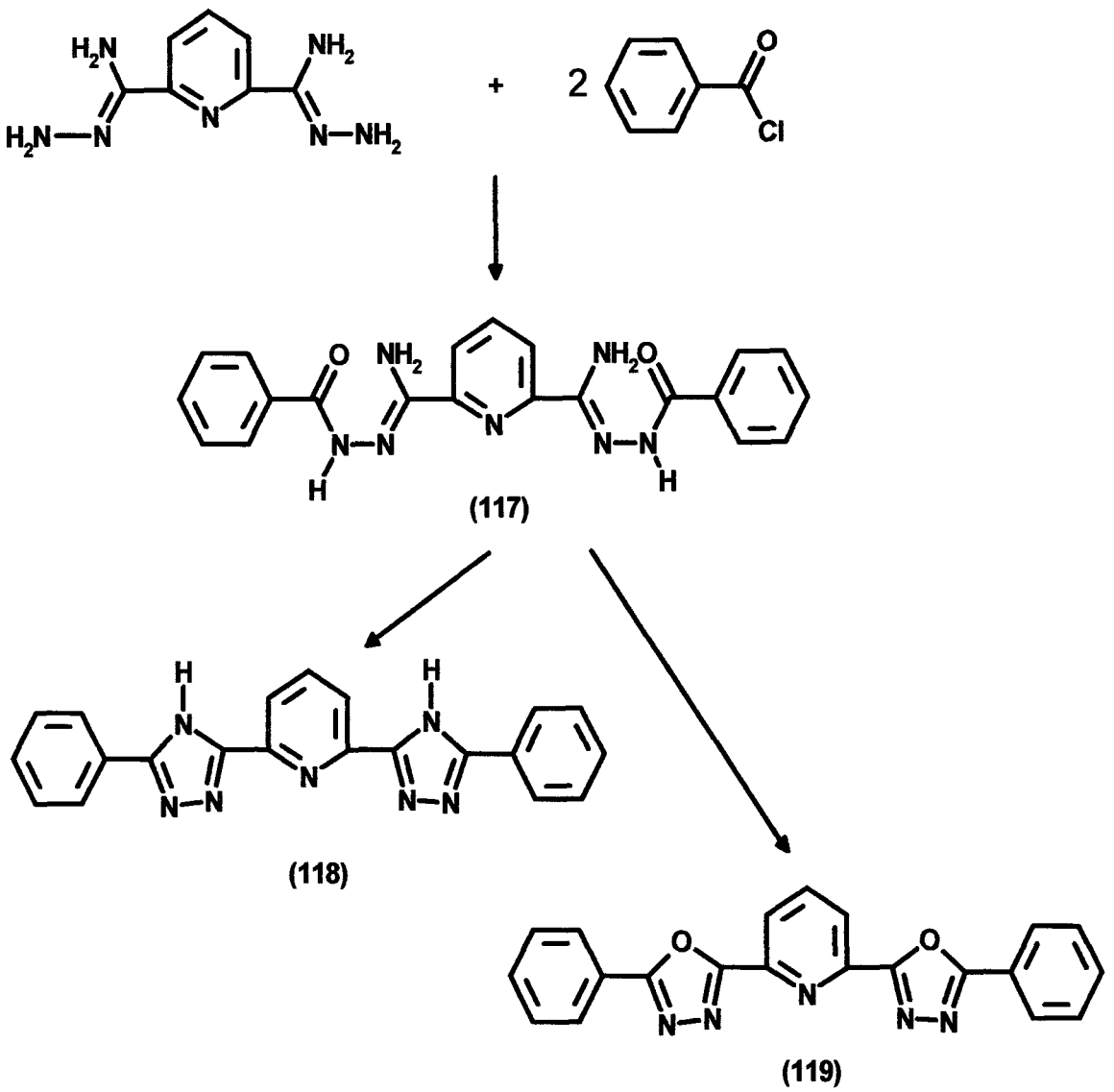

Scheme [2.3]

- The *N*-acylhydrazidines were prepared by low temperature solution condensation in polar solvents such as *N,N*-dimethylacetamide and hexamethylphosphoramide Hergenrother also made use of an "interfacial method" which will be discussed later

To obtain quantitative formation of 1,3,4-oxadiazoles **(116)** and **(119)** from the corresponding acylamidrazones requires the use of elevated temperatures in solution using strong acids such as dichloroacetic , trifluoroacetic, phosphoric or sulfuric acids

- Predominant formation of the corresponding 1,2,4-triazoles was achieved by heating acylamidrazones at elevated temperatures (250-300°C) in a melt or in refluxing solvents such as *N*-methylpyrollidine, *m*-cresol or hexamethyl phosphoramide
- When forming 1,2,4-triazoles, small amounts of ammonia were often detected during the cyclization process due to the formation of the corresponding 1,3,4-oxadiazoles The amount of ammonia formed depended on the heating rate
- Introduction of a tube containing the acylamidrazone under N_2 into a preheated oil bath at 300°C usually resulted in maximum ammonia evolution whereas heating in *m*-cresol from room temperature to reflux temperature resulted in minimum formation of oxadiazole (0 8%)

This general route for the synthesis of 1,2,4-triazoles and 1,3,4-oxadiazoles dates back to 1889 when Bladin combined carboxylic acid anhydrides and acid chlorides with aryl substituted amidrazones to obtain aryl-1,2,4-triazoles[8] In a related report, Pinner treated N-acylamidrazones with nitrous acid to obtain 1,3,4-oxadiazoles[4] It is also interesting to note that 1,3,4-oxadiazoles were among the Pellizari reaction products[9], which involves heating hydrazides and amides at high temperatures in the absence of a solvent to yield triazoles He proposed the formation of a diacylhydrazide **(120)** with elimination of ammonia to account for 1,3,4-oxadiazole formation whereas Potts[10] proposed the formation of an intermediate acylhydrazidine which cyclizes to **(100)** and **(4)** as in Scheme [2 4]

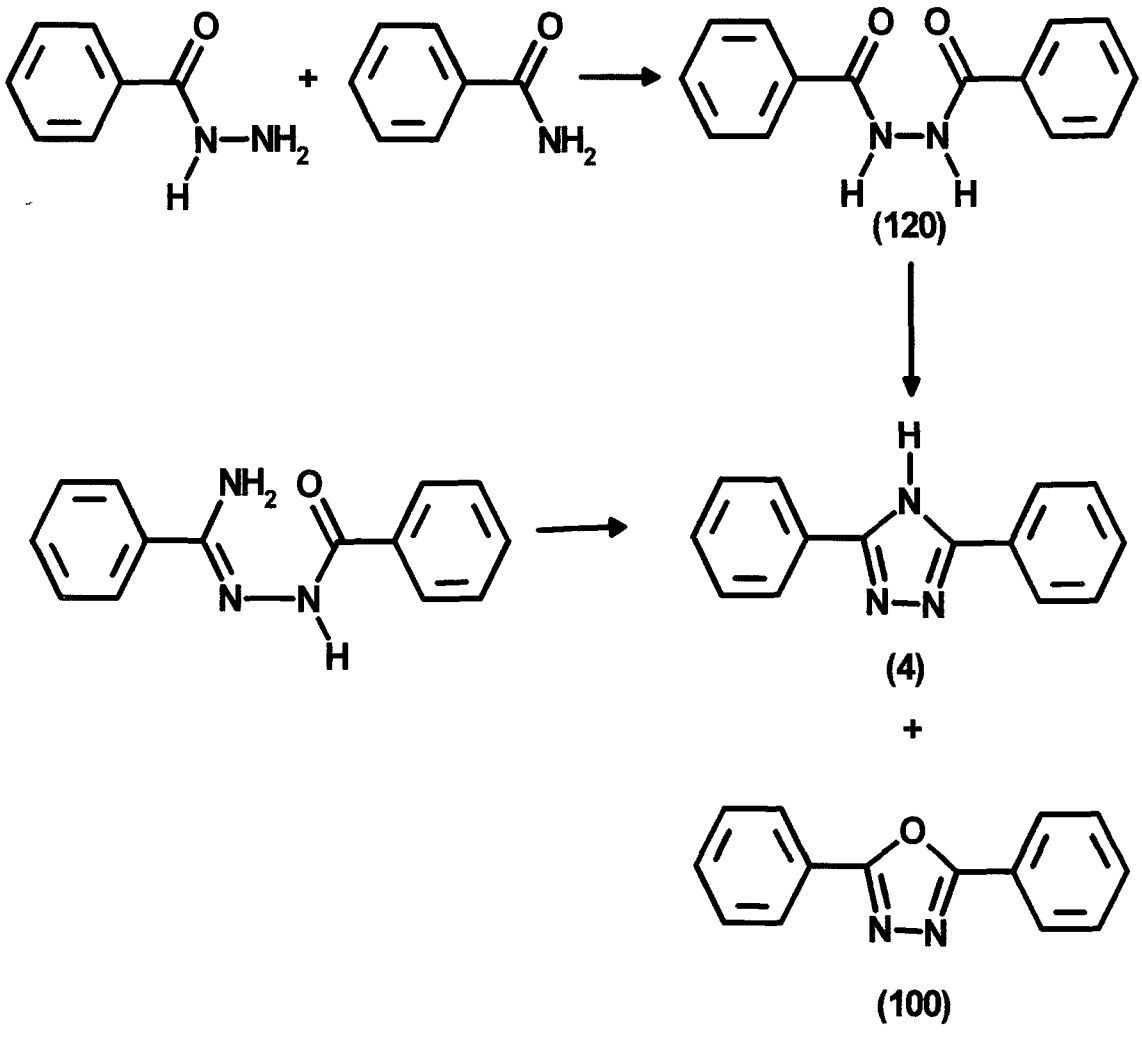

Scheme [2.4]

Hergenrothers work on the synthesis of large molecules containing triazoles, came about as part of an investigation into the formation of poly-triazoles[11 12,13,] and poly-oxadiazoles[14] Mono- and bis-triazoles (and oxadiazoles) were formed as model compounds It was during this timeframe (early 1970's) that much of the information that we use today was gathered by Hergenrother and other polymer chemists, through model compound synthesis

In Scheme [2 5] the reaction of 2,6-pyridine-dihydrazidine and isophthaloyl chloride is illustrated

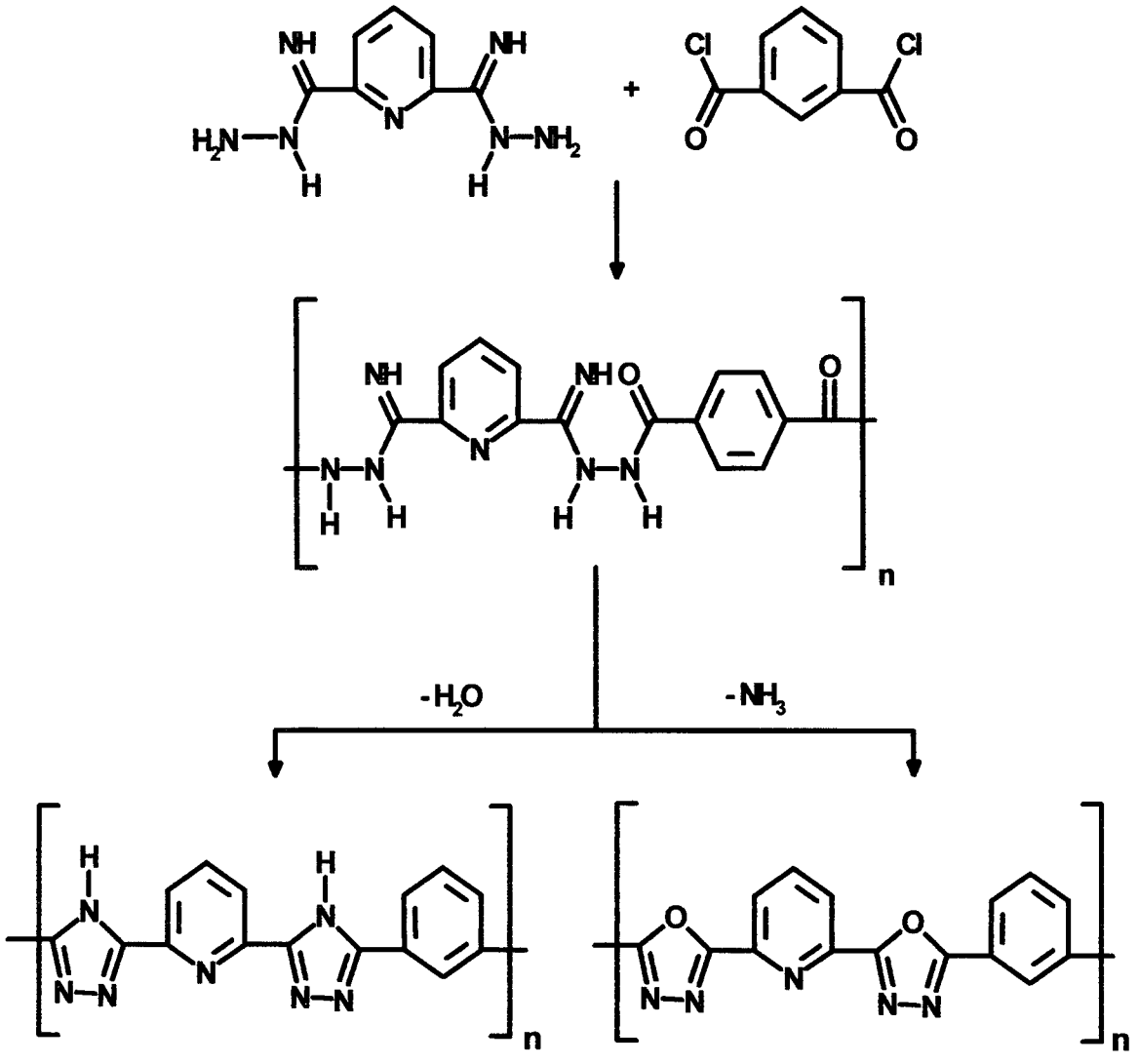

Scheme [2.5]

Two methods were used in this synthesis of **(117)**, **(118)** and **(119)** shown in Scheme [2 3]

(1) **General method** Both the amidrazone (and anhydrous K_2CO_3) and the acid chloride were dissolved in *N,N*-dimethylacetamide The acid chloride was added drop wise to the amidrazone over time, followed by stirring for 3 hours at ambient temperature

(2) **Interfacial Method** The benzoyl chloride in chloroform was added rapidly to a vigorously stirred solution of the amidrazone and sodium carbonate in water The reaction was complete after approximately 10 minutes

Hergenrother investigated other means of converting the *N*-acylamidrazones to triazoles or oxadiazoles such as by refluxing in acetic anhydride[1], thionyl chloride or *m*-cresol containing a catalytic amount of *p*-toluenesulphonic acid but the crude products obtained were either too impure or not the desired compound

For example when the reaction shown in Scheme [2 6] was carried out

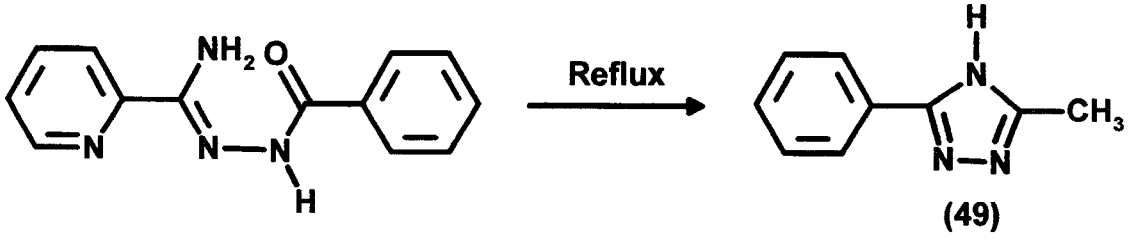

Scheme [2.6]

N-benzoyl(2-pyridyl) hydrazidine was refluxed in acetic anhydride, the product was mainly 3-(2-pyridyl)-5-methyl-1,2,4-triazole All the model compounds were noted to be hygroscopic with the relative affinity for hydration decreasing from

acylamidrazone to triazole to oxadiazole. In most cases drying at 120°C for 4 hours removed the hydrated water except for the diacylamidrazone **(117)** (Scheme [2.3]) when heated to temperatures as high as 200°C failed to achieve removal of the tightly bound water.

The 2-pyridyl-amidrazone molecule **(104)** used in the preparation of many triazoles is a very versatile reactant. Hergenrother used the amidrazones to synthesize 1,2,4-triazolines[15] such as **(121)** and triazoles e.g. (115) shown in Scheme [2.7] by reaction with aromatic aldehydes and aromatic dialdehydes.

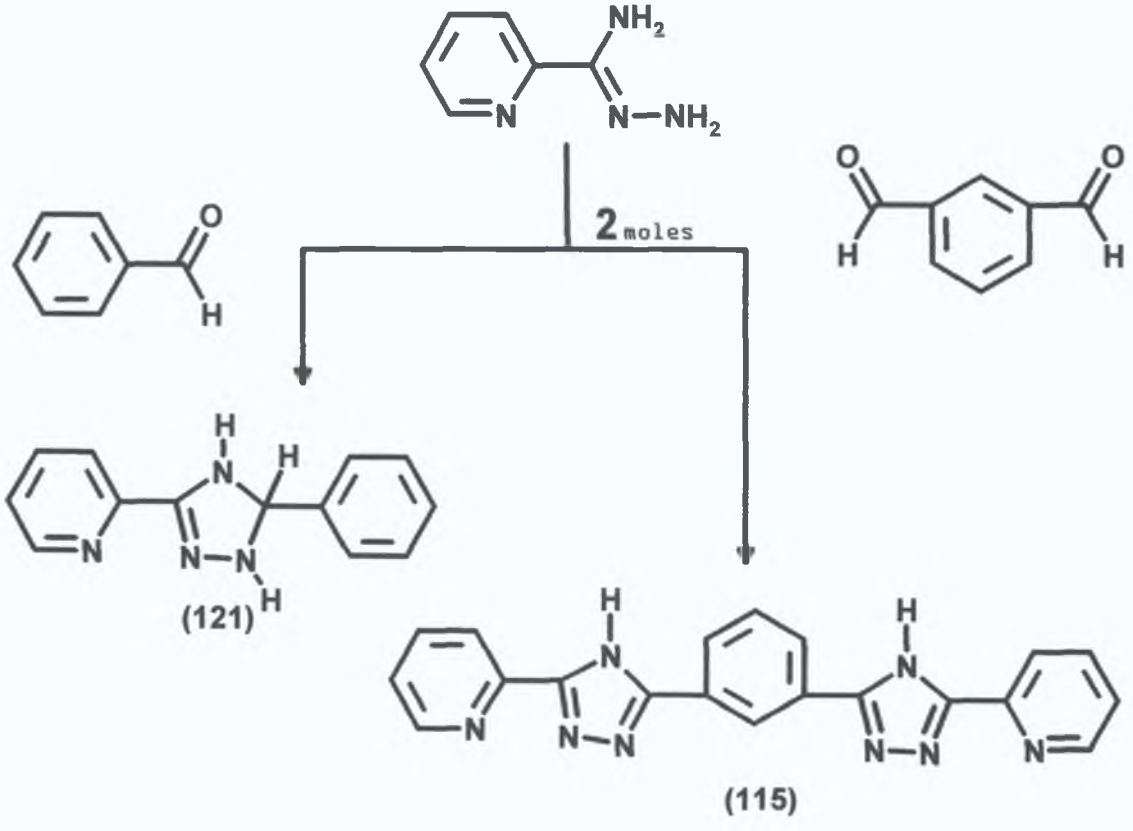

Scheme [2.7]

These triazoline compounds were prepared in quantitative yields by refluxing stoichiometric quantities of the two reactants in ethanol, followed by pouring onto

ice to precipitate the product Carrying out the reaction by melt condensation failed to produce good yields of product, due to the decomposition which occurred when triazolines were heated at temperatures of ~250°C Hergenrother attempted to convert them to the more thermally stable 1,2,4-triazoles by dehydrogenation as shown in Scheme [2 8]

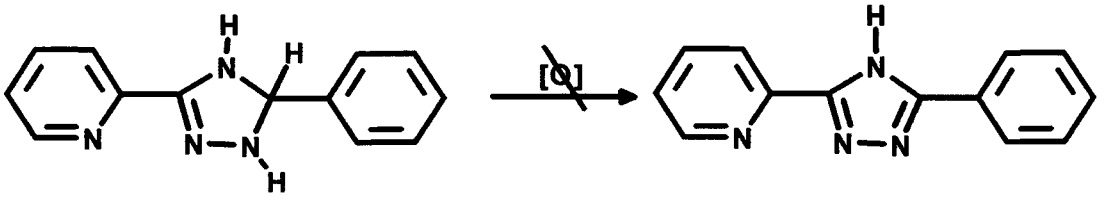

Scheme [2.8]

Reaction conditions including the use of sulfur, chloranil, ferric chloride and dimethyl sulfoxide only resulted in partial oxidation with purple/black products forming Hergenrother went on to explore another avenue in triazole synthesis by producing amino-triazoles[16,17], the amine group being available for further reaction to form even larger and more complex heterocyclic polymers The same procedure was again employed to produce the triazole **(122)** and **(123)**, only this time nitrobenzoyl chloride was reacted with the amidrazone as in Schemes [2 9] and [2 10]

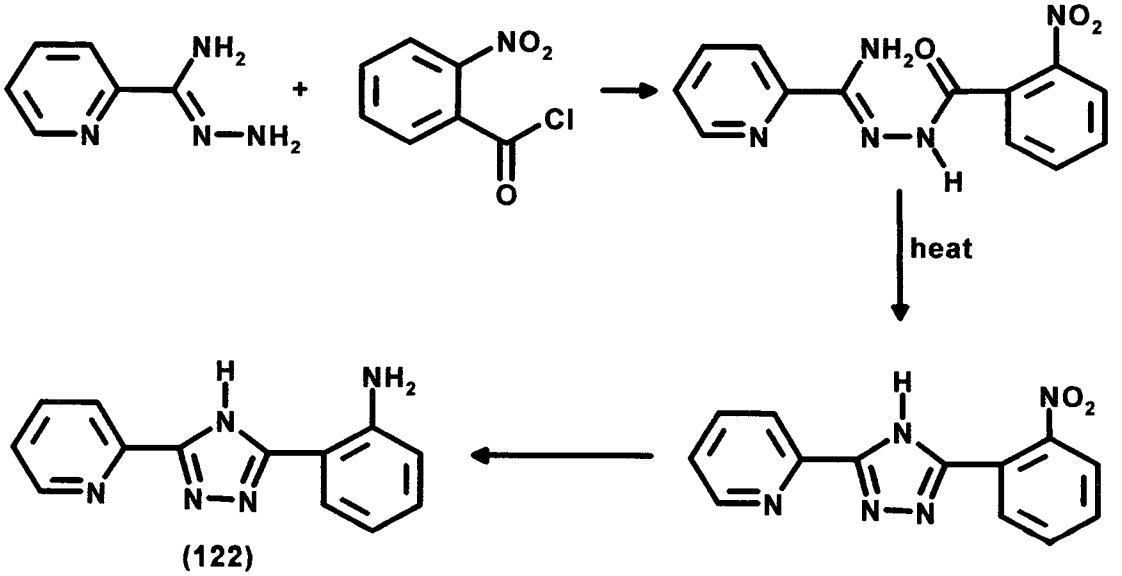

(122)

Scheme [2.9]

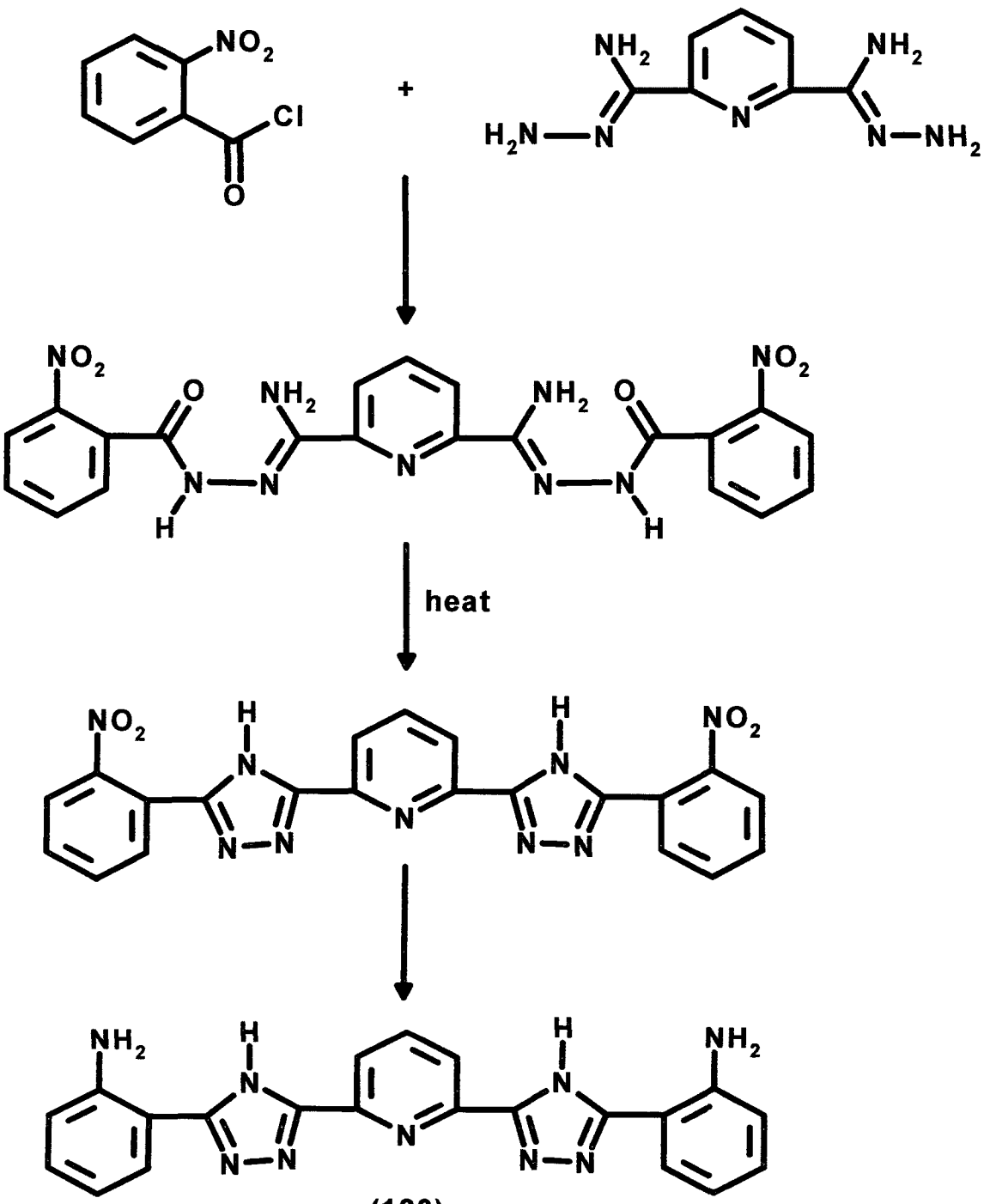

(123)

Scheme [2.10]

The nitro- product was reduced using sodium sulfide monohydrate in ethylene glycol at 115°C for 4 hours The resultant solution when neutralized with hydrochloric acid yielded the product, the amino triazole The amino-triazoles **(122)** and **(123)** then became the precursors to further reactions as shown in Schemes [2 11] and [2 12] respectively resulting in the formation of quinazolo-1,2,4-triazoles **(124),(126),** and **(128)**

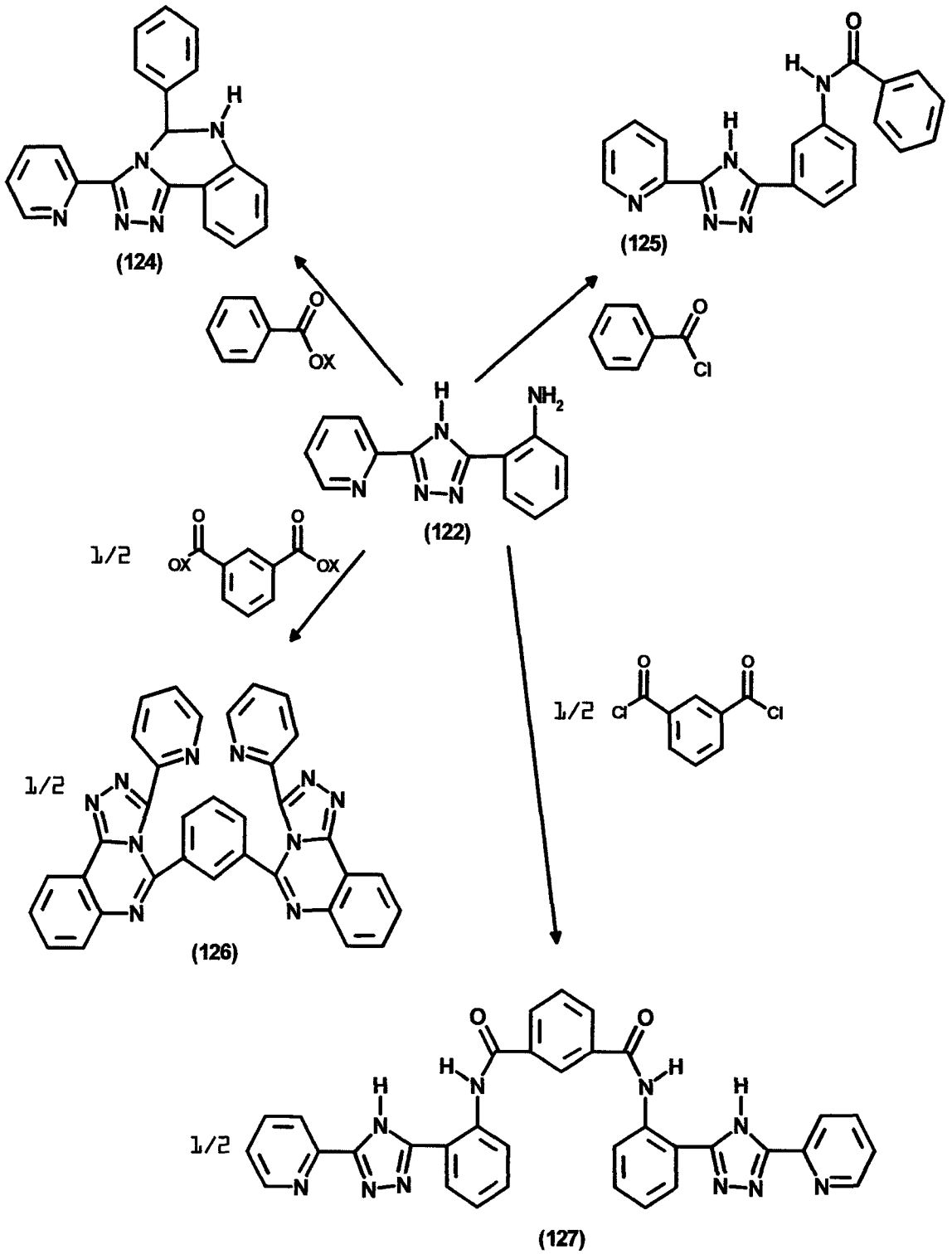

Scheme [2.11]

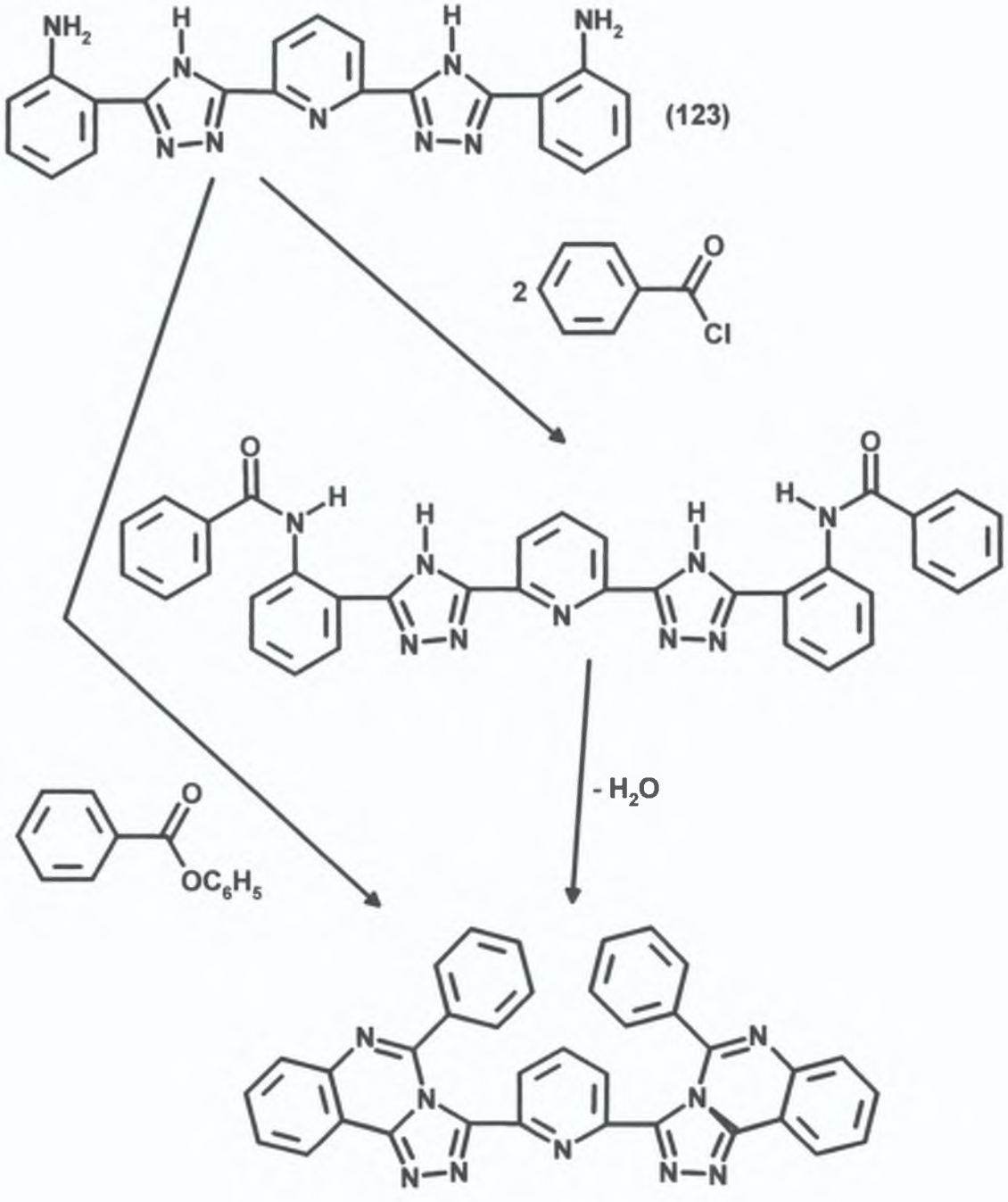

(128)

Scheme [2.12]

The aminophenyl triazole reacted readily with the acid chloride at 0°C in dimethylacetamide under inert conditions. Again pouring onto water precipitated the product. The precursor amide then formed the final product through a melt

condensation in a preheated oil bath The quinazolotriazole (128) could also be formed by mixing the aminophenyltriazole and benzoic acid in polyphosphoric acid with heating to 250°C for 3 hours When X= C_6H_5 **(129)** the product was formed by a melt process at 340°C from the aminophenyltriazole and phenylbenzoate

After reaction of the amidrazone with the carboxylic acid chloride the *N*-acylamidrazone can be preferentially turned into a 1,3,4-oxadiazole using strong acids such as trifluoroacetic acid Small amounts of 1,3,4-oxadiazole (<5%) often accompany the 1,2,4-triazole but can be removed by recrystallization and thus does not present any serious purification problems The melting points of these triazoles were determined by differential scanning calorimetry as the average melting point apparatus is unreliable above 300°C
Similar to Hergenrother, Korshak and co-workers carried out their research in the field of heterocyclic polymers and used the synthesis of triazoles and their derivatives as model reactions[18] Starting with diamines, 1,3-bis[5-(2-aminophenylene)-1,2,4-triazol-3-yl]benzene **(130)**, 1,4-bis[5-(2-aminophenylene)-1,2,4-triazol-3-yl]benzene **(131)** and 2,6-bis[5-(2-aminophenylene)-1,2,4-triazol-3-yl]pyridine **(132)** were synthesized by two pathways

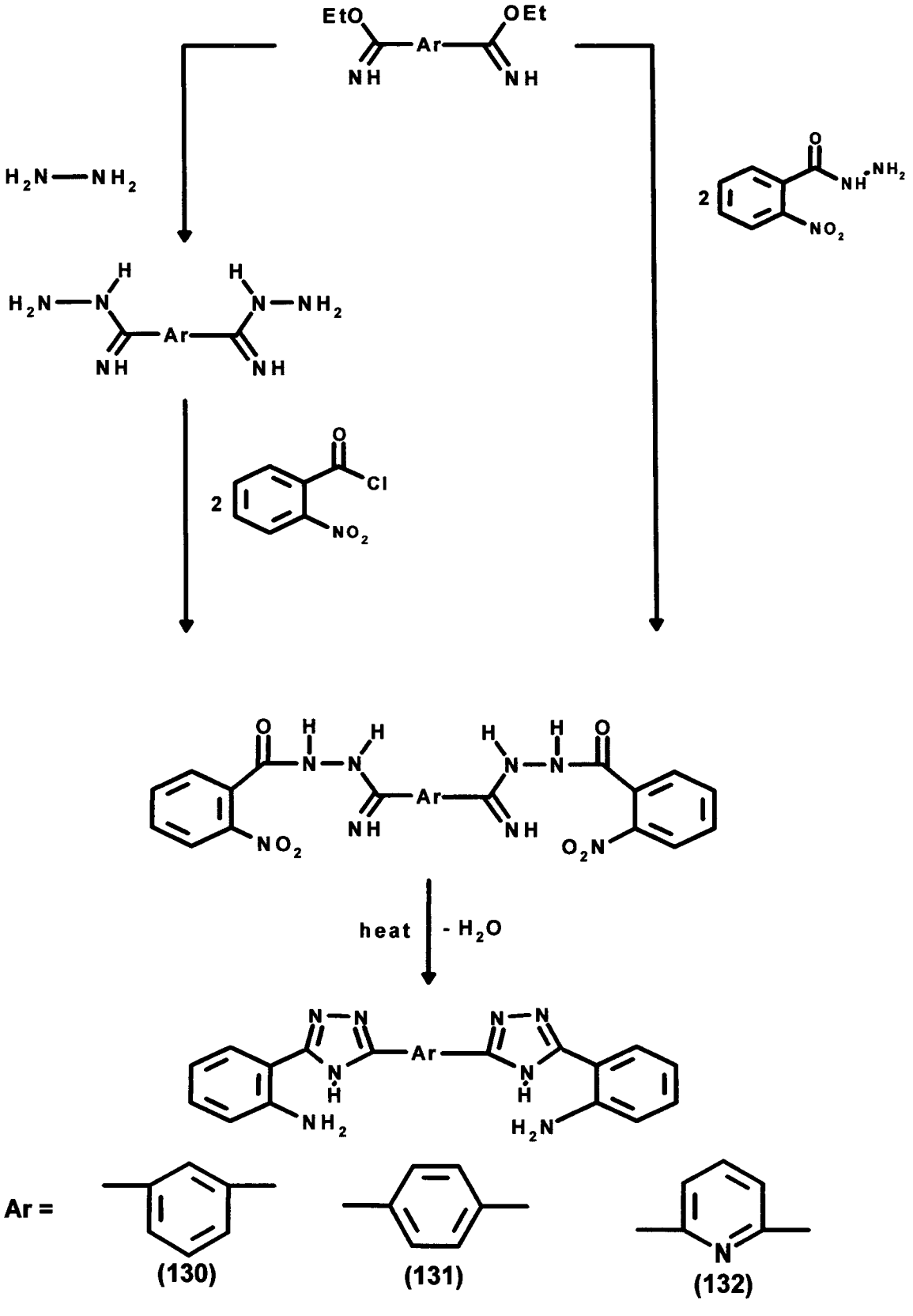

Scheme [2.13]

In a model reaction 3-phenyl-5-(2-benzamidophenylene) **(135)** and 3,5-diphenyl-*s*-triazolo[**4**,3-c]quinazoline **(134)** have been obtained by the interaction of 3-phenyl-5-(2-aminophenylene) **(133)** with benzoic acid in polyphosphoric acid

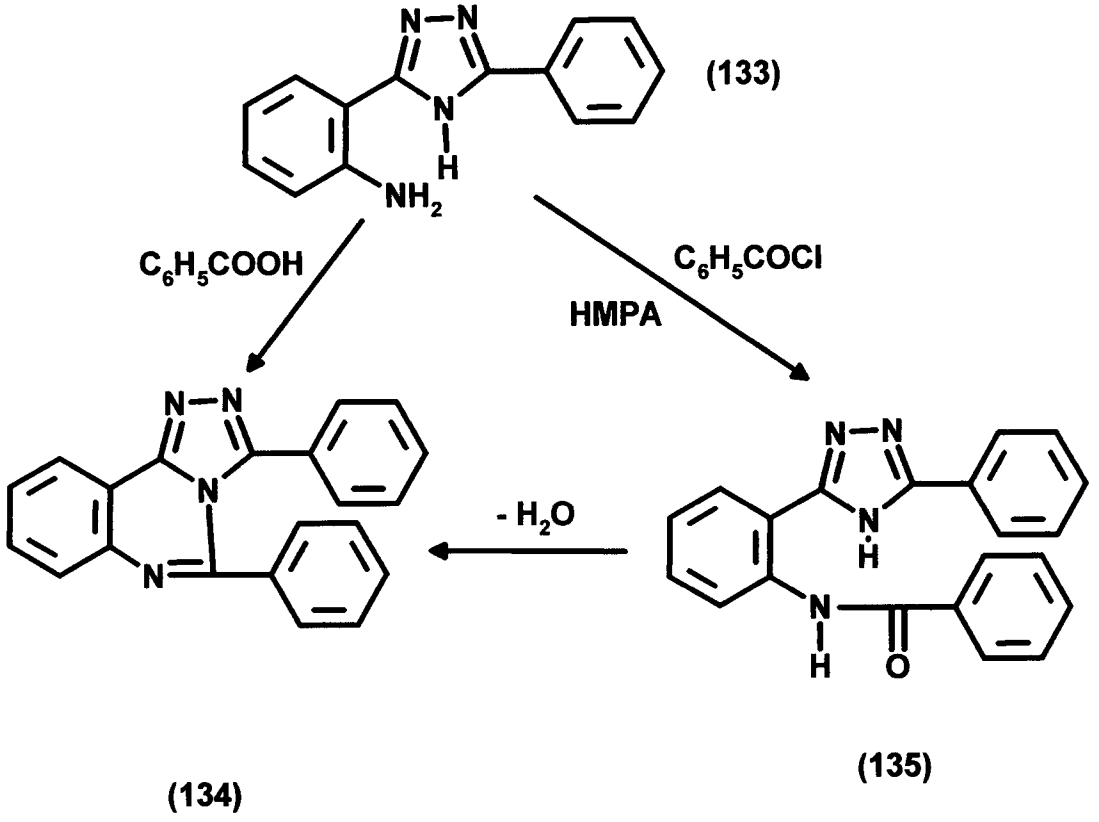

Scheme [2.14]

Not only has an amine group in the triazole molecule been involved in a reaction, in this the N in the 4-position has lost its proton and bonded to the carbonyl carbon in the ring closure reaction These properties were then taken a stage further to produce even more complex molecules[18] By reacting **(133)** with aromatic dicarboxylic acid dichlorides in HMPA followed by thermal cyclodehydration of the reaction products the resultant molecules **(136)-(140)** shown in Scheme [2 15] were formed

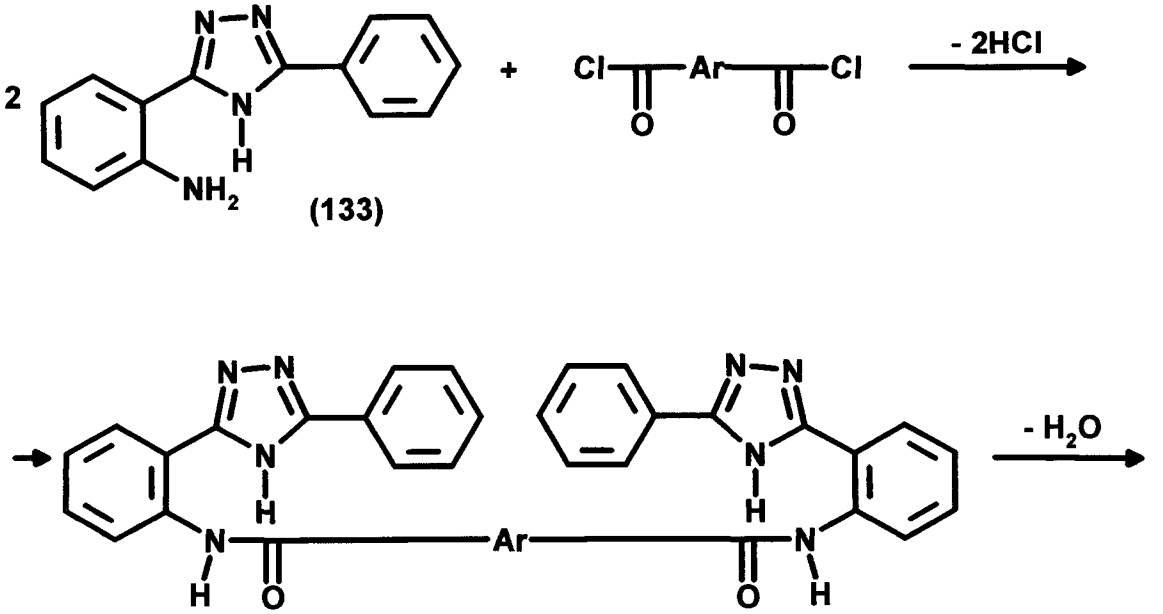

Ar= Substituents 136-140

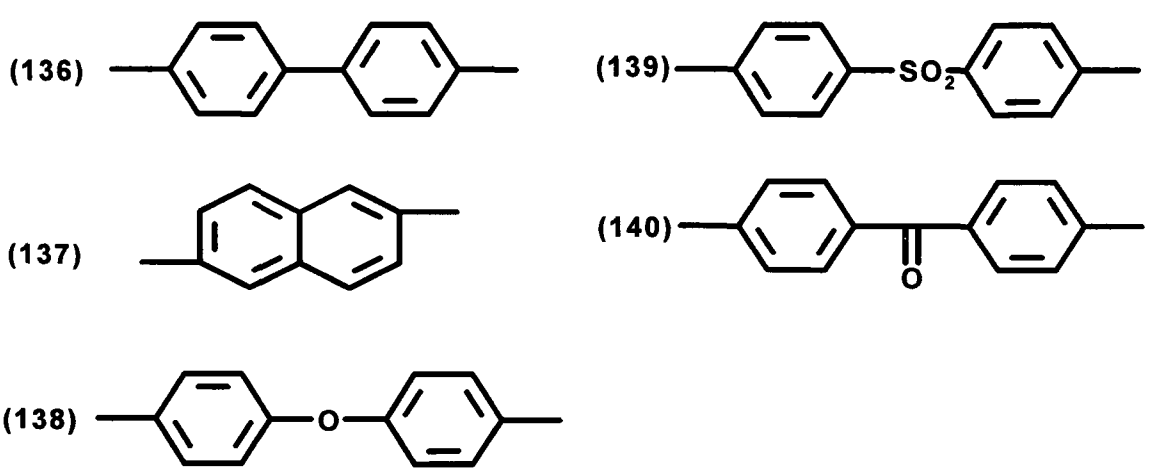

Scheme [2.15]

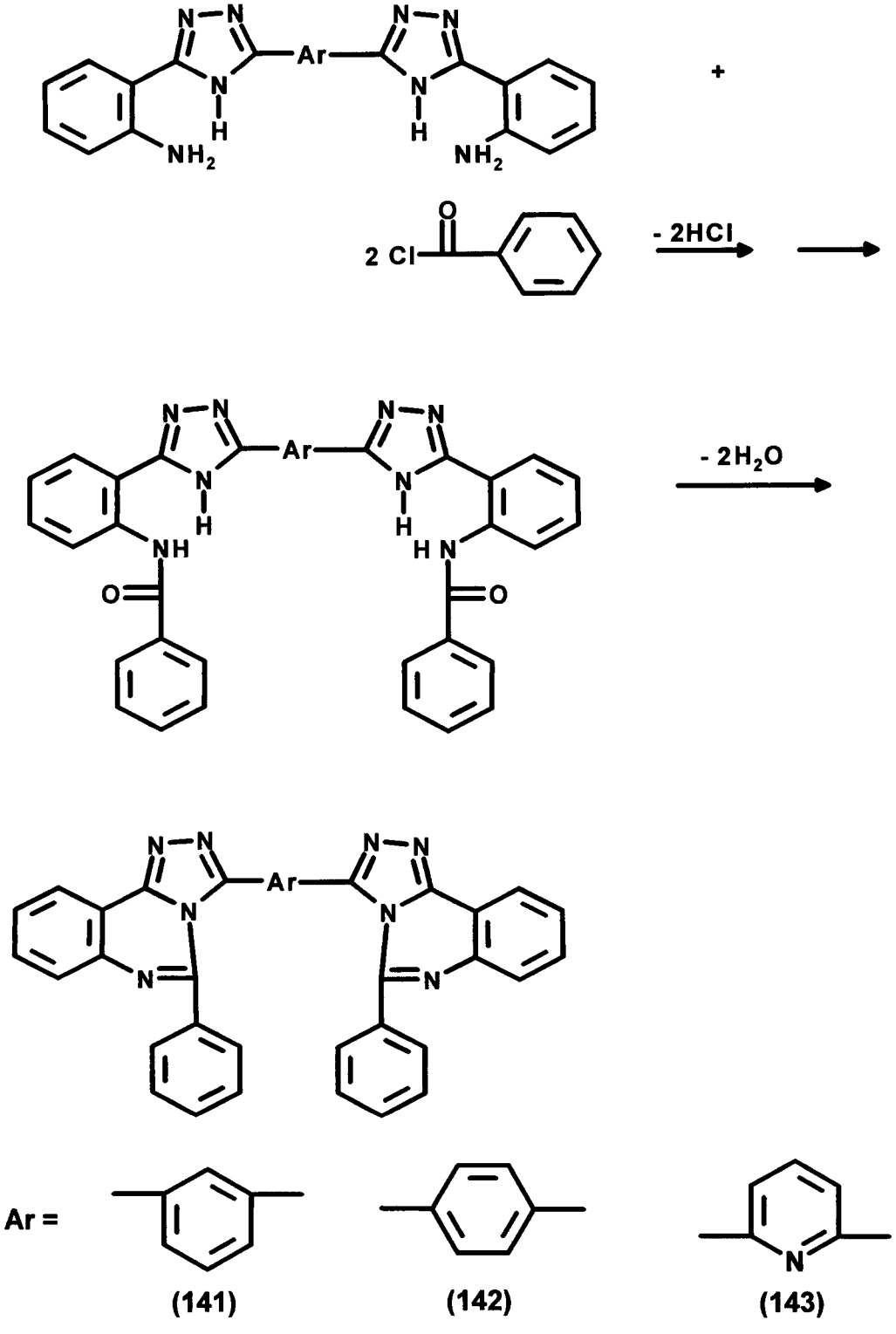

Scheme [2.16]

Different products were also obtained by reacting bis[5-(2-aminophenyl)-1,2,4-triazol-3-yl]arylenes with benzyl chloride in HMPA followed by heating of the reaction products as shown in Scheme [2 16]

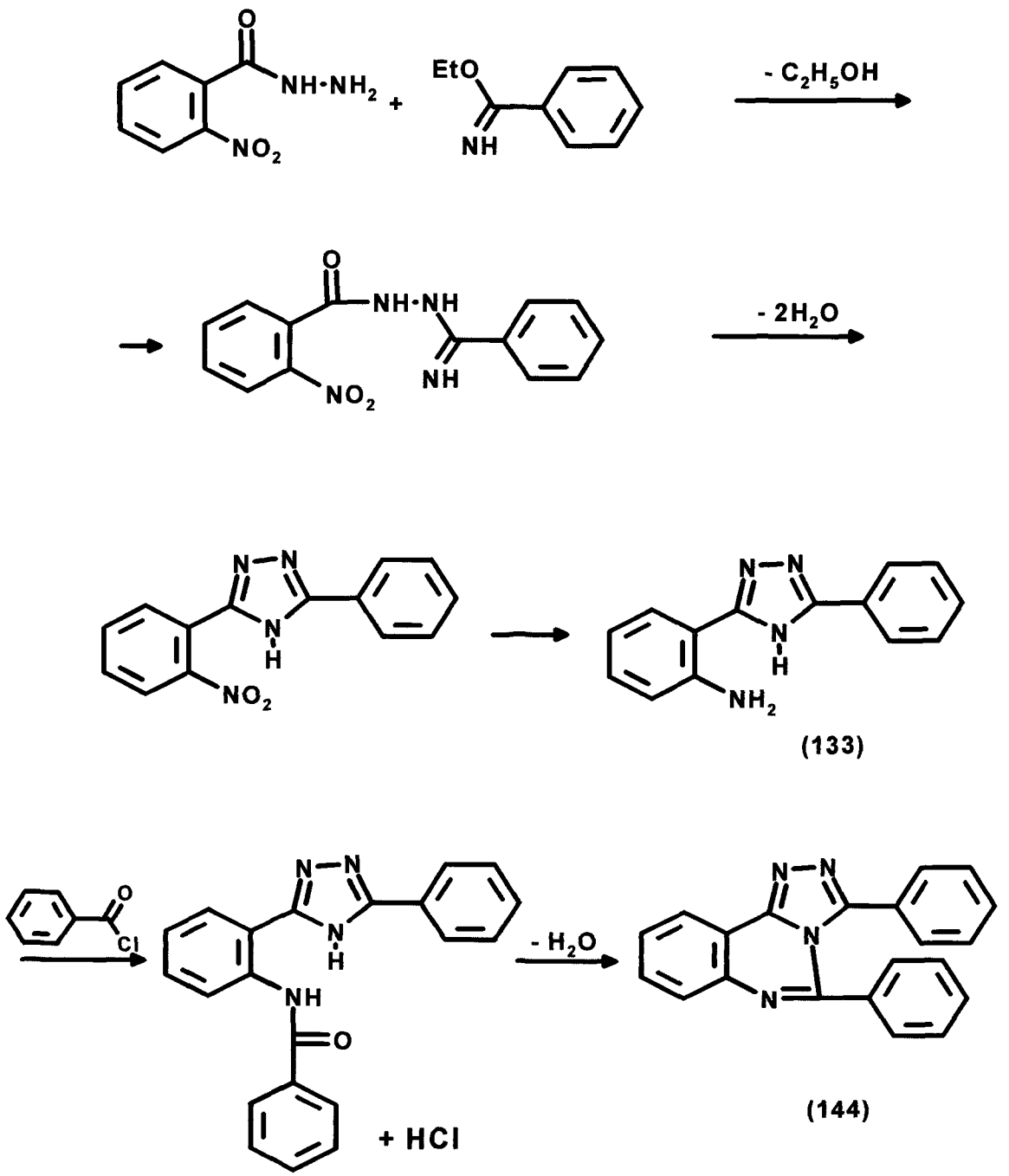

Scheme [2.17]

Korshak and co-workers synthesized their triazoles by reaction of acid chloride and amidrazone In preparation for these reactions they earlier produced triazoles e g **(133)** via the hydrazide/iminoether reaction pathway[19]

In the reaction, the imido ester of benzoic acid was reacted with *o*-nitrobenzoic acid hydrazide by boiling an alcoholic solution of equimolar amounts of the compounds for one hour The resulting yellow crystalline *o*-nitrobenzoyl benzamidrazone was subjected to cyclodehydration by heating under vacuum at 200°C for 2–2 5 hours The resulting nitrophenylene-1,2,4-triazole was reduced with hydrazine hydrate in ethanol in the presence of Raney Nickel catalyst to the aminophenylene triazole With this amino group now present quinazoline formation **(144)** then ensued on thermal cyclodehydration The reaction of the bis-(imidoester) of isophthalic acid with *o*-nitrobenzoic acethydrazide in boiling ethanol gave the corresponding bis-acylamidrazone **(145)** which was converted to the triazole **(146)** on heating under vacuum at 250°C for three hours as in Scheme [2 18]

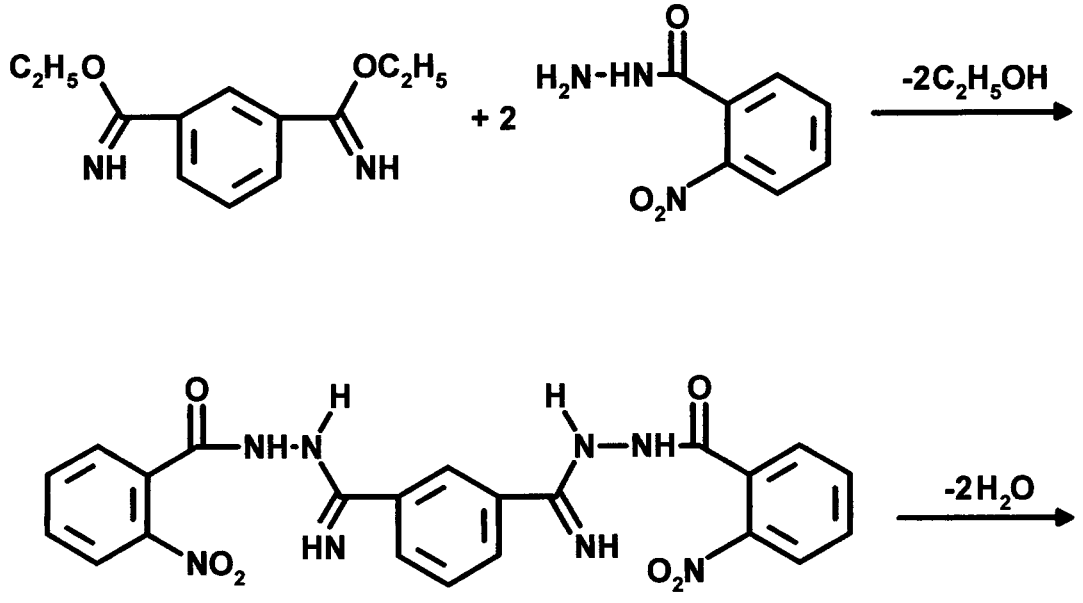

(145)

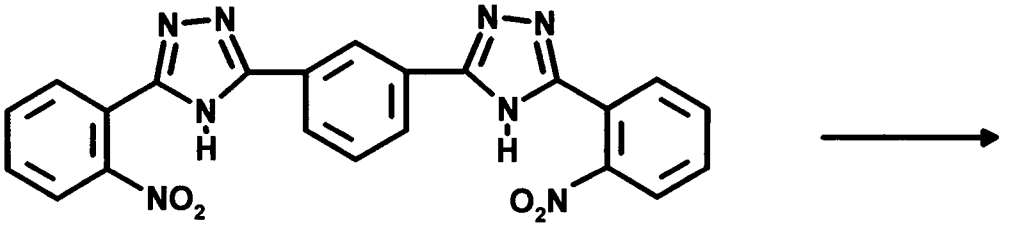

(146)

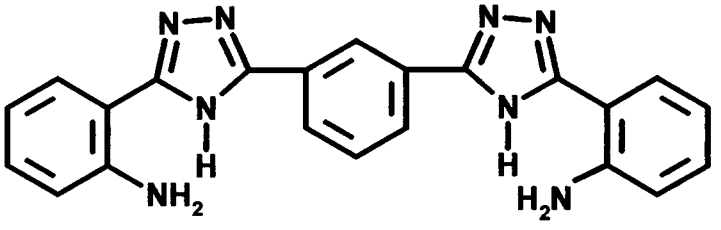

Scheme [2.18]

Further advancements in this area of research saw the use of 4,6-diamino-1,3-bis(5-phenyl-1,2,4-triazol-3-yl)benzene **(147)** as a monomer in model compound synthesis[20] The diamine was prepared from 4,6-dinitroisophthalic acid dichloride as shown below in Scheme [2 19]

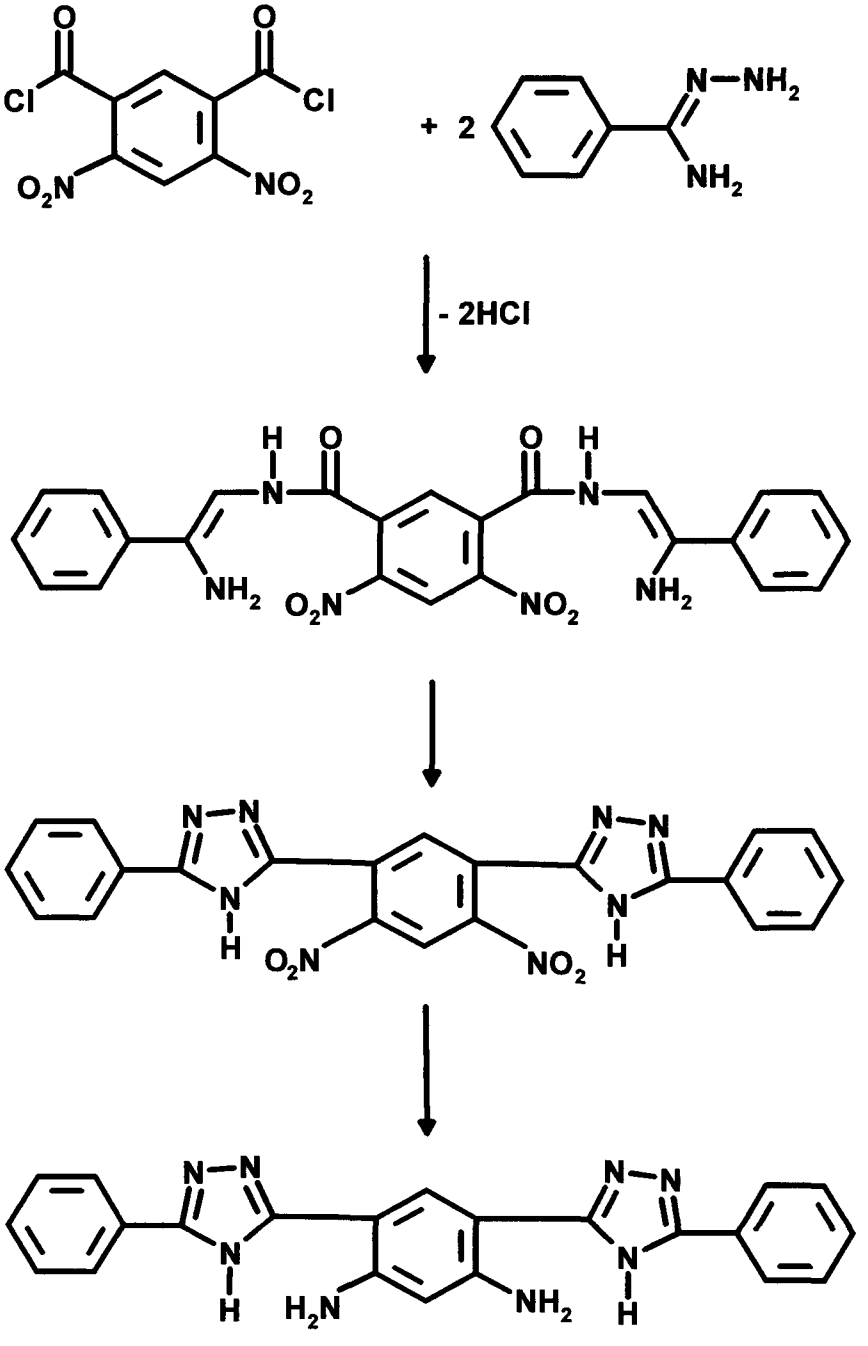

(147)

Scheme [2.19]

Reaction of these diamino triazoles with benzoyl chloride with subsequent dehydration gave rise to the new heterocyclic system 3,5,9,11-tetra-phenylbenz[1,2-g 4,5-g^1]bis(1,2,4)-triazole[4,3-c]pyridine **(148)**

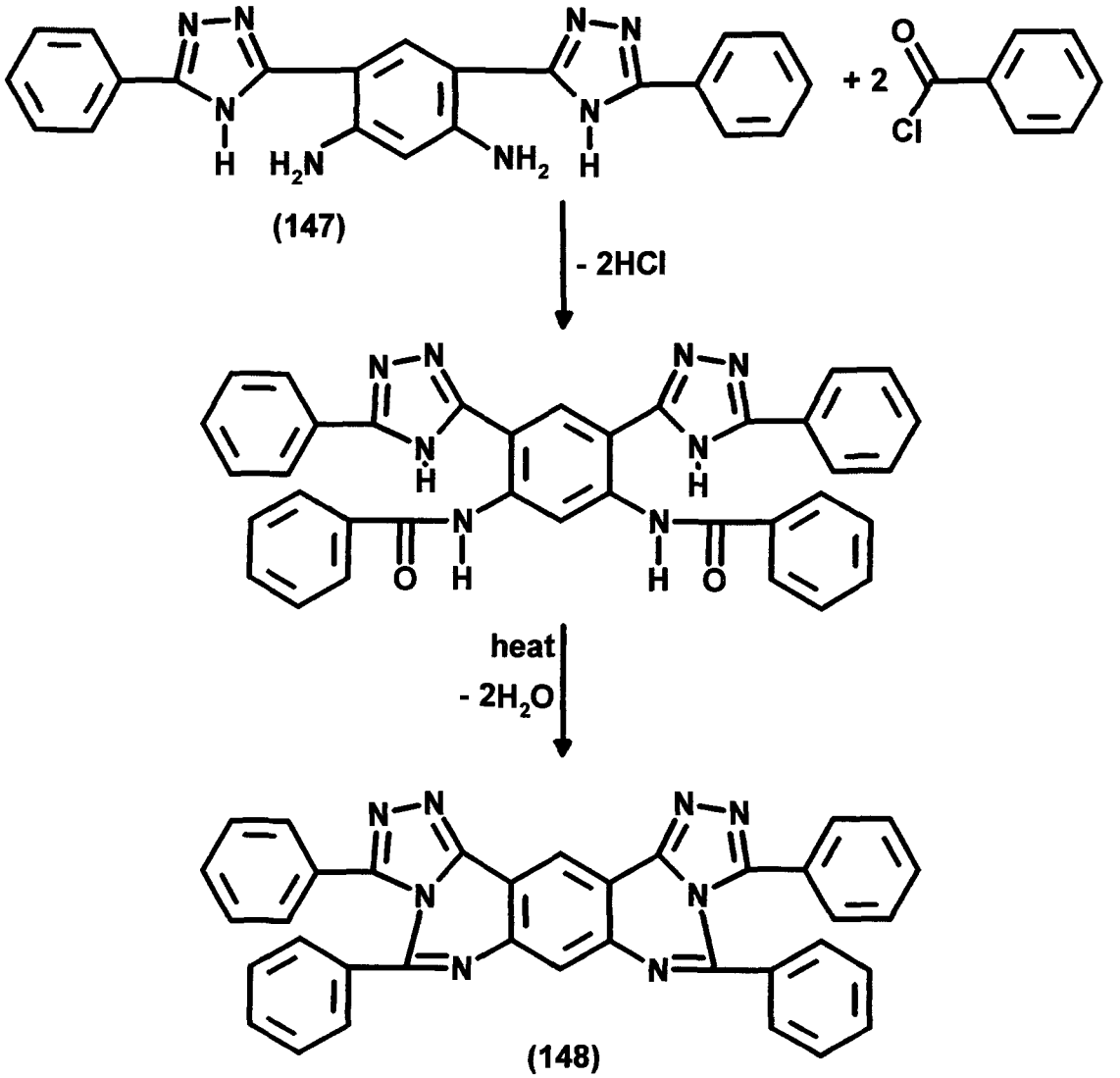

(147)

(148)

Scheme [2.20]

2.2 RESULTS AND DISCUSSION

2 2 1 Introduction

The aim of this chapter was to develop a successful method for the production of the following four ligands

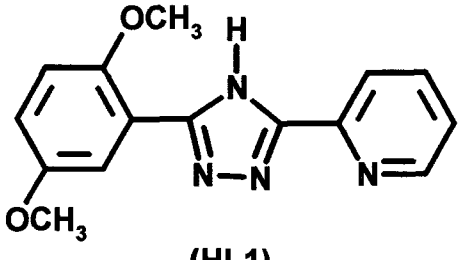

(HL1)

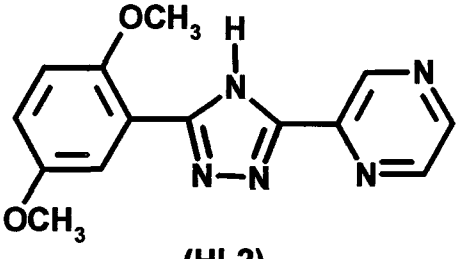

(HL2)

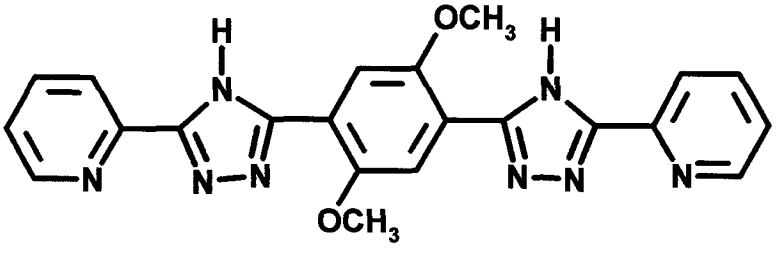

(H_2L3)

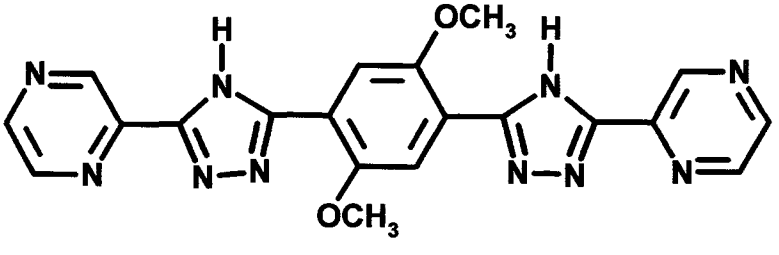

(H_2L4)

Fig. [2.1]

These ligands when complexed with ruthenium metal, could ultimately undergo a "deprotection" of their methoxy groups to corresponding hydroxyl groups. In the synthesis of the bis-triazoles above, one of the starting materials (the central aromatic ring of the molecule) was 2,5-dihydroxyterephthalate. It was decided to initially protect the hydroxyl functionality as its corresponding methyl ether. In doing this we are eliminating the chance of semiquinone or quinone formation which can occur at high temperatures in 1,4-dihydroxy aromatic molecules. Also blocking the hydroxyl centres eliminates the chance of ruthenium metal bonding at this site during the complexation reaction. This indirectly promotes coordination at the desired nitrogen sites. The starting material for the bis-triazole ligand synthesis is shown below.

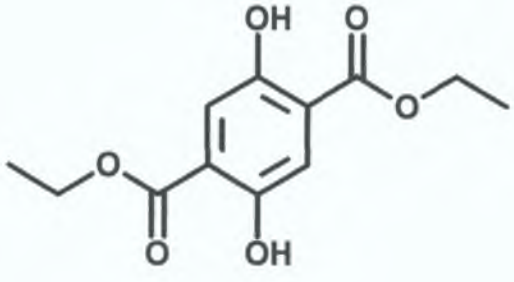

Fig. [2.2]

This molecule was purchased from the Aldrich chemical company. The initial protection reaction was adapted from a method described by Vogel[21] and produced quantitative yields of the dimethoxy product **(149)**.

The conversion is carried out by refluxing the dihydroxy starting material with methyl iodide in dry acetone in the presence of a base. It is imperative that an extra-long condenser be fitted to the reaction vessel during heating as methyl iodide is so volatile that it may escape through the top of an ordinary condenser thus reducing yields. The longer condenser provides the extra cooling glass surface to prevent loss of methyl iodide. Potassium carbonate is used to remove iodide ions produced in the reaction. Work-up of this reaction has the

advantage of being extremely quick and clean Filtration of the reaction mixture removes potassium carbonate while the removal of excess methyl iodide and acetone by rotary evaporation results in excellent yields of **(149)** The next step in the synthesis involves two stages, conversion of the diethyl esters to carboxylic acids **(150)** followed by diacid chloride formation **(151)**

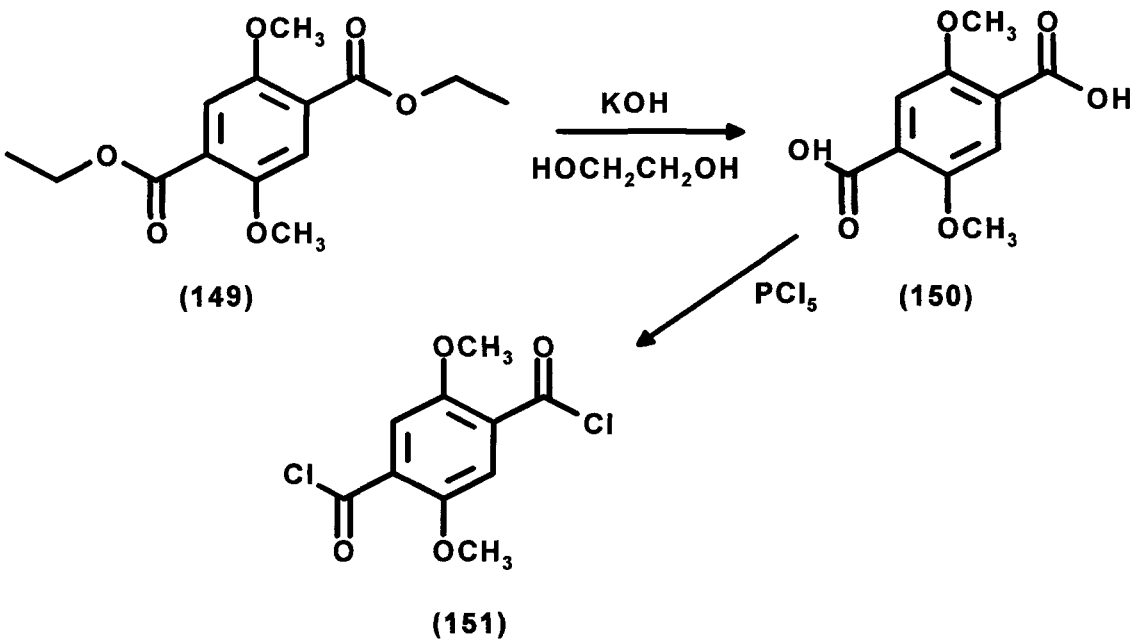

(149) **(150)** **(151)**

Scheme [2.22]

The saponification step was carried out with complete conversion The diester crystals **(149)** were added to a hot solution of potassium carbonate dissolved in ethylene glycol Initially ethanol is produced in the reaction which must be removed by distillation to eliminate ethyl ester reformation The addition of water completes dicarboxylic acid formation **(150)** The diacid precipitates on lowering the pH of the solution Great care must be taken to thoroughly dry the dicarboxylic acid before reaction with PCl_5 This is effectively achieved using P_2O_5 as drying agent in a Kugelrohr oven The presence of even trace amounts of water can adversely affect the acid chloride formation reaction
Also, when the diacid is thoroughly dried the solid-solid reaction with PCl_5 proceeds with only a small amount of heat activation being required The diacid chloride **(151)** formed was used immediately for acylamidrazone formation **(152)**

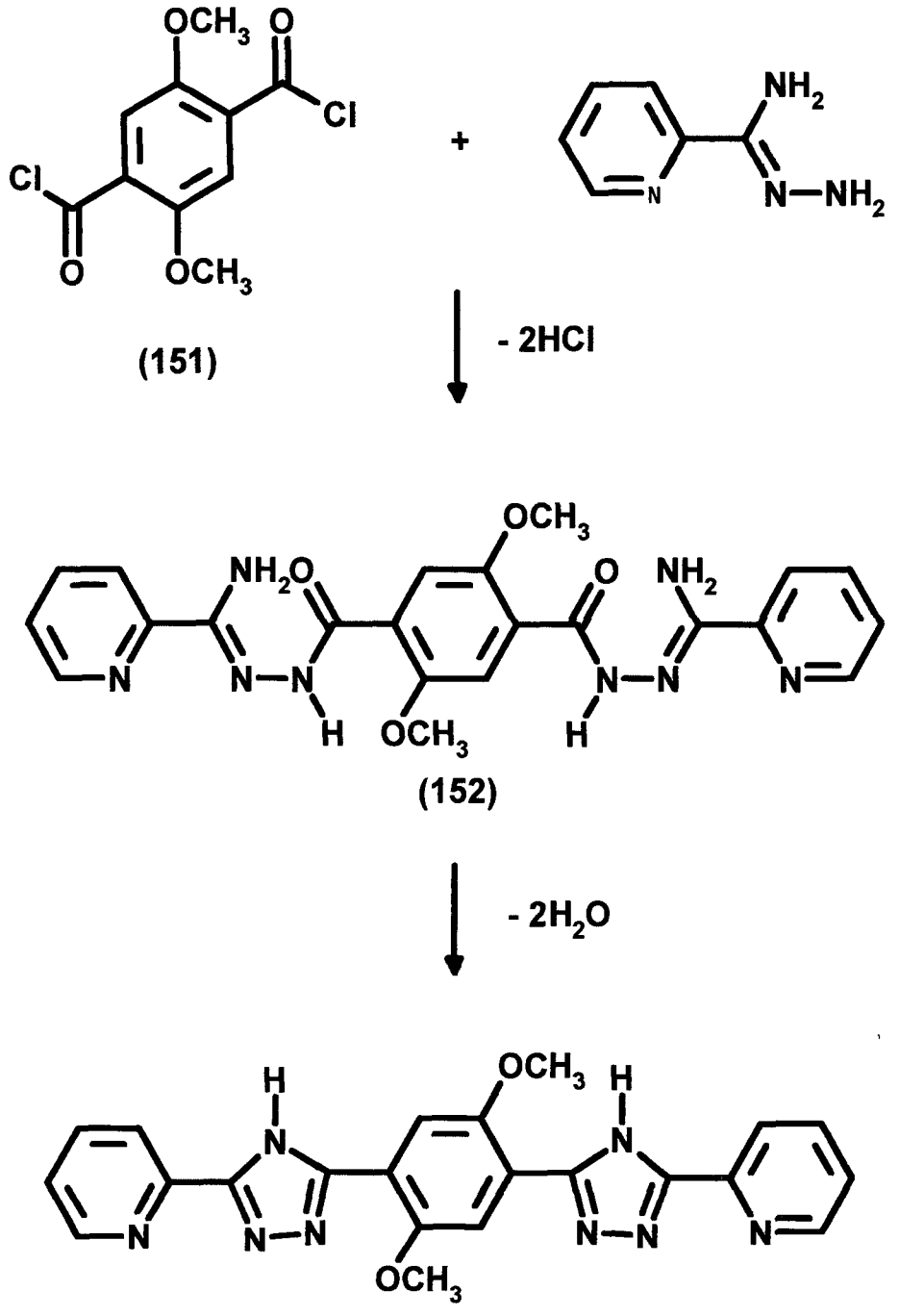

Scheme [2.23]

Pyridine or pyrazine amidrazone (the former is shown in Scheme [2 23] above) enters the synthesis at this stage to facilitate acylamidrazone formation

The acylamidrazone, if purified prior to cyclization with DMSO, results in purer triazole production As with the other triazoles described in chapter one, the thermal cyclization step is the least predictable Heating the yellow acylamidrazone in ethylene glycol until completely dissolved followed by refluxing until the clear yellow colour changes to clear brown, produces the best yields of triazoles

The triazolic products can sometimes be recrystallized from DMSO, however to obtain a suitable crystal for X-ray analysis the recrystallization solvent of choice was ethylene glycol The solvating properties of this solvent prevent recrystallization from ocurring too quickly which promotes better crystal formation DMSO has the disadvantage of allowing the product to precipitate rapidly often resulting in powder like products being formed The X-ray crystal structure of three of the four target ligands have been obtained while the structure of the pyrazine-bis-triazole which was recrystallized with excellent purity from DMSO remained elusive due its uncontrollably rapid rate of recrystallization from this solvent The mono-triazole target ligands (HL1) and (HL2) were synthesized using the same synthetic procedures as described for the bis-triazoles (H_2L3) and (H_2L4) The synthesis of these mono-triazoles proved more facile than their bis-triazole analogues Indeed good crystals of the mono-triazoles suitable for X-ray analysis were obtained using DCM as recrystallization solvent following cyclization with ethylene glycol

2.2.2 Spectroscopic analysis

Note: All ^{1}H-NMR spectra of acylamidrazones and triazoles were carried out in DMSO-d^{6} unless otherwise stated.

2.2.2.1 Acylamidrazones (154) and (155)

Having examined the NMR spectrum of the model acylamidrazone in Chapter one, the NMR spectra **(154)** and **(155)** were obtained and compared.

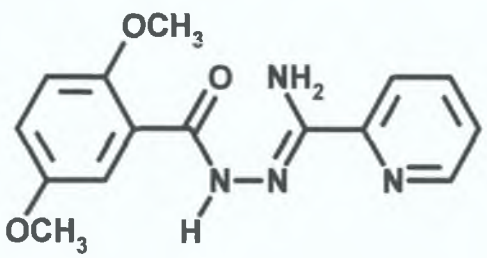

(154)

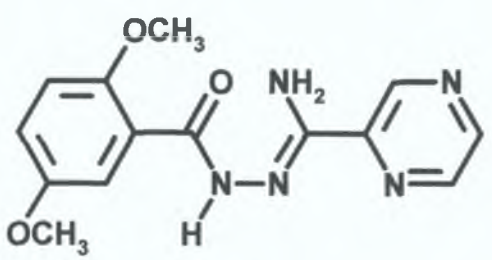

(155)

(154) and **(155)** both contain methoxy groups at the 1" and 4" positions of the benzene ring. The shielding effect of these groups on the aromatic protons results in an upfield shift being observed. In the model **(110)** the benzyl proton chemical shifts ranged from 7.54–8.04 ppm while **(154)** ranges from 7.05–7.15 ppm and **(155)** from 7.26–7.47 ppm.

A knock-on effect can be seen for the N–H proton. This proton, **(110),** appeared at 11.54 ppm, which we attributed to the deshielding effect of the nearby carbonyl group. Similar to the benzyl protons this N–H proton experiences an

upfield shift appearing at 10.15 ppm for **(154)** and 10.71 for **(155)**. Comparing the heteroaromatic parts of the molecule, the pyrazine protons of **(155)** appear further downfield than the pyridyl protons of **(110)** and **(154)**. H3 of **(155)** appears at 9.59 ppm compared with 8.47 ppm and 8.17 ppm for H3 of the **(110)** and **(154)** respectively. The absence of a proton within a three bond radius and no apparent long range coupling effects simplifies H3 of the pyrazine ring to a characteristic sharp singlet. Another characteristic feature of all three acylamidrazone spectra is the presence of a broad singlet of integration two. This peak represents the $-NH_2$ protons of the molecule. The presence of chemical exchange and hydrogen bonding effects both contribute to the unpredictability of the chemical shift of this peak. The $-NH_2$ peak appeared at 10.18 ppm in **(110)**, at 6.75 ppm in **(154)** and 9.92 ppm in **(155)**. Shown in Figures [2.3] is the ^{1}H-NMR spectra of **(154)**.

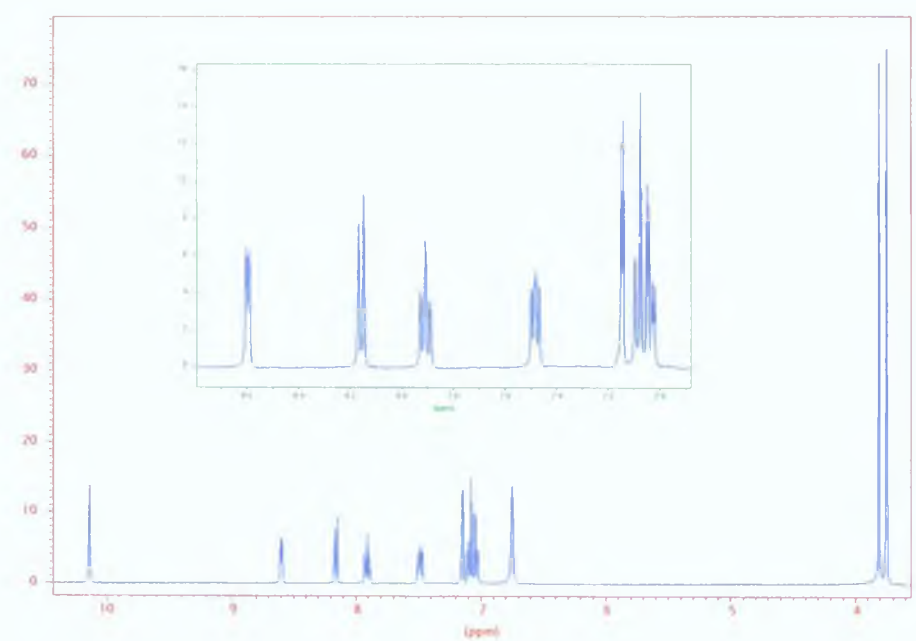

Fig. [2.3] NMR spectrum of (154).

In **(154)** and **(155)** the methoxy protons appear at similar chemical shifts The $-OCH_3$ protons in the 1" position appear further downfield in both cases at 3 81 ppm for **(154)** and 3 88 ppm for **(155)** the $-OCH_3$ of 4" at 3 75 ppm for **(154)** and 3 77 ppm for **(155)**

2.2.2.2 Acylamidrazones (152) and (153):

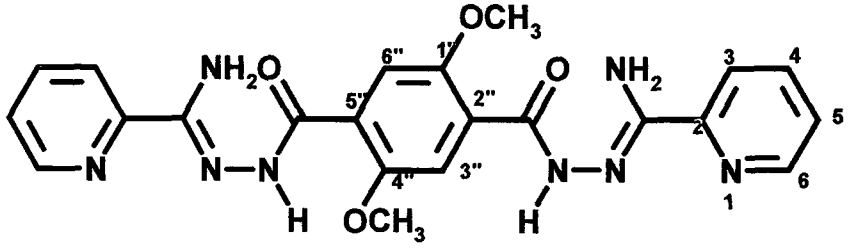

(152)

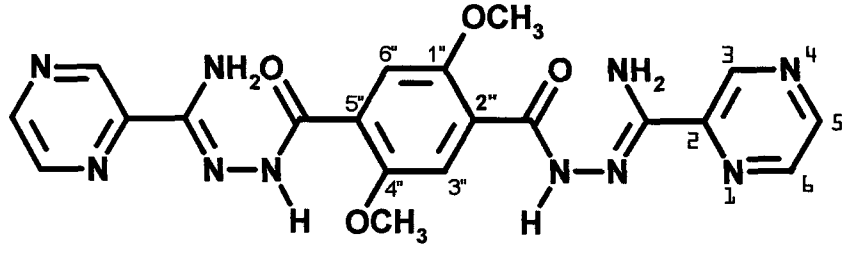

(153)

Fig. [2.4] (1520 and (153). Numbering shown.

These acylamidrazones possess very similar fundamental characteristics as the smaller type, i e the presence of a broadened singlet for –NH and the broadened singlet of integration four for $-NH_2$ However, these acylamidrazones possess a plane of symmetry running through the central aromatic ring and as such, only one set of NMR signals representing half of the molecule is seen The result is a greatly simplified spectrum

Comparing **(152)** and **(153)** to the model made in Chapter one, the first point of note is that the model **(107)** has four chemically equivalent aromatic protons with a signal at 8 06 ppm This is compared to H3" of **(152)** at 7 38 ppm and H3" of **(153)** at 7 37 ppm, leading to the same conclusion that the dimethoxy groups on the ring have a shielding effect on the aromatic protons The $-OCH_3$ signal appears at 4 03 ppm in **(152)**, which is significantly further downfield than **(153)** at 3 84 ppm Whereas with **(154)** and **(155)** there appeared to be a relation between the presence of methoxy groups on the benzene ring and the position of the –NH signal, this is not seen with the acylamidrazones **(152)** and **(153)** The –NH signal of the **(107)** is at 10 36 ppm, that of **(152)** is 10 21 ppm and **(153)** is 10 32 ppm The $-NH_2$ signals of the three acylamidrazones appear at similar chemical shifts, ranging from 6 81–7 04 ppm The less random appearance of these characteristic peaks aid structure elucidation greatly

As with **(155)**, **(153)** also exhibits pyrazine proton peaks at downfield shifts Whereas H6 of **(107)** and **(152)** both appear at 8 6 ppm and is the furthest downfield pyridine proton, H6 of **(153)** has a chemical shift of 8 74 ppm H3 of **(153)** again feels the electronegative effects of the proximal N atoms and results in a chemical shift of 9 32 ppm

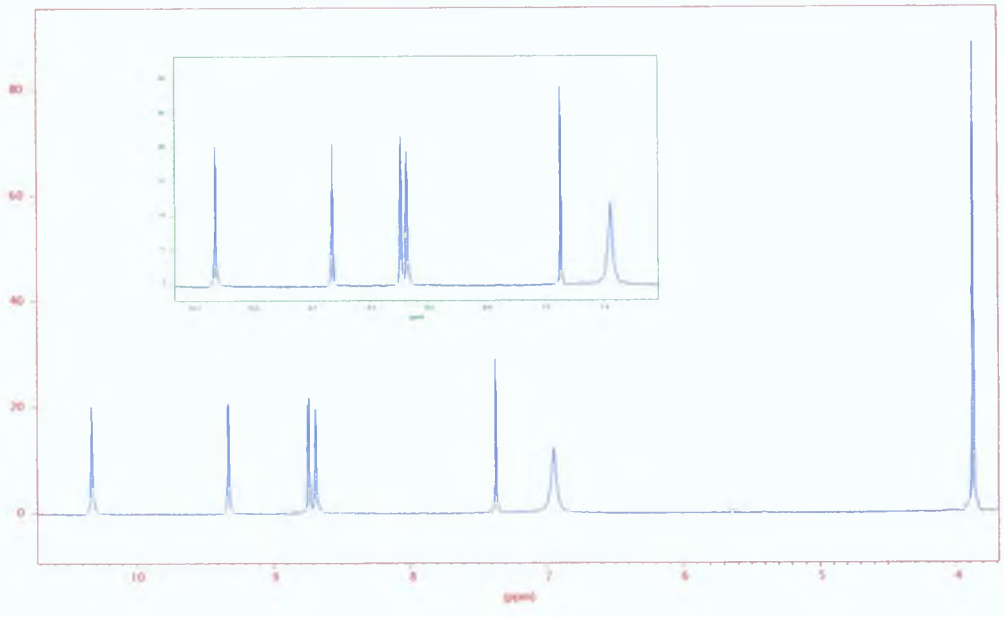

Fig. [2.5] (153) ^{1}H-NMR spectrum with expanded aromatic region.

2.2.2.3 Triazoles HL1 and HL2

In Chapter one we discussed the spectral changes observed on converting an acylamidrazone to a triazole. The replacement of the characteristic –NH and $-NH_2$ signals by one broad triazolic N–H signal between 14 and 15 ppm is the most notable difference in the spectrum.

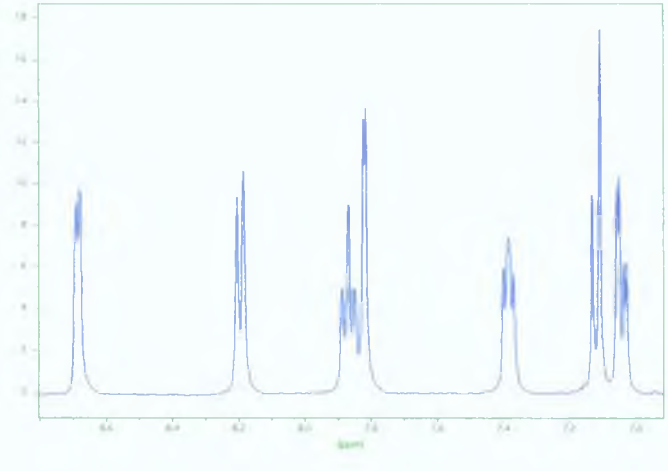

Fig. [2.6] Aromatic region of ^{1}H–NMR spectrum of HL1.

In **HL1** the $-OCH_3$ signal of position 1"appears at 3.99 ppm while that of position 4" is at 3.83 ppm. H3" of the benzene ring appears as a singlet at 7.82 ppm and H5" and H6" are the doublets in the region 7.0–7.2 ppm. H6" is the slightly more deshielded of the two peaks owing to its closer proximity to the triazole ring. H5" is the doublet of doublets due to interaction with H6" on one side and long range coupling to H3" on the other. The benzyl moieties of **HL1** and **HL2** have almost identical chemical shifts but again the pyrazine protons of **HL2** appear further downfield than the pyridine protons of **HL1**.

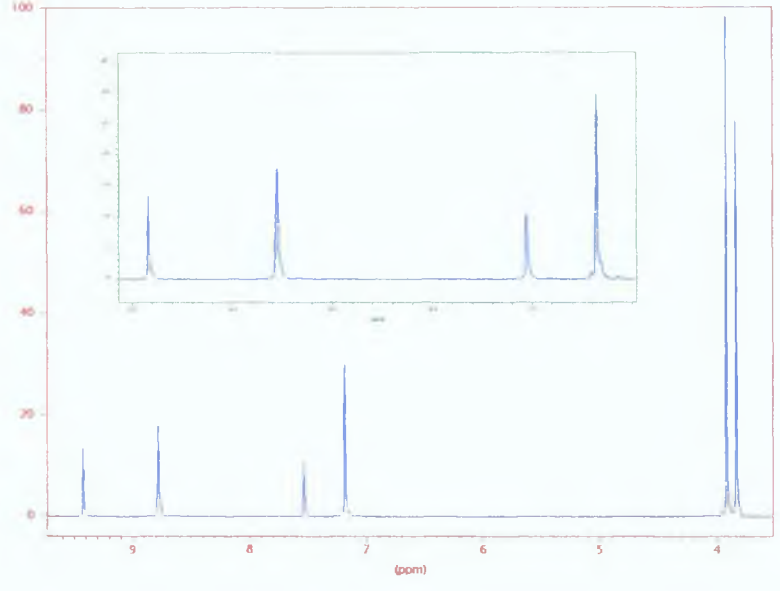

Fig. [2.7] ^{1}H-NMR of HL2 with aromatic region expanded.

These shift patterns can be viewed in terms of electron distribution using a software program called "Spartan"[22]. The "Spartan" program is used for molecular modelling. In general these programs perform mathematical calculations to give the resultant stereochemical representation of inputted hypothetical molecules. In this case the actual X-ray crystallographic data was available for HL1 and HL2 allowing us to view the electronic distribution in these

molecules. Electron density is portrayed in the pictures as coloured clouds surrounding atoms. Regions of high electron density are coloured red and areas of lower electron density as blue. The pictures may be used simply as a guide to aid NMR confirmation and to provide a view of the molecule from the point of view of electron density. Protons in proximity to electronegative atoms (appearing as regions of red) may experience a deshielding effect with resultant downfield signals in the NMR spectrum.

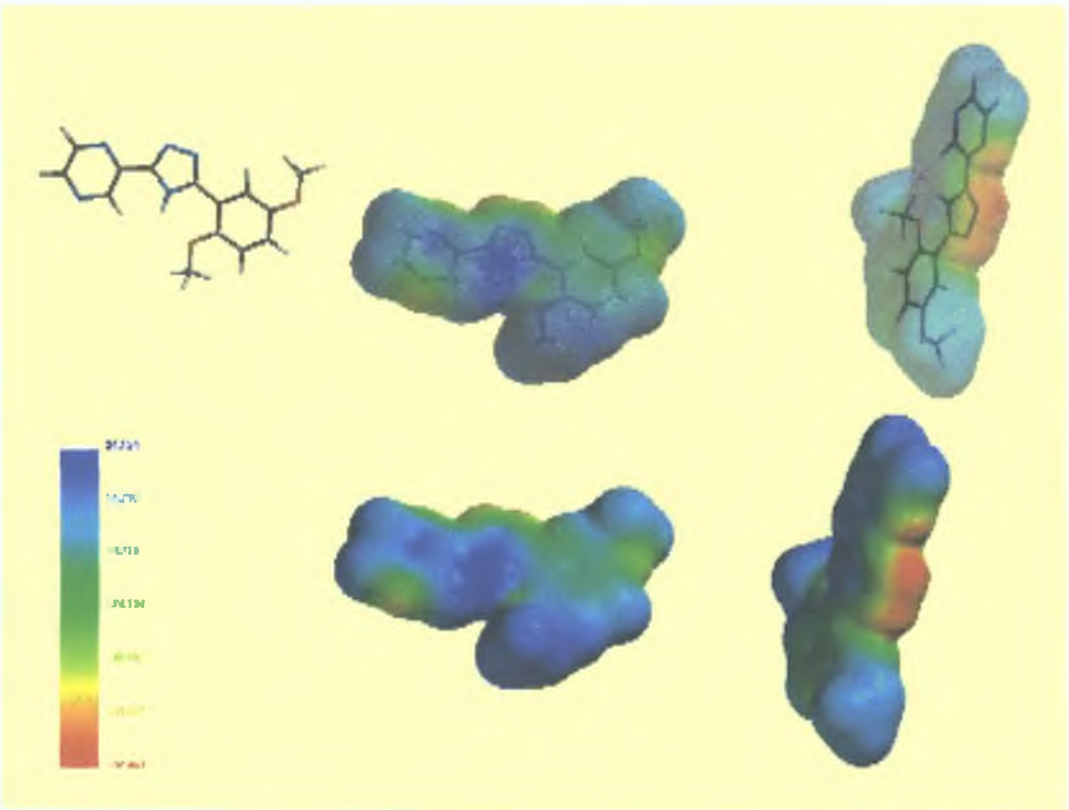

Fig. [2.8]: Spartan representations of HL2.

Triazoles H_2L3 and H_2L4

The spectra of these triazoles again reveal a greatly simplified picture due to the plane of symmetry existing in each of the molecules The model triazole had four chemically equivalent benzyl peaks but because only half the symmetric molecule is portrayed in the spectrum, one strong sharp singlet of integration two is seen at 8 25 ppm Since the central rings of **H_2L3** and **H_2L4** are 1",4"-dimethoxy substituted, only one benzylic proton at 7 94 ppm in **H_2L3** and 7 96 ppm in **H_2L4** is observed The $-OCH_3$ singlet has a similar chemical shift in **H_2L3** and **H_2L4** having values of 4 03 and 4 08 ppm respectively The triazolic –NH proton, which was seen in the model at 14 91 ppm, is at 14 11 in **H_2L3** but not seen below 15 ppm in **H_2L4** This may be due to the strong deshielding effect of the pyrazine ring with H3(9 37 ppm), H5(8 72 ppm) and H6(8 79 ppm) Note A common feature of these ligands is the broad appearance of the signals in ^{1}H-NMR spectra Zooming in on the tops of the peaks shows splitting is occurring as doublets, triplets as clearly visible on close inspection The broadening effects may be due to one of the reasons outlined in the NMR discussion in Chapter One

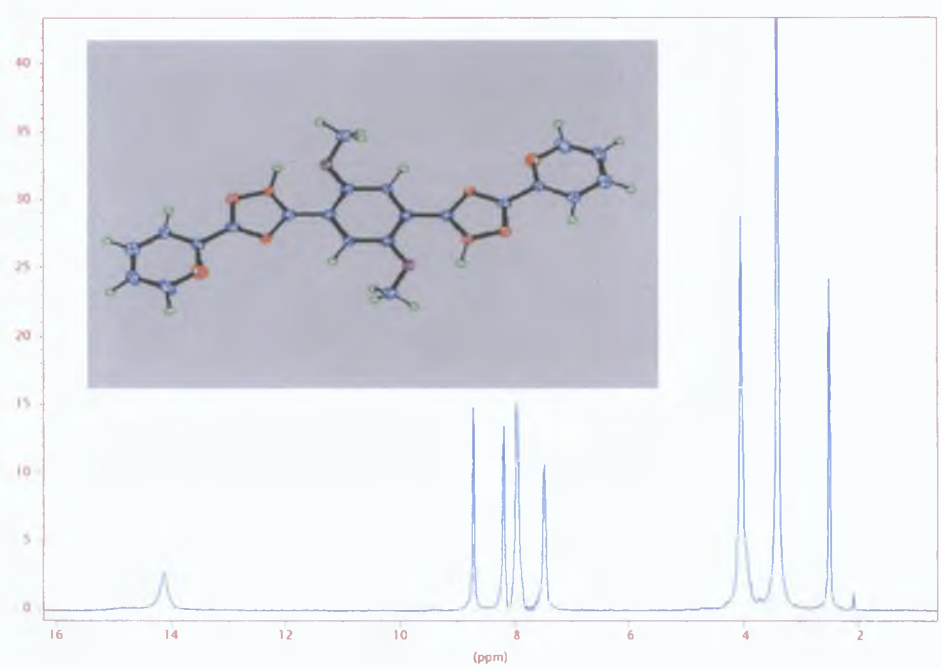

Fig. [2.9] ^{1}H-NMR of H_2L3

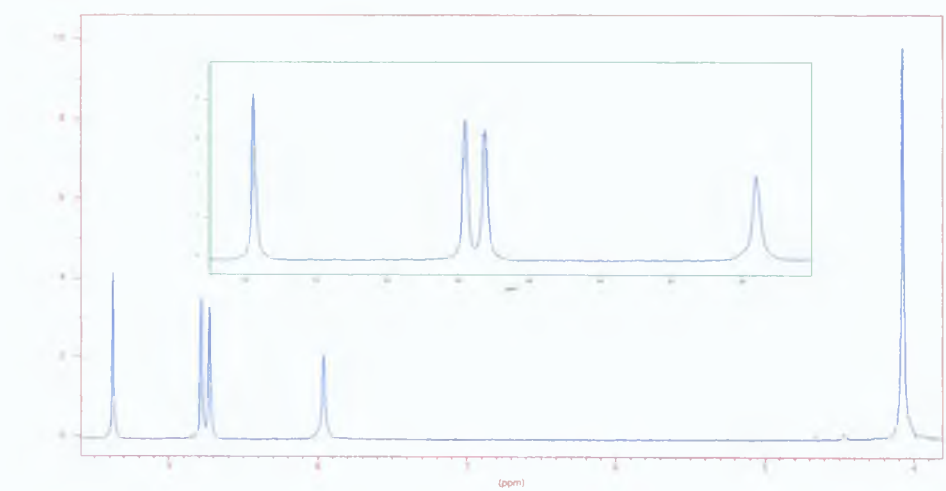

Fig. [2.10] ^{1}H-NMR of H_2L4 with aromatic region expanded.

2 2 3 X-ray Structure Determination

2.2.3.1 X-ray crystal structure of 3-(1,4-dimethoxyphenyl)-5-pyridinyl-1H-1,2,4-triazole (HL1)

This structure determination was carried out by Mr Mark Niewenhuyzen of Queen's University Belfast The molecular structure of HL1 is shown in fig [2 12] from two perspectives for clarity The first picture has the crystallographers atomic labeling shown

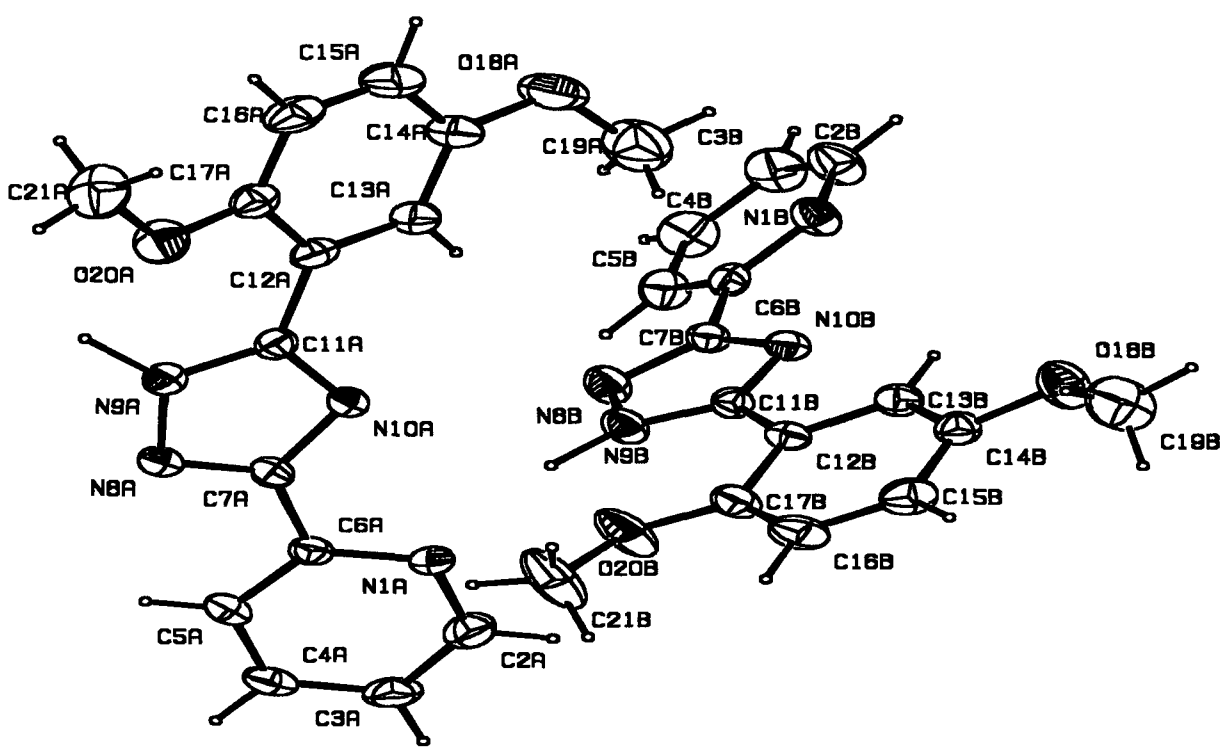

Fig. [2.11] Structure of HL1. Crystallographers numbering shown.

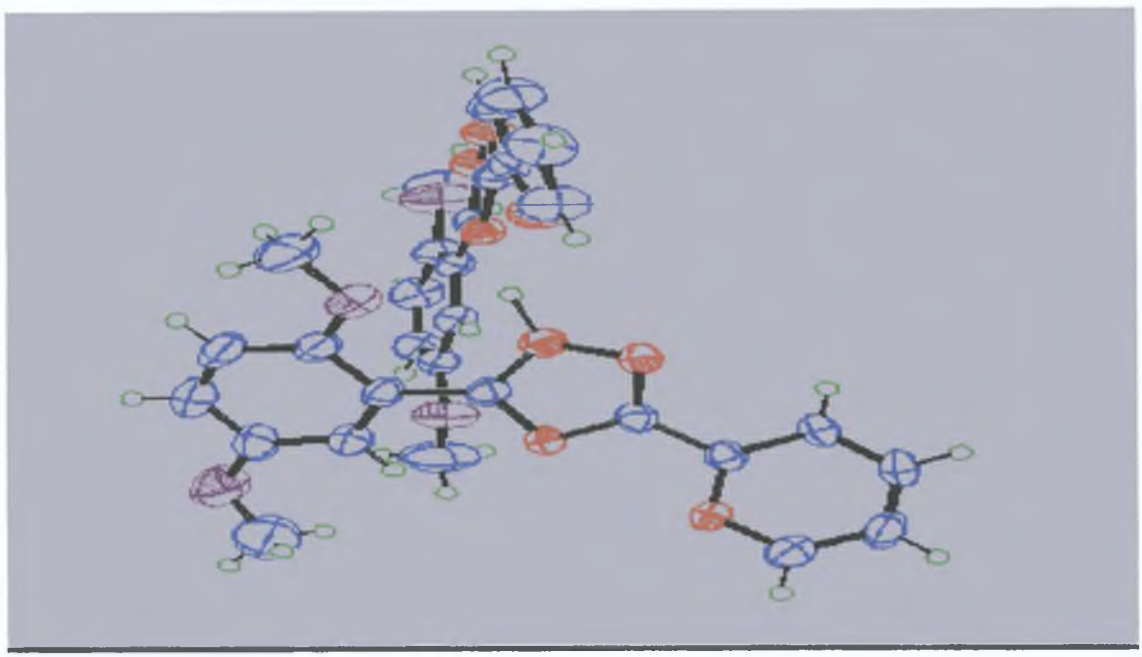

Fig. [2.12] Structure of HL1 shown from another angle.

HL1 has a $P2_1/n$ space group (with Cu radiation). There are eight molecules in the unit cell (two in the asymmetric unit). The unit cell contains no residual or *potential* solvent volume. An approximate fit between the two molecules 1 and 2 (*inverted*) is 3.83 A (this *presumes* that the labelling scheme is identical pairwise between the two molecules).

Intra- and Intermolecular H-bonding distances are:

N9B...O20B is 2.70 Å Intra

N9B...N1A is 2.94 Å Intra

N9B...N10A is 3.28 Å Intra

C13A...N10A is 2.88 Å Intra

C13B...N10B is 2.84 A Intra

N9A...N1B is 2.93 Å Inter [2655.02]

N9A...N10B is 3.33 Å Inter [2655.02]

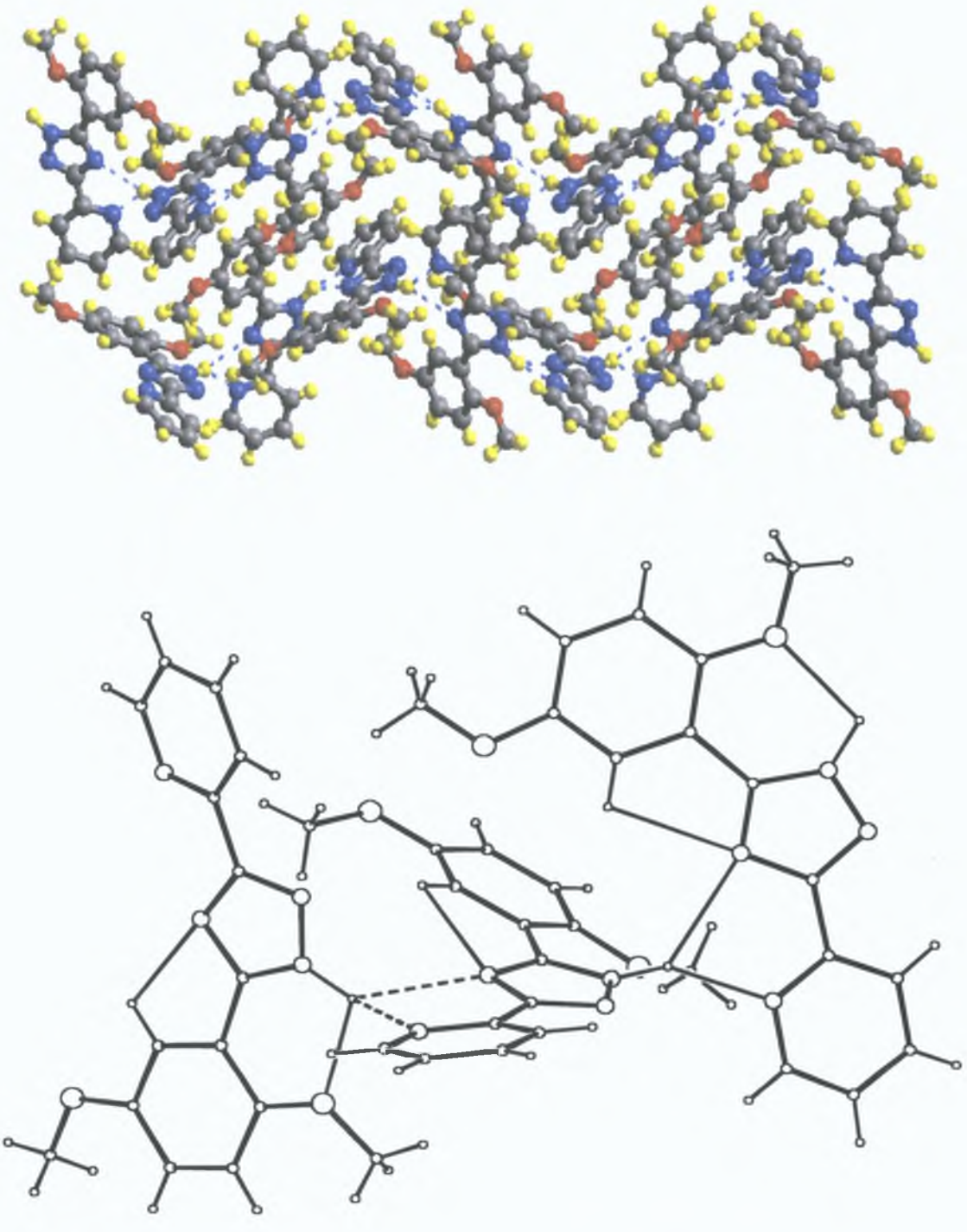

Fig. [2.13] Two views of crystal packing structure of HL1 with hydrogen bonding illustrated.

Bond	Length (Angstroms)	Bond	Length (Angstroms)
N(1A)-C(2A)	1 341(6)	N(1B)-C(2B)	1 330(6)
N(1A)-C(6A)	1 344(5)	N(1B)-C(6B)	1 336(6)
C(2A)-C(3A)	1 377(7)	C(2B)-C(3B)	1 366(7)
C(3A)-C(4A)	1 366(7)	C(3B)-C(4B)	1 368(7)
C(4A)-C(5A)	1 378(6)	C(4B)-C(5B)	1 373(7)
C(5A)-C(6A)	1 390(6)	C(5B)-C(6B)	1 377(6)
C(6A)-C(7A)	1 472(6)	C(6B)-C(7B)	1 471(6)
C(7A)-N(8A)	1 316(5)	C(7B)-N(8B)	1 320(5)
C(7A)-N(10A)	1 359(5)	C(7B)-N(10B)	1 356(5)
N(8A)-N(9A)	1 359(5)	N(8B)-N(9B)	1 355(5)
N(9A)-C(11A)	1 345(5)	N(9B)-C(11B)	1 343(5)
N(10A)-C(11A)	1 334(5)	N(10B)-C(11B)	1 335(5)
C(11A)-C(12A)	1 470(6)	C(11B)-C(12B)	1 462(6)
C(12A)-C(17A)	1 395(6)	C(12B)-C(13B)	1 383(6)
C(12A)-C(13A)	1 404(6)	C(12B)-C(17B)	1 394(6)
C(13A)-C(14A)	1 386(7)	C(13B)-C(14B)	1 381(6)
C(14A)-O(18A)	1 366(6)	C(14B)-O(18B)	1 371(6)
C(14A)-C(15A)	1 379(7)	C(14B)-C(15B)	1 379(7)
C(15A)-C(16A)	1 376(7)	C(15B)-C(16B)	1 380(7)
C(16A)-C(17A)	1 388(7)	C(16B)-C(17B)	1 380(7)
C(17A)-O(20A)	1 369(6)	C(17B)-O(20B)	1 361(6)
O(18A)-C(19A)	1 360(7)	O(18B)-C(19B)	1 383(6)
O(20A)-C(21A)	1 433(6)	O(20B)-C(21B)	1 408(6)

Table [2.1]: Bond Lengths of HL1.

ıd	Angle (degrees)	Bond	Angle (degrees)
A)-N(1A)-C(6A)	116 8(4)	C(2B)-N(1B)-C(6B)	117 2(4)
A)-C(2A)-C(3A)	123 9(5)	N(1B)-C(2B)-C(3B)	123 9(5)
A)-C(3A)-C(2A)	118 6(5)	C(2B)-C(3B)-C(4B)	118 7(5)
A)-C(4A)-C(5A)	119 1(5)	C(3B)-C(4B)-C(5B)	118 5(5)
A)-C(5A)-C(6A)	119 0(5)	C(4B)-C(5B)-C(6B)	119 5(5)
A)-C(6A)-C(5A)	122 5(4)	N(1B)-C(6B)-C(5B)	122 2(4)
A)-C(6A)-C(7A)	115 8(4)	N(1B)-C(6B)-C(7B)	116 1(4)
A)-C(6A)-C(7A)	121 7(4)	C(5B)-C(6B)-C(7B)	121 7(4)
A)-C(7A)-N(10A)	115 2(4)	N(8B)-C(7B)-N(10B)	114 7(4)
A)-C(7A)-C(6A)	122 9(4)	N(8B)-C(7B)-C(6B)	121 8(4)
0A)-C(7A)-C(6A)	121 8(4)	N(10B)-C(7B)-C(6B)	123 5(4)
A)-N(8A)-N(9A)	102 4(4)	C(7B)-N(8B)-N(9B)	102 3(4)
1A)-N(9A)-N(8A)	110 1(4)	C(11B)-N(9B)-N(8B)	110 7(4)
1A)-N(10A)-C(7A)	102 8(4)	C(11B)-N(10B)-C(7B)	103 4(4)
0A)-C(11A)-N(9A)	109 5(4)	N(10B)-C(11B)-N(9B)	108 8(4)
0A)-C(11A)-C(12A)	124 0(4)	N(10B)-C(11B)-C(12B)	123 1(4)
)A)-C(11A)-C(12A)	126 4(4)	N(9B)-C(11B)-C(12B)	128 0(4)
7A)-C(12A)-C(13A)	119 2(4)	C(13B)-C(12B)-C(17B)	118 5(4)
7A)-C(12A)-C(11A)	124 0(5)	C(13B)-C(12B)-C(11B)	118 0(4)
3A)-C(12A)-C(11A)	116 7(4)	C(17B)-C(12B)-C(11B)	123 5(4)
4A)-C(13A)-C(12A)	120 6(5)	C(12B)-C(13B)-C(14B)	121 5(4)
8A)-C(14A)-C(15A)	116 4(5)	O(18B)-C(14B)-C(15B)	125 0(4)
8A)-C(14A)-C(13A)	124 7(5)	O(18B)-C(14B)-C(13B)	115 6(4)
5A)-C(14A)-C(13A)	118 9(6)	C(15B)-C(14B)-C(13B)	119 4(5)
6A)-C(15A)-C(14A)	121 5(5)	C(16B)-C(15B)-C(14B)	119 7(5)
5A)-C(16A)-C(17A)	120 0(5)	C(15B)-C(16B)-C(17B)	121 0(5)
20A)-C(17A)-C(16A)	124 2(5)	O(20B)-C(17B)-C(16B)	124 0(4)
20A)-C(17A)-C(12A)	116 0(4)	O(20B)-C(17B)-C(12B)	116 2(4)
6A)-C(17A)-C(12A)	119 7(5)	C(16B)-C(17B)-C(12B)	119 7(5)
9A)-O(18A)-C(14A)	117 8(5)	C(14B)-O(18B)-C(19B)	118 2(5)
7A)-O(20A)-C(21A)	118 6(4)	C(17B)-O(20B)-C(21B)	118 7(4)

Table [2.2]: Bond angles of HL1.

2.2.3.2 X-ray crystal structure of 3-(1,4-dimethoxyphenyl)-5-pyrazin-2-yl)-1H-1,2,4-triazole (HL2)

The structure determination was carried out by Mr. Mark Niewenhuyzen of Queen's University Belfast.

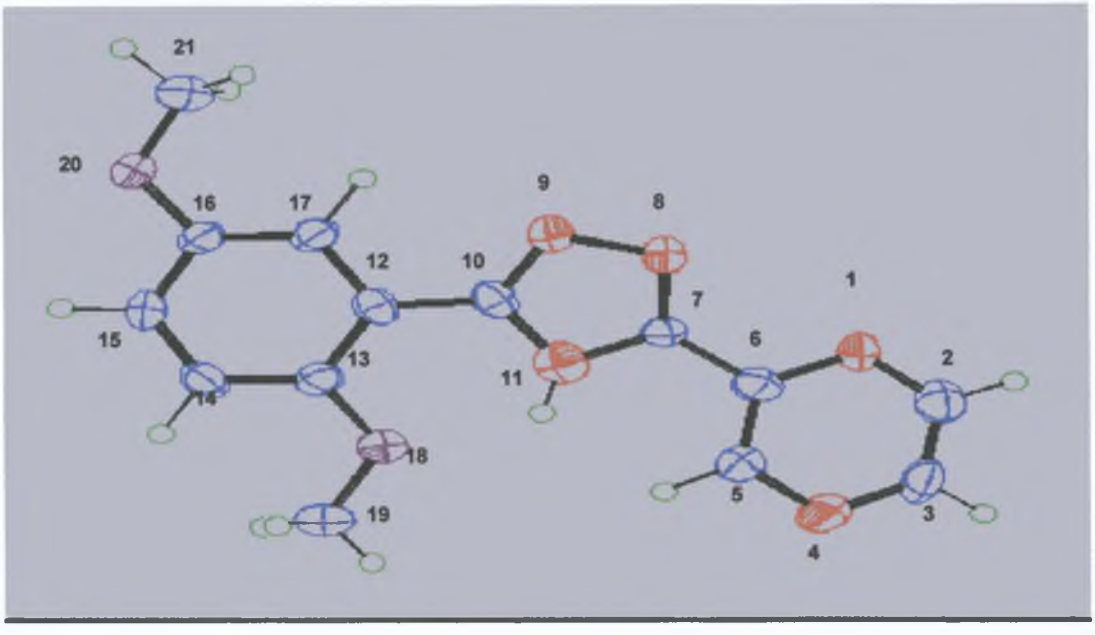

Fig. [2.14] X-ray crystal structure of HL2 with crystallographers numbering scheme shown.

The space group of HL2 is $P2_1$ (with Cu radiation). There are two molecules in the unit cell (one in the asymmetric unit). The unit cell contains no residual or *potential* solvent volume.

Intra- and Intermolecular H-bonding distances are:

N11...O18 is 2.60 Å Intra

C2...N9 is 3.50 Å Inter [2555]

C14...N4 is 3.65 Å Inter [2746]

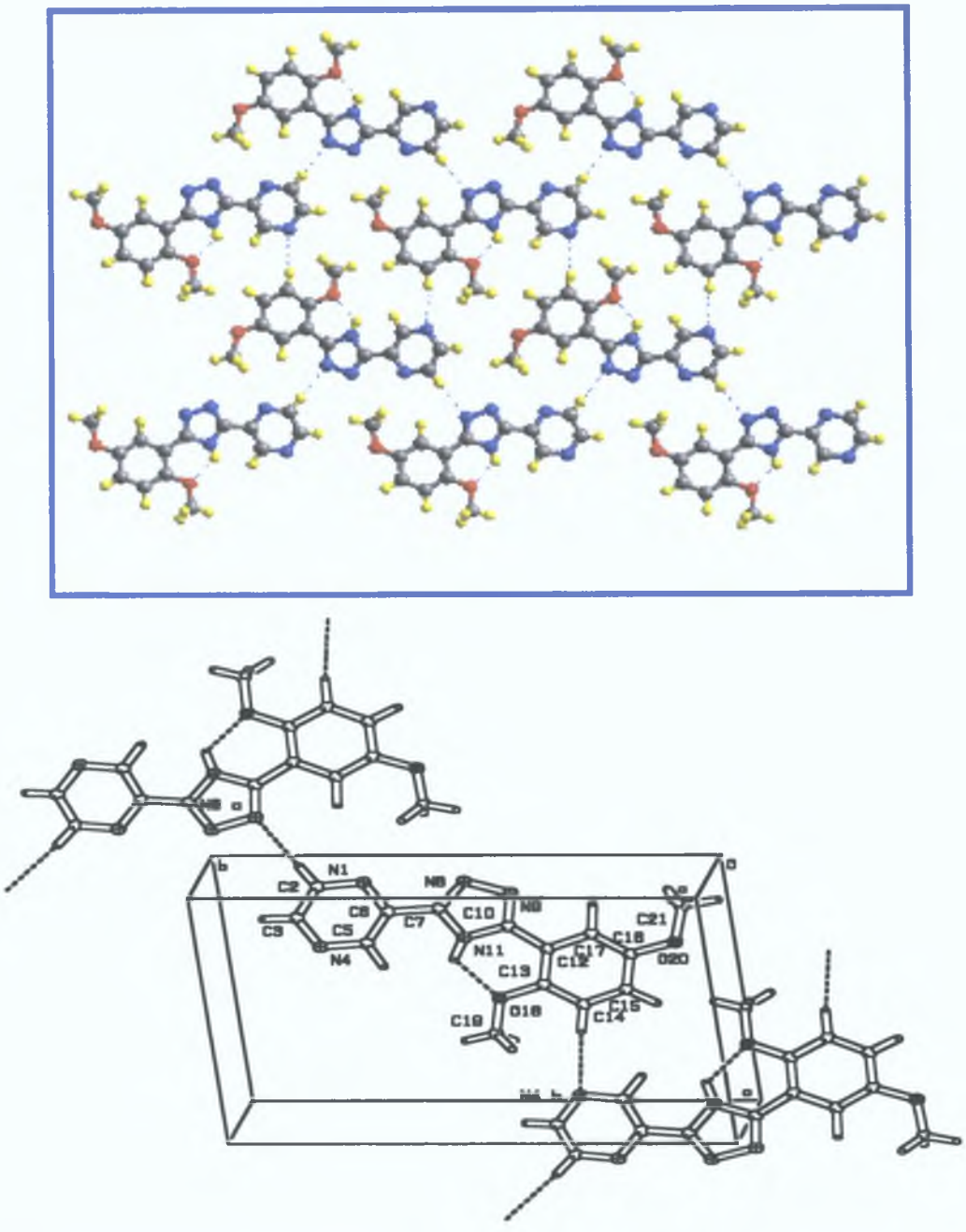

Fig. [2.15] Two views of crystal packing structure of HL2 with hydrogen bonding illustrated.

Bond	Length (Angstroms)	Bond	Length (Angstroms)
N(1)-C(2)	1.329(9)	C(10)-C(12)	1.452(9)
N(1)-C(6)	1.345(8)	C(12)-C(17)	1.406(8)
C(2)-C(3)	1.369(10)	C(12)-C(13)	1.410(9)
C(3)-N(4)	1.331(9)	C(13)-O(18)	1.380(8)
N(4)-C(5)	1.345(9)	C(13)-C(14)	1.387(9)
C(5)-C(6)	1.381(9)	C(14)-C(15)	1.367(9)
C(6)-C(7)	1.458(9)	C(15)-C(16)	1.394(8)
C(7)-N(8)	1.299(8)	C(16)-C(17)	1.370(9)
C(7)-N(11)	1.351(8)	C(16)-O(20)	1.381(8)
N(8)-N(9)	1.411(8)	O(18)-C(19)	1.433(8)
N(9)-C(10)	1.291(8)	O(20)-C(21)	1.438(8)
C(10)-N(11)	1.344(8)		

Table [2.3]: Bond Lengths of HL2.

nd	Angle (degrees)	Bond	Angle (degrees)
2)-N(1)-C(6)	115.5(6)	C(10)-N(11)-C(7)	103.7(4)
1)-C(2)-C(3)	122.5(7)	C(17)-C(12)-C(13)	119.1(5)
4)-C(3)-C(2)	123.0(6)	C(17)-C(12)-C(10)	117.3(5)
3)-N(4)-C(5)	115.1(6)	C(13)-C(12)-C(10)	123.6(6)
4)-C(5)-C(6)	122.1(7)	O(18)-C(13)-C(14)	123.3(6)
1)-C(6)-C(5)	121.9(6)	O(18)-C(13)-C(12)	117.1(5)
1)-C(6)-C(7)	117.6(6)	C(14)-C(13)-C(12)	119.6(6)
5)-C(6)-C(7)	120.5(6)	C(15)-C(14)-C(13)	120.6(6)
3)-C(7)-N(11)	112.5(5)	C(14)-C(15)-C(16)	120.2(6)
3)-C(7)-C(6)	128.9(6)	C(17)-C(16)-O(20)	124.6(5)
11)-C(7)-C(6)	118.5(6)	C(17)-C(16)-C(15)	120.5(6)
7)-N(8)-N(9)	105.0(5)	O(20)-C(16)-C(15)	114.9(6)
10)-N(9)-N(8)	106.8(5)	C(16)-C(17)-C(12)	119.9(6)
9)-C(10)-N(11)	112.0(5)	C(13)-O(18)-C(19)	116.9(5)
9)-C(10)-C(12)	125.8(6)	C(16)-O(20)-C(21)	118.2(5)
11)-C(10)-C(12)	122.3(5)		

Table [2.4]: Bond angles of HL2.

2.2.3.3 X-ray crystal structure of 1,4-dimethoxy-2,5-bis(pyridin-2-yl-1,2,4-triazol-3-yl)benzene (H_2L3)

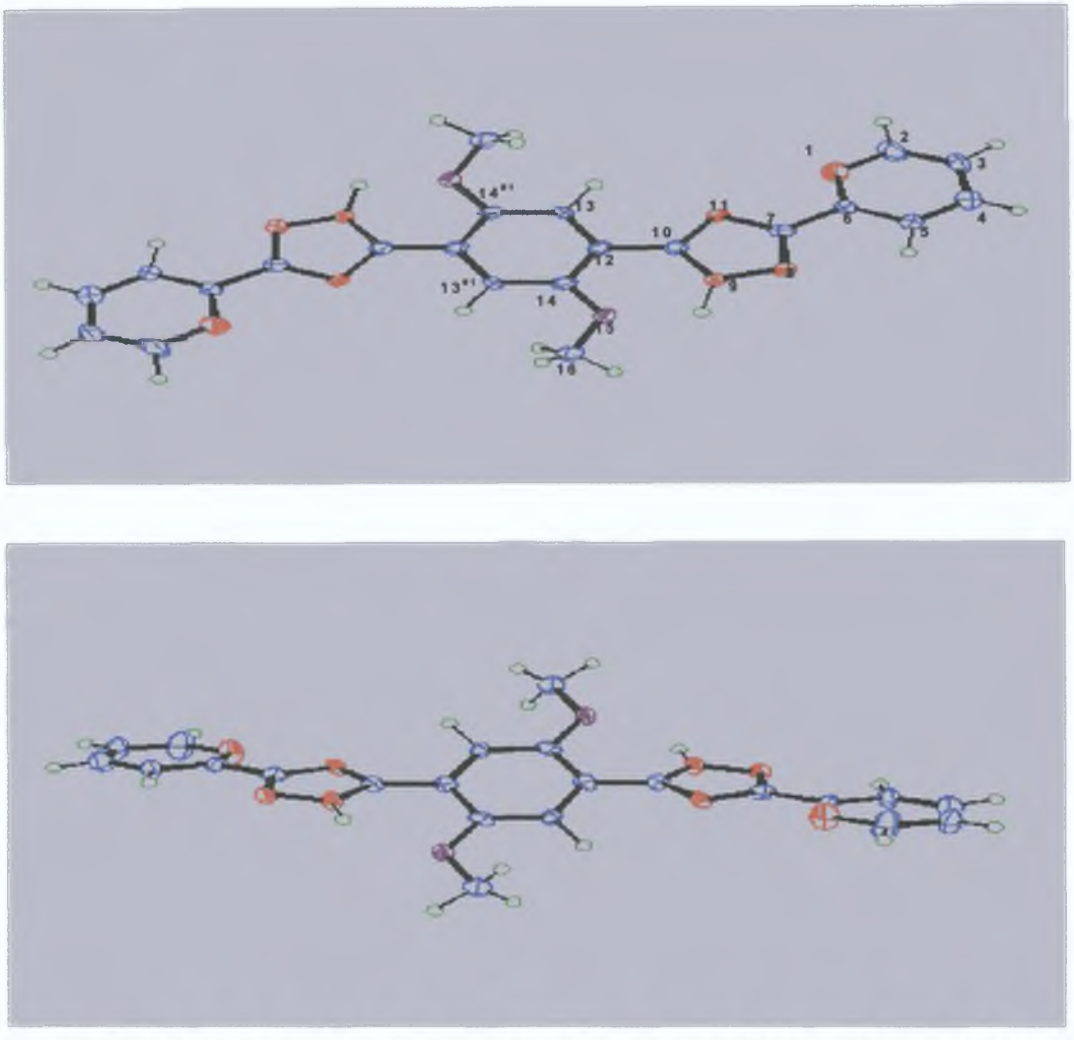

Fig. [2.16]: Two perspectives of the X-ray crystal structure of H_2L3. (Crystallographers numbering shown (top)).

The space group of H2L3 is $P2_1/c$ (with Mo radiation). There are two molecules in the unit cell (half molecule in the asymmetric unit). The unit cell contains no residual or *potential* solvent volume.

Intra- and Intermolecular H-bonding distances are:

N9...N11 is 2.90 Å Inter [4554]

C5...N8 is 2.91 Å Intra

C13...N8 is 3.65 Å Inter [2554]

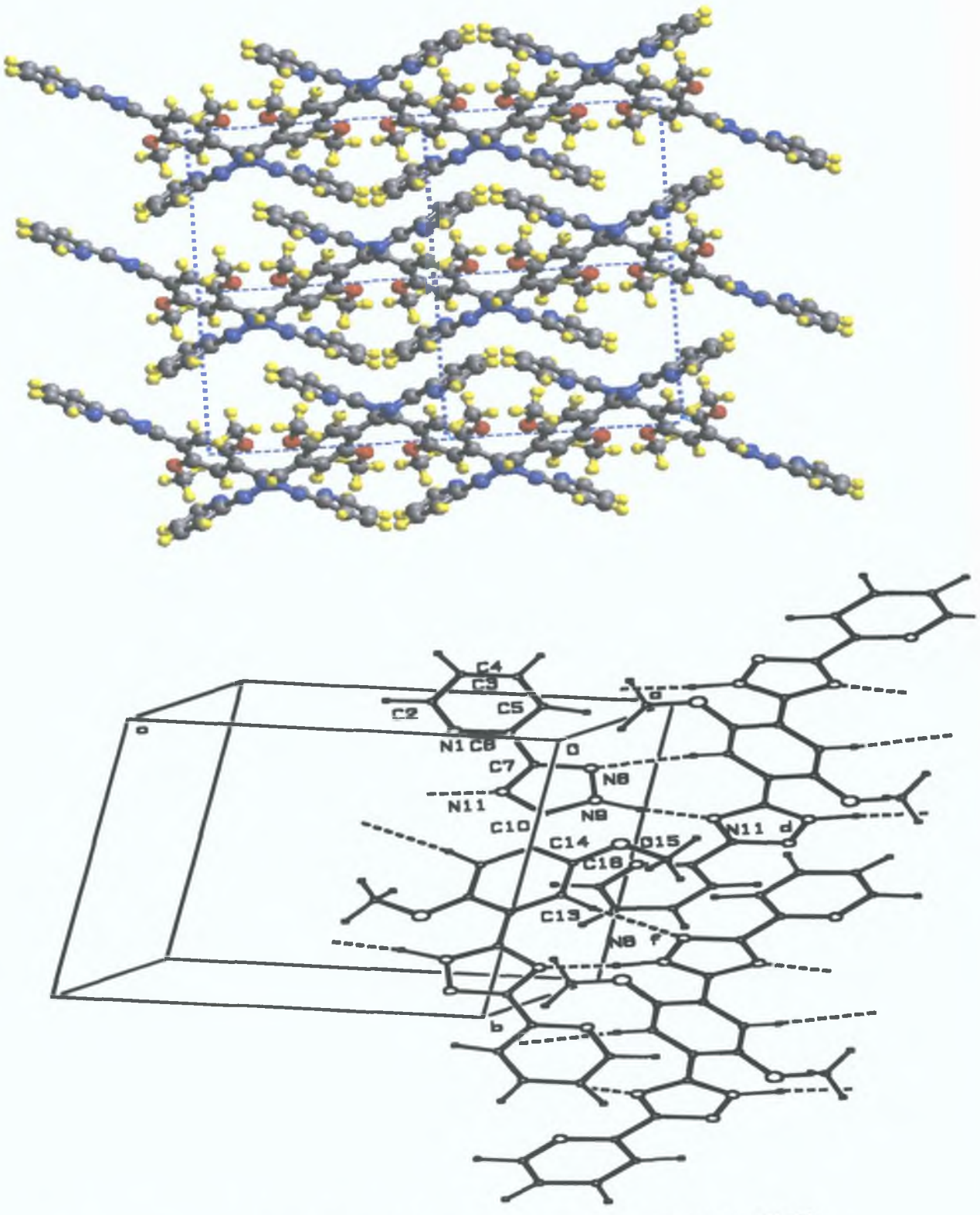

Fig. [2.17] Two views of crystal packing structure of H_2L3 with H-bonding illustrated (bottom).

Bond	Length (Angstroms)	Bond	Length (Angstroms)
N(1)-C(6)	1.333(5)	N(9)- C(10)	1.344(5)
N(1)- C(2)	1.348(6)	C(10)- N(11)	1.350(5)
C(2)- C(3)	1.380(7)	C(10)- C(12)	1.466(6)
C(3)- C(4)	1.372(7)	C(12)- C(13)	1.397(6)
C(4)- C(5)	1.380(7)	C(12)- C(14)	1.406(6)
C(5)- C(6)	1.395(6)	C(13)- C(14)#1	1.394(6)
C(6)- C(7)	1.480(6)	C(14)- O(15)	1.365(5)
C(7)- N(8)	1.338(5)	C(14)- C(13)#1	1.394(6)
C(7)- N(11)	1.356(6)	O(15)- C(16)	1.439(5)
N(8)- N(9)	1.369(5)		

Table [2.5]: (a) Bond lengths of H_2L3

Bond	Angle (degrees)	Bond	Angle (degrees)
C(6)-N(1)-C(2)	116.8(5)	N(9)-C(10)-N(11)	109.4(4)
N(1)-C(2)-C(3)	124.1(5)	N(9)-C(10)-C(12)	124.8(4)
C(4)-C(3)-C(2)	118.0(5)	N(11)-C(10)-C(12)	125.7(4)
C(3)-C(4)-C(5)	119.4(5)	C(10)-N(11)-C(7)	103.1(3)
C(4)-C(5)-C(6)	118.7(4)	C(13)-C(12)-C(14)	120.2(4)
N(1)-C(6)-C(5)	122.9(4)	C(13)-C(12)-C(10)	119.2(4)
N(1)-C(6)-C(7)	115.7(4)	C(14)-C(12)-C(10)	120.6(4)
C(5)-C(6)-C(7)	121.4(4)	C(14)#1-C(13)-C(12)	120.3(4)
N(8)-C(7)-N(11)	115.0(4)	O(15)-C(14)-C(13)#1	124.6(4)
N(8)-C(7)-C(6)	121.5(4)	O(15)-C(14)-C(12)	115.9(4)
N(11)-C(7)-C(6)	123.5(4)	C(13)#1-C(14)-C(12)	119.5(4)
C(7)-N(8)-N(9)	102.1(4)	C(14)-O(15)-C(16)	117.4(4)
C(10)-N(9)-N(8)	110.4(3)		

Table [2.6]: (b) Bond angles of H_2L3

2.3 EXPERIMENTAL

2.3.1 1-(pyridin-2-yl)-4-(1'',4''-dimethoxy-benz-2''-yl)-acylamidrazone (154)

2,5 dimethoxybenzoic acid (182 18, 10 g, 0 055 mol) and PCl_5 (FW 208 24, 11 45 g, 0 055 mol) were stirred in a clean dry 50 ml round bottomed flask fitted with a reflux condenser The two solids reacted immediately forming a clear yellow product The apparatus was then arranged for distillation and the $POCl_3$ formed was removed with slight heating (40°C) under a weak vacuum The clear yellow liquid was left to crystallize overnight under bench vacuum The acid chloride (FW 200 5, 11 03 g, 0 05 mol) was then dissolved in THF (30 ml) and transferred to an equilibrated dropping funnel This was fitted to a 250 ml round bottomed flask containing pyridin-2-yl amidrazone (FW 137, 6 85 g, 0 05 mol) dissolved in dry THF (40 ml) and sodium carbonate (FW 106, 2 65 g, 0 025 mol) was added to the stirred solution Dropwise addition of the acid chloride solution to the amidrazone resulted in the immediate precipitation of the pale yellow acylamidrazone When addition was complete, the reaction mixture was stirred for a further 4 h to allow completion of the reaction The THF was removed by suction filtration through a sintered funnel and the yellow product the stirred in ice water again filtered before oven drying m p 190°C

The acylamidrazone (FW 300, 10 95 g, 0 037 mol, 73% yield) was sufficiently pure for use in the next stage

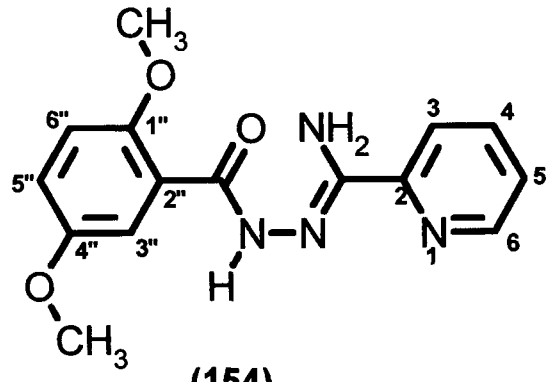

(154)

2 3 2 3-(1,4-dimethoxyphenyl)-5-pyridin-2-yl-1H-1,2,4-triazole **(HL1)**

1-(pyridin-2-yl)-4-(1,4-dimethoxy)-acylamidrazone (FW 300, 6 g, 0 02 mol) was dissolved in a minimum of ethylene glycol (30 ml) and heated at reflux temperature After approximately 30 min a colour change from clear yellow to clear brown was observed indicating product formation On cooling, the triazole product precipitated from solution and was collected by filtration

Recrystallization from DCM with decolourising charcoal treatment produced fine white product crystals The crystals were sufficiently pure for X-ray crystallography

^{1}H NMR (acetone-d^6) (δ, ppm, J,Hz) 12 54 (1H, s), 8 69 (1H, d, J=3 9), 8 20 (1H, d, J=7 9), 7 87 (1H, t, J=7 9), 7 82 (1H, s, J=3 0), 7 39 (1H, t, J=4 9), 7 12 (1H, d, J=9 9), 7 04 (1H,dd, J=3 0,8 9), 3 99 (3H, broad s), 3 83 (3H, s)
C,H,N Analysis($C_{15}H_{16}N_4O_2$) (% Theory/Found) C(63 82/63 62), H(5 00/5 15), N(19 85/18 74)

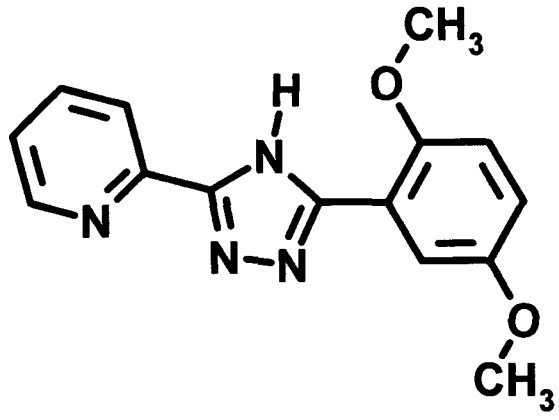

2.3.3 1-(pyrazın-2-yl)-4-(1,4-dımethoxy)-acylamıdrazone **(155)**

The method was the same as that used for the synthesıs of 1-(pyrıdın-2-yl)-4-(1,4-dımethoxy)-acylamıdrazone wıth the exceptıon that pyrazın-2-yl amıdrazone was used ın the place of pyıdın-2-yl amıdrazone ın the previously descrıbed reactıon m p 152°C

^{1}H NMR (dmso-d^6) (δ, ppm, J,Hz) 10 71 (1H, broad s), 9 93 (2H, broad s), 9 59 (1H, s), 9 05 (1H, s), 8 95 (1H, s), 7 47 (1H, s), 7 26 (2H, broad s), 3 88 (3H, broad s), 3 77 (3H, broad s)

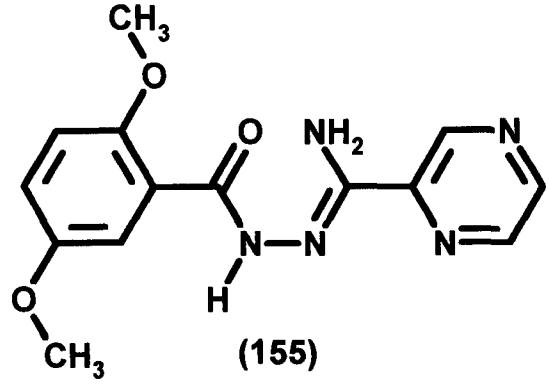

(155)

2 3 4 3-(1,4-dimethoxyphenyl)-5-pyrazin-2-yl-4H-1,2,4-triazole (HL2)

The method used was the same as that described for the formation of 3-(1,4-dimethoxyphenyl)-5-pyridin-2-yl-1H-1,2,4-triazole with the exception that 1-(pyrazin-2-yl)-4-(1,4-dimethoxy)-acylamidrazone was cyclized in the reaction m p>200°C

^{1}H NMR (dmso-d^6) (δ, ppm, J,Hz) 9 42 (1H, s), 8 78 (2H, s), 7 53 (1H, s), 7 18 (2H, s), 3 91 (3H, s), 3 83 (3H, s)
C,H,N Analysis($C_{14}H_{13}N_5O_2$) (% Theory/Found) C(59 36/59 62), H(4 63/4 75), N(24 52/24 71)

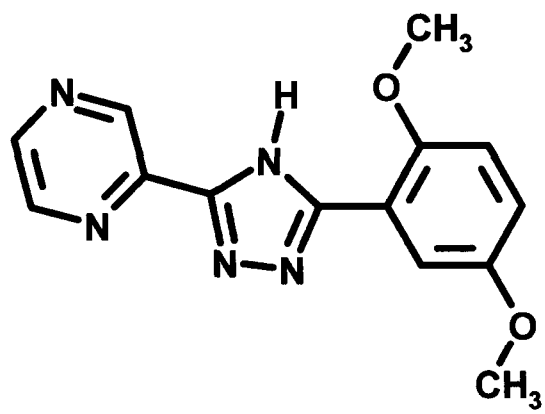

2 3 5 1,4-bis(acyl-pyridin-2-yl-amidrazone)-1,4-dimethoxy-benzene($C_{22}H_{18}N_8O_2$) **(152)**

2 3 5 1 Step One Diethyl-2,5-dimethoxyterephthalate formation ($C_{14}H_{18}O_6$) **(149)**

5 09 g (0 02 mol) of diethyl-2-5-dihydroxyterephthalate and 13 8 g (0 1 mol) potassium carbonate were stirred with 100 ml dry acetone in a round bottomed flask fitted with a long reflux condenser and a $CaCl_2$ drying tube 14 2 g (0 1 mol) iodomethane was added and the mixture heated at reflux temperature for approximately 48 h or until the product spot is visible with consumption of the

starting material on TLC (mobile phase: pet ether 2:1 diethyl ether). On cooling, the white product was filtered through a sintered funnel and washed with acetone. The methoxy product was verified by NMR: yield, 5.36 g (0.019 mol), 95%;

^{1}H NMR ($CDCl_3$) (δ, ppm; J,Hz) 7.36(1H, s); 4.36(2H, q, J=7.4); 3.87(3H, s); 1.37(3H, t, J=7.4).

2.3.5.2 Step Two: Preparation of 2,5-dimethoxyterephthalic acid ($C_{10}H_{10}O_6$) **(150)**

5 g (0.09 mol) of potassium hydroxide and 15 ml ethylene glycol were placed in a 50 ml round bottomed flask and the mixture heated with an air gun until it became homogeneous. 5 g (0.018 mol) of diethyl-2,5-dimethoxyterephthalate was added along with a few bumping chips and the apparatus arranged for reflux. The mixture was heated at 100°C until one layer was visible (10 min) ignoring any remaining solid. The flask was allowed to cool and arranged for distillation. The ethanol formed during heating was removed by distillation at reduced pressure. The potassium salt of the acid was cooled, 20 ml H_2O added, and 20% H_2SO_4 added until slightly acidic to litmus. The white diacid product precipitated on acidification and was filtered and washed with water and acetone. The diacid was dried in a Kugelrohr apparatus *in vacuo* over P_2O_5 at 100°C: yield 3.9 g (0.017 mol) 94.44%;. mp = 265°C;

^{1}H NMR (dmso-d^6) (δ, ppm; J,Hz) 7.28(1H, s); 3.77(3H, s)

2.3.5.3 Step Three: 2,5-Terephthaloyldichloride formation **(151)**

3.5 g (0.015 mol) of Kugelrohr dried 2,5-dimethoxyterephthalic acid was placed in a dry 50 ml beaker equipped with a magnetic stirring bar. 6.25 g (0.03 mol) of phosphorous pentachloride was carefully added and the solids stirred to affect

good mixing After 10 min of gentle stirring the solids were heated gently with an air gun causing melting, becoming a yellow liquid with the evolution of HCl gas and phosphoryl oxychloride, $POCl_3$ The reaction was then heated gradually to 200°C and the phosphoryl oxychloride removed by distillation at ordinary pressure On cooling, the flask was heated again at reduced pressure to remove any residual traces of phosphoryl oxychloride The solid yellow diacid chloride (whose reactivity made it unsuitable for analysis) was used immediately

2 3 5 4 Step Four 1,4-dimethoxy-2,5-bis(acyl-pyridin-2-yl-amidrazone)-benzene (Acylamidrazone Formation) ($C_{22}H_{22}N_8O_4$) **(152)**

All glassware used was rigorously dried before carrying out this step
To a stirred solution of 4 76 g (0 035 mol) of 2-pyridyl amidrazone and 1 59 g (0 015 mol) sodium carbonate in 30 ml dry THF was added 3 95 g (0 015 mol) of 2,5 dimethoxyterephthaloyl dichloride dissolved in 50 ml dry THF This addition was dropwise while the reaction was cooled in an ice bath A yellow product precipitated immediately and the reaction vessel was stirred overnight The reaction contents were then poured into 100 g ice water, stirred for 30 min and the yellow solid filtered, washed with water and acetone, and dried under vacuum Impurities present in the acylamidrazone were removed by heating the crude product in DMSO, filtering and washing with acetone m p 189°C

The product acylamidrazone, a fine yellow powdery solid was characterised by NMR yield 5 g (0 01 mol), 66 67%,

^{1}H NMR (dmso-d^6) (δ, ppm, J,Hz) 10 21(2H, s, –NH), 8 61(2H, d, J=5 6, H6), 8 17(2H, d, J=7 4, H3), 7 76(2H, t, J=7 4, H4), 7 50(2H, t, J=7 4, H5), 7 38(2H, s, Benz-H), 6 81(4H, s, $-NH_2$), 4 03(6H, 2, $-OCH_3$)

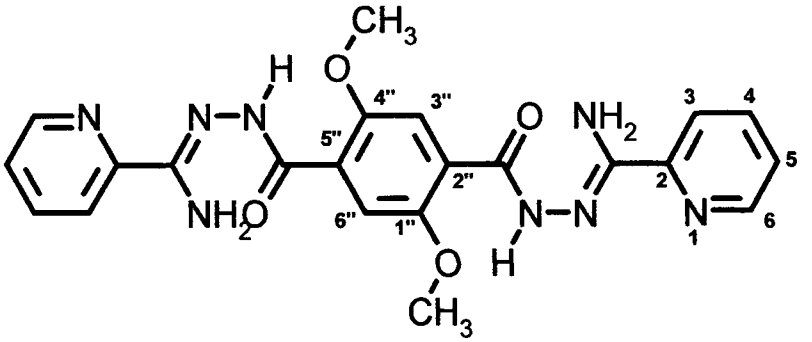

(152)

2 3 6 1,4-dimethoxy-2,5-bis(pyridin-2-yl)-1,2,4-triazol-3-yl)benzene **(H_2L3)**

5 g (0 01 mol) of 1,4-dimethoxy-2,5-bis(acyl-pyridin-2-yl-amidrazone)-benzene was heated to reflux temperature in 40 ml ethylene glycol until the reaction mixture turned a clear brown colour The product, a tan solid, precipitated from solution overnight

Recrystallisation from DMSO yielded crystals of the triazole which was characterised by NMR, microanalysis and its molecular structure established by X-ray crystallography yield, 2 **3** g (5 4 x 10^{-3} mol), 54 %,

^{1}H NMR (dmso-d^6) (δ, ppm, J,Hz) 14 11(2H, broad s, –NH), 8 70(2H, broad s, H6), 8 18(2H, d, J=7 4, H3), 7 94(4H, broad s, H4 and Benz-H), 7 47(2H, s, H5), 4 03(6H, broad s, –OCH_3), C,H,N Analysis($C_{22}H_{18}N_8O_2$ 1H_2O) (% Theory/Found) C(60 95/59 46), H(4 50/4 20), N(25 23/25 42)

Note The microanalytical N deviation was considered not significant in view of the obtaining of a confirmatory crystal structure

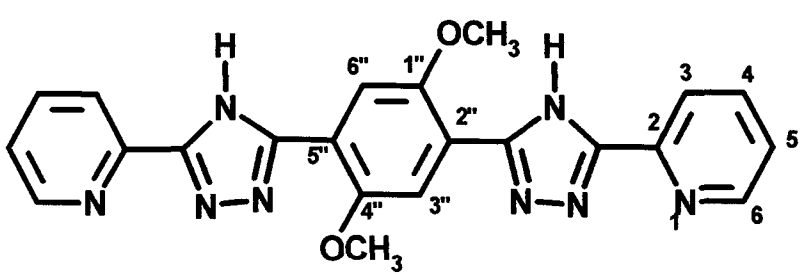

2 3 7 1,4-dihydroxy-2,5-bis(5-pyridin-2-yl)-1,2,4-triazol-3-yl)-benzene **(H_2L7)**

0 5 g (1 2 x 10^{-3} mol) of 1,4-dimethoxy-2,5-bis(pyridin-2-yl)-1,2,4-triazol-3-yl)benzene in 30 ml (excess) hydrobromic acid (48%) and acetic acid (<10 ml) were placed in a 100 ml round bottomed flask and heated at reflux temperature overnight On cooling, a tan solid (possibly the HBr salt) precipitated out The cooled reaction solution became very hot and appeared an orange colour when exposed to the air The solid salt product was removed by filtration and neutralized with saturated sodium carbonate solution to leave a solid which was filtered, washed with water and diethyl ether and dried m p >200°C

The deprotected product was characterised by NMR with DMSO-d^6 and d-acetic acid yield, 0 37 g (9 3 x 10^{-4} mol), 77 5%,

^{1}H NMR (dmso-d^6) (δ, ppm, J,Hz), 8 84(2H, d, J=5 55, H6), 8 44(4H, m, H3,H4), 7 87(2H, t, J=5 55, H5), 7 78(2H, s, Benz-H) Hydroxy signals not seen in spectrum

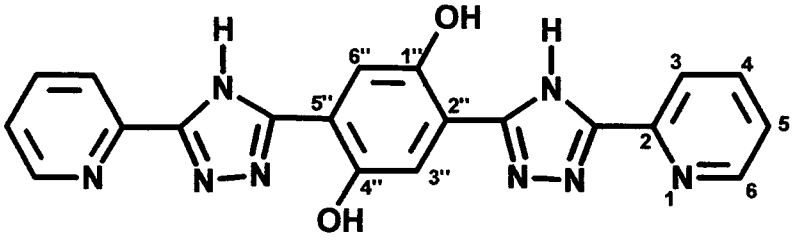

2 3 8 1,4 - dimethoxy-2,5-bis([acyl-pyrazin-2-yl]-amidrazone)-benzene **(153)**

All glassware was oven dried overnight prior to carrying out this step

To a stirred solution of 12 06 g (0 088 mol) pyrazine amidrazone and 4 66 g (0 044 mol) of sodium carbonate in 50 ml dry THF, was added 11 57 g (0 044 mol) of 2,5-dimethoxyterephthaloyl dichloride dissolved in 100 ml dry THF over the course of about 30 min A pale yellow milky precipitate formed immediately and the solution stirred overnight The THF solvent was removed by suction through a sintered funnel and the yellow solid subsequently poured into ice water and stirred for 30 min The yellow solid was again filtered and washed with water and acetone

Recrystallization was carried out from DMSO followed by suction and oven (40°C) drying afforded the desired acylamidrazone yield, 10 20 g (0 026 mol), 58 % yield),

^{1}H NMR (dmso-d^6) (δ, ppm, J,Hz) 10 32 (2H, s, –NH), 9 32 (2H, s, H3), 8 74 (2H, d, J=3 0, H6), 8 69 (2H, s, H5), 7 37 (2H, s, Benz-H), 6 94 (4H, s, $-NH_2$), 3 87 (6H, broad s, $-OCH_3$)

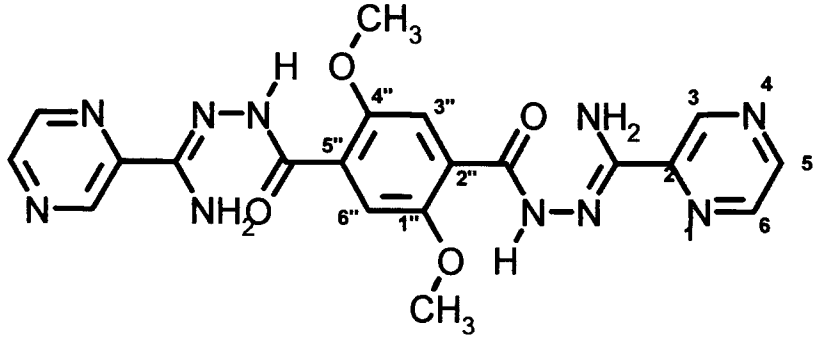

(153)

2 3 9 1,4-dimethoxy-2,5-bis([5-pyrazin-2-yl]-1,2,4-triazol-3-yl)-benzene **(H_2L4)**

5 g (0 011 mol) of 1,4-dimethoxy-2,5-bis([acyl-pyrazin-2-yl]-amidrazone)-benzene was heated in 40 ml ethylene glycol at reflux temperature until the colour changed from clear yellow to clear brown (approximately 2 h) The

reaction vessel was allowed to cool, was stoppered, and placed in a freezer overnight A tan powder precipitated which was filtered and washed with ethanol and acetone

Purification using DMSO yielded the pale brown triazole, yield, 1 3 g, (2 97 x 10^{-3} mol), 27% yield),

^{1}H NMR (dmso-d^6) (δ, ppm, J,Hz) 9 37 (2H, s, H3), 8 79 (2H, s, H6), 8 72 (2H, s, H5), 7 96 (2H, s, Benz-H), 4 08 (6H, broad s, $-OCH_3$), NH signal not seen
C,H,N Analysis($C_{20}H_{16}N_{10}O_2$) (% Theory/Found) C(56 07/55 39), H(3 76/4 14), N(32 69,31 77)

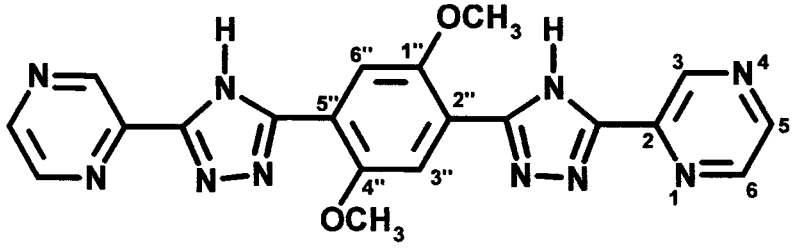

2.4 CONCLUSIONS

Four new dimethoxy protected triazole ligands are described in this chapter Of the four, the crystal structures of three were obtained One of the ligands H_2L3 underwent a deprotection reaction to form its dihydroxy analogue being formed All the ligands were formed from corresponding acylamidrazones which are also described All the triazole ligands when purified produced clean ^{1}H-NMR spectra in dmso-d^6 In general however, all triazole ligands showed poor peak resolution The larger ligands containing two triazole rings produced symmetrical ^{1}H-NMR spectra and dissolve with difficulty in DMSO Packing structures obtained for the ligands show H-bonding effects Sufficient quantities

of the ligands were produced to allow production of their corresponding ruthenium bis-bipyridyl complexes

Note that experimental details of the deprotection of H_2L3 are presented This reaction was carried using 48% hydrobromic acid This was the only ligand on which a successful deprotection was carried out

As discussed earlier the aim of the work is to produce deprotected complexes Arguably the production of deprotected hydroquinone ligand is useful for a number of reasons, not least of which is as a comparative molecule

The reason why we did not concentrate on forming the hydroquinone analogues of the ligands described in this chapter should be explained Hydroquinone ligands do not undergo complexation reactions to ruthenium as successfully as the protected ligands The –OH groups provide coordination sites for ruthenium promoting the formation of unwanted reaction side products

Also the HBr procedure which was successfully used in the deprotection of H_2L3 was not carried out successfully in the cases of the other ligands Difficulties were encountered in these cases with controlling the amount of oxidation taking place Newly formed hydroquinone molecules may have been further oxidized to semiquinones and quinones

Since the ruthenium complexes of the ligands synthesized in this chapter possess greater solvation properties deprotection reactions on the complexes could be carried out with more control All our efforts at deprotection were thus concentrated on the complexes as described in chapter three

2.5 REFERENCES

[1] P Hergenrother, *J Heterocyclic Chem* , 965, (1969)

[2] J A Bladin, *Chem Ber* , **22**, 3114, (1889)

[3] E Bamberger, P deGruyter, *Chem Ber* , **26**, 2385, (1893)

[4] A Pinner, *Justus Liebigs Ann Chem* , **297**, 221, (1897)

[5] E L Rinnan, *Chem Ber* , **30**, 1193, (1897)

[6] P M Hergenrother, *Polymer Prepnnts*, **10**, 772, (1969)

[7] M Saga, T Shono, *J Polymer Sci B*, **4**, 869, (1966)

[8] J A Bladin, *Ber* , **22**, 3114, (1889)

[9] G Pellizari, *Gazz Chim Ital* , **41**, 20, (1911)

[10] K T Potts, *Chem Rev* , **61**, 87, (1961)

[11] A H Frazer, F T Wallenberger, I M Sarasohn, *J Polym Sci* A-1, **4**, 1147, (1964)

[12] A H Frazer, F T Wallenberger, *J Polym Sci* A-2, 1171, (1964)

[13] A H Frazer, W Sweeney, F T Wallenberger, *J Polym Sci* A-2, 1157, (1964)

[14] V V Korshak, Y S Krongauz, A L Rusanov, *Izv Akad Nauk SSSR, Ser Khim* , **11**, 2663, (1968)

[15] P M Hergenrother, L A Carlson, *J Polym Sci A-1*, **8**, 1003, (1970)

[16] P M Hergenrother, *J Heterocyclic Chem* , **9**, 131, (1972)

[17] P M Hergenrother, *J Polym Sci A-1*, 9, 2377, (1971)

[18] V V Korshak, A L Rusanov, T G Iremashvili, I V Zhuraleva, E L Baranov, *Macromolecules*, **6**, 483, (1973)

[19] V V Korshak, A L Rusanov, E L Baranov, T G Iremashvili, T I Bezhuashvili, *Dokl Akad Nauk SSSR, Engl Trans* , **196**, 149, (1971)

[20] V V Korshak, A L Rusanov, L K Plieva, M K Kereselidze, T V Lekae, *Macromolecules*, **9**, 627, (1976)

[21] A I Vogel, Vogel's Textbook of Practical Organic Chemistry, Wiley, New York, 1989

[22] http //www wavefun com/

3 Synthesis of Ruthenium Complexes of 1,2,4-Triazoles

3.1 INTRODUCTION

Complexes discussed in this chapter

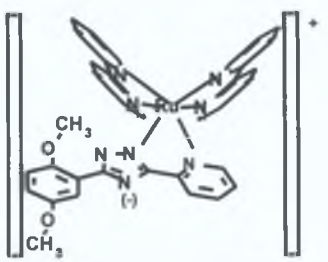

$Ru(bpy)_2L1$

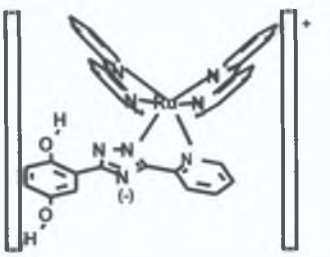

$Ru(bpy)_2L5$

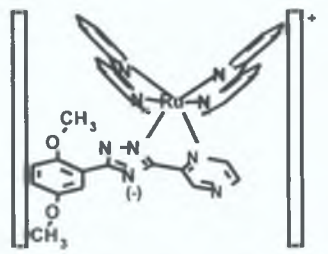

$Ru(bpy)_2L2$

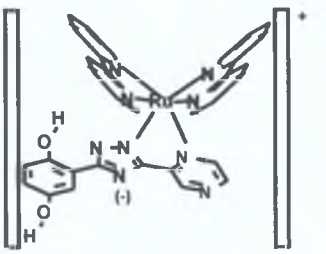

$Ru(bpy)_2L6$

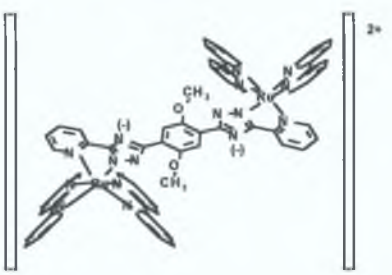

$[Ru(bpy)_2]_2L3$

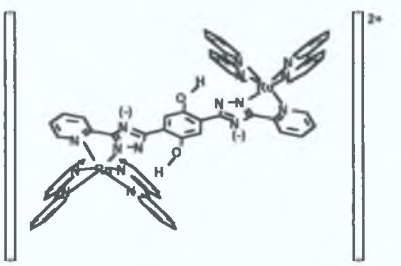

$[Ru(bpy)_2]_2L7$

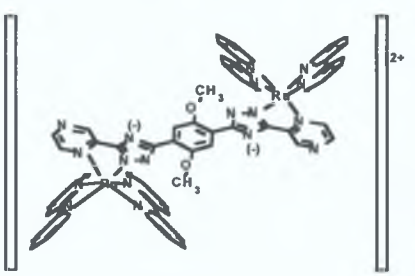

$[Ru(bpy)_2]_2L4$

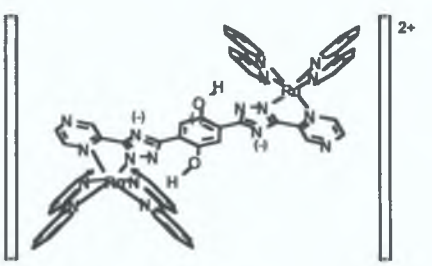

$[Ru(bpy)_2]_2L8$

$Ru(bpy)_2L1 = [Ru(bpy)_2(1,4\text{-dimethoxyphenyl})\text{-}5\text{-pyridin-2-yl-}1,2,4\text{-triazole}]PF_6.2H_2O$

$Ru(bpy)_2L2 = [Ru(bpy)_2(1,4\text{-dimethoxyphenyl})\text{-}5\text{-pyrazin-2-yl-}1,2,4\text{-triazole}]PF_6.2H_2O$

$[Ru(bpy)_2]_2L3 = [Ru\{(bpy)_2\}_2(1,4\text{-bis}(5\text{-pyridin-2-yl-}1,2,4\text{-triazol-3-yl})\text{-}2,5\text{-dimethoxybenzene})](PF_6)_2.4H_2O$

$[Ru(bpy)_2]_2L4 = [Ru\{(bpy)_2\}_2(1,4\text{-bis}(5\text{-pyrazin-2-yl-}1,2,4\text{-triazol-3-yl})\text{-}2,5\text{-dimethoxybenzene})](PF_6)_2.4H_2O$

$Ru(bpy)_2L5 = [Ru(bpy)_2(1,4\text{-dihydroxyphenyl})\text{-}5\text{-pyridin-2-yl-}1,2,4\text{-triazole}]PF_6.2H_2O$

$Ru(bpy)_2L6 = [Ru(bpy)_2(1,4\text{-dihydroxyphenyl})\text{-}5\text{-pyrazin-2-yl-}1,2,4\text{-triazole}]PF_6.2H_2O$

$[Ru(bpy)_2]_2L7 = [(Ru\{(bpy)_2\}_2(1,4\text{-bis}(5\text{-pyridin-2-yl-}1,2,4\text{-triazol-3-yl})\text{-}2,5\text{-dihydroxybenzene})](PF_6)_2.4H_2O$

$[Ru(bpy)_2]_2L8 = [(Ru\{(bpy)_2\}_2(1,4\text{-bis}(5\text{-pyrazin-2-yl-}1,2,4\text{-triazol-3-yl})\text{-}2,5\text{-dihydroxybenzene})](PF_6)_2.4H_2O$

This chapter is concerned with the synthesis of ruthenium bis-bipyridyl complexes of the ligands described in chapter two. The target ligands discussed, all contained 1,4-dimethoxy groups on the central aromatic ring. While it was desirable to investigate the ruthenium complexes of these dimethoxy ligands, considerable importance was also attached to the synthesis of the hydroquinone analogues of the complexes. An illustration of one of the desired dihydroxy complexes is shown in fig. [3.1].

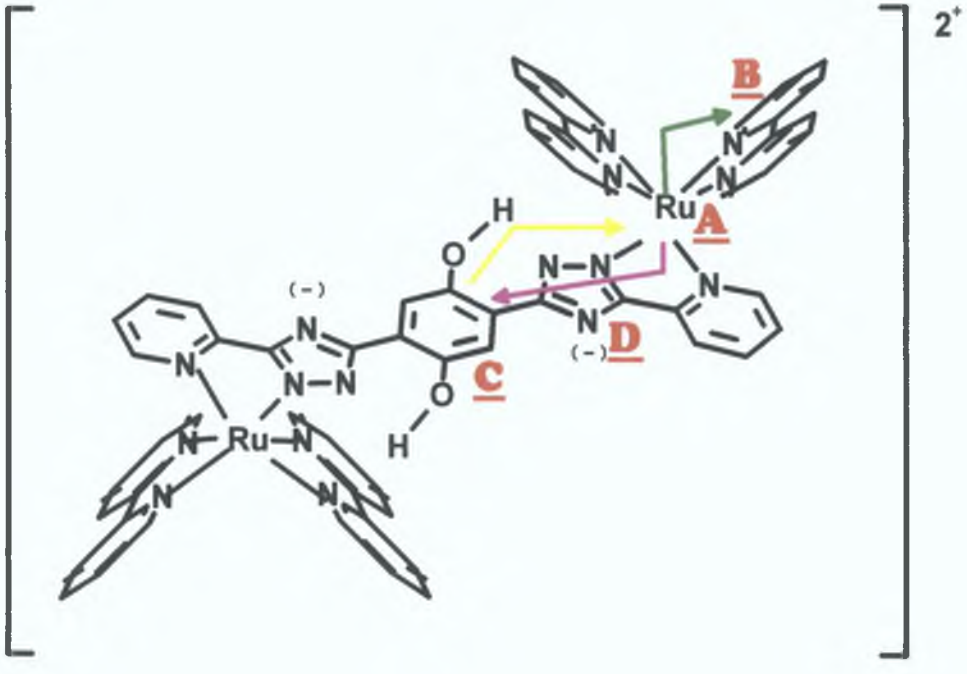

Fig. [3.1]

Why is this molecule important? Research into complexes of this type has stemmed from the success of $[Ru(bipy)_3]^{2+}$, which is known as a potential photocatalyst.[12] This means $[Ru(bipy)_3]^{2+}$ possesses properties which allow it act as a catalyst in solar energy conversion. Solar energy conversion, which is the conversion of light into electrical energy, is possible because of the electrochemical and photophysical properties of $[Ru(bipy)_3]^{2+}$. We will introduce these later in this chapter. When $[Ru(bipy)_3]^{2+}$ absorbs a photon of light, an electron is excited from the Ru(II) metal centre leaving the metal with an electron

hole and a +3 charge[3]. This makes the complex a strong oxidant. Also, the irradiated electron is excited from the metal centre onto a bipy ligand. From there this electron can easily be transferred to another compound causing reduction. Thus $[Ru(bipy)_3]^{2+}$ is a better oxidiser and reductor in the excited state than in the ground state. By changing the ligand systems around the metal centre we aim to improve on the successes of $[Ru(bipy)_3]^{2+}$.

The molecule in Fig. [3.1] will potentially play a key role in artificial photosynthetic systems. A key element in such systems is that when the sun shines on a leaf, an electron is excited on a specialized molecule and this electron subsequently embarks on a journey termed the photosynthetic pathway. What the molecule above represents is a custom made specialized molecule (or mimic) which when irradiated excites an electron in an artificial system.
By looking at the labels in the figure we can simplify the discussion. In the molecule shown only one side is labelled while in practice the molecule is symmetrical and what occurs on one side can potentially occur on the other. When the complex is irradiated, an electron is excited from the ruthenium Ru(II) metal centre A into a π^* orbital on the bipyridyl groups at B. This excited electron could then decay back onto the ruthenium, now Ru(III), at A, but before it can do so an electron is given to the ruthenium from the central dihydroxy aromatic C. Now because C is such a distance away from A, we have attained a good charge separation in the molecule giving the excited state a longer "lifetime" and thus greater stability because the electron now has a potentially long journey back to its ground state. Furthermore, if the pathway the electron takes back is D (shown by the purple arrow), then the electron must travel through a negatively charged triazole region (shown in Fig 3.1), which effectively slows down the electron transfer. Thus the molecule is designed to have a long lifetime in the excited state.

The aim of this thesis is to synthesize this and similar molecules Thereafter the properties of the molecule will be investigated by photophysical methods Two choices are available to the researcher when synthesizing these complexes One can either produce the ligand in its hydroquinone (dihydroxy) form and produce the ruthenium complex from that, or form the complex as the dimethoxy protected version and carry out a deprotection of the complex to produce the hydroquinone form We have chosen to proceed via the latter route for a number of reasons

- Ruthenium can potentially bind to an oxygen atom during coordination If coordinating a hydroquinone containing triazole ligand, this would introduce the possibility of isomers and unwanted by-product formation
- Experience has shown that 1,2,4-triazole ligands containing hydroquinones can be unstable when heated to high temperatures, probably becoming semiquinones and quinones[4]
- The greater solubility that is inherent in ruthenium complexes allows for easier manipulation as opposed to the insoluble ligands

Having decided that deprotection of the complexes (i e cleavage of the methyl ethers when in the complex form) was the best course of action we investigated possible methods of deprotection While boron tribromide was eventually chosen as the reagent of choice the following options were considered

3 1 1 Cleavage of Methyl Ethers

A number of methods are available for the cleavage of methyl ethers[5]
Here we describe some of the most successful methods with the emphasis on applicability and practicality

3.1.1.1 Boron tribromide

At present boron tribromide could be considered the reagent of choice for the cleavage of ethers[5] What has made it successful is its ability to cleave ether protecting groups under mild conditions without affecting a large number of other functional groups Hence its wide and varied use in natural product synthesis where selective cleavage is vitally important Another advantage of boron tribromide is that it operates under mild conditions, often only requiring a reaction medium such as dichloromethane Thus a cleavage can be effected without the use of strongly acidic or alkaline reaction conditions as are often required, with alternative reagents
Boron tribromide was used for ether cleavage as early as 1942 when a general procedure was developed[6]

General Procedure: A weighed quantity of the ether (usually 15–20 g) was introduced into the reaction flask and cooled in an ice bath Boron tribromide was then slowly introduced via a dropping funnel In all cases boron tribromide and ether were allowed to react in the ratio 1 mol of boron tribromide to 3 mol of ether After addition of boron tribromide the mixture was heated on a water bath for 40 min The alkyl bromide was distilled directly from the reaction mixture After alkyl bromide removal, the residue remaining in the flask was hydrolyzed with a minimum amount of 10% sodium hydroxide solution The resulting solution was acidified with hydrochloric acid and extracted with ether

This procedure then largely disappeared before being reintroduced in 1963[7,8] The use of milder reaction conditions than those described in the general procedure were recommended The reaction is usually carried out in dichloromethane, pentane or benzene at room temperature for 12–15 h Work-up involved hydrolysis with water and extraction of the product from the reaction mixture with ether as in Scheme [3 1]

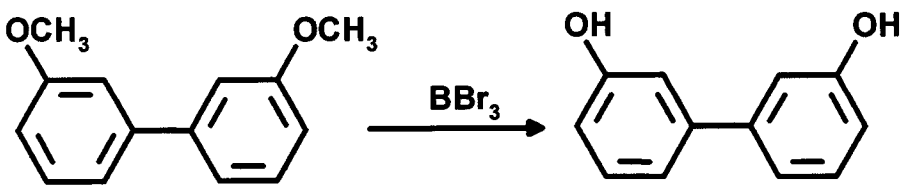

Scheme [3.1]

The deprotection of 3,3'-dimethoxy-biphenyl employed even milder reaction conditions 3,3'-Dimethoxy-biphenyl was dissolved in DCM in a flask which was placed in an acetone–dry ice bath at -80°C The flask was fitted with an air condenser Boron tribromide, one equivalent for each methoxy group) in dichloromethane was then added through the condenser On completion of the addition, a calcium chloride tube was fitted to the top of the condenser to protect the reaction mixture from moisture The mixture was allowed to attain room temperature overnight with stirring before being hydrolyzed by careful shaking with water Ether was then added and the organic layer separated and extracted with 2N NaOH The alkaline extract was neutralized with dil HCl and the product was obtained by extraction into ether with its subsequent removal

It is important to note that boron tribromide is a heavy colourless liquid (d=2 6) when pure, but begins to decompose on exposure to light, liberating free bromine (and thus turning a brown colour) It fumes vigorously in air, being rapidly hydrolyzed to boric acid, with the evolution of heat Recently boron tribromide was used for ether cleavage in the formation of symmetrically meta-disubstituted benzene derivatives with functionalities in terminal positions[9] The cleavage of the methyl ether shown in Scheme [3 2] affords a 93% yield of the deprotected product

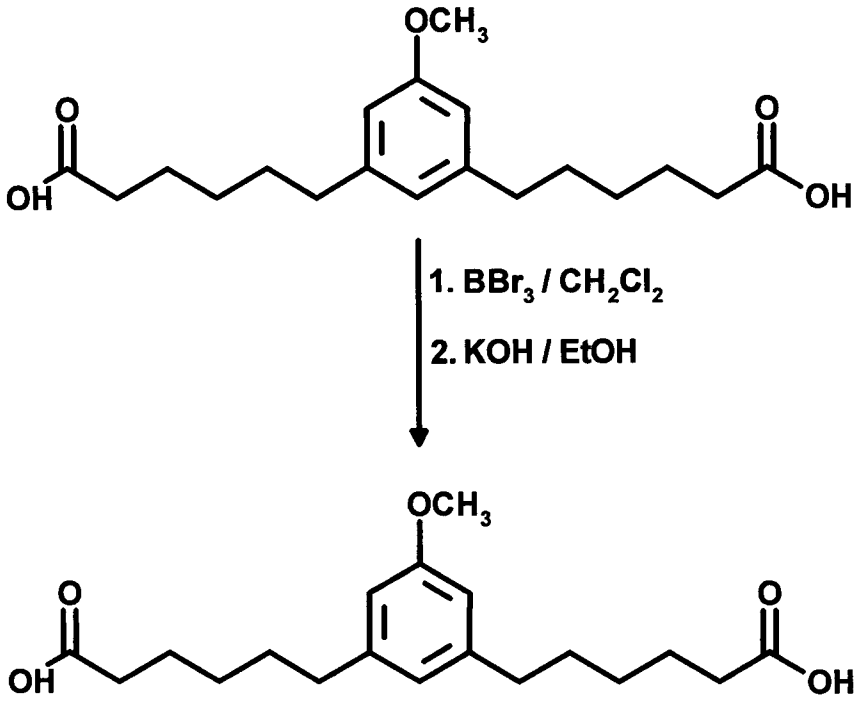

93%

Scheme [3.2]

The first stage in the reaction of BBr_3 with an ether is the formation of a Lewis acid complex[10] as in the Scheme [3 3]

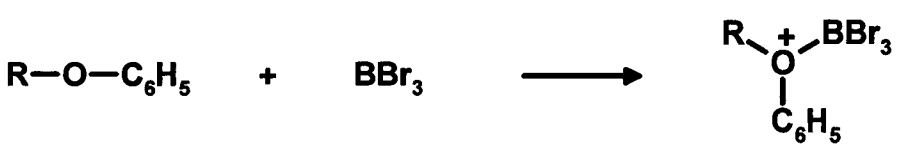

Scheme [3.3]

The complex then proceeds via an S_N1 mechanism to give the alkyl bromide and the phenyl di-bromo-boron molecule

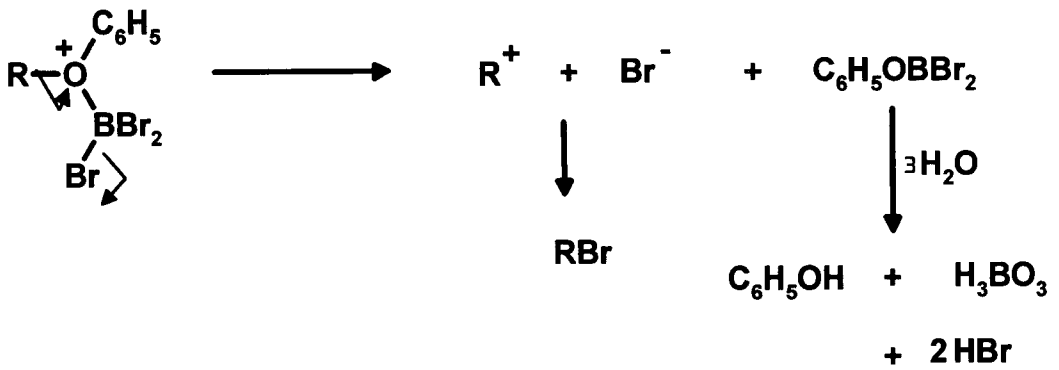

Scheme [3.4]

The final part of the reaction involves the hydrolysis of the boron intermediate with water to form the alcohol Hydrogen bromide and boric acid are by-products of the reaction depicted in Scheme [3 4]

Niwa and co-workers observed that the cleavage pattern of boron tribromide is dramatically modified in the presence of sodium iodide and a crown- ether[11]

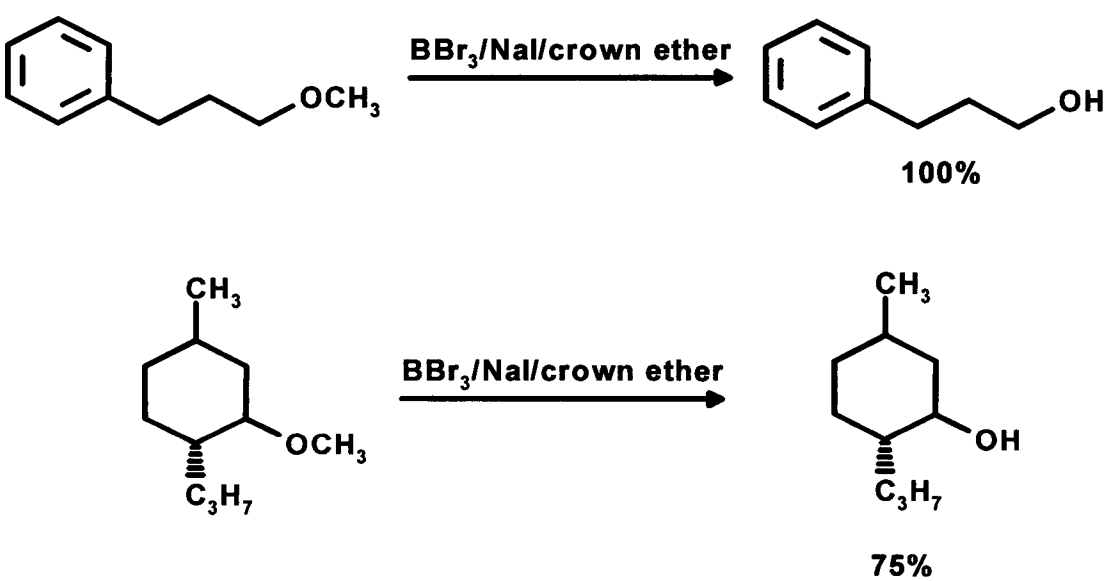

Scheme [3.5]

In Scheme [3 5], this system of reagents in dry methylene chloride cleaved very efficiently primary and secondary aryl methyl ethers under mild conditions to give the corresponding alcohols

The general procedure involves addition to a stirred solution of methyl ether in dry DCM of 0.3 M solution of 15-crown-5-ether, saturated with sodium iodide in DCM followed by the addition of a 1 M solution of boron tribromide in DCM at -30°C under argon. After stirring at this temperature for 3 h the reaction was quenched by the addition of saturated aqueous sodium hydrogen carbonate solution and worked up in the usual manner.

3.1.1.2 Boron Trihalide–Methyl Sulfide complexes

One of the difficulties with using boron tribromide arises from its tendency to fume profusely in air. Generally the boron tribromide has to be transferred into the reaction via syringe under a blanket of nitrogen.
Boron tribromide–dimethyl sulfide complexes[12] are solids which are stable in air and handled easily.

The boron tribromide is released in solution as follows

$$Br_3B{\cdot}S(CH_3)_2 \leftrightarrow Br_3B + S(CH_3)_2$$

Using a two- or four-fold excess of the reagent, methoxy and methylenedioxy groups attached to aromatic rings have been successfully cleaved. The general procedure initially involves a flame-dried flask under an atmosphere of N_2, to which is added 1,2-dichloroethane and the required amount of boron trihalide-dimethyl sulfide complex. The desired number of equivalents of aryl ether are then added to this solution, before stirring at reflux temperature. The reaction can be monitored by TLC. When the starting material disappears, the reaction mixture is hydrolyzed by adding water, stirred and diluted with ether. The organic phase is separated and washed with sodium hydrogen carbonate. The phenol is then taken up in 1N sodium hydroxide, acidified, and the product

extracted with ether Removal of the ether then furnishes the product in Scheme [3 6]

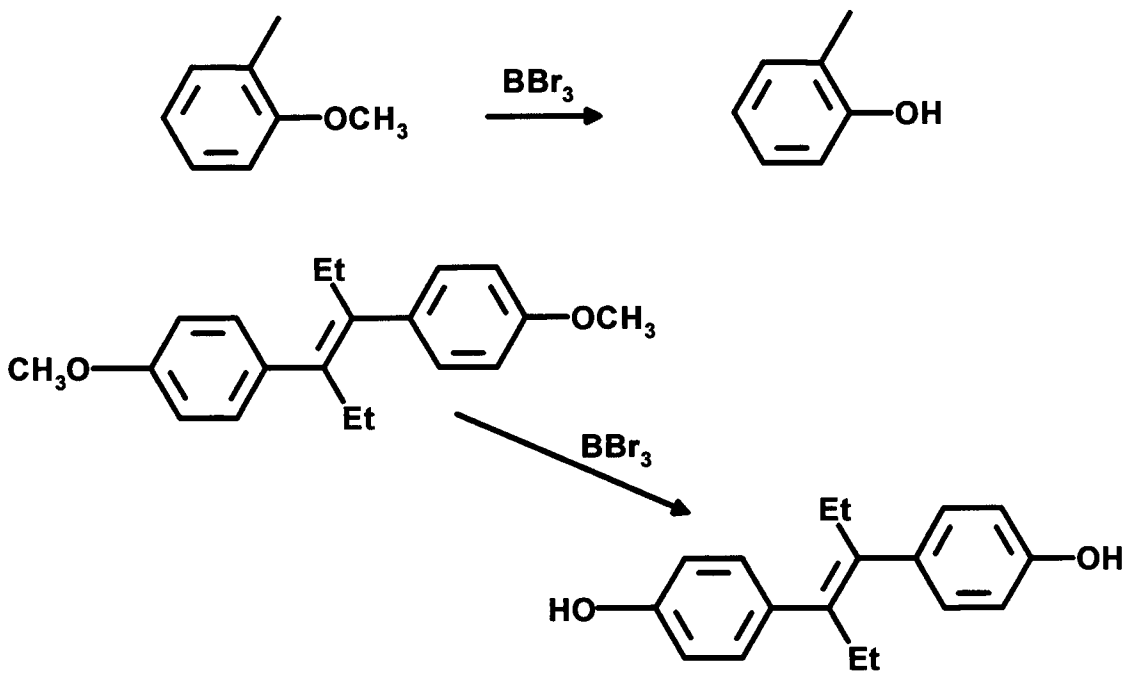

Scheme [3.6]

3.1.1.3 Iodotrimethylsilane.

Another method regarded as being among the best for cleavage of ethers involves the use of iodotrimethylsilane[5] The reagent can be bought commercially but can also be easily produced from readily available silicon derivatives, as shown in Scheme [3 7] in the three reactions

$$(CH_3)_3SiCl + NaI \rightarrow (CH_3)_3SiI + NaCl$$

$$3(CH_3)_3Si{-}O{-}Si(CH_3)_3 + 2Al + 3I_2 \rightarrow 6(CH_3)_3SiI + N_2O_3$$

$$C_6H_5{-}Si(CH_3)_3 + I_2 \rightarrow (CH_3)_3SiI + C_6H_5{-}I$$

Scheme [3.7]

The reagent also cleaves esters, but does so more slowly than ethers; thus the possibility exists of cleaving ethers in the presence of esters. Aryl alkyl ethers react significantly slower than dialkyl ethers, so dialkyl ethers can be cleaved completely under conditions that result in only a 5–10% cleavage of phenolic ethers. Although methyl ethers have been used extensively as protecting groups for phenols, they are not generally used in aliphatic systems due the difficulty of their removal. Jung and Lyster[13] have, in this context, studied in detail the simple and efficient dealkylation of aromatic and aliphatic ethers with iodotrimethylsilane, providing the deprotected alcohols and phenols in good yield.

$$R{-}O{-}R' \text{ (A)} + 2Me_3Si{-}I \text{ (B)} \rightarrow R{-}O{-}SiMe_3 \text{ (C)} + R'{-}O{-}SiMe_3 \text{ (D)} + R'I \text{ (E)} + RI \text{ (F)}$$

$$\downarrow H_2O$$

$$R{-}OH \text{ (G)} + R'{-}OH \text{ (H)}$$

Scheme [3.8]

Alkyl methyl ethers (R'=Me) react with TMS–I to afford mixtures of dealkylated products, the trimethylsilylethers C and D and the alkyl iodides E and F in which in general, the products C and E greatly predominate.

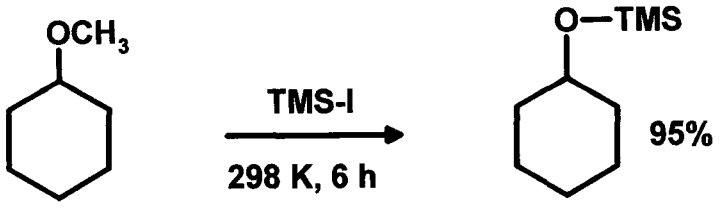

Scheme [3.9]

Cyclohexyl methyl ether when treated with a 1 1 equivalent of TMS–I gave 95% cyclohexyl-trimethylsilyl ether and methyl iodide

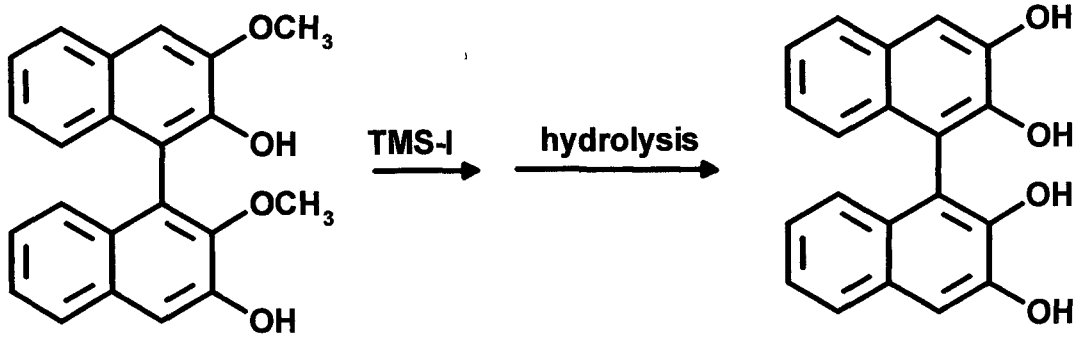

Scheme [3.10]

Aryl alkyl ethers such as that shown Scheme [3 10] are cleaved when treated with trimethylsilyl iodide to afford only the aromatic trimethylsilyl ethers and the alkyl iodides which are easily converted into the corresponding alcohols or phenols in high yield upon simple hydrolysis[5]

Cleavage of methyl ethers with TMS–I tolerates many functional groups, e g triple bonds, double bonds, ketone groups, amino groups and aromatic halide groups A chlorotrimethylsilane / sodium iodide system has been found in some cases to cleave ethers at a faster rate than iodotrimethylsilane itself For example anisole is demethylated by chlorotrimethylsilane and sodium iodide in 10 h Under similar conditions pure TMS–I required 24 h The catalytic influence

of the iodide ions in the former case is attributed to the faster rate of ether cleavage[14].

The conversion of ethers to iodides by chlorotrimethylsilane / sodium iodide is generally carried out in a flask fitted with a reflux condenser and flushed continuously with dry N_2. To a solution of the ether and sodium iodide in acetonitrile is added chlorotrimethylsilane slowly with continuous stirring. The contents are stirred at room temperature until completion of the reaction as indicated by TLC. Heating under reflux is sometimes necessary to complete the reaction. On completion, the reaction mixture is quenched with water and extracted with ether. The ether layer is washed with sodium thiosulfate (to remove the iodine) and brine, and dried with Na_2SO_4. Removal of the ether gives the phenolic products[14] shown in Scheme [3.11].

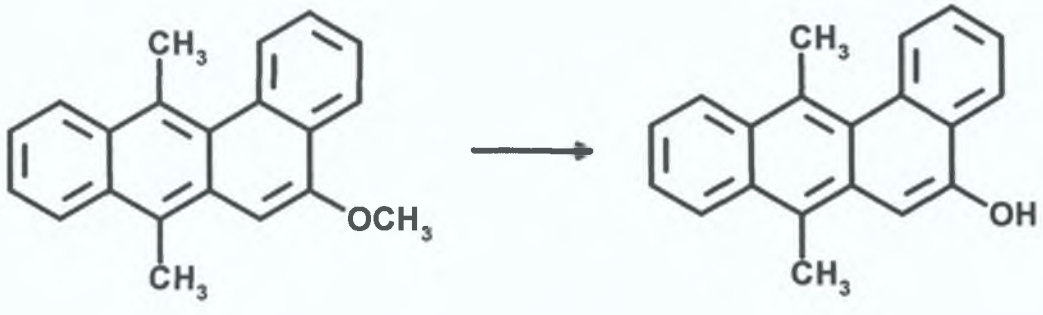

Scheme [3.11]

The aryl methyl ether shown above has successfully cleaved the corresponding hydroxyl compound both by heating in DMF with sodium ethyl mercaptide and by heating with sulfide in *N*-methylpyrrolidine at 140–145°C for 2–4 h. The use of sodium sulfide has advantages over the former method in that the reagent is simpler to prepare and the work-up is less malodorous. Several similar anthracene derivatives have also been cleaved by this method in high yields.

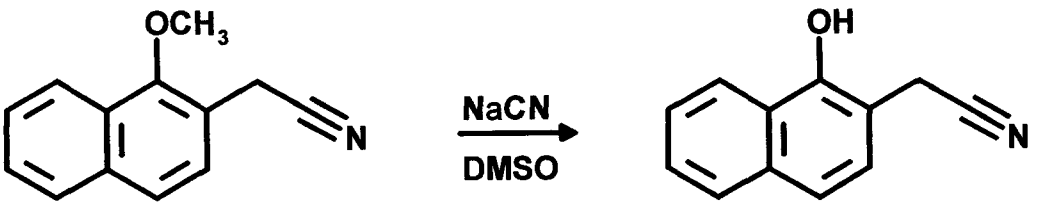

Scheme [3.12]

In his work on the synthesis of antidepressants McCarthy and co-workers[15] needed a convenient method for the demethylation reaction above One of his suggested methods involved the use of lithium iodide in collidene, a procedure developed by Harrison[16]

The best method found for the above reaction, according to McCarthy involved the use of sodium cyanide–dimethylsulfoxide In a typical experiment the methoxy naphthalene derivatives and a five-fold excess of sodium cyanide were added to DMSO and heated to 180°C under nitrogen After pouring into water and acidifying with strong acid, the free alcohol precipitates Hydrogen cyanide gas is evolved in the reaction Compounds having functionalities like carboxyl, carboxamide and keto groups all emerged from the reaction intact

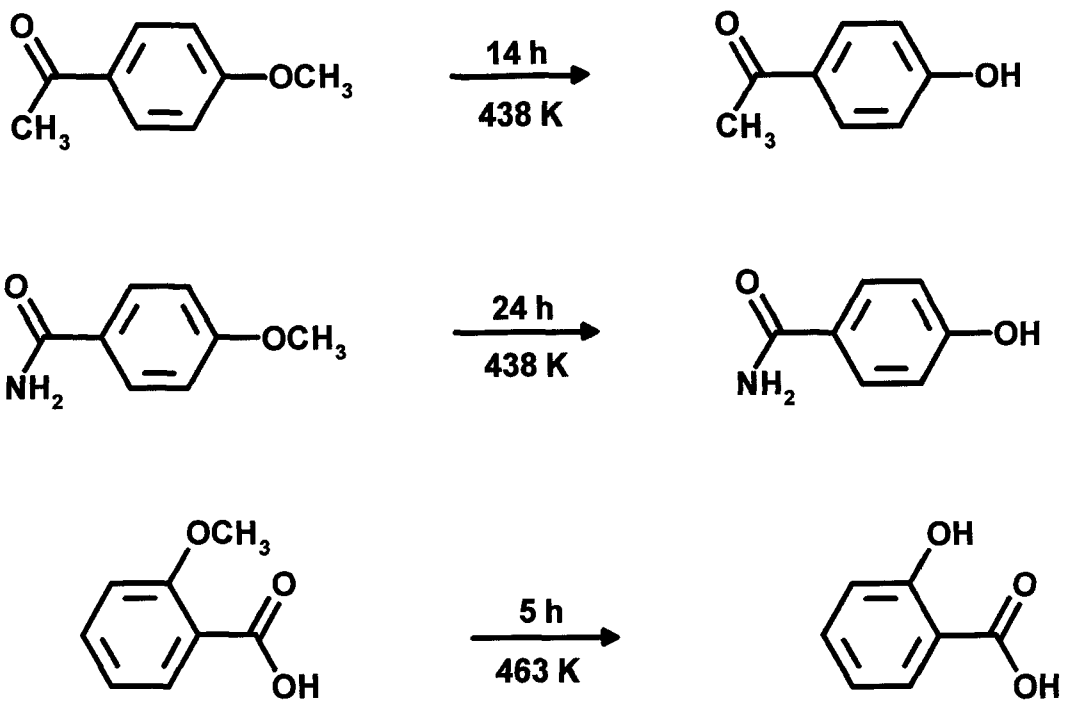

Scheme [3.13]

In one case it was reported that an anisole derivative having a carbonyl in the *para* position, which was resistant to cleavage with boron tribromide even under forcing conditions, was cleaved with this reagent A summary of the reaction is shown in Scheme [3 13]

3.1.1.4 Hydrobromic Acid

Constant boiling aqueous hydrobromic acid (b p 130°C/760 torr, d=1 5, 45–47%, 9 M) has been widely used to cleave methyl ethers[17] It is most effective when used with acetic acid as a co-solvent Anisole for instance is demethylated to phenol in almost quantitative yield, in 2 h at 130°C The efficiency of hydrobromic acid is significantly increased and reaction times shortened when a phase transfer catalyst is used[18]

The yields and reaction times do not depend on the nature of the phase transfer catalyst but only on its concentration The only requirement for an effective catalysis is that the catalyst must be soluble in the organic phase Catalysts such as hexadecyltributylphosphonium bromide and trioctylmethylammonium chloride have been used

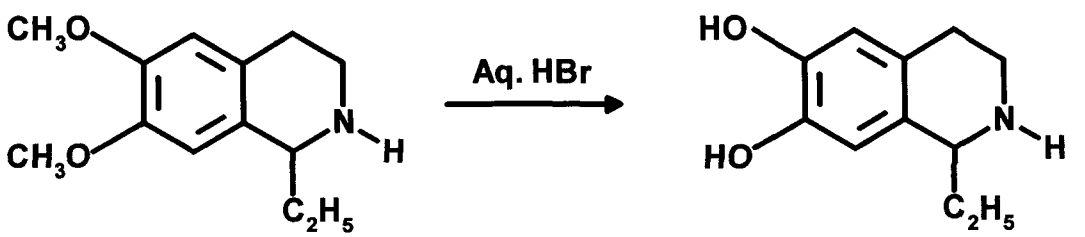

Scheme [3.14]

In Scheme [3 14], 6,7-dimethoxy-1-ethyl-1,2,3,4-tetrahydroisoquinoline was demethylated using a typical hydrogen bromide procedure[19]
The demethylation can be carried out with either the free base or the hydrochloride A 10% excess of the 48% hydrobromic acid (redistilled over a trace of 50% hypophosphorous acid, 1 g for each 100 g of 48% hydrobromic acid) were heated together On removal of the aqueous fore-run the liquid temperature reached 126°C The reaction time can vary from 1–3 h and in some cases even longer and is complete when the evolution of methyl bromide ceases When the excess hydrobromic acid is removed under pressure the product can be crystallized from ethanol

3.2 RESULTS AND DISCUSSION

3.2.1 Counter-ion Comments

The compound used to precipitate all of the complexes synthesized in this work was ammonium hexafluorophosphate The hexafluorophospate (PF_6^-) moiety of the compound serves as a single negatively charged counter-ion The complexes of the termed "smaller ligands" HL1 and HL2, emerge from the complexation reaction with the triazolic proton removed A single PF_6^- counter-ion per molecule is used to precipitate the salts of these complexes

The "larger ligands" H_2L3 and H_2L4 which each contain two triazolic protons, when complexed require two PF_6^- ions per molecule to facilitate salt formation Dissolution of the complexes in H_2O followed by addition of acid allows re-protonation of the triazole rings Further acidification may result in the protonation of the bipyridyl nitrogen atoms Growth of crystals of these complexes (in the deprotonated form) was sometimes aided by the addition of a small amount of base (ammonia) to the recrystallising solution

The complexes formed have very high molecular weights Microanalytical values in some cases are slightly deviant, but this should not be taken as evidence of impurity Bound water, acetone etc can cause these deviations The predicted X-ray structure was obtained in one case where the microanalytical results were not as expected

3.2.2 NMR Analysis of Small Triazoles

All ^{1}H-NMR spectra were obtained in **acetone-d^6** unless otherwise stated.

3.2.2.1 $[Ru(bpy)_2L1](PF_6).2H_2O$

The hydroquinone analogue of this molecule $[Ru(bipy)_2L6]$ was reported by Dr. Tia Keyes[4] in 1994. This complex is the dimethoxy protected version of that molecule.

Shown in Fig. [3.2] below is the ^{1}H-NMR spectrum of $[Ru(bpy)_2L1](PF_6).2H_2O$. At first glance the spectral peak pattern seems complex, but worthy of note is the purity of the complex. No impurity peaks are visible in the spectrum and the relative aromatic integration total is correct at 23. Though complex, the peak pattern shows good separation between the peaks, making the sample very suitable for COSY experiments.

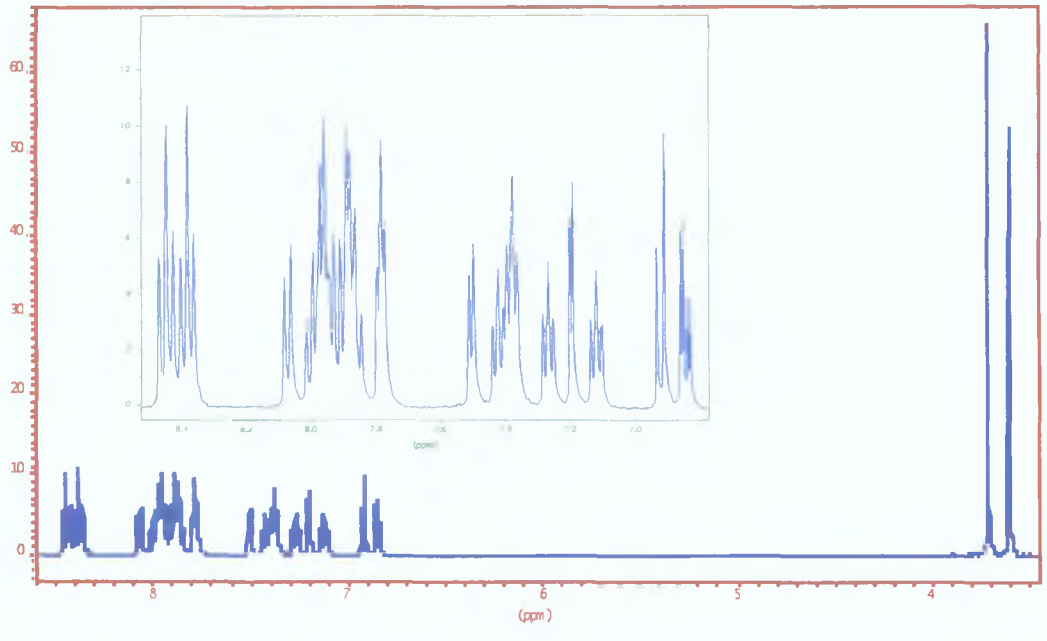

Fig. [3.2]: ^{1}H-NMR spectrum (ACN-d^3) of $[Ru(bpy)_2L1](PF_6).2H_2O$ with aromatic region enlarged (inset).

In Fig. [3.3], the pair of doublets at 6.93 ppm and 6.83 ppm can be reasonably attributed to H6" and H5" of the benzene ring. Identifying these peaks and their corresponding contours one can locate H3" at 7.20 ppm (see contour marked A on the COSY). H3" appears as a finely split doublet due to long range coupling to H5" which on close inspection is seen to be a doublet of doublets with the same J-value as H3". Thus H5" is the doublet of doublets at 6.93 ppm.

The doublet at 8.08 ppm in the complex spectrum can be related to position B in the COSY. Following the arrows across the map, this doublet is coupled (related) to a peak in the multiplet at 7.95 ppm, a doublet at 7.51 ppm and a triplet at 7.12 ppm. These four peaks are assigned as the pyridyl portion of the ligand in the molecule. This is deduced by the fact that the pyridyl peaks can be distinguished from the bipyridyl peaks by the absence of any long range coupling signals in the COSY map (shown in Fig. 3.3). The order of the pyridyl peaks in the ligand has changed from (moving downfield from) H6(8.69), H3(8.21), H4(7.87), H5(7.39) to having in the complex H3(8.08) as the furthest downfield peak followed by H4(7.95), H6(7.51), H5(7.12).

The obvious upfield shift of the pyridyl H6 proton in the complex is due to this proton experiencing a shielding effect from the bipyridyl rings. H6 can be seen in the crystal structure to lie in close proximity to these rings whose ring current imparts a shielding effect on the proton resulting in its upfield shift[3,20,21,22] This phenomenon is known as a diamagnetic anisotropic interaction of the H6 proton with the adjacent bipyridyl rings.

With the phenyl and pyridyl protons of the ligand assigned, the remaining peaks in the COSY spectrum correspond to the bis-bipyridyl protons. These 16 protons appear in four groups of four protons, each group representing a particular site on each of the bipyridyl (bipy) rings. The bipy protons appear in the ranges 8.06–8.47 ppm, 7.78–7.91 ppm, 7.25–7.44 ppm and from 7.93–8.01 ppm.

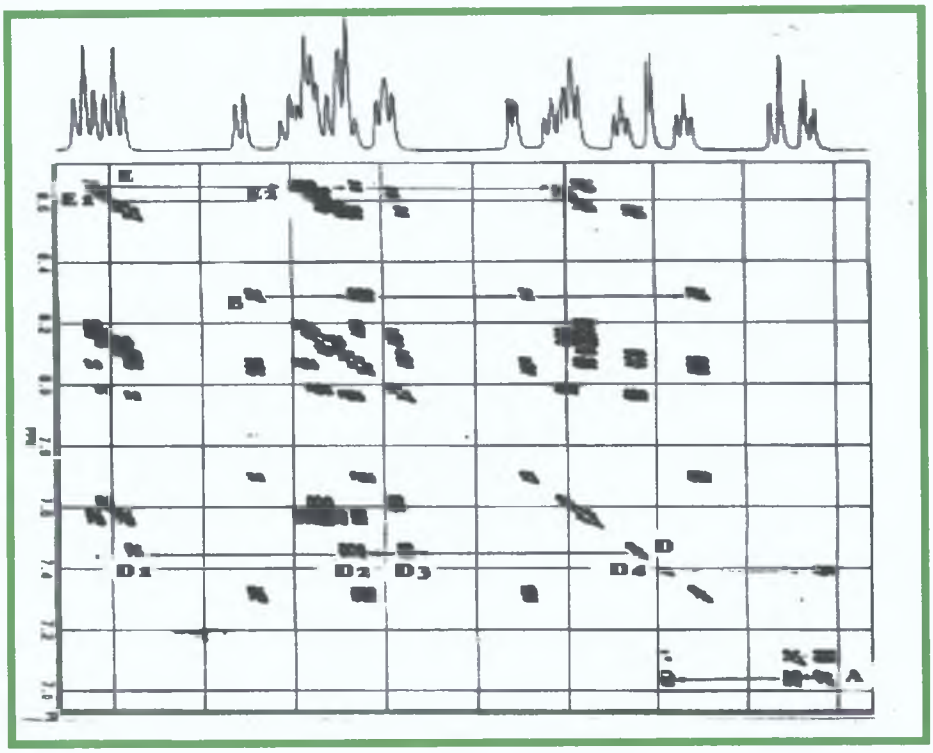

Fig. [3.3]: COSY spectrum (ACN-d^3) of $[Ru(bpy)_2L1](PF_6).2H_2O$.

Using the COSY shown in Fig. [3.3] these peaks can be assigned to their positions on the bipy (=bipyridyl) rings. Point D along the diagonal of the COSY shows most clearly the couplings of the bipy protons. D1 corresponds to overlapping doublets which appear as a triplet. D1 represents either H3 or H6. Since H3 in general is the furthest downfield bipy signal[4], it is assigned to D1. D2 and D4 correspond to triplets representing bipy H4 and H5. To assign these peaks one should look at point E on the COSY. E1 corresponds to the H3 bipy protons and judging by the amplitudes of the contours on the map H3 protons are most strongly coupled to the set of triplets closest to them at E2 (7.93–8.00 ppm). They are assigned to bipy H4. Thus the bipyridyl protons appears from the furthest downfield upwards in the order H3, H4, H6, H5.

3.2.2.2 $[Ru(bpy)_2L2](PF_6).2H_2O$

The ^{1}H-NMR spectrum of this, the pyrazine analogue of $[Ru(bpy)_2L1](PF_6).2H_2O$ is shown in fig. [3.4] below. The presence of a pyrazine ring results in changes of chemical shift and coupling values. H3 of the pyrazine ring of the ligand is located at 9.51 ppm while the other pyrazine protons are present at 8.64 and 8.10 ppm. We deduce this, not from the ^{1}H-NMR spectrum, but from the COSY map. One might expect coupling of the H3 proton to H5 which is often observed in spectra containing pyrazine groups. Though no splitting of the H3 signal is visible in the ^{1}H-NMR spectrum, if one observes the H3 contour on the diagonal of the COSY shown in Fig. 3.5 (at point **A**), by following the arrow across, H3 is seen to be coupled to a doublet at 8.10 ppm which is assigned to H5. The doublet at 8.64 ppm represents H6. The H6 proton does not appear to experience the same upfield shift as H6 of $[Ru(bpy)_2L1](PF_6).2H_2O$. The pyrazine complex may not experience the same shielding effect of the bipyridyl ring current as did its pyridine analogue.

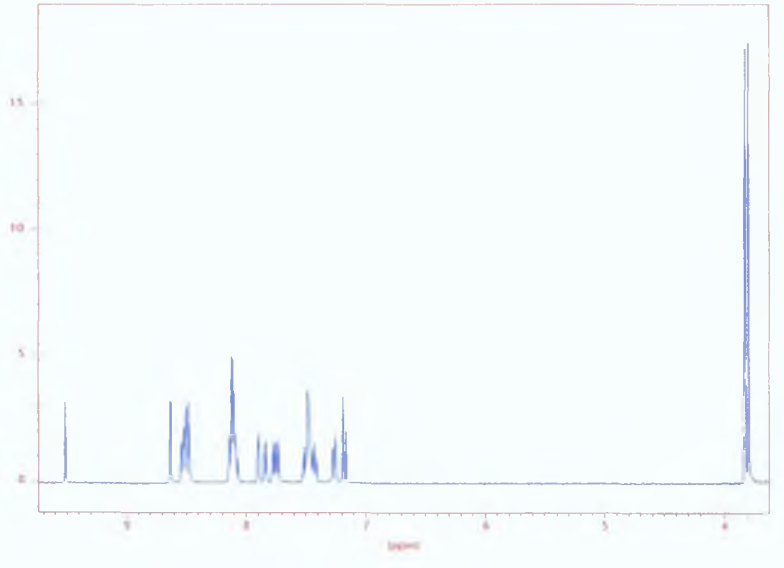

Fig. [3.4]: ^{1}H-NMR spectrum of $[Ru(bpy)_2L2](PF_6).2H_2O$

Switching attention to the benzyl protons in the complex, H3" is observed as the prominent doublet at 7.47 ppm emerging from the multiplet in the region. The J-value of 2.95 for the fine doublet shows that it is coupled to the doublet of doublets at 7.28 ppm which has the same J-value. This is the coupling of H3" to H5" which can also be observed at point B in the COSY in fig. [3.5]. Point C shows the contour of H5" coupling to H6" to its right and H3" to its left.

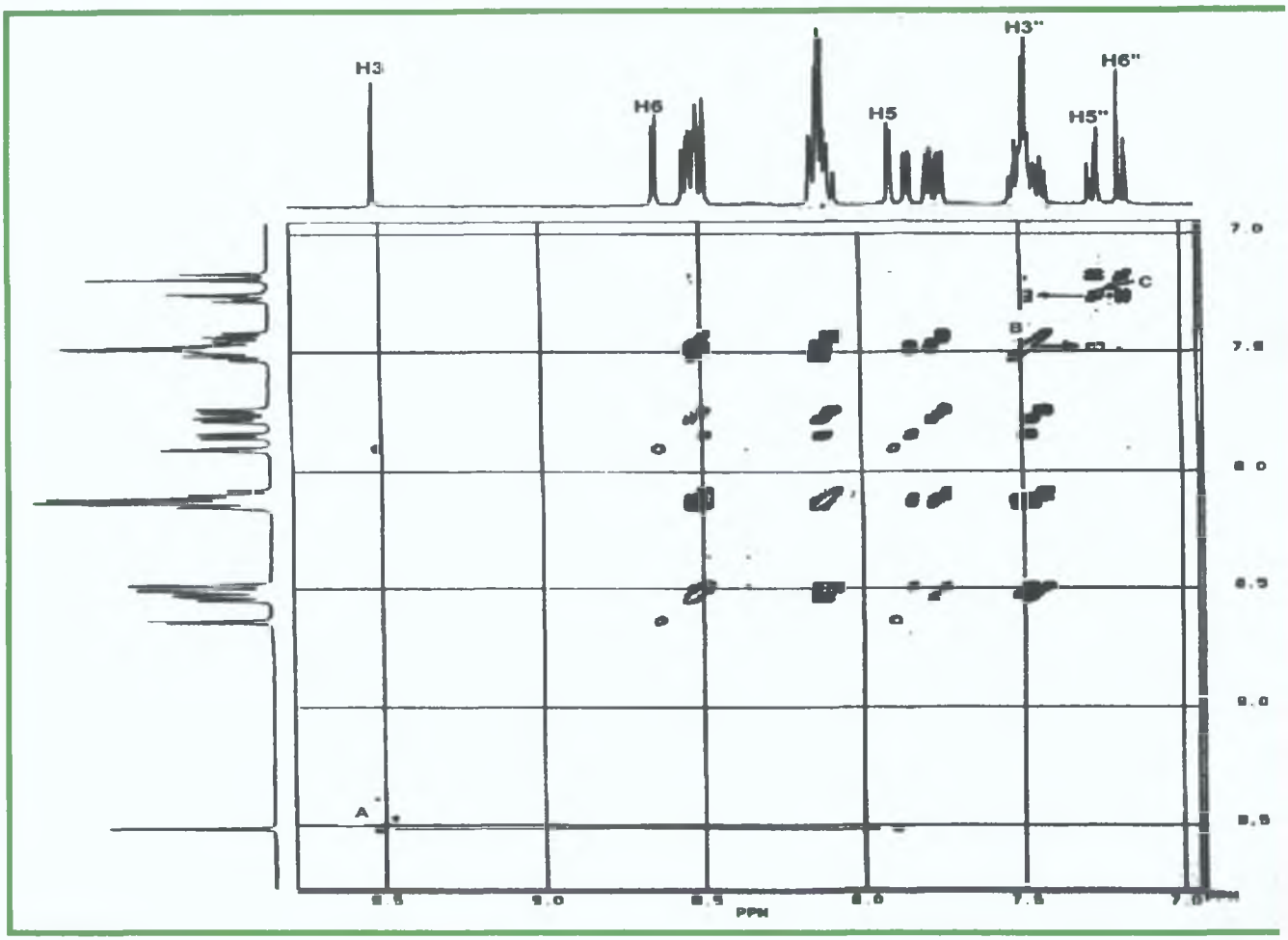

Fig. [3.5]: COSY of $[Ru(bpy)_2L2](PF_6).2H_2O$.

H5" in this complex is further downfield than H6". H5" is in closer proximity to the bipyridyl rings (and their ring currents). This is the reverse of the situation in $[Ru(bpy)_2L1](PF_6).2H_2O$.

Reason: The reason for these changes in shift can be understood by viewing the crystal structures of HL1 (Fig 2 12) and its corresponding ruthenium bipyridyl complex (Fig 3 35) and HL2 (Fig 2 14) On complexation the pyridine N of HL1 (which is adjacent to N4 of the triazole) flips through approx 180° so that in the complex it is now in proximity to N1 of the triazole Looking at the structure of the complex in Fig 3 35, the H6" proton appears to be in closer proximity to the bipyridyl protons than H5" and thus would be expected to appear further downfield Now, although the crystal structure of the complex of HL2 was not obtained, it is clear from the structure of the ligand HL2 (Fig 2 14) that N1 of the pyrazine ring and N1 of the triazole ring are already perfectly positioned for complexation to ruthenium, i e no flipping of the pyrazine ring should occur in this case Thus if ruthenium metal complexes with HL2, without any ligand rearrangement, H5" of the resultant complex would be in closer proximity to the bipyridyl groups than H6" Accordingly, in the ^{1}H-NMR of the complex of HL2, H5" is shifted further downfield than H6" This could explain the observed difference in the H5", H6" shifts in the spectra of the two complexes

Further work involving obtaining of the crystal structure of $[Ru(bpy)_2L2](PF_6)\ 2H_2O$ may prove this explanation The bipyridyl protons of $[Ru(bpy)_2L2](PF_6)\ 2H_2O$ are present in the regions H3(8 48–8 54 ppm), H4(8 07–8 14 ppm), H6(8 07–8 14 ppm), H5(7 41–7 51 ppm)

3.2.2.3 $[Ru(bpy)_2L5](PF_6).2H_2O$

This complex has been described previously in detail by Dr Tia Keyes in her Ph D thesis[4] No attempt was made to duplicate this work

3.2.2.4 $[Ru(bpy)_2L6](PF_6).2H_2O$

The deprotection of $[Ru(bpy)_2L2](PF_6).2H_2O$ with boron tribromide results in the formation of the 1",4"-hydroquinone complex, $[Ru(bpy)_2L6](PF_6).2H_2O$. The spectrum shown in fig. [3.6] is very similar to the dimethoxy complex. H3 appears at 9.55 ppm as opposed to 9.51 ppm for the protected complex. The benzyl protons which were in the range 7.18–7.37 for $[Ru(bpy)_2L2](PF_6).2H_2O$ have experienced the expected upfield shift to the range 6.92–7.41 ppm in $[Ru(bpy)_2L6](PF_6).2H_2O$.. The prediction is based on calculations of approximate chemical shift effect on the *ortho*-, *meta*- and *para*- positions by functional groups[23]. No –OH signal was seen in the spectrum. This is not unusual and may be due to solvent effects. Its non-appearance could also be attributable to H-bonding effects, which we would expect to see with neighbouring N atoms

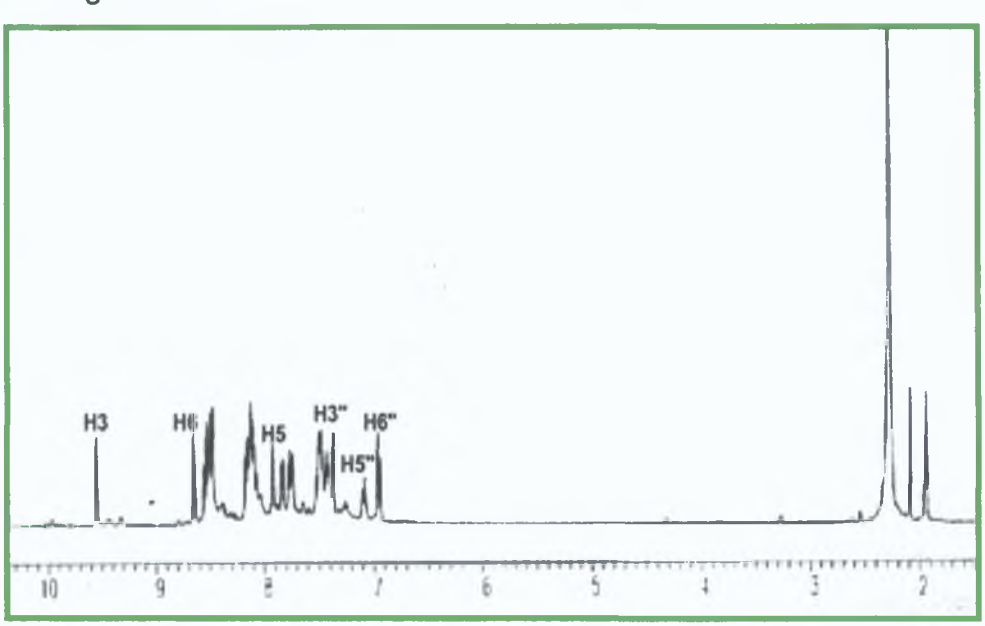

Fig. [3.6]: ^{1}H-NMR of $[Ru(bpy)_2L6](PF_6).2H_2O$

3.2.2.5 $[Ru(bpy\text{-}d^8)_2L2](PF_6).2H_2O$

If ruthenium bis-bipyridyl dichloride undergoes a deuteriation reaction whereby all the bipyridyl protons are converted to deuterium atoms the product can be complexed to a ligand as normal. The resulting deuteriated complexes are very useful for a number of NMR experiments. Firstly, the bipy proton signals are removed from the spectrum resulting in a much simplified set of peaks belonging only to the undeuteriated ligand. Secondly, the chemical shifts of the peaks in the deuteriated spectrum can validate the original spectrum (assuming both spectra are carried out in the same solvent, their chemical shifts are often very similar).

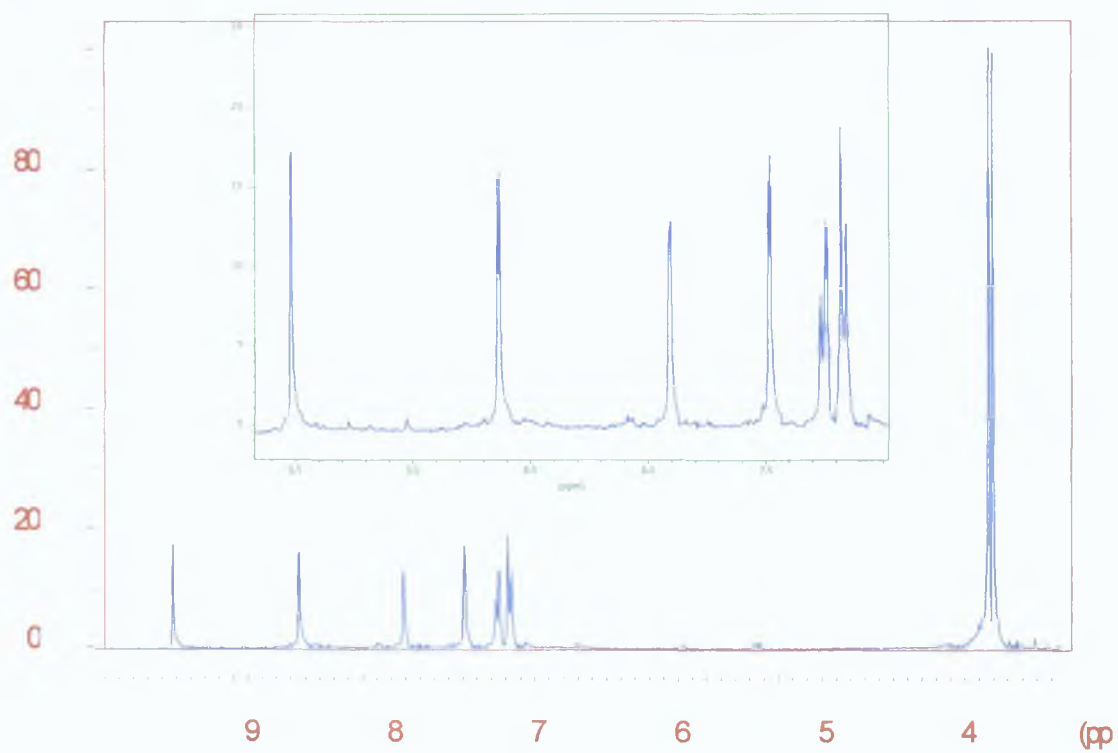

Fig. [3.7]: ^{1}H-NMR of $[Ru(bpy\text{-}d^8)_2L2](PF_6).2H_2O$ with expanded aromatic region (inset).

The spectrum of $[Ru(bpy\text{-}d^8)_2L2](PF_6).2H_2O$ is shown in fig. [3.7]. The chemical shifts are equal to that of the deuteriated complex throughout. The doublet of H3" which was engulfed in a multiplet of bipy-H4 peaks in the ordinary complex can now be clearly distinguished. Immediately upfield from H3", the doublet of doublets of H5" is also clarified. The original and deuteriated spectra can also be compared by overlaying both spectra as shown in Fig. [3.8].

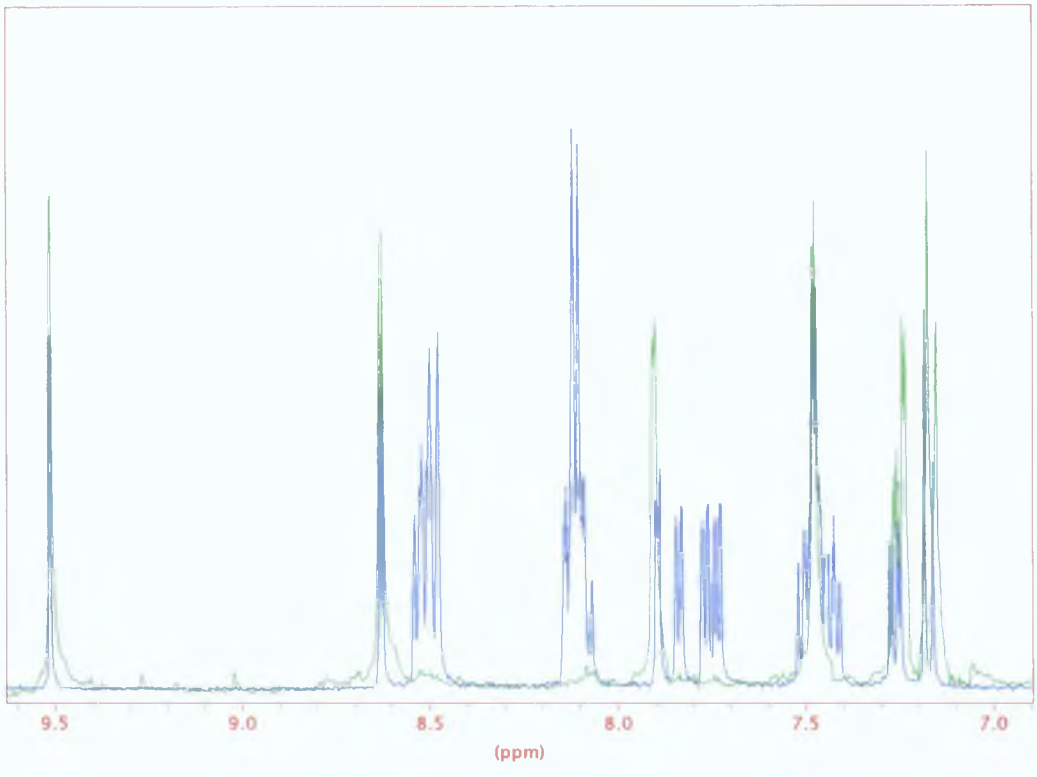

Fig. [3.8] :Overlay of $[Ru(bpy\text{-}d^8)_2L2](PF_6).2H_2O$ and $[Ru(bpy)_2L2](PF_6).2H_2O$

Finally subtracting the peaks of the deuterated spectrum (shown in Fig. [3.9]) from the original complex spectrum results in a difference spectrum containing only the bipyridyl peaks of the original complex. This gives a good feel for the H3, H4, H6, H5 (from downfield up) bipyridyl grouping.

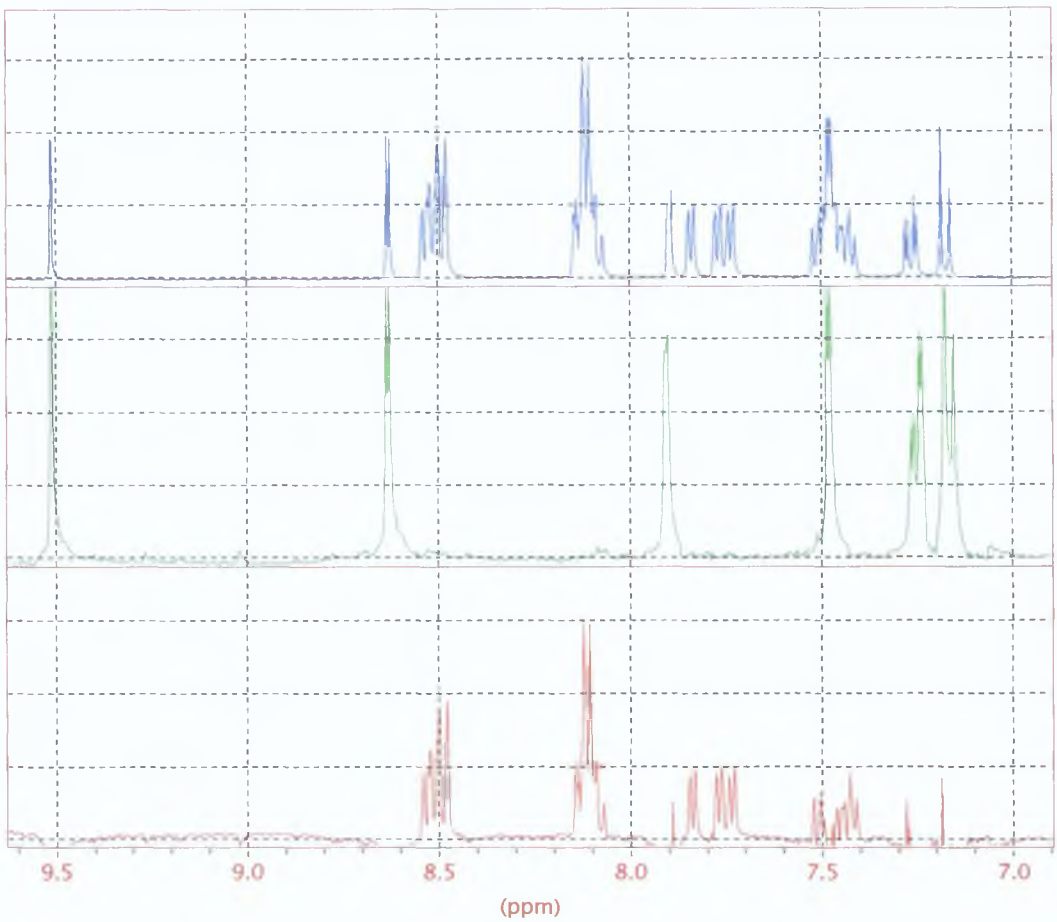

Fig. [3.9]: Subtraction of [Ru(bpy-d^8)$_2$L2](PF$_6$).2H$_2$O from [Ru(bpy)$_2$L2](PF$_6$).2H$_2$O leaving bis-bipyridyl peaks.

3.2.3 NMR Analysis of Large Metal complexes Containing Triazoles

3.2.3.1 $[(Ru(bpy)_2)_2L3](PF_6)_2.4H_2O$

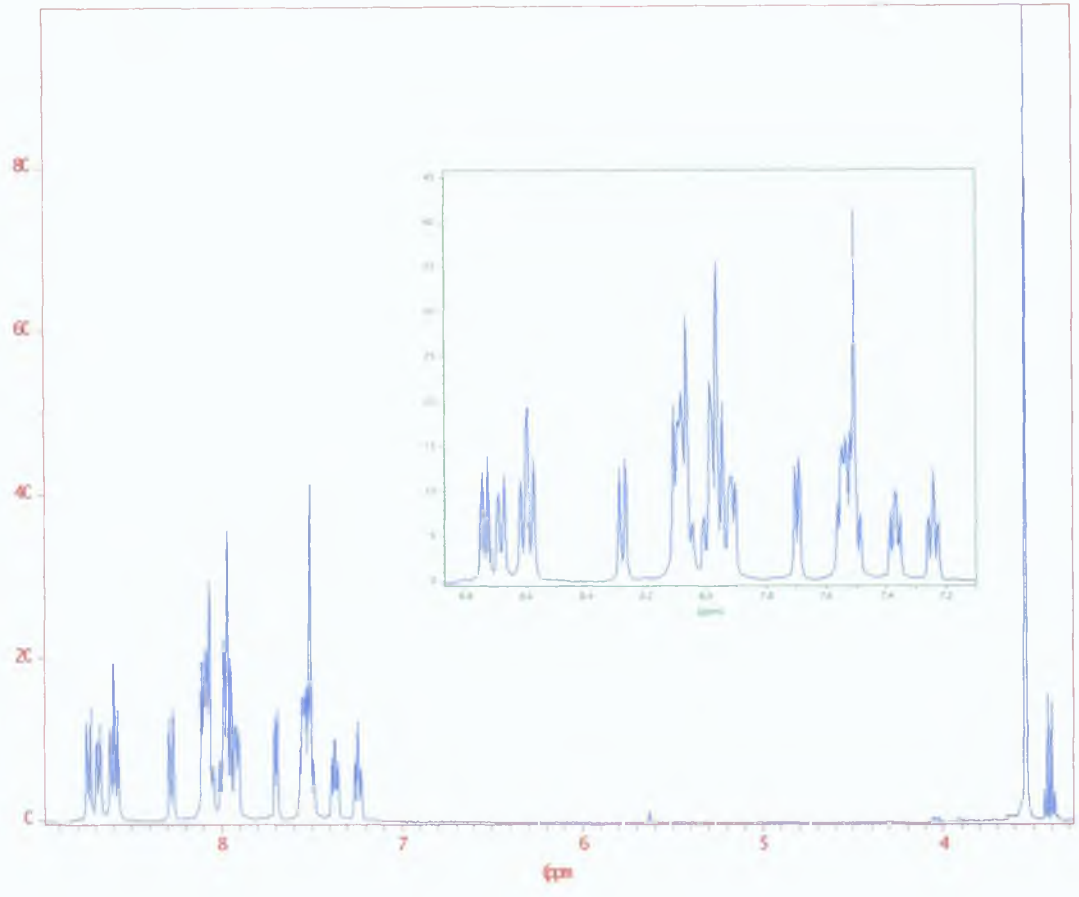

Fig. [3.10]: ^{1}H-NMR (ACN-d^3) of $[(Ru(bpy)_2)_2L3](PF_6)_2.4H_2O$ with enlarged aromatic region (inset).

The methoxy proton signal can be seen in fig.[3.10] at 3.54 ppm. The benzyl H3" proton again emerges from a multiplet at 7.51 ppm and the pyridyl protons of the ligand appear at 8.29 ppm(H3), 7.96 ppm(H4), 7.71 ppm(H6) and 7.24 ppm(H5). These peaks are distinct from the bipy peaks by the coupling in the

COSY spectrum. Long range coupling of the bipy peaks is seen in the COSY. It is difficult to pinpoint H4 and H5 in the proton spectrum however and again the COSY spectrum aids elucidation.

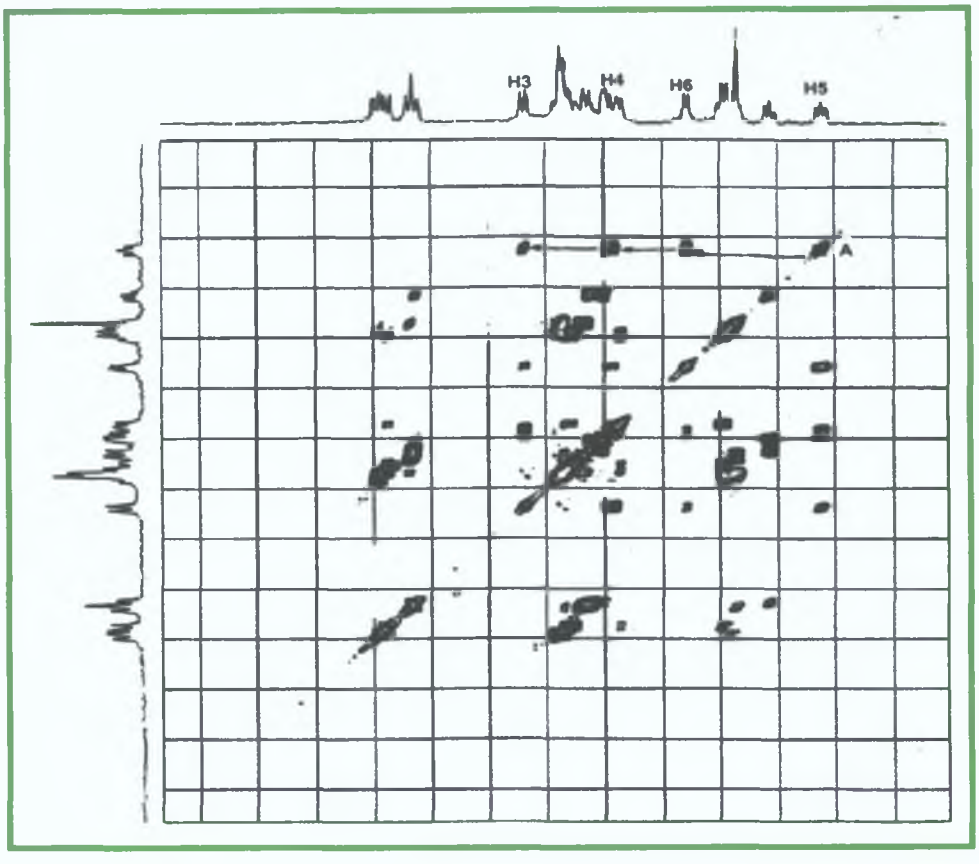

Fig. [3.11]: COSY (ACN-d^3) of [(Ru(bpy)$_2$)$_2$L3](PF$_6$)$_2$.4H$_2$O.

Point A on the COSY spectrum in Fig. [3.11] lies beside the contour representing H5 of the pyridyl ring. We know this from the information provided by the ^{1}H-NMR spectrum of the deuteriated complex. Following the arrows across, we have H6 (doublet), H4 in the multiplet at 7.95 ppm and H3 (doublet), the furthest downfield pyridyl signal. The bipy protons appear in the range H3 (8.56–8.75 ppm), H4(8.04–8.11 ppm), H6(7.90–8.00 ppm) and H5(7.35–7.56 ppm)

3.2.3.2 $[(Ru(bpy\text{-}d^8)_2)_2L3](PF_6)_2.4H_2O$

Forming the deuteriated bipy analogue of $[(Ru(bpy)_2)_2L3](PF_6)_2.4H_2O$ (in fig.[3.12]) again provides interesting spectral data which allows us to clearly see the ligand peaks as they appear in the complex. The bipy grouping can also be seen in the subtraction spectrum fig. [3.13].

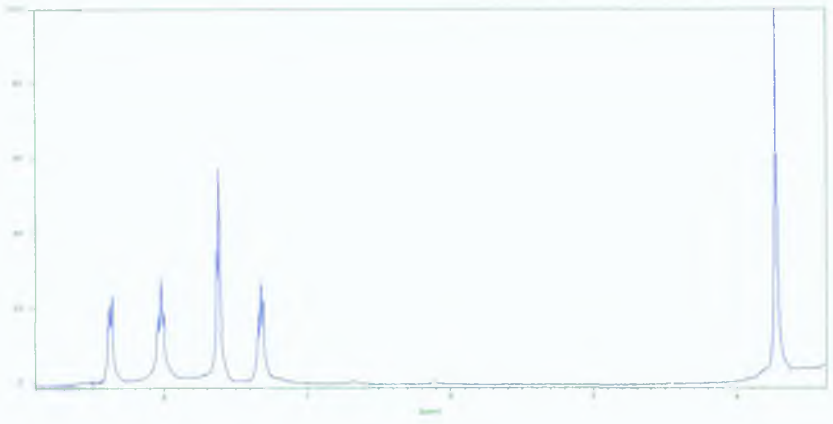

Fig. [3.12]: ^{1}H-NMR of $[(Ru(bpy\text{-}d^8)_2)_2L3](PF_6)_2.4H_2O$.

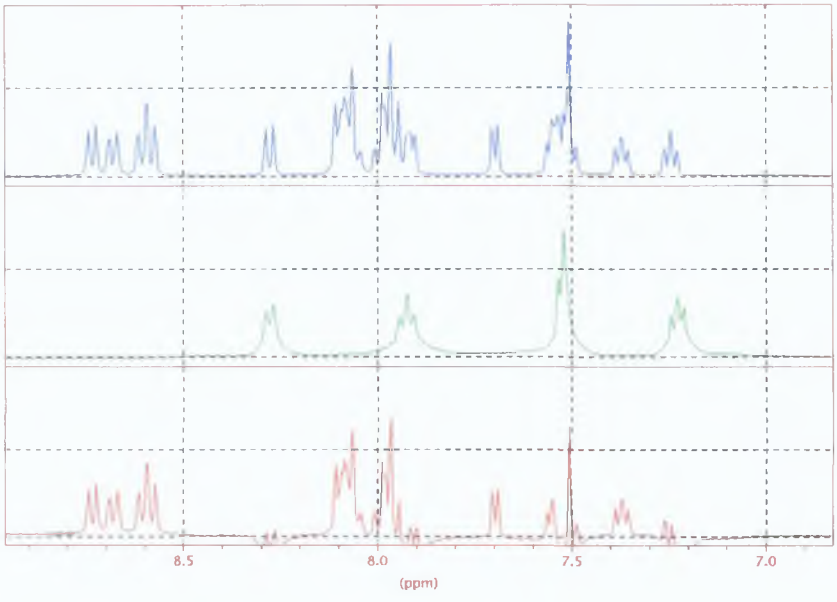

Fig. [3.13]: Comparison of ^{1}H-NMR spectra of $[(Ru(bpy\text{-}d^8)_2)_2L3](PF_6)_24H_2O$ ($ACN\text{-}d^3$) to $[(Ru(bpy\text{-}d^8)_2)_2L3](PF_6)_24H_2O$. Subtraction of the spectra exposes bis-bipyridyl peaks.

3.2.3.3 $[(Ru(bpy)_2)_2L7](PF_6)_2.4H_2O$

NMR studies of this hydroquinone complex are of great significance in the investigation of this complex. ^{1}H-NMR and COSY spectra were obtained in deuteriated DMSO and acetone. The COSY obtained in DMSO provides the good indication of purity and allows easiest peak assignment. DMSO as an NMR solvent is excellent and its solvent effects often produce helpful chemical shift changes to clarify otherwise difficult spectra.

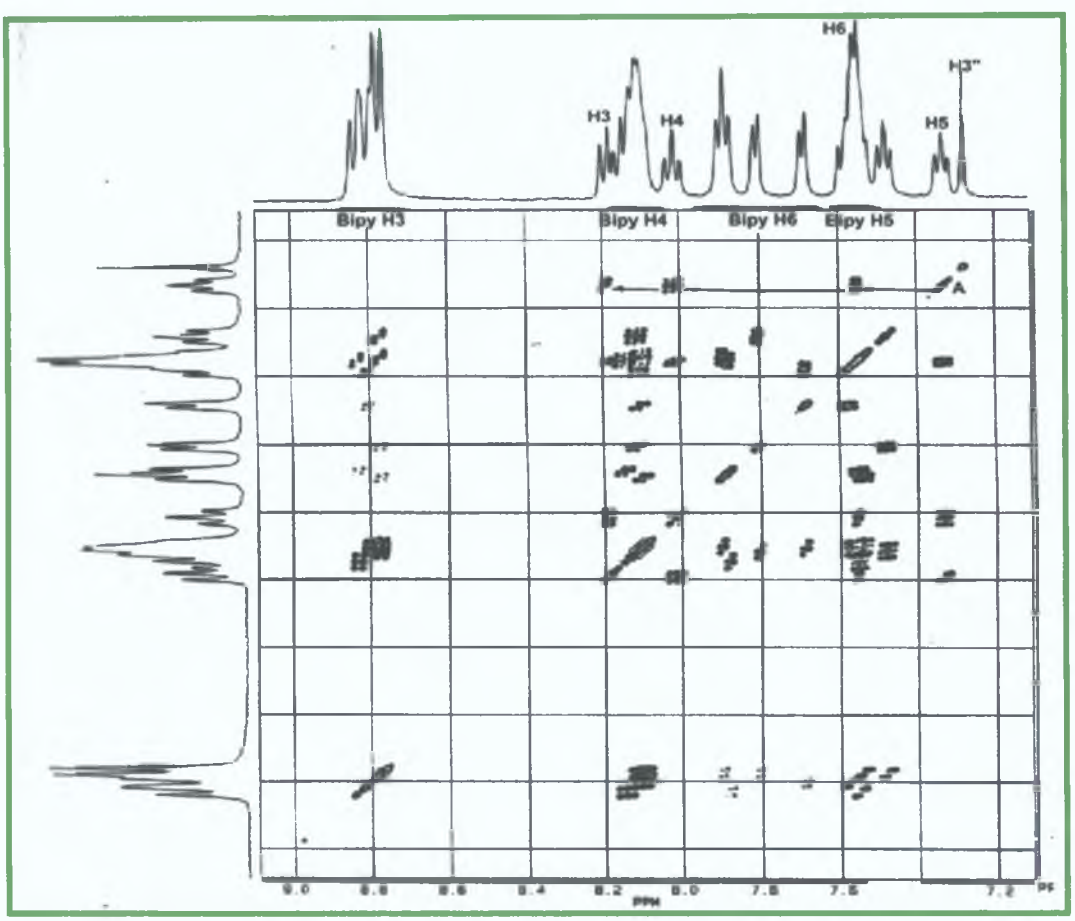

Fig. [3.14]: COSY of $[(Ru(bpy)_2)_2L7](PF_6)_2.4H_2O$ in DMSO-d^6.

Owing to the spectral similarities of the protected and deprotected complexes, we can say the contour at point A on the COSY map in fig. [3.14] corresponds to

the triplet representing H5 of the ligand pyridine. H6 is located in the multiplet immediately downfield. Further downfield and more deshielded is the triplet of H4 with H3 the furthest downfield signal. The benzylic proton appears as the most shielded proton in the region. The underlined areas in the spectrum labelled H3–H6 represent the bipyridyl protons.

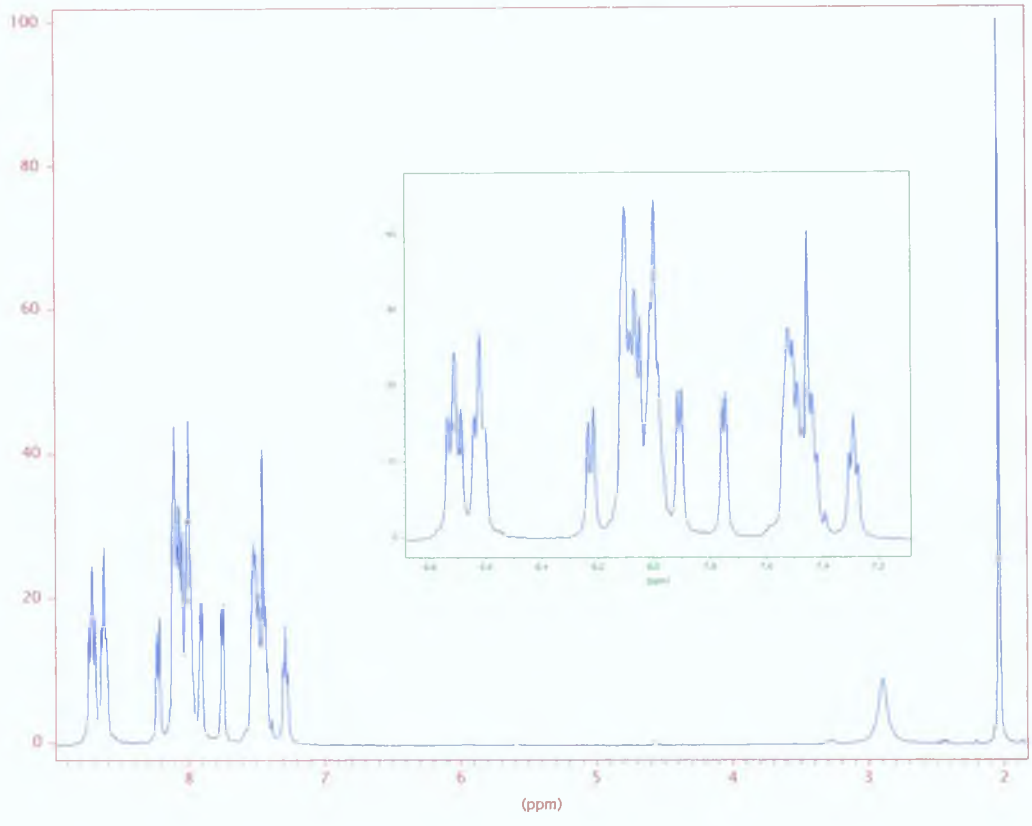

Fig. [3.15]: ^{1}H-NMR spectrum of $[(Ru(bpy)_2)_2L7](PF_6)_2.4H_2O$ in acetone-d^{6} with aromatic region enlarged (inset).

The proton spectra shown in fig. [3.15] was carried out in deuteriated acetone solvent to allow some comparison with the dimethoxy analogue of the complex (the hydroquinone complexes often showed anomolous solubility properties and in this case no spectrum in deuteriated acetonitrile was obtainable). The absence of the $-OCH_3$ signal in the 3.5–4.0 ppm indicates that deprotection has been successful. A broad singlet (not shown in the spectrum) corresponding to the new –OH proton of the central hydroquinone is present at 10.90 ppm.

Hydrogen bonding effects between the –OH and the triazole N (among others) can be attributed to the downfield appearance of the hydroxyl proton. H3 of the pyridine ring appears at 8.24 ppm but H4 is clearly defined being part of the multiplet in the range 7.80–8.00 ppm. H6(7.75 ppm), and H5(7.29 ppm) are clear and the benzylic proton is visible at 7.42 ppm.

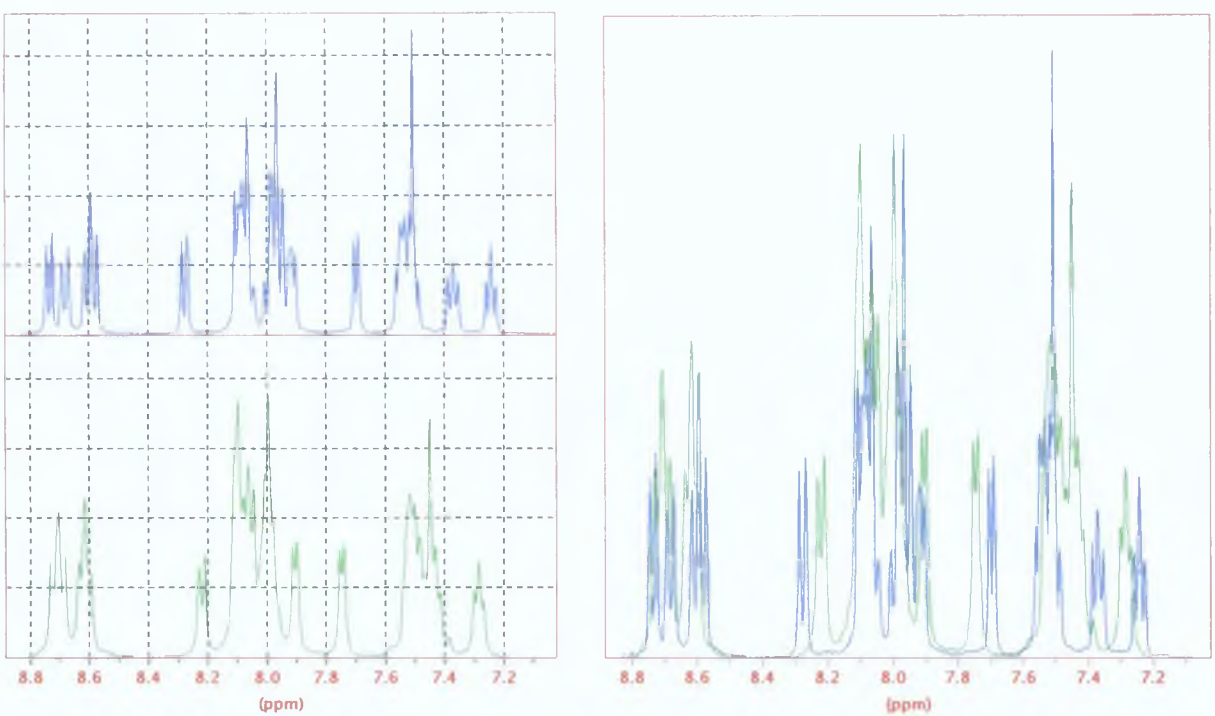

Fig. [3.16]: Comparison of ^{1}H-NMR spectra of [(Ru(bpy)$_2$)$_2$L3](PF$_6$)2.4H$_2$O (ACN-d^3) to [(Ru(bpy)$_2$)$_2$L7](PF$_6$)2.4H$_2$O (left). An overlay of both spectra is shown (right).

The overlay plot in fig. [3.16] shows that in the deprotected complex, the pyridyl ligand H3 and H4 have shifted slightly upfied while H6 and H5 moved slightly downfield. As expected, the benzylic proton has been shifted upfield to 7.42 ppm.

3.2.3.4 $[(Ru(bpy)_2)_2L4](PF_6)_2.4H_2O$

The ^{1}H-NMR spectrum of the pyrazine analogue of $[(Ru(bpy)_2)_2L3](PF_6)_2.4H_2O$ is shown in fig. [3.17]. Compared to $[(Ru(bpy)_2)_2L3](PF_6)_2.4H_2O$ the benzylic proton has shifted upfield from 7.51 to 7.36 ppm. H3 in $[(Ru(bpy)_2)_2L3](PF_6)_2.4H_2O$ was at 8.29 ppm whereas in the pyrazine spectrum, the expected downfield shift of H3 at 9.21 ppm has occurred. H6, which was shifted upfield in $[(Ru(bpy)_2)_2L3](PF_6)_2.4H_2O$ by the shielding effects of the bipyridyl ring current, in this case is not as affected appearing at 8.23 ppm.

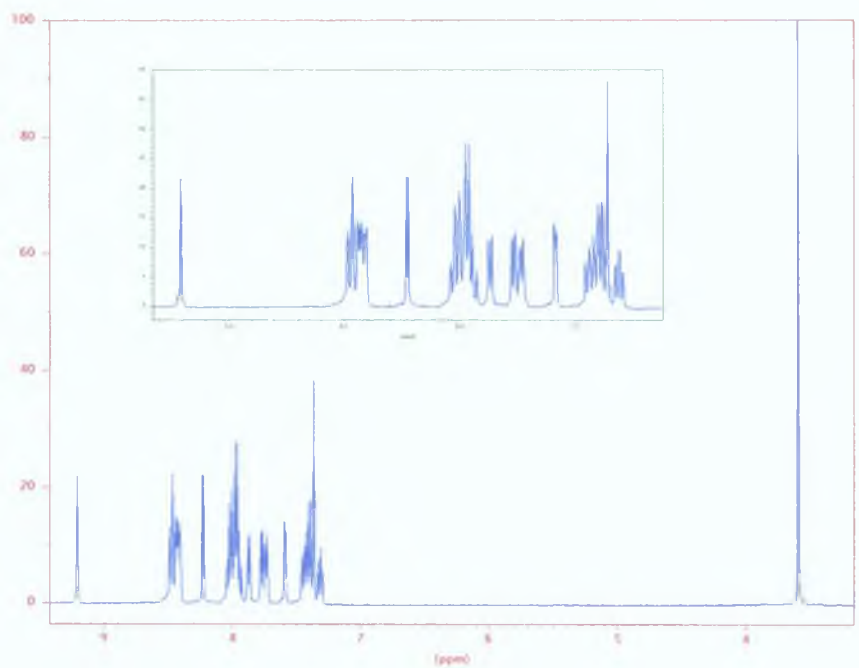

Fig. [3.17]: ^{1}H-NMR spectrum of $[(Ru(bpy)_2)_2L4](PF_6)2.4H_2O$ in (ACN-d^3) with aromatic region enlarged (inset).

3.2.3.5 $[(Ru(bpy\text{-}d^8)_2)_2L4](PF_6)_2.4H_2O$

The deuteriated complex was also prepared and the comparison of the proton NMR's is illustrated in fig. [3.18].

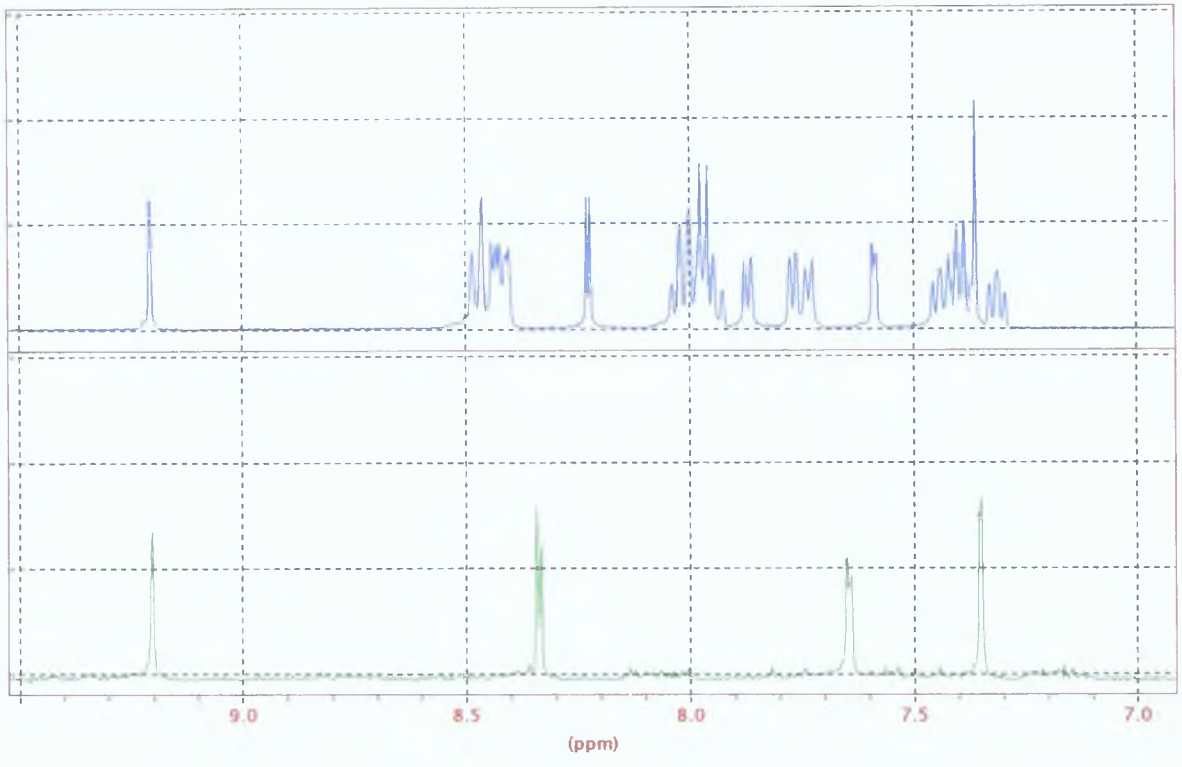

Fig. [3.18]: Comparison of ^{1}H-NMR spectra of $[(Ru(bpy)_2)_2L4](PF_6)_2.4H_2O$ (ACN-d^3) to $[(Ru(bpy\text{-}d^8)_2)_2L4](PF_6)_2.4H_2O$

3.2.3.6 $[(Ru(bpy)_2)_2L8](PF_6)_2.4H_2O$

The spectrum of this hydroquinone complex shows the absence of the $-OCH_3$ signal between 3 and 4 ppm. However no –OH signal is in evidence further down the spectrum. An explanation for this lies in the fact that acidic protons such as triazolic and hydroxyl protons are subject to exchange effects and are

often not seen. Note that no triazolic proton signal was seen in the pyrazine ligand HL2 spectrum but was confirmed present by X-ray structure determination.

Apart from this anomaly the chemical shifts of the protected and deprotected complexes are in good agreement. The comparison and overlay spectra (fig.[3.19]) show this.

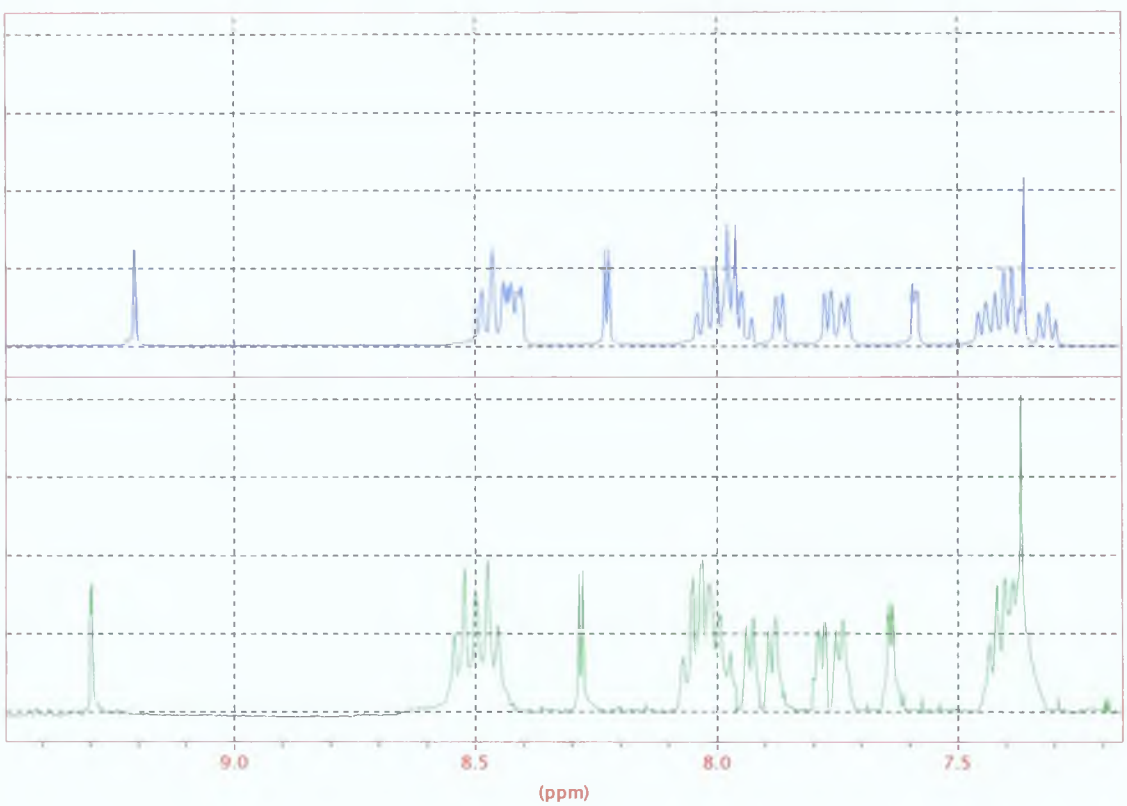

Fig. [3.19]: Comparison of ^{1}H-NMR spectra of $[(Ru(bpy)_2)_2L4](PF_6)_2.4H_2O$ (ACN-d^3) to $[(Ru(bpy)_2)_2L8](PF_6)_2.4H_2O$ (ACN-d^3).

The chemical shift values reported in this chapter are summarized in tables 3 1 and 3 2

Complex (Solvent d-acetone unless stated)	H3	H4	H5	H6
$[Ru(bpy)_2L1](PF_6)\ 2H_2O$ (ACN-d^3)	8 08	7 95	7 12	7 51
$[Ru(bpy)_2L2](PF_6)\ 2H_2O$	9 51	–	~8 10	8 64
$[Ru(bpy)_2L6](PF_6)\ 2H_2O$	9 55	–	8 13	8 67
$[Ru(bpy\text{-}d^8)_2L2](PF_6)\ 2H_2O$	9 52	–	7 91	8 64
$[(Ru(bpy)_2)_2L3](PF_6)_2\ 4H_2O$ (ACN-d^3)	8 29	7 96	7 24	7 71
$[(Ru(bpy)_2)_2L7](PF_6)_2\ 4H_2O$	8 24	7 98–8 0	7 29	7 76
$[(Ru(bpy\text{-}d^8)_2)_2L3](PF_6)_2\ 4H_2O$	8 39	8 03	7 33	7 64
$[(Ru(bpy)_2)_2L4](PF_6)_2\ 4H_2O$ (ACN-d^3)	9 21	–	7 59	8 23
$[(Ru(bpy)_2)_2L8](PF_6)_2\ 4H_2O$ (ACN-d^3)	9 30	–	7 64	8 28
$[(Ru(bpy\text{-}d^8)_2)_2L4](PF_6)_2\ 4H_2O$	8 76	–	7 20	7 90

Table [3.1] List of chemical shifts for pyridinyl/pyrazinyl protons of ruthenium complexes

Complex					
$[Ru(bpy)_2L1](PF_6)\ 2H_2O$	7 20(H2')	6 86(H5')	6 93(H6')	3 71($OCH_3^{1'}$)	3 61($OCH_3^{4'}$)
$[Ru(bpy)_2L2](PF_6)\ 2H_2O$	7 47(H3')	7 18(H5')	7 28(H6')	3 83($OCH_3^{1'}$)	3 80($OCH_3^{4'}$)
$[Ru(bpy)_2L6](PF_6)\ 2H_2O$	7 41(H3')	6 92(H5')	7 09(H6')	no –OH signal	
$[Ru(bpy\text{-}d^8)_2L2](PF_6)\ 2H_2O$	7 49(H3')	7 18(H5')	7 27(H6')	3 83($OCH_3^{1'}$)	3 80($OCH_3^{4'}$)
$[(Ru(bpy)_2)_2L3](PF_6)_2\ 4H_2O$	7 51(Benz-H)	3 54(OCH_3)			
$[(Ru(bpy)_2)_2L7](PF_6)_2\ 4H_2O$	~7 41(Benz-H)	10 90(OH)			
$[(Ru(bpy\text{-}d^8)_2)_2L3](PF_6)_2\ 4H_2O$	7 64(Benz-H)	3 73(OCH_3)			
$[(Ru(bpy)_2)_2L4](PF_6)_2\ 4H_2O$	7 36(Benz-H)	3 59(OCH_3)			
$[(Ru(bpy)_2)_2L8](PF_6)_2\ 4H_2O$	7 37(Benz-H)	no –OH signal			
$[(Ru(bpy\text{-}d^8)_2)_2L4](PF_6)_2\ 4H_2O$	7 36(Benz-H)	3 06(OCH_3)			

Table [3.2] List of chemical shifts for benzylic protons of ruthenium complexes.

3 2 4 Absorption and Emission Discussion

The importance of the synthesis of ruthenium complexes of the ligands described in this work has been established by the fact that changing the ligand systems around the ruthenium (II) centre, from those in $[Ru(bipy)_3]^{2+}$, it is possible to alter the ground and excited state properties of the complexes [3] In essence, the ability of these complexes to form long-lived charge separated species complexes is desired and will be investigated at a future date within the research group Though the scope of the thesis deals with the synthetic routes to these complexes, a cursory report of absorption and emission characteristics of the complexes is described in this chapter The results obtained are related to the complexes in a broad sense only Results obtained from complexes HL1 and HL2 were not sufficiently clear for inclusion in this work

UV absorption and emission experiments were carried out using the same conditions and equipment as outlined by Dr Tia Keyes in her Ph D thesis [4] Measurements were taken in acetonitrile unless stated with an excitation slit width of 5 nm and an emmision slit of 10 nm Measurements at 77 K were conducted in an ethanol/methanol 4 1 mixture with excitation and emission slit widths at 5 nm Diethylamine (or conc aqueous ammonia) was used to deprotonate complexes and 60% (w/v) perchloric acid was used to protonate complexes In any case no more than 10% acid or base was added

3.2.4.1 Absorption and emission properties of H_2L3 Complexes

Ruthenium bipyridyl complexes containing triazole ligands in general show an intense absorption band in the region of 450 nm This is attributed to $d\pi$-π^* metal to ligand charge transfer (MLCT)[24] Also complexes containing electron rich ligands tend to have strong σ-donating properties from the ligand to the metal This results in the MLCT bands having lower energy and absorption bands at higher wavelengths in the spectrum[4]

On deprotonation of the triazolic proton of the complex, the ligand becomes more electron rich and thus a better σ-donor This causes the MLCT bands to have lower energy and can be seen in the spectrum as absorption bands at higher wavelengths Shown in fig [3 20] are the absorption spectra for $[(Ru(bipy)_2)_2L3]^{2+}$ and $[(Ru(bipy)_2)_2L7]^{2+}$ The blue line in both spectra represents the protonated complex, the black and white lines denote the deprotected species In both cases the absorption maxima are seen to move to higher wavelengths (~480 nm) on deprotonation of the complexes The appearance of these $d\pi$-π^* bands at higher wavelengths is commonly seen in these pyridyl triazole ligand containing complexes[25]

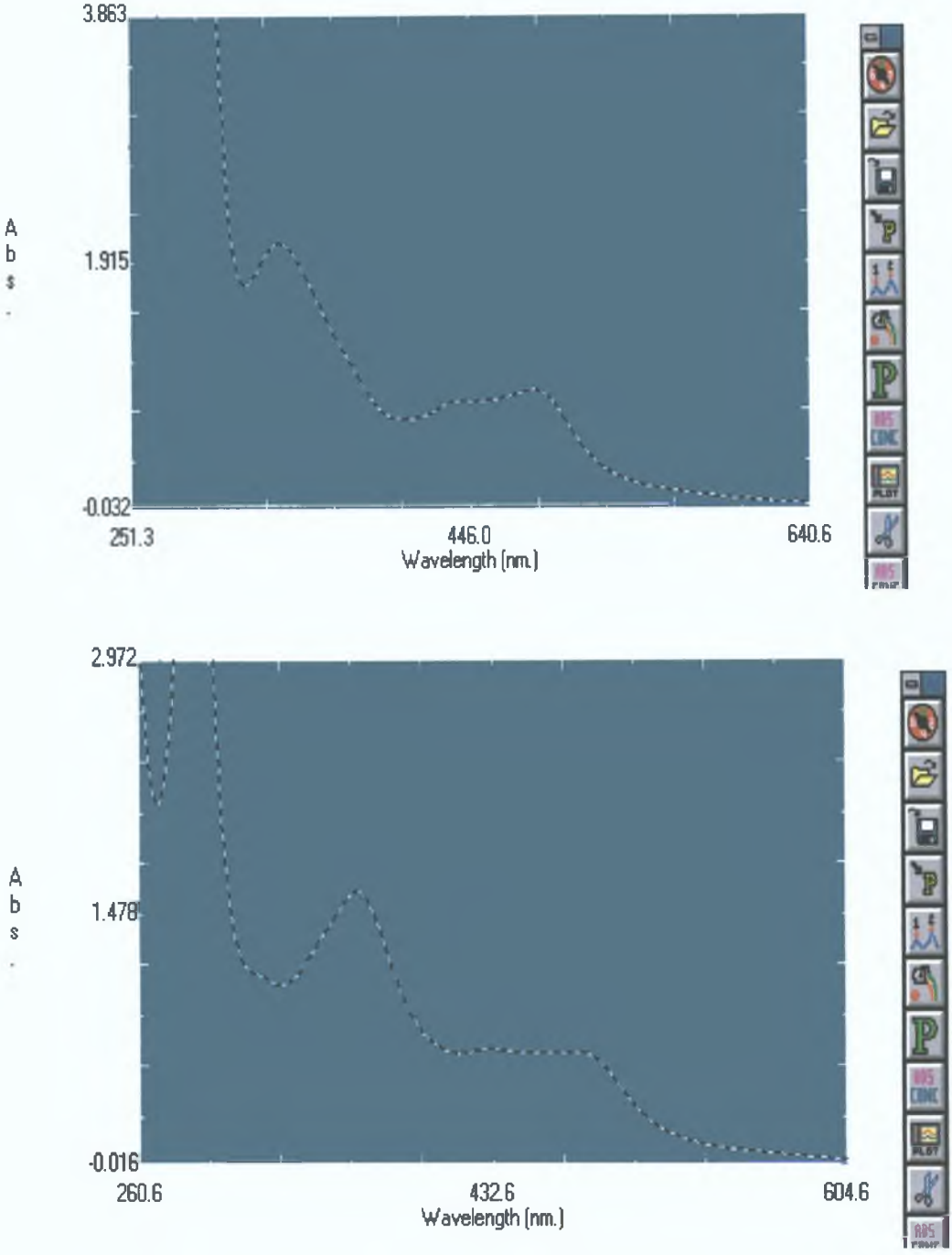

Fig. [3.20]: UV absorbance of protonated (blue)/deprotonated (B/W) of $[(Ru(bipy)_2)_2L3]^{2+}$ (top) and deprotected $[(Ru(bipy)_2)_2L7)]^{2+}$ (bottom) complexes.

When the triazole of the complex is protonated the ligand has less σ-donating (and greater π-accepting) ability because it is less electron rich The ruthenium metal (t_{2g} level) is then more stable because of the increased π-accepting ability of the ligand and so the MLCT gap increases resulting in a UV peak shift to lower wavelength, called a blue shift A shift to high wavelength is called a red shift A red shift of both deprotonated complexes $[(Ru(bipy)_2)_2L3]^{2+}$ and $[(Ru(bipy)_2)_2L7)]^{2+}$ with respect to $[Ru(bipy)_3]^{2+}$ is observed due to σ-donation from the electron rich ligands in fig [3 21]

3.2.4.2 Room (298 K) and low (77 K) temperature emission spectra.

Note: In the following graphs, the peaks labeled "protonated" were obtained on addition of acid and those labeled "deprotonated" were obtained on addition of base.

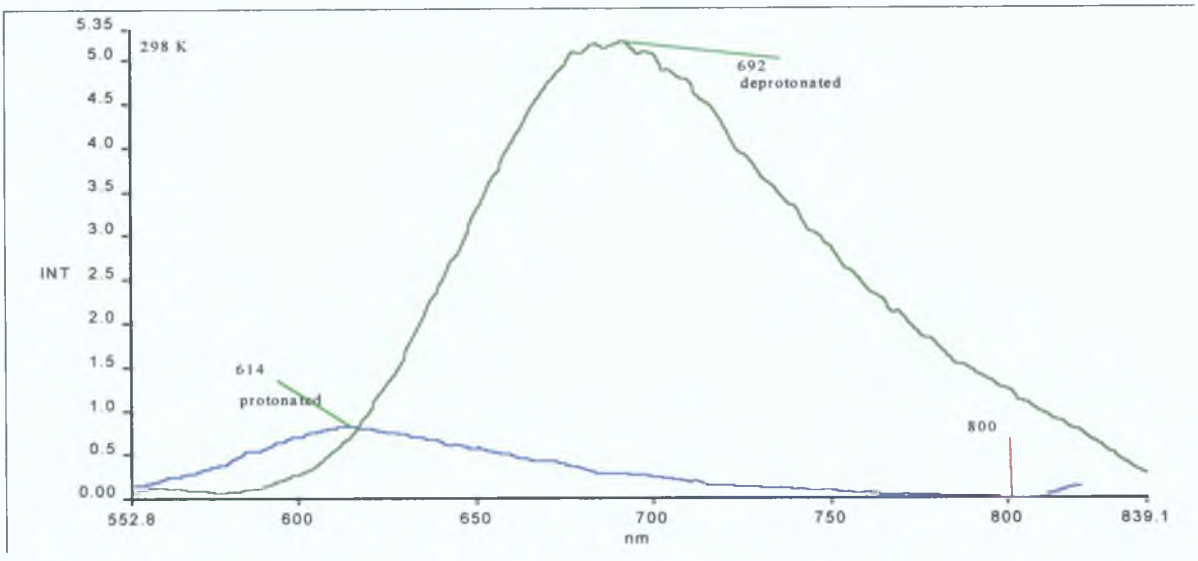

Fig. [3.21a]: Emission spectra of $[\{Ru(bipy)_2\}_2L3]^{2+}$ at 298 K in acetonitrile.

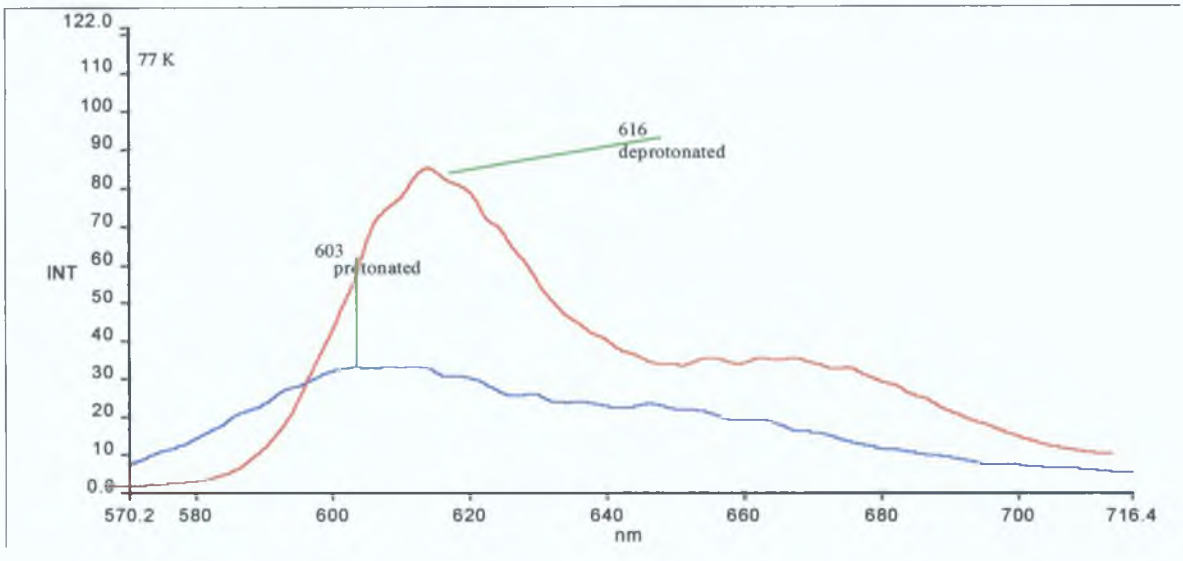

Fig. [3.21b]: Emission spectra of $[\{Ru(bipy)_2\}_2L3]^{2+}$ at 77 K in MeOH:EtOH 4:1.

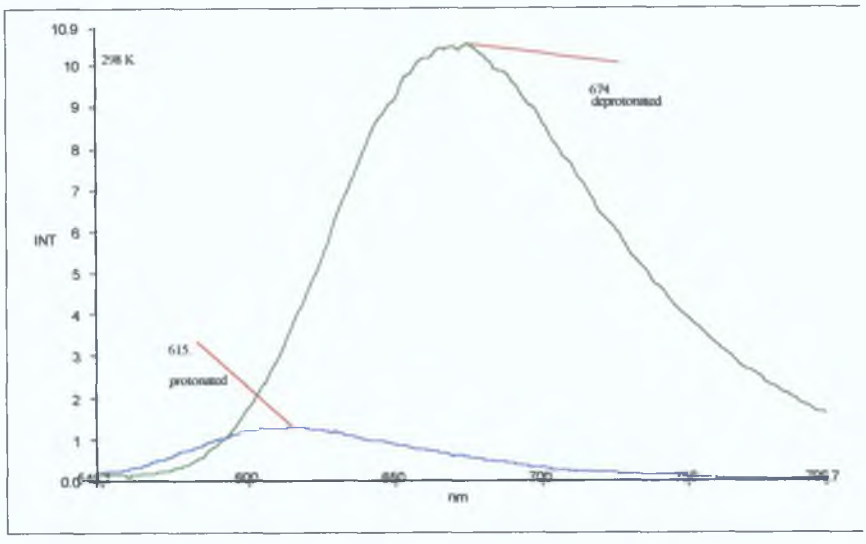

Fig. [3.22a]: Emission spectra of $[\{Ru(bipy)_2\}_2L7)]^{2+}$ at 298 K in acetonitrile.

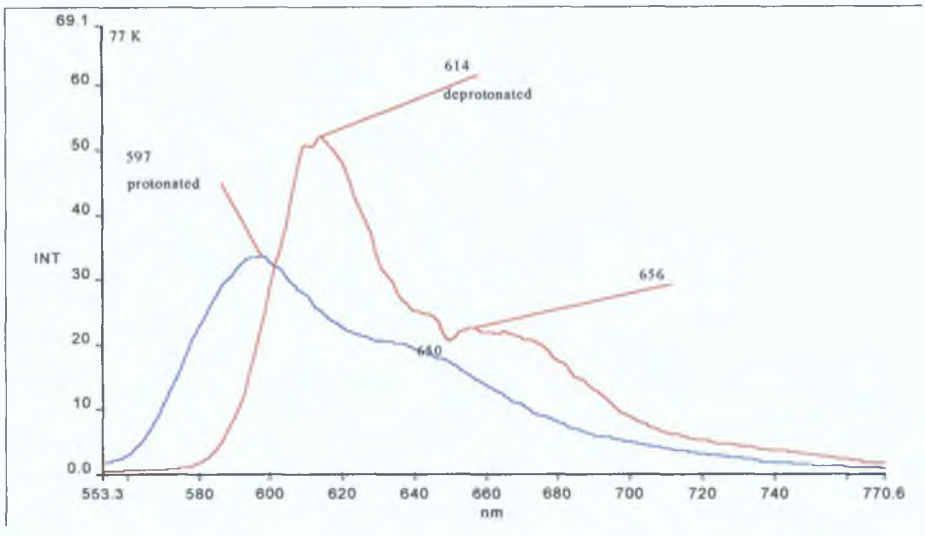

Fig. [3.22b]: Emission spectra of $[\{Ru(bipy)_2\}_2L7]^{2+}$ at 77 K in MeOH:EtOH 4:1.

The emission spectra of $[Ru(bipy)_2L3]^{2+}$ and $[Ru(bipy)_2L7]^{2+}$ carried out at 298 and 77K are shown in fig. [3.22]. Both complexes showed emission at both temperatures, whether protonated or deprotonated.

Emission experiments provide information regarding decay from the MLCT excited state. The deprotonated (green) line in the spectrum of $[Ru(bipy)_2L3]^{2+}$

(fig. [3.21a]) at 298 K has a λ_{max} of 692 nm. When the complex is protonated and its emission again measured (blue line), a λ_{max} of 614 nm is now seen. This blue shift to higher energy can again be explained by the fact that on protonation of the triazole the ligand, it has decreased σ-donation to the metal resulting in an increased MLCT gap and the peak appearing at lower wavelength in the emission spectrum. Another consequence of the lower σ-donation of the protonated ligand is that the ligand field splitting (Δ_0) is lower, allowing thermal population of the ^{3}MC state. This population results in faster radiation-less decay; thus the intensity of the emission peak of the protonated species is low. While the room temperature emission spectra were carried out in ACN, experiments at 77 K were carried out in MeOH:EtOH (4:1) which forms a glass at this temperature. At low temperature a large difference in peak intensity is observed. This is due partly to the decreased solvent interaction with the complex, which can contribute to faster decay[24]. Low frequency vibrations, which also cause faster decay, are also reduced because the solids vibrate at high frequency. The other factor influencing the intensity of the peak at 77 K relates to the point made earlier regarding population of the ^{3}MC state. Since lower σ-donation of the ligand resulted in lower ligand field splitting and thermal population of the ^{3}MC (eg) level with faster decay, at 77 K the thermal energy required to populate the ^{3}MC level is insufficient which results in longer lifetimes. Whereas at 298 K in $[\{Ru(bipy)_2\}_2L3]^{2+}$ the intensity of the deprotonated peak is five times that of the protonated peak, at 77 K the deprotonated:protonated intensity ratio was 3:1. This is because protonation leads to stabilization of the t_2g level and an increase in the t_2g-^{3}MLCT gap, which results in a slower rate of decay and a larger intensity for the protonated species.

Comparing the emission maxima at 298 K of 692 nm for deprotonated $[\{Ru(bipy)_2\}_2L3]^{2+}$ to 674 nm for deprotonated $[\{Ru(bipy)_2\}_2L7]^{2+}$ one may explain the difference in terms of the groups present on the central ring of the ligand. $[\{Ru(bipy)_2\}_2L7]^{2+}$ contains hydroxyl groups which can interact with the nearby N

of the triazole This leads to a decrease in σ-donation of the ligand resulting in an increase in MLCT energy and the appearance of the emission peak of $[\{Ru(bipy)_2\}_2L7]^{2+}$ at a lower wavelength

3.2.4.3 Absorption and emission spectra of H_2L4 containing complexes.

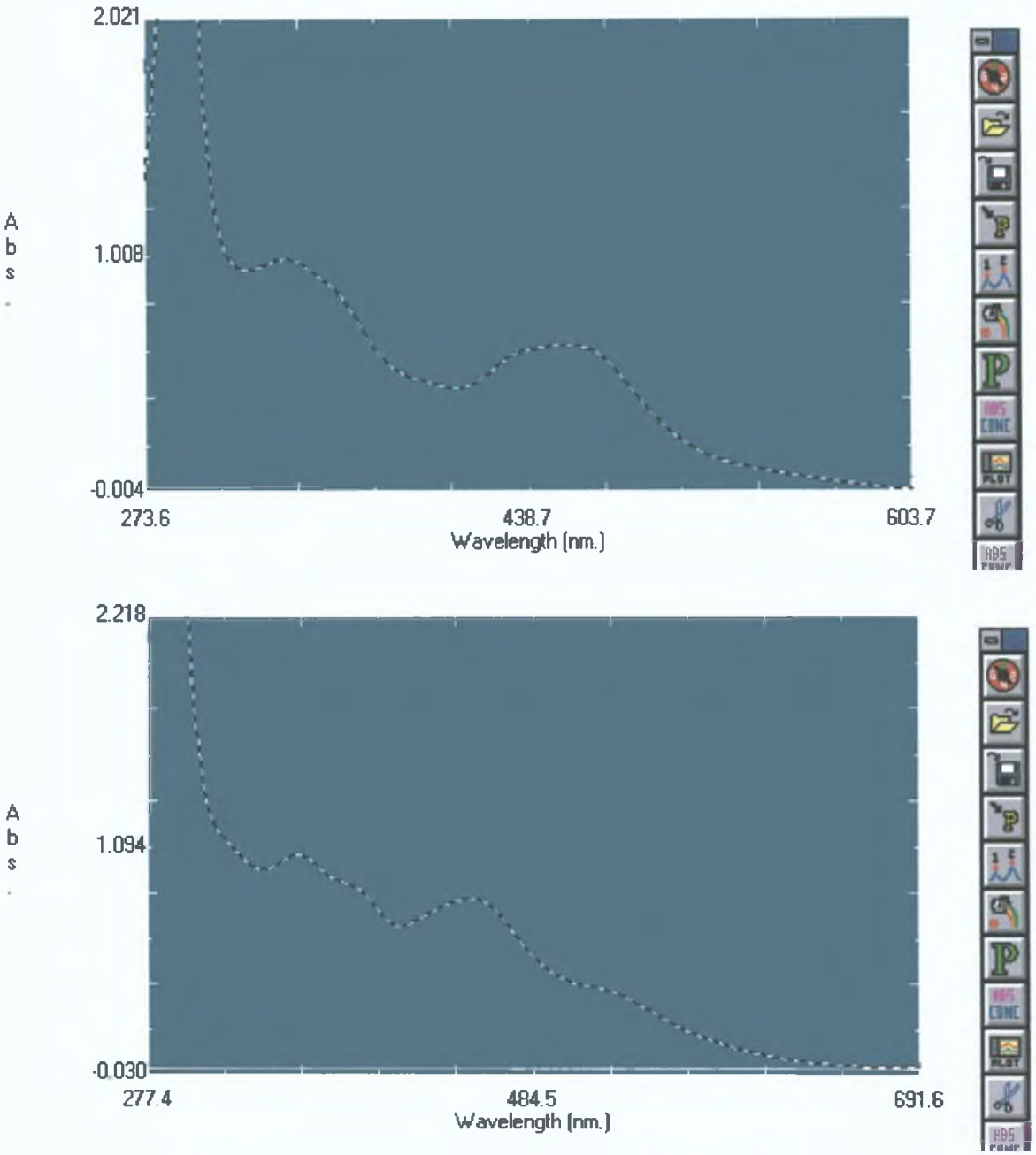

Fig. [3.23] UV absorbance of protonated (blue)/deprotonated (B/W) of $[\{Ru(bipy)_2\}_2L4]^{2+}$ complex (top) and $[\{Ru(bipy)_2\}_2L8]^{2+}$ (bottom).

The protonated complexes [{Ru(bipy)$_2$}$_2$(H$_2$L4)] and [{Ru(bipy)$_2$}$_2$(H$_2$L8)] have high dπ-π* MLCT bands[26,23] at ~530 nm in the absorption spectrum (It is possible that during protonation by addition of acid, that we may not only have protonated the triazole portion of the molecule but also the pyrazine part This has been suggested as the reason for the band at 530 nm This has not been taken into account in the following discussion) This red shift of peaks compared to those of the pyridyl triazole complex analogues, suggest that the pyrazine triazoles are strong σ-donors which results in lower MLCT energy and higher wavelength spectral peaks (The electron rich pyrazine ring can be seen in the spartan picture of the pyrazine triazole ligand) When the pyrazyl triazole complexes are deprotonated however, an MLCT band at 450 nm is observed The expected increase in σ-donation (on deprotonation of the ligand) from ligand to metal and subsequent decrease in MLCT energy is not observed in this case Instead, a decrease in the wavelength of the absorption bands was observed This behaviour is also seen for the smaller pyrazyl triazole complexes [Ru(bipy)$_2$L2]$^+$ and [Ru(bipy)$_2$L6]$^+$ The difference in behaviour of the pyrazyl triazole to the pyridyl triazoles complexes can be explained after investigation of the emission spectra

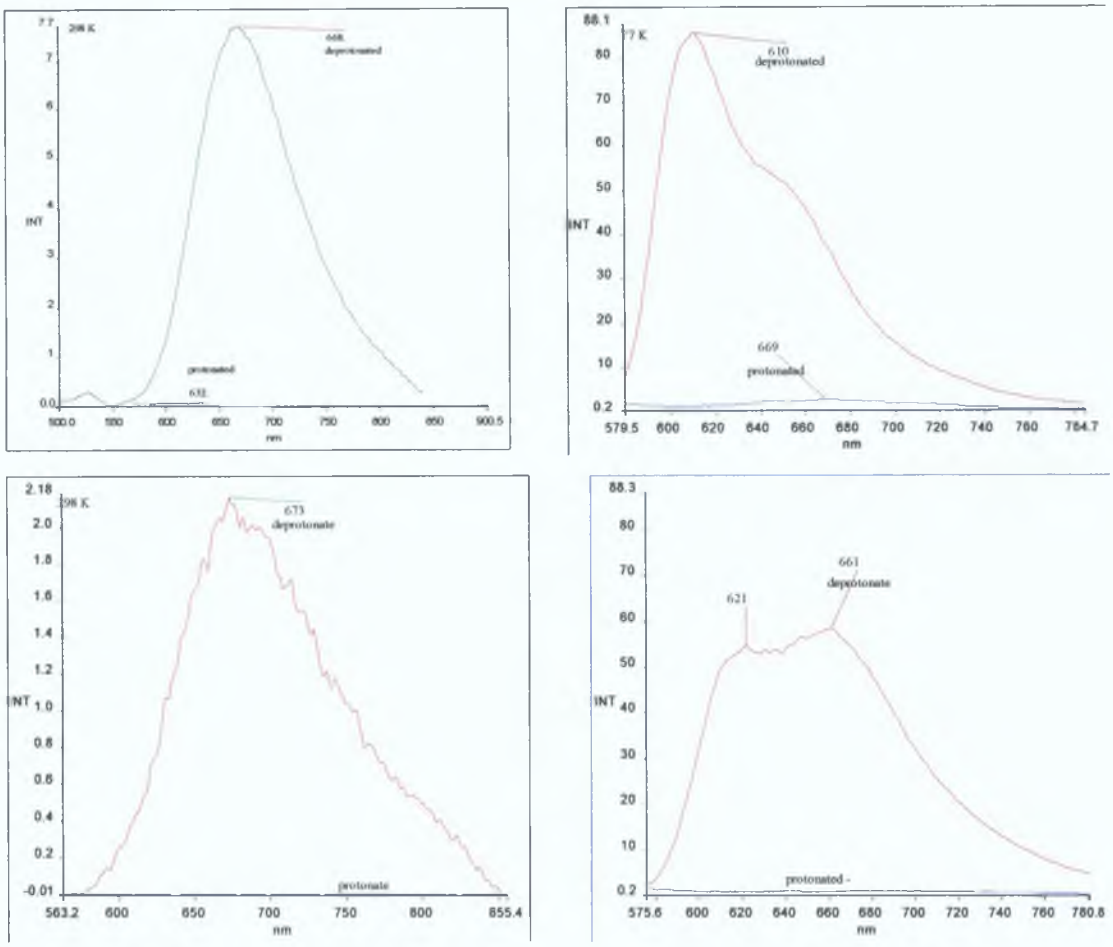

Fig. [3.24]: Emission spectra of $[\{Ru(bipy)_2\}_2L4]^{2+}$ (top) and $[\{Ru(bipy)_2\}_2L8]^{2+}$ (bottom) at 298 K in acetonitrile (left) and at 77 K in MeOH:EtOH 4:1 (right).

The emission spectra of protonated $[\{Ru(bipy)_2\}_2H_2L4]$ and $[\{Ru(bipy)_2\}_2H_2L8)]$ show almost no emission. (This may be due to the addition of too much acid during the protonation. The same pattern was observed in protonated $[Ru(bipy)_2HL2]$ and $[Ru(bipy)_2L6)]$ where no emission was observed at 298 K while the emissions of the deprotonated complexes were of very low intensity. At 77 K both protonated and deprotonated $[Ru(bipy)_2L2]^+$ and $[Ru(bipy)_2L6)]^+$ emitted to some extent; but again the protonated emission peak appeared at a higher wavelength than the deprotonated complex.

Another explanation for this difference in absorption and emission spectra can be given by considering that in the protonated pyrazyl triazole complexes, the lowest unoccupied molecular orbital (LUMO) of the pyrazyl triazole ligand is lower than the LUMO of bipyridine Thus on excitation an electron is excited from the ruthenium metal onto the pyrazyl triazole ligand rather than onto bipy (which is the case in pyridyl triazole complexes) This results in the poor emission spectra for the protonated pyrazyl triazole complexes The observed red shift in the absorption spectra is attributed to a stabilization of the π^* orbital In effect the MLCT energy is lower, the UV band is at a higher wavelength and the emission decays faster However on deprotonation of the complexes the LUMO is no longer on the ligand, it is on the bipyridyl (bipy) and the emission is said to be bipy based Some emission is seen for these deprotonated complexes

3.2.4.4 Investigation of ground and excited states of pyridyl triazole complexes.

The change in the UV-vis absorption spectra with changing pH is shown in fig. [3.25] for $[\{Ru(bipy)_2\}_2L3]^{2+}$ and $[\{Ru(bipy)_2\}_2L7]^{2+}$.

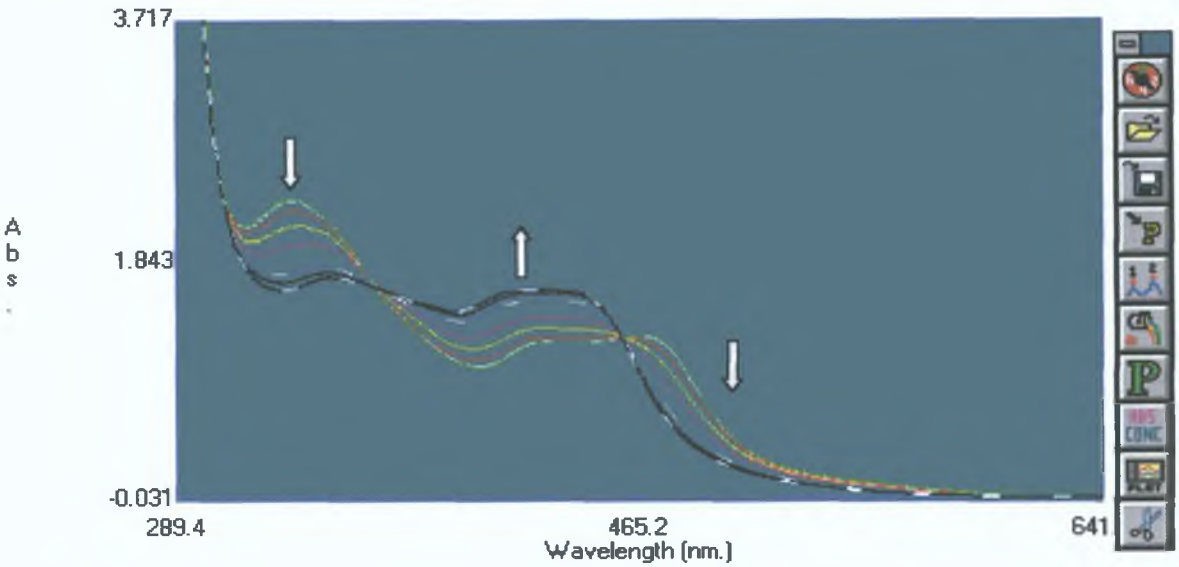

Fig. [3.25] pH-dependence of the absorption spectra of $[\{Ru(bipy)_2\}_2L3]^{2+}$. pH= 1.37,1.71, 2.37, 3.17, 4.08, 4.62, 5.20, 5.99, 6.50, 7.00.

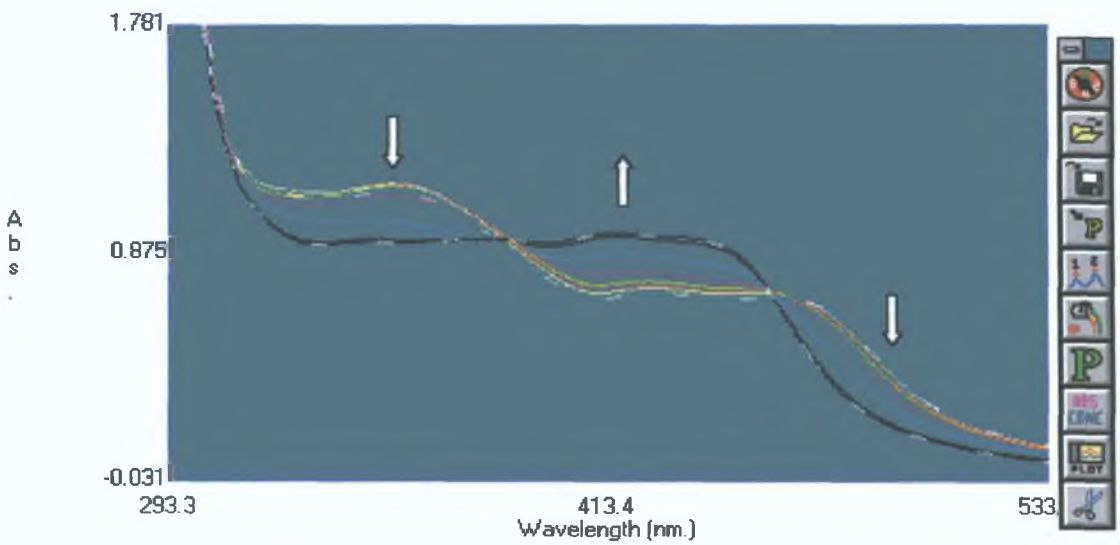

Fig. [3.26]: pH-dependence of the absorption spectra of $[\{Ru(bipy)_2\}_2L7]^{2+}$. pH = 1.13, 1.21, 1.70, 2.83, 3.75, 4.36, 4.87, 5.51, 6.16, 6.77.

The spectra were obtained in a Britton-Robinson buffered solution. In each case, a plot of pH versus % change in absorbance gave a pK_a value; for example the graph for $[\{Ru(bipy)_2\}_2L3]^{2+}$ is shown in Fig. [3.27] here.

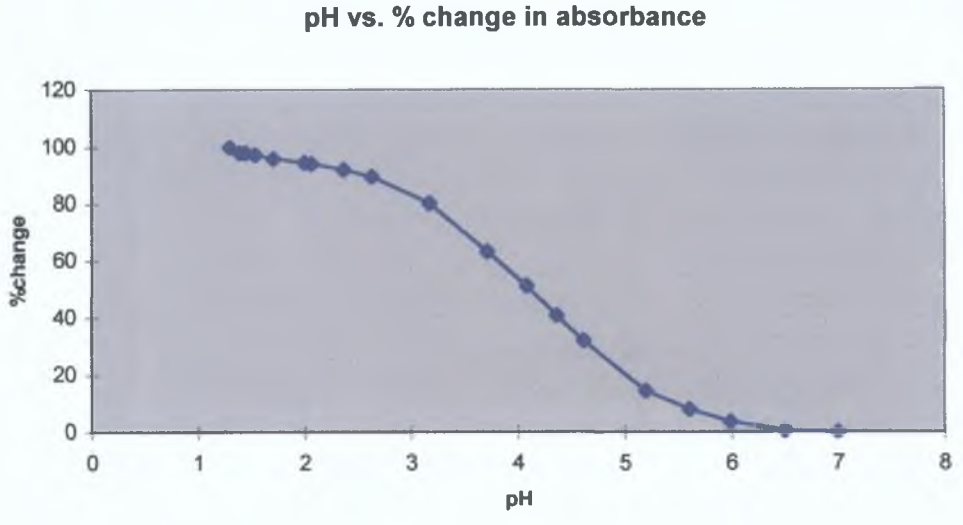

Fig. [3.27]: Plot of pH versus % change in absorbance.

$[\{Ru(bipy)_2\}_2L7)]^{2+}$ differs from $[\{Ru(bipy)_2\}_2L3]^{2+}$ only by the presence of hydroxyl groups on the central ligand ring in the former which are protected as methoxy groups in the latter. The possibility of the formation of a H-bridge between the hydroxyl groups and the triazole nitrogen has been cited previously[27] as the reason for the lower pK_a in $[\{Ru(bipy)_2\}_2L7)]^{2+}$.

X-ray structure analysis has also been used to prove that in a similar complex H-bridging can occur. The higher wavelength absorption band in the UV absorption spectrum of $[\{Ru(bipy)_2\}_2L7]^{2+}$ indicates greater σ-donation than for $[\{Ru(bipy)_2\}_2L3]^{2+}$ causing the triazole to possess less electron density and thus have a lower pK_a. Increasing the pH of $[\{Ru(bipy)_2\}_2L7]^{2+}$ further leads to deprotonation of the hydroxyl groups which can be seen as small changes in the absorption spectrum shown in Fig.[3.28].

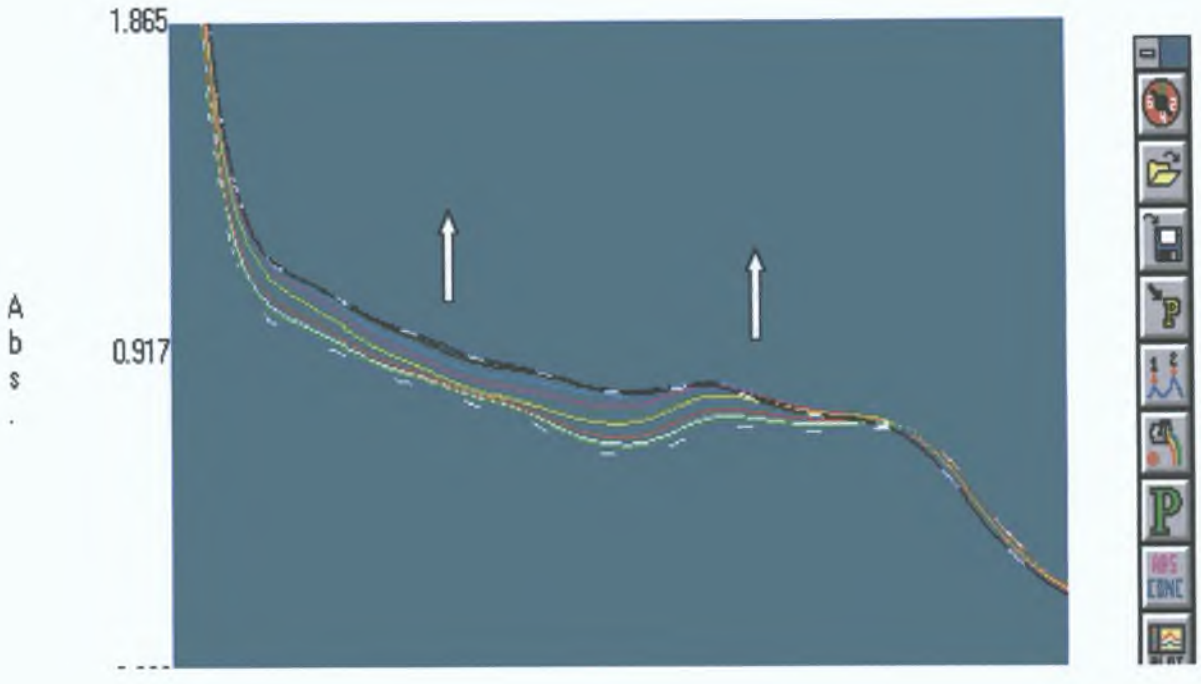

Fig. [3.28]: pH-dependence of the absorption spectra of $[\{Ru(bipy)_2\}_2L7]^{2+}$ at pH= 9.30, 9.59, 9.92, 10.53, 10.98, 11.49, 11.97, 12.46, 12.73, 12.94. All compounds measured in Britton-Robinson buffer.

The pH dependance of the emission of $[\{Ru(bipy)_2\}_2L3]^{2+}$ and $[\{Ru(bipy)_2\}_2L7]^{2+}$ were measured. An estimation of the pK_a* could be made for the complexes by plotting peak intensity against p*H*. The pK_a* of $[\{Ru(bipy)_2\}_2L3]^{2+}$ was estimated to be 2.43 and that of $[\{Ru(bipy)_2\}_2L7]^{2+}$ was 2.15. These values require correction for lifetimes of the protonated and deprotonated species[28] but for the scope of this work estimation will suffice.

In both $[\{Ru(bipy)_2\}_2L3]^{2+}$ and $[\{Ru(bipy)_2\}_2L7]^{2+}$ the excited state pK_a value is lower than that of the ground state as can be seen in fig.[3.29] and [3.30] respectively. This means the coordinated ligands are more acidic in the excited state than in the ground state. This proves that an electron excited from the ruthenium metal goes onto the bipyridine rather than the ligand. When an

electron is excited onto the bipyridine the pyridyl triazole donates electron density to appease the Ru^{3+} charge. The resultant decrease in electron density in the ligand makes it more acidic and the pK_a* value is lowered. The fact that the pyridyl triazole ligand is not involved in the excitation causes it be called a "spectator ligand".

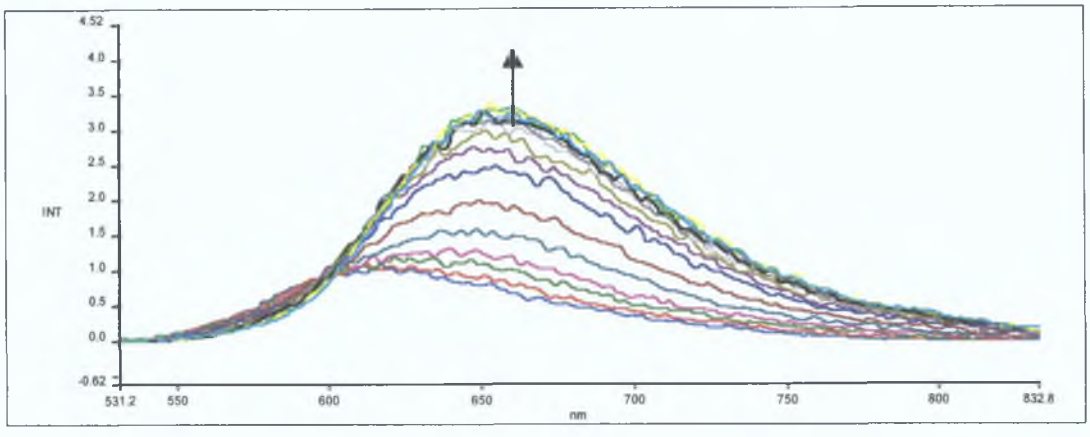

Fig. [3.29]: pH-dependence of the emission spectra of the $[(Ru(bipy)_2)_2L3]^{2+}$: pH= 1.2,1.36,1.57, 1.75, 2.00, 2.31, 2.78, 3.06, 3.29, 3.58, 3.72, 3.93, 4.43, 4.75, 4.94, 5.20, 5.58, 6.00, 6.30, 6.57 and 6.98, measured in a Britton - Robinson buffer; conc. 10^{-5}M.

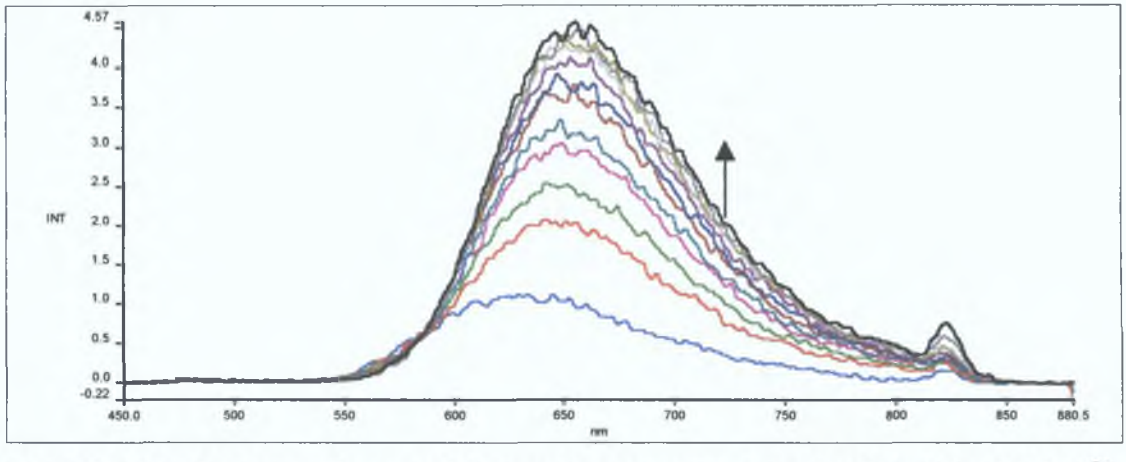

Fig. [3.30]: pH-dependence of the emission spectra of : $[\{Ru(bipy)_2\}_2L7]^{2+}$ (with increasing peak intensity), pH= 1.27, 1.59, 1.83, 2.17, 2.42, 2.87, 3.25, 3.59, 3.91, 4.13, 4.46 and 4.72

The absorption and emission spectra with changing pH for $[[\{Ru(bipy)_2\}_2L4]^{2+}$ and $[\{Ru(bipy)_2\}_2L8]^{2+}$ are shown in Figs.[3.31]-[3.33] respectively. Their pK_a values of 3.2 and 2.18 respectively are both lower than those of their pyridyl triazole analogues $[[\{Ru(bipy)_2\}_2L3]^{2+}$ and $[\{Ru(bipy)_2\}_2L7]^{2+}$. This indicates the pyrazinyl triazoles are better σ-donors, having reduced ligand electron density and becoming more acidic. The pK_a* values for $[[\{Ru(bipy)_2\}_2L4]^{2+}$ and $[[\{Ru(bipy)_2\}_2L3]^{2+}$ were estimated to be 2.15 and 2.40 respectively using the Forsters equation[29]

$pK_a^* = pK_a + (0.625/T)(\upsilon_B - \upsilon_{HB})$

Where υ_B- and υ_{HB} are the $E_{0\text{-}0}$ values (in cm^{-1})of the deprotonated and protonated complexes respectively. These values are taken from the λ_{max} of the emission spectra at 77 K. T is 77 K.

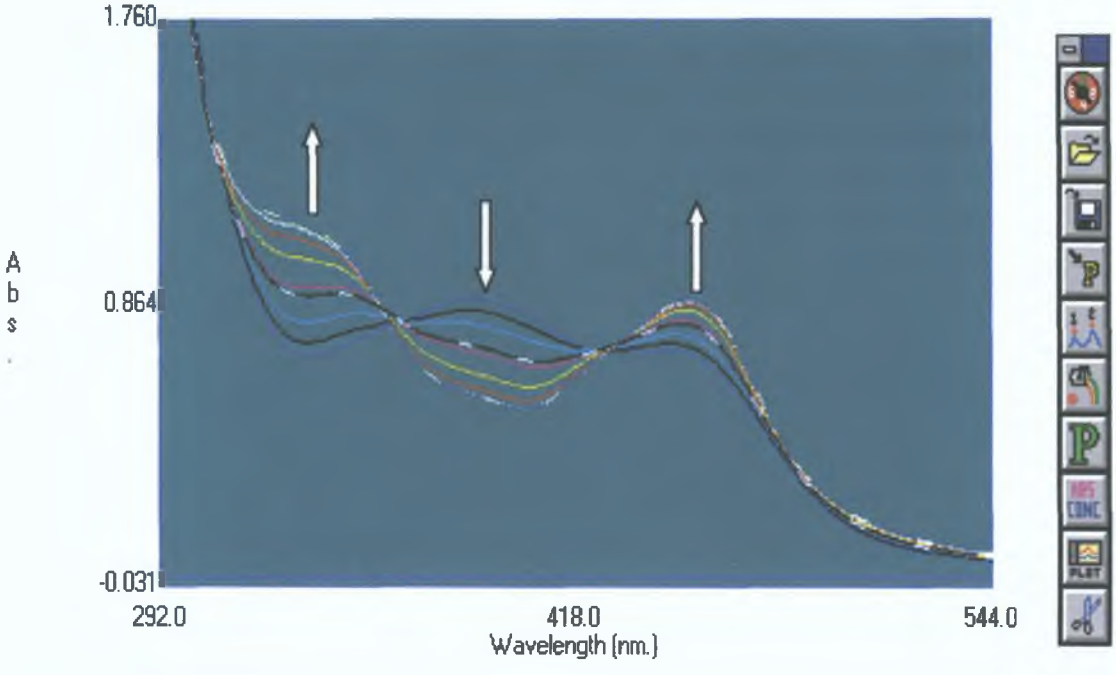

Fig. [3.31]: pH-dependence of the absorption spectra of $[\{Ru(bipy)_2\}_2L4]^{2+}$:pH= 1.22, 2.30, 2.81, 3.33, 3.47, 4.01, 4.53, 5.30, 5.96, 6.40.

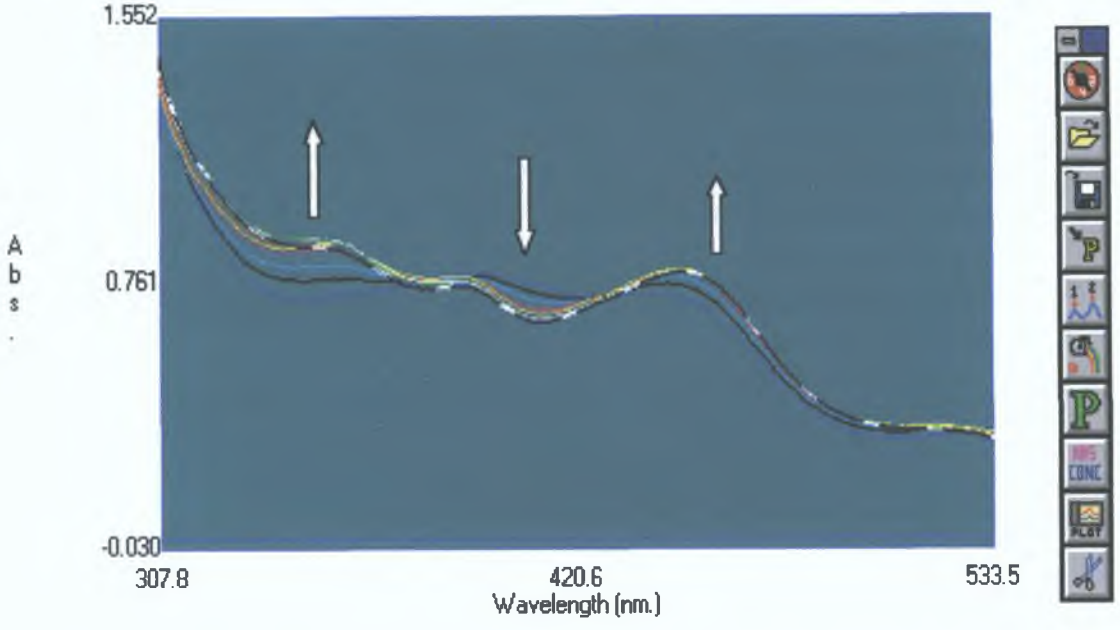

Fig. [3.32]: pH-dependence of the absorption spectra of $[\{Ru(bipy)_2\}_2L8]^{2+}$: pH=1.43, 1.96, 2.49, 3.22, 3.70, 4.47, 5.06, 5.61, 6.32, 7.10

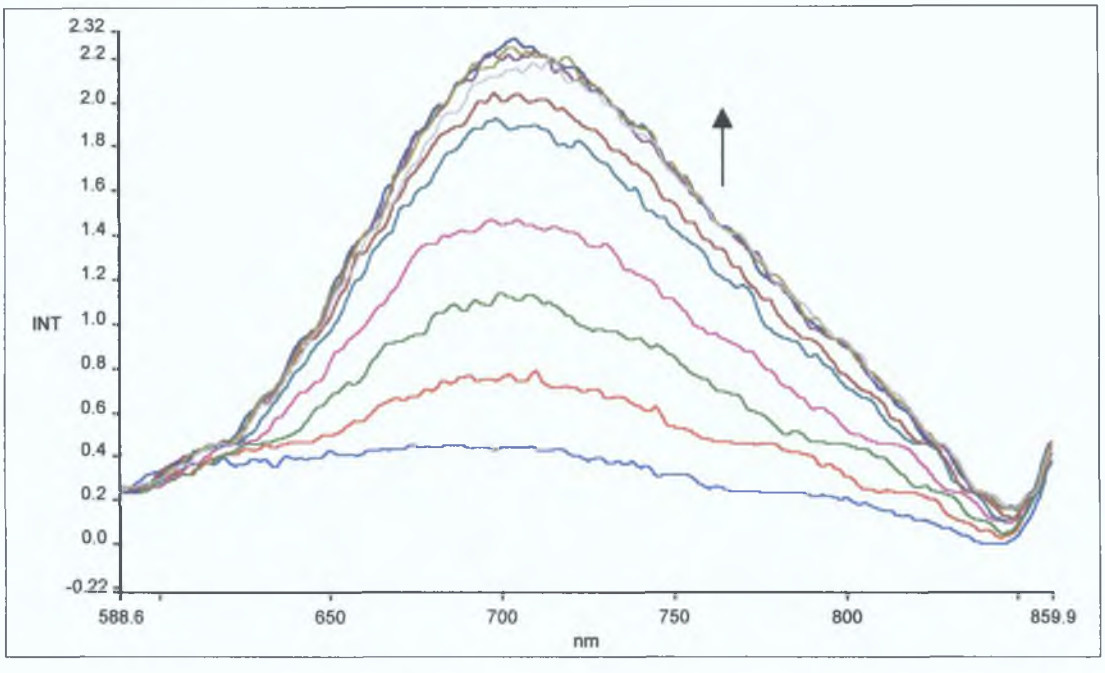

Fig. [3.33]: $[\{Ru(bipy)_2\}_2L4]^{2+}$complex, with increasing peak intensity. pH= 1.49, 1.79, 1.96, 2.24, 2.75, 3.03, 3.20, 3.41, 3.62, 3.89 and 4.14. Measured in a Britton-Robinson buffer.

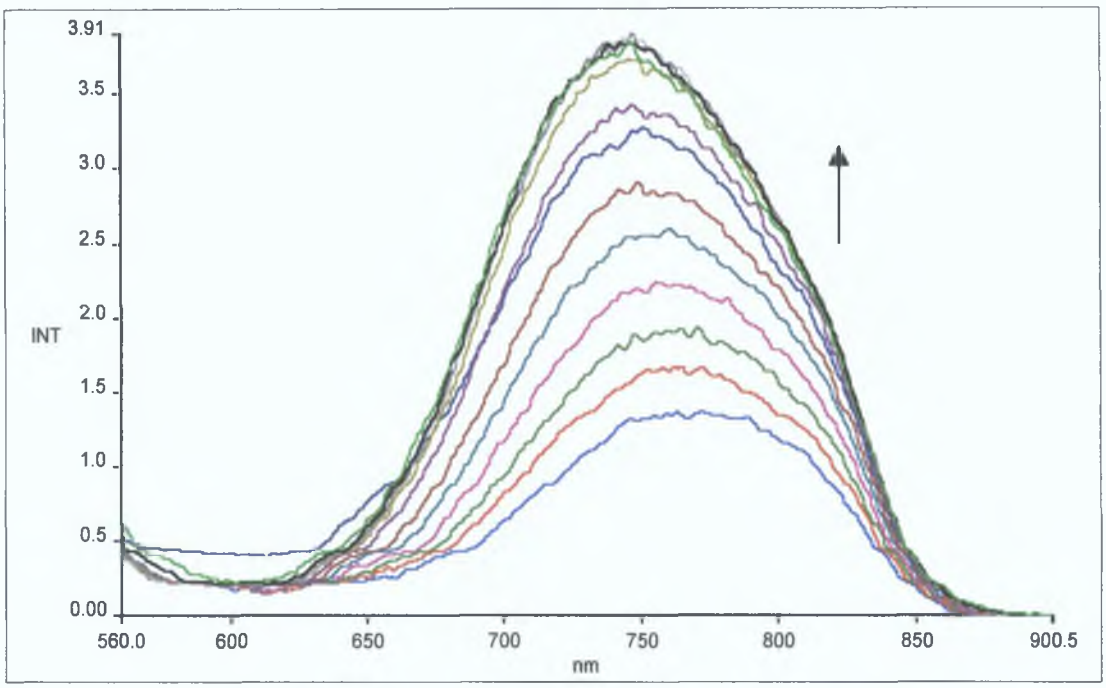

Fig. [3.34]: [{Ru(bipy)$_2$}$_2$L4]$^{2+}$complex, with increasing peak intensity. pH= 1.22, 1.47, 1.65, 2.01, 2.34, 2.54, 2.77, 2.95, 3.27, 3.60, 3.75 and 3.96.

Complex	Absorbance λ_{max}, nm	Emission λ_{max}, nm	
		300 K	77 K[a]
$([Ru(bpy)_2]_2L3)^{2+}$	(337) **482**	**692**	**616**
$([Ru(bpy)_2]_2H2L3)^{4+}$	**416**	**614**	**603**
$([Ru(bpy)_2]_2L7)^{2+}$	(367) **481**	**674**	**614** (656)
$([Ru(bpy)_2]_2H2L7)^{4+}$	**426**	**615**	**597**
$([Ru(bpy)_2]_2L4)^{2+}$	(336) **457**	**668**	**610**
$([Ru(bpy)_2]_2H2L4)^{4+}$	(383) **537**	**682**	**609**
$([Ru(bpy)_2]_2L8)^{2+}$	(360) **452**	**673**	**621,661**
$([Ru(bpy)_2]_2H2L8)^{4+}$	(395) **535**	**Not seen**	**Not seen**

[a] Measured in EtOH/MeOH 4:1.

Table [3.3]: Table of absorption and emission data for discussed complexes in their protonated and deprotonated forms.

Unless otherwise stated all measurements were carried out in acetonitrile. Protonation of the complexes was achieved by the addition of perchloric acid.

3.2.5 X-ray Structure Determination

A crystal suitable for X-ray analysis was grown from acetone/water during a recrystallization period of approx. three weeks. The structure determination was carried out by Mr. Mark Niewenhuyzen of Queen's University Belfast. The crystal exhibits a pseudo herring-bone configuration. The protons on one of the methoxy groups were disordered, thus their spatial orientation is not shown. The complex crystallized out with a molecule of acetone and a hexafluorophosphate ion which were removed from the crystal structure for clarity of view. However they can be seen in the packing picture, ({PF_6= purple and green}; {acetone= blue and red}) in fig. [3.36].

From the crystal structure it is clear that the ligand is bound through the pyridine-N and N1 of the triazole ring (or via N(25) and N(32) using the crystallographic numbering scheme). The angle that N(25) and N(32) make with ruthenium is called the "bite angle" of the ligand and is 77.8°. This corresponds well with the bite angle of 77.9° obtained by Hage[24] for $[Ru(bpy)_2(pyridyltriazole)]PF_6.CH_3COCH_3$. Ruthenium to nitrogen distances of 2.033-2.098 angstroms are also comparable to those found in other complexes[24]. Ruthenium coordinates to two bipyridine molecules in the *–cis* configuration. The ruthenium to N(25) (of pyridine ring) at 2.098 angstroms is the longest Ru-N bond. One attributable factor to this length is limited π-backbonding in the complex[24]. Bite angles of 79.5° and 78.8° for bipyridine ligands are also considered normal.

Looking at the crystal structure of this complex with respect to its free ligand HL1, some comments can be made. We have mentioned that in the crystal the nitrogen atoms bonded to the ruthenium metal are in the *-cis* configuration. In the ligand the same nitrogens are *–trans* to each other. The ligand crystal structure is packed in such a way that the triazolic proton on N2 of the triazole is

intermolecular H-bonded to the pyridine-N and N4 of the triazole of another molecule On complexation, the ligand is deprotonated and the H-bonding removed allowing the pyridine ring to rotate sufficiently so that the pyridine-N and N1 (which were *–trans* to each other in the ligand) are now in a *–cis* configuration The corresponding nitrogen atoms in HL2 are in a –cis configuration in the ligand, thus no rotation is expected on complexation In the case of HL2 the triazolic proton is H-bonded to the adjacent methoxy oxygen HL1 is similar to H_2L3 in that the triazole-N1 and the pyridine are in a *-trans* configuration

3.2.5.1 $[Ru(bipy)_2L1](PF_6).2H_2O$

The space group of the molecule is P-1 or P1bar (with Cu radiation) There are two molecules in the unit cell (one in the asymmetric unit) The unit cell contains residual or *potential* solvent volume of 570 4 A^3 which is 29 2% of the unit cell, (the drawing does not contain the anion)

C45 is disordered over two sites and *only* one is shown in the diagrams The C5/C8 hydrogen bond about an inversion centre is *bi-furcated* with some pi-pi stacking between the two bipyridyl rings

Intra- and Intermolecular H-bonding distances

C5 N33 is 3 49 A Inter [2565]

C8 N33 is 3 37 A Inter [2565]

C14 N32 is 3 14 A Intra

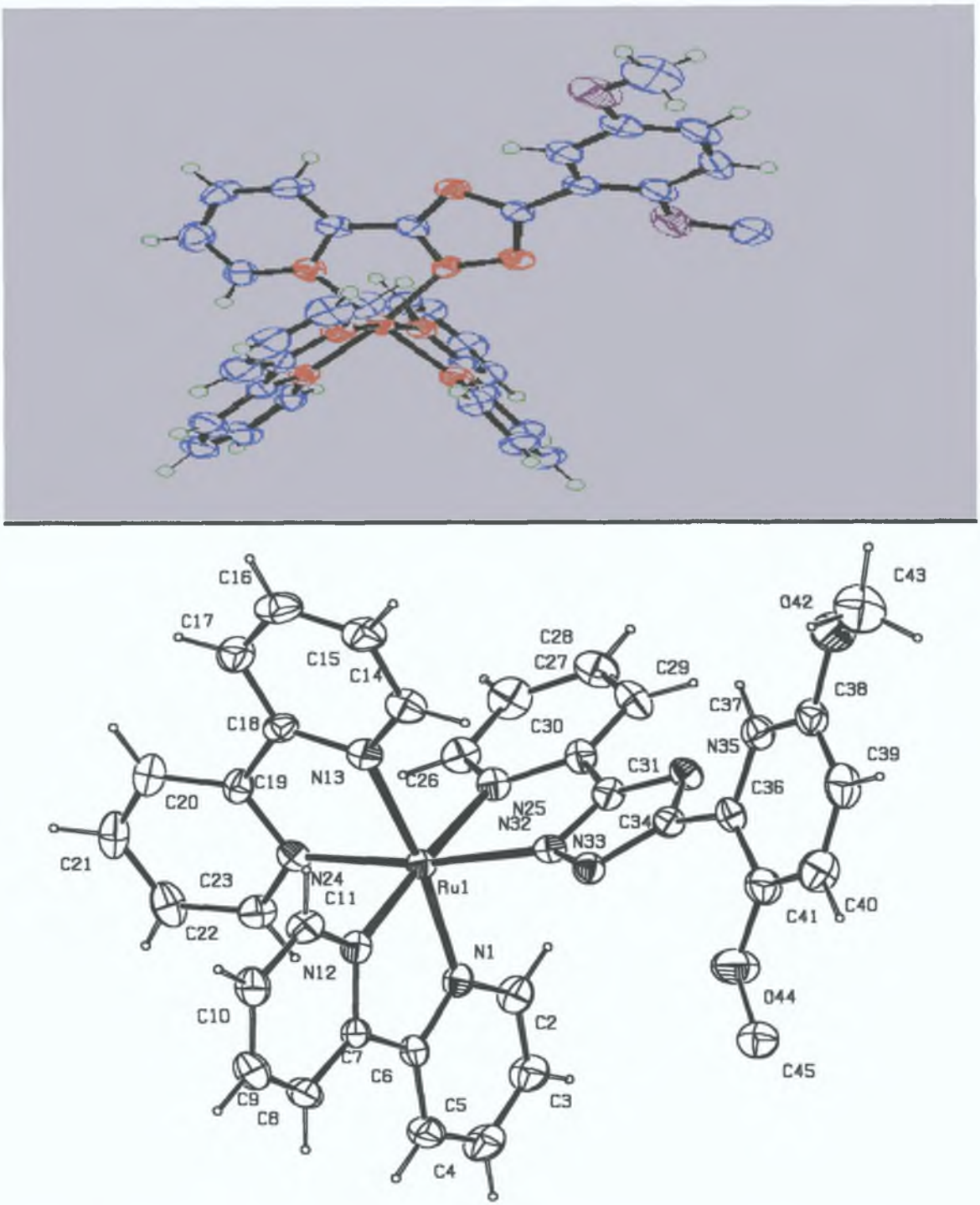

Fig. [3.35] Crystal structure (two views) of. [Ru(bipy)$_2$L1] cation. PF_6 and acetone molecules have been omitted for clarity.

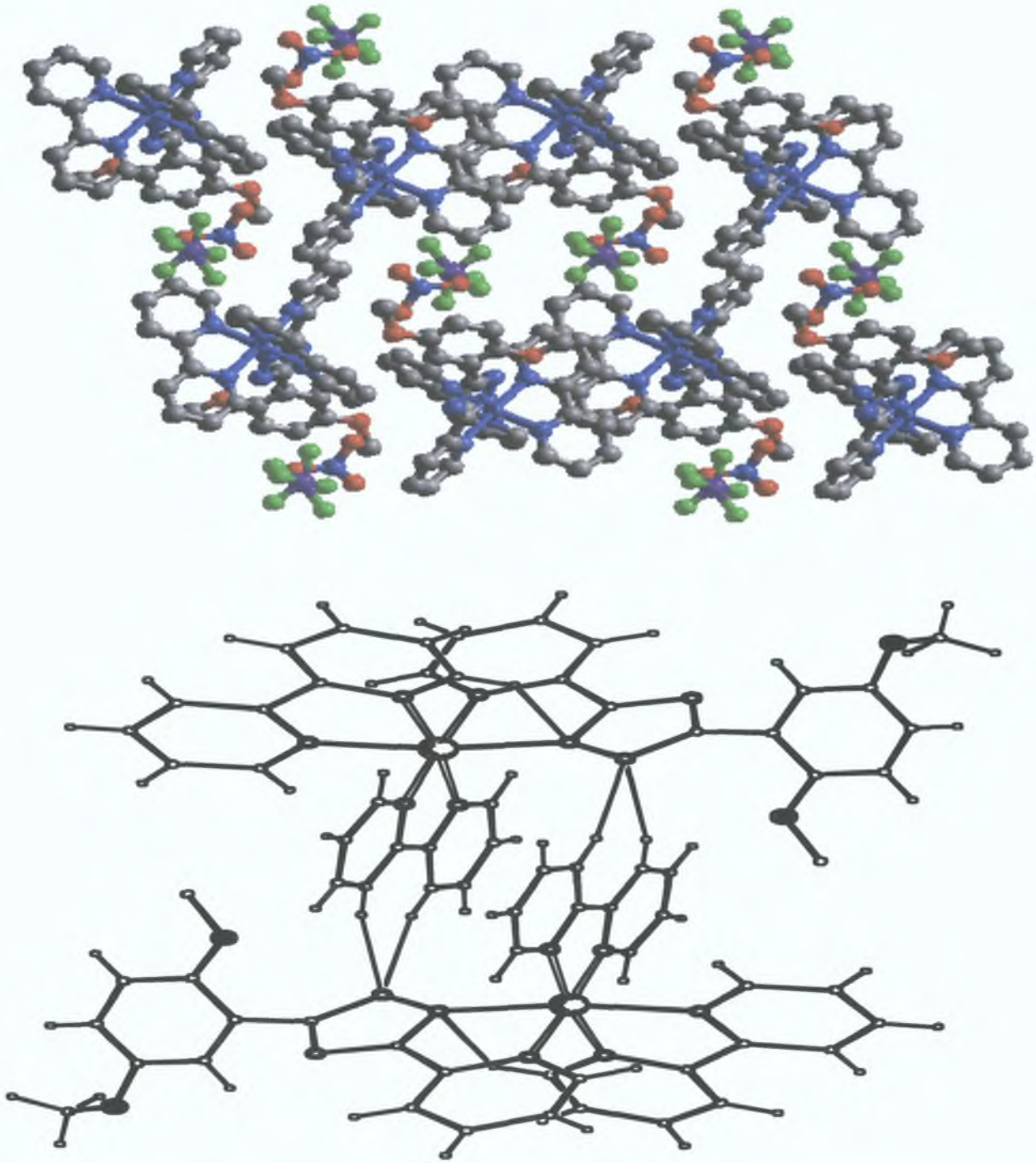

Fig. [3.36] Packing of $[Ru(bipy)_2L1](PF_6).2H_2O$ with H-bonding illustrated (bottom).

Bond	Length (Angstroms)	Bond	Length (Angstroms)	Bond	Length (Angstroms)
Ru(1)-N(12)	2 033(7)	N(13)-C(18)	1 331(11)	C(30)-C(31)	1 476(11)
Ru(1)-N(1)	2 051(7)	N(13)-C(14)	1 375(11)	C(31)-N(32)	1 326(10)
Ru(1)-N(13)	2 056(7)	C(14)-C(15)	1 389(13)	C(31)-N(35)	1 349(10)
Ru(1)-N(24)	2 052(7)	C(15)-C(16)	1 40(2)	N(32)-N(33)	1 368(9)
Ru(1)-N(32)	2 062(7)	C(16)-C(17)	1 382(14)	N(33)-C(34)	1 335(10)
Ru(1)-N(25)	2 098(7)	C(17)-C(18)	1 404(12)	C(34)-N(35)	1 350(10)
N(1)-C(2)	1 352(10)	C(18)-C(19)	1 496(12)	C(34)-C(36)	1 493(11)
N(1)-C(6)	1 367(10)	C(19)-N(24)	1 360(10)	C(36)-C(37)	1 390(12)
C(2)-C(3)	1 388(13)	C(19)-C(20)	1 399(12)	C(36)-C(41)	1 386(12)
C(3)-C(4)	1 386(14)	C(20)-C(21)	1 388(14)	C(37)-C(38)	1 394(12)
C(4)-C(5)	1 410(13)	C(21)-C(22)	1 378(14)	C(38)-C(39)	1 360(14)
C(5)-C(6)	1 392(12)	C(22)-C(23)	1 383(13)	C(38)-O(42)	1 378(11)
C(6)-C(7)	1 495(11)	C(23)-N(24)	1 360(11)	C(39)-C(40)	1 399(14)
C(7)-N(12)	1 366(10)	N(25)-C(26)	1 348(11)	C(40)-C(41)	1 413(13)
C(7)-C(8)	1 393(12)	N(25)-C(30)	1 373(11)	C(41)-O(44)	1 370(11)
C(8)-C(9)	1 388(12)	C(26)-C(27)	1 401(13)	O(42)-C(43)	1 426(12)
C(9)-C(10)	1 405(13)	C(27)-C(28)	1 383(14)	O(44)-C(45)	1 479(14)
C(10)-C(11)	1 396(12)	C(28)-C(29)	1 416(14)		
C(11)-N(12)	1 359(10)	C(29)-C(30)	1 372(12)		

Table [3.4]: Bond lengths of $[Ru(bipy)_2L1](PF_6).2H_2O$

ond	Angle	Bond	Angle	Bond	Angle
I(12)-Ru(1)-N(1)	79 5(3)	C(11)-C(10)-C(9)	119 3(8)	C(27)-C(28)-C(29)	119 8(9)
I(12)-Ru(1)-N(13)	94 8(3)	N(12)-C(11)-C(10)	122 8(8)	C(30)-C(29)-C(28)	117 4(9)
I(1)-Ru(1)-N(13)	172 1(3)	C(11)-N(12)-C(7)	117 0(7)	C(29)-C(30)-N(25)	123 7(8)
I(12)-Ru(1)-N(24)	86 1(3)	C(11)-N(12)-Ru(1)	126 8(6)	C(29)-C(30)-C(31)	125 0(8)
I(1)-Ru(1)-N(24)	95 2(3)	C(7)-N(12)-Ru(1)	115 7(5)	N(25)-C(30)-C(31)	111 3(7)
I(13)-Ru(1)-N(24)	78 8(3)	C(18)-N(13)-C(14)	118 9(8)	N(32)-C(31)-N(35)	114 4(7)
I(12)-Ru(1)-N(32)	100 9(2)	C(18)-N(13)-Ru(1)	116 6(6)	N(32)-C(31)-C(30)	118 6(7)
I(1)-Ru(1)-N(32)	93 0(2)	C(14)-N(13)-Ru(1)	124 5(6)	N(35)-C(31)-C(30)	126 9(8)
I(13)-Ru(1)-N(32)	93 5(3)	N(13)-C(14)-C(15)	120 1(9)	C(31)-N(32)-N(33)	106 2(6)
I(24)-Ru(1)-N(32)	170 1(2)	C(14)-C(15)-C(16)	120 1(9)	C(31)-N(32)-Ru(1)	115 4(5)
I(12)-Ru(1)-N(25)	176 3(2)	C(17)-C(16)-C(15)	119 8(9)	N(33)-N(32)-Ru(1)	137 1(5)
I(1)-Ru(1)-N(25)	97 1(3)	C(16)-C(17)-C(18)	117 1(10)	C(34)-N(33)-N(32)	104 3(6)
I(13)-Ru(1)-N(25)	88 8(3)	N(13)-C(18)-C(17)	123 9(8)	N(33)-C(34)-N(35)	115 1(7)
I(24)-Ru(1)-N(25)	95 6(3)	N(13)-C(18)-C(19)	114 4(7)	N(33)-C(34)-C(36)	123 6(7)
I(32)-Ru(1)-N(25)	77 8(2)	C(17)-C(18)-C(19)	121 6(8)	N(35)-C(34)-C(36)	120 9(7)
C(2)-N(1)-C(6)	117 6(7)	N(24)-C(19)-C(20)	123 0(8)	C(31)-N(35)-C(34)	100 0(7)
C(2)-N(1)-Ru(1)	126 8(6)	N(24)-C(19)-C(18)	114 3(7)	C(37)-C(36)-C(41)	119 4(8)
C(6)-N(1)-Ru(1)	115 5(5)	C(20)-C(19)-C(18)	122 7(8)	C(37)-C(36)-C(34)	116 4(7)
N(1)-C(2)-C(3)	122 0(9)	C(21)-C(20)-C(19)	117 8(9)	C(41)-C(36)-C(34)	124 2(8)
C(4)-C(3)-C(2)	120 5(9)	C(22)-C(21)-C(20)	120 0(9)	C(36)-C(37)-C(38)	120 3(9)
C(3)-C(4)-C(5)	118 4(9)	C(21)-C(22)-C(23)	119 4(9)	C(39)-C(38)-O(42)	124 0(9)
C(6)-C(5)-C(4)	117 9(9)	N(24)-C(23)-C(22)	122 2(9)	C(39)-C(38)-C(37)	121 3(9)
N(1)-C(6)-C(5)	123 4(8)	C(19)-N(24)-C(23)	117 6(7)	O(42)-C(38)-C(37)	114 7(8)
N(1)-C(6)-C(7)	113 8(7)	C(19)-N(24)-Ru(1)	115 8(5)	C(38)-C(39)-C(40)	119 2(9)
C(5)-C(6)-C(7)	122 7(8)	C(23)-N(24)-Ru(1)	126 7(6)	C(41)-C(40)-C(39)	120 2(9)
N(12)-C(7)-C(8)	123 1(8)	C(26)-N(25)-C(30)	117 9(7)	O(44)-C(41)-C(36)	116 6(8)
N(12)-C(7)-C(6)	114 3(7)	C(26)-N(25)-Ru(1)	125 5(6)	O(44)-C(41)-C(40)	123 8(8)
C(8)-C(7)-C(6)	122 6(8)	C(30)-N(25)-Ru(1)	116 5(5)	C(36)-C(41)-C(40)	119 6(9)
C(9)-C(8)-C(7)	119 4(8)	N(25)-C(26)-C(27)	122 1(9)	C(38)-O(42)-C(43)	118 1(9)
C(8)-C(9)-C(10)	118 3(8)	C(28)-C(27)-C(26)	119 0(9)	C(41)-O(44)-C(45)	117 5(9)

Table [3.5]: Bond angles of $[Ru(bipy)_2L1](PF_6).2H_2O$

3.3 EXPERIMENTAL

3 3 1 $[Ru(bpy)_2L1](PF_6)\ 2H_2O$

3-(1,4-dimethoxyphenyl)-5-pyridin-2-yl-1H-1,2,4-triazole (HL1) (200 mg, 7 1x10^{-4} mol) and $Ru(bpy)_2Cl_2$ (370 mg, 7 1x10^{-4} mol) were reacted in the manner described previously for complex preparation[4] The desired complex was recrystallized from acetone/H_20 yield, 495 mg (5 8x10^{-4} mol), 82%

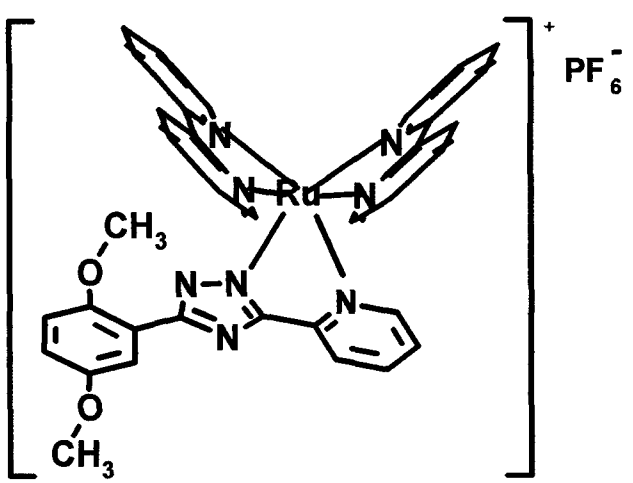

^{1}H NMR (ACN-d^3) (δ, ppm, J,Hz) 8 45(2H, t, J=8 9), 8 38(2H, t, J=8 9), 8 08(1H, d, J=7 9, H3), 7 95(7H, m, containing H4), 7 79(2H, t, J=4 9), 7 51(1H, d, J=5 9, H6), 7 42(1H, t, J=6 9), 7 38(2H, t, J=5 9), 7 27(1H, t, J=5 9), 7 20(1H, d, J= 2 9, H3"), 7 12(1H, t, J=6 9, H5), 6 93(1H, d, J=8 9, H6"), 6 83(1H, dd, J=2 9, 8 9, H5"), 3 71(3H, s, -$OCH_3$1"), 3 61(3H, s, -$OCH_3$4") C,H,N Analysis $C_{35}H_{33}N_8O_4PF_6Ru$(% Theory/Found) C(48 0/48 2); H(3 8/4 0), N(12 8/12 4)

3 3 2 $[Ru(bpy)_2L2](PF_6)\ 2H_2O$

3-(1,4-dimethoxyphenyl)-5-pyrazin-2-yl-1H-1,2,4-triazole (HL2) (200 mg, 7 1x10-4 mol) and $Ru(bpy)_2Cl_2$ (370 mg, 7 $1x10^{-4}$ mol) were reacted in the manner described previously for complex preparation[4] The desired complex was recrystallized from acetone/H_20 yield, 510 mg (5 0x10-4 mol), 70 4%

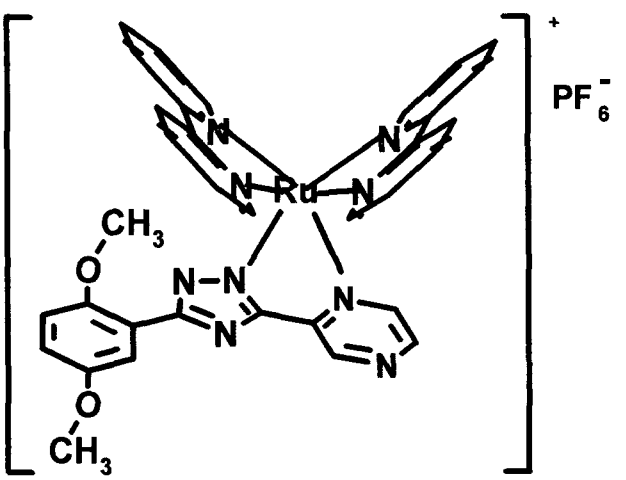

^1H NMR (Acetone-d^6) (δ, ppm, J,Hz) 9 51(1H, s, H3), 8 64(1H, d, J=3 0, Hf), 8 51(4H, m), 8 10(5H, m, containing H5{doublet}), 7 89(1H, d, J=4 9), 7 84(1H, d, J=4 9), 7 77(1H, d, J=5 9), 7 73(1H, d, J=4 9), 7 47(5H, m, containing H3"{doublet, J=3 0}), 7 28(1H, dd, J=3 0, 8 9, H5"), 7 18(1H, d, J=8 9, H6"), 3 83(3H, s, -$OCH_3$1"), 3 80(3H, s, -$OCH_3$4") C,H,N Analysis $C_{34}H_{32}N_9O_4PF_6Ru$ (% Theory/Found) C(48 2/48 0), H(3 9/3 5), N(14 9/14 3)

3 3 3 $[Ru(bipy\text{-}d^8)_2L2](PF_6)\ 2H_2O$

The deuteriated form of the complex was made using the same complexation method as for the normal complex Deuteriated ruthenium bis-bipyridyl dichloride, which is used in place of normal ruthenium bis-bipyridyl dichloride was provided (pre-made) for use in this reaction

^1H NMR (Acetone-d^6) (δ, ppm, J,Hz) 9 52(1H, s, H3), 8 64(1H, d, J=3 0, H6), 7 91(1H, d, J=3 0, H5), 7 49(1H, d, J=3 0, H3"), 7 27(1H, dd, J=3 0, 8 9, H5"), 7 18(1H, d, H6"), 3 83(3H, s, -$OCH_3$1"), 3 80(3H,s, -$OCH_3$4")

3 3 4 $[Ru(bpy)_2L6](PF_6)\ 2H_2O$

$[Ru(bpy)_2L2](PF_6)\ 2H_2O$ (100 mg, 9 8x10^{-5} mol) and BBr_3 (1 M in DCM, 5 ml, excess) were reacted using the following procedure The protected complex in a 50 ml round bottomed flask was dissolved in a small amount of dry DCM The flask was fitted with a rubber septum and placed in an acetone/dry ice bath (-80°C) A steady stream of N_2 gas was flushed through the flask The boron tribromide solution was then injected through the septum On completion of the addition the N_2 stream aws removed and the flask sealed The mixture was then allowed to attain room temperature overnight with stirring The appearance of the complex at this stage was as a paste in the flask

The product, a HBr salt of the complex was insoluble in DCM The contents of the reaction flask were poured onto ice water (to quench excess BBr_3) and stirred for 30 minutes The workup was then transferred to a separatory funnel and the DCM layer removed The remaining aqueous layer was neutralized with saturated sodium bicarbonate solution At neutral pH the product solid precipitated from solution, was collected by suction and washed with ether The deprotected product was recrystallized from acetone/H_20 yield, 71 mg (7 2x10^{-5} mol), 73 5%

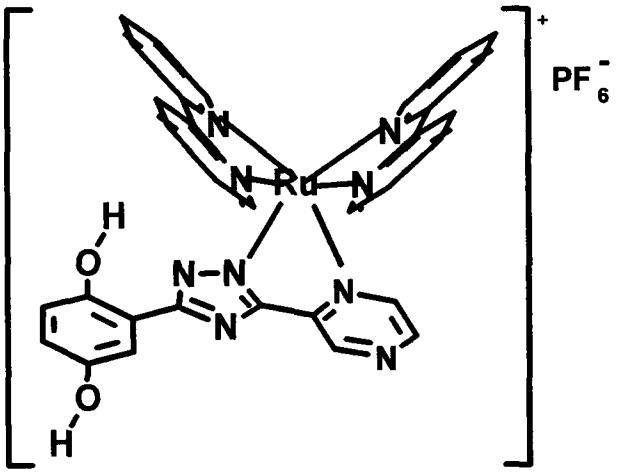

^{1}H NMR (Acetone-d^6) (δ, ppm, J,Hz) 9 55(1H, s, H3), 8 67(1H, d, H6), 8 51(4H, m), 8 13(5H, m, H5+Benz H6'), 7 92(1H,d), 7 85(1H, d), 7 80(2H, dd), 7 41(5H, m, Benz H3"), 7 09 (1H, d, Benz H5"), 6 92(1H, d, Benz H6")
details C,H,N Analysis $C_{32}H_{28}N_9O_4PF_6Ru$ (% Theory/Found) C(47 0/46 6), H(3 5/3 0), N(15 4/15 6)

3 3 5 [{Ru(bipy)$_2$}$_2$L3](PF$_6$)$_2$ 4H$_2$O)

To a solution of Ruthenium bis bipyridyl dichloride [Ru(bipy)$_2$(Cl)$_2$] 2H$_2$O (0 25 g, 4 8 x 10^{-4} mol) in ethanol(100 cm^3) was added 1,4-bis(5-pyridin-2-yl-1,2,4-triazol-3-yl)-1,4-dimethoxy benzene (H$_2$L3) (0 1 g, 2 35 x 10^{-4} mol) in water (50 cm^3) and ethanol (50 cm^3) The mixture was heated at reflux temperature on a heating mantle for approx 24 h to afford product

The solvent was then reduced by distillation to 20 cm^3 and a solution of NH$_4$PF$_6$ (200 mg) in water (10 cm^3) was added dropwise to precipitate the hexaflourophosphate salt of the complex The precipitate was removed by suction filtration and washed with water and ether The wine coloured solid was dried *in vacuo* over P$_2$O$_5$ and recrystallised from acetone/water yield 0 32 g (2.1x10^{-4} mol), 89%.

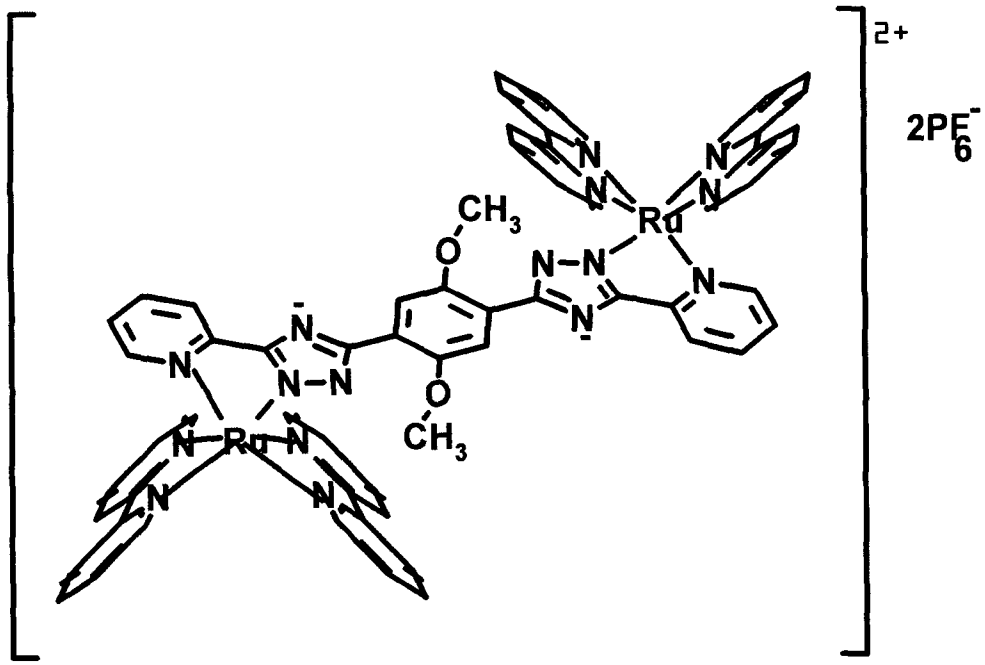

^{1}H NMR (acetone-d^6) (δ, ppm, J,Hz) 8 71(2H, d, J=7 4), 8 65(2H, d, J=7 4), 8 57(4H, t, J=7 4), 8 25(2H, d, J=7 4), 8 04(8H, m), 7 94(10H, m), 7 67(2H, d, J=5 55), 7 48(8H, m), 7 35(2H, t, J=7 4), 7 22(2H, t, J=7 4), 3 51(6H, s)
^{1}H NMR (ACN-d^3) (δ, ppm, J,Hz) 8 47(2H, d, J=7 4), 8 68(2H, d, J=7 4), 8 59(4H, t, J=7 4), 8 29(2H, d, J=7.4, H3), 8 07(8H, m), 7 96(10H, m, H4), 7 71(2H, d, J=5 5, H6), 7 50(8H, m, Benz-H), 7 37(2H, t, J=7 4), 7 24(2H, t, J=7 4, H5), 3 54(6H,s, -OCH$_3$) C,H,N Analysis $C_{62}H_{56}N_{16}O_6P_2F_{12}Ru_2$ (% Theory/Found) C(43 7/44 7), H(3 0/3 4), N(13 1/13 1)

3 3 6 $[(Ru[bipy\text{-}d^8]_2)_2L3](PF_6)_2\ 4H_2O)$

This deuteriated dimer was made using the same complexation method as for the normal complex Deuteriated ruthenium bis-bipyridyl dichloride, which is used in place of normal ruthenium bis-bipyridyl dichloride was provided (pre-made) for use in this reaction

^{1}H NMR (acetone-d^6) (δ, ppm, J,Hz) 8 55(2H, d, J=7 4), 8 16(2H, t, J=7 4), 7 91(2H, d, J=4 6), 7 73(2H, broad s), 7 49(2H, d, J=7 4), 3 77(6H, s)
^{1}H NMR (ACN-d^3) (δ, ppm, J,Hz) 8 39(2H, d, J=7 9, H3), 8 03(2H, t, J=7 9, H4), 7 64(4H, m, H6 and Benz-H), 7 33(2H, t, J=7 9, H5), 3 73(6H, s, -OCH_3)

3 3 7 $[(Ru[bipy]_2)_2L7](PF_6)_2\ 4H_2O$

Dry $[(Ru\{bipy\}_2)_2L3](PF_6)_2\ 4H_2O$ (100 mg, 6 5 x 10^{-5} mol) was placed in a thoroughly dried 50 ml two neck round bottom flask and was dissolved in a small amount of dry DCM The flask was fitted with a rubber septum and placed in an acetone/dry ice bath (-80°C) A steady stream of N_2 gas was flushed through the flask Boron tribromide (1M soln in DCM, 10 cm^3 –excess) was then added via syringe On completion of the addition the N_2 stream was removed and the flask sealed The mixture was then allowed to attain room temperature overnight with stirring The appearance of the complex at this stage was as a paste in the flask

The product, a HBr salt of the complex was insoluble in DCM The contents of the reaction flask were poured onto ice water (to quench excess BBr_3) and stirred for 30 minutes The workup was then transferred to a separatory funnel and the DCM layer removed The remaining aqueous layer was neutralized with saturated sodium bicarbonate solution At neutral pH the

product solid precipitated from solution, was collected by suction and washed with ether yield, 63 mg (4 2x10^{-5} mol), 65%

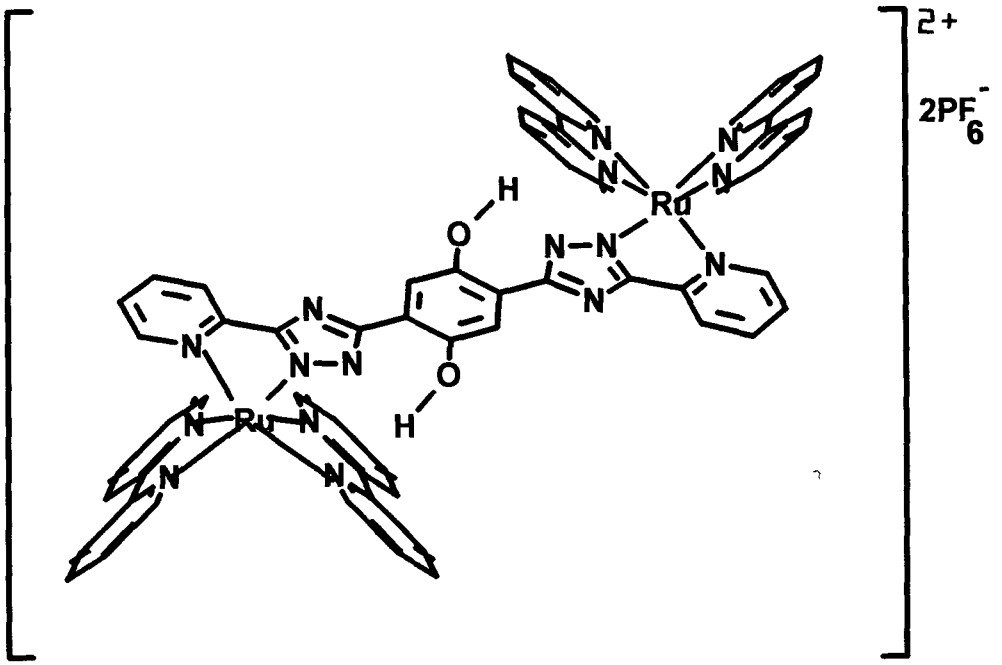

^{1}H NMR (dmso-d^6) (δ, ppm, J,Hz) 10 70(2H, s), 8 78(10H, m), 8 12(12H, m), 8 01(2H, t, J=7 4), 7 88(4H, t, J=5 55), 7 55(8H, m), 7 47(2H, t, J=7 4), 7 33(2H, t, J=7 4), 7 28(2H, s)

^{1}H NMR (ACN-d^3) (δ, ppm, J,Hz) 10 90(2H, broad s, -OH) 8 71(4H,t {overlapping doublets}), 8 62(4H, t {overlapping doublets}), 8 24(2H, d, J=7 8, H3), 8 04(16H, m, H4), 7 91(2H, d, J=5 9), 7 75(2H, d, J=4 9, H6), 7 47(10H, m, Benz-H), 7 29(2H, t, J=5 9, H5) C,H,N Analysis $C_{60}H_{52}N_{16}O_6P_2F_{12}Ru_2$ (% Theory/Found) C(45 5/45 9), H(3 3/3 3), N(14 1/14 9)

3 3 8 $[(Ru[bipy]_2)_2L4](PF_6)_2\ 4H_2O$

To a solution of Ruthenium bis bipyridyl dichloride $[Ru(bipy)_2(Cl)_2]\ 2H_2O$ (0 91 g, 1 86 x 10^{-3}mol) in ethanol(100 ml) was added 1,4-bis(5-pyrazin-2-yl-1,2,4-triazol-3-yl)-1,4-dimethoxy benzene (H_2L4) (0 4 g, 9 3 x 10^{-4} mol) in ethanol (50 cm^3) and water (50 ml) This solution was placed bath for 30 min to ensure good dissolution The mixture was then heated at reflux temperature for 24 h The volume in the reaction vessel was then reduced to 15 ml and allowed to cool before adding NH_4PF_6 (200 mg) to precipitate the hexaflourophosphate salt of the complex The ruthenium complex was filtered and washed with water (to remove excess NH_4PF_6) and diethyl ether (to dry) The complex was recrystallized from acetone/H_20 and further purification was achieved by dissolving the complex in acetonitrile and carrying out a gravity filtration through an alumina column yield 1 28 g (8 3x10^{-4}), 89%

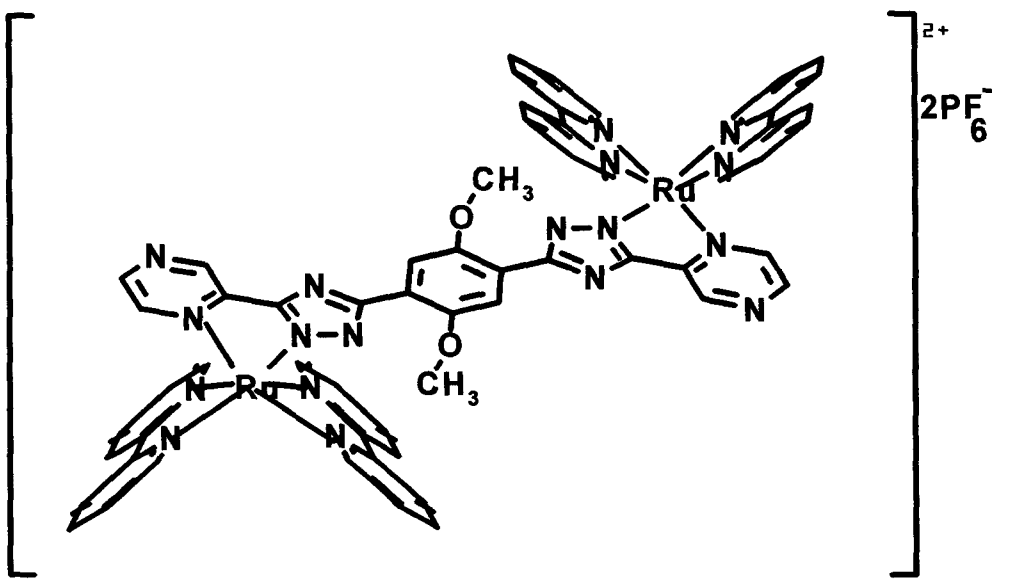

^{1}H NMR (ACN-d^3) (δ, ppm, J,Hz) 9 21(1H, s, H3), 8 45(4H, m), 8 23(1H, d, J=2 95, H6), 7 98(5H, m), 7 87(1H, d, J=5 9), 7 77(1H, d, J=5 9), 7 73 (1H, d, J=5 9), 7 59(1H, d, J=1 97, H5), 7 41(4H, m, containing Benz-H), 7 31(1H, t,

J=5 9), 3 59(3H, s) C,H,N Analysis (% Theory/Found) $C_{60}H_{54}N_{18}O_6P_2F_{12}Ru_2$ C(41 3/41 7), H(3 1/2 6), N(14 4/14 9)

3 3 9 $[(Ru[bpy\text{-}d^8]_2)_2L4](PF_6)_2\ 4H_2O$

This deuteriated dimer was made using the same complexation method as for the normal complex Deuteriated ruthenium bis-bipyridyl dichloride, which is used in place of normal ruthenium bis-bipyridyl dichloride was provided (pre-made) for use in this reaction

^{1}H NMR (acetone-d^6) (δ, ppm, J,Hz) 8 76(1H, s, H3), 7 90(1H, d, H6), 7 36(1H, d, Benz-H), 7 20(1H, d, H5), 3 06(3H, s, OCH_3) Splitting was not sufficiently good to obtain accurate coupling constants

3 3 10 $[(Ru[bipy]_2)_2L8](PF_6)_2\ 4H_2O$

All equipment used in this reaction was thoroughly cleaned and dried prior to use

$[(Ru\{bipy\}_2)_2L4](PF_6)_2\ 4H_2O$) (150 mg, 9 7 x 10 $^{-5}$ mol) was placed in a 25 ml two necked round bottomed flask, and dissolved in DCM (5 cm^3) and a minimum of ACN (approx 1 ml) The flask was stoppered with heavy duty rubber bungs and an argon atmosphere established inside the flask The flask was then cooled in a toluene/N_2 bath Boron tribromide (1M soln in DCM, 10 cm^3 -excess) was then added via syringe The reaction contents were maintained at low temperature for 2 h, then allowed to return to ambient temperature with continuous stirring for a further 10 h After this time the solid reaction product had fallen out of solution The solvent was removed by rotary evaporation and the fuming acidic contents of the reaction vessel neutralized with dil KOH solution The demethylated complex was obtained by suction filtration and washed thoroughly with H_20

Recrystallization from acetone/toluene yielded a fine wine powder of the desired complex yield 53 mg (3 5x10^{-5} mol), 36%

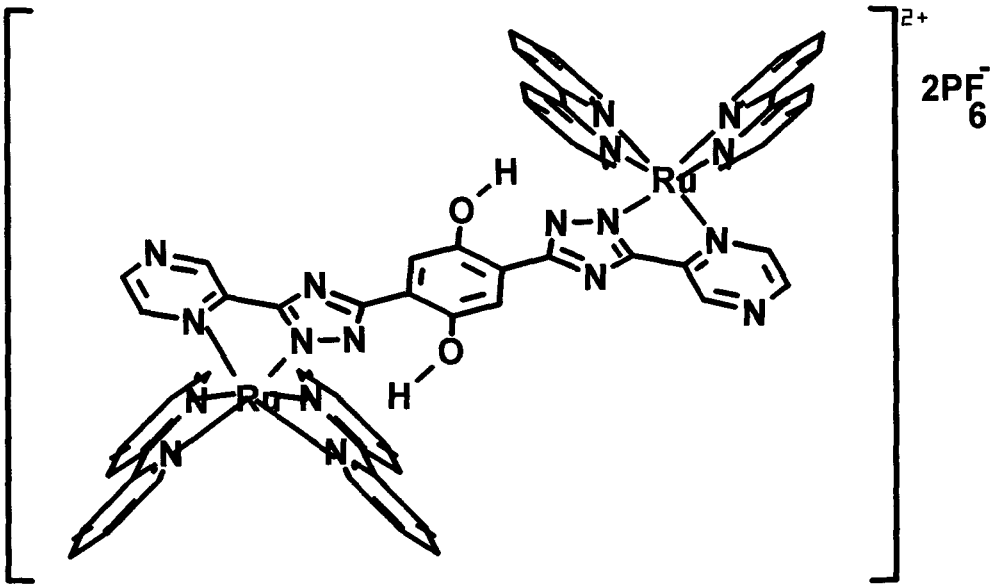

^{1}H NMR (ACN-d^3) (δ, ppm, J,Hz) 9 30(1H, s, H3), 8 50(4H, m), 8 28 (1H, d, J=3 5, H6), 8 02(4H, m), 7 93(1H, d, J=5 4), 7 88(1H, d, J=5 4), 7 78(1H, d, J=5 4), 7 64(1H, dd, J=1 0,3 2, H5), 7 40(5H, m, Benz-H) C,H,N Analysis $C_{58}H_{50}N_{18}O_6P_2F_{12}Ru_2$ (% Theory/Found) C(43 9/44 2), H(3 2/3 0), N(15 9/15 5)

3.4 CONCLUSIONS

Ruthenium complexes of HL1, HL2, H_2L3 and H_2L4 were successfully synthesized and obtained as their PF_6 salts The ruthenium complex of HL1 was successfully crystallized and the X-ray structure obtained The ruthenium binds through N1 of the triazole The crystal structure fits well with previously obtained complex structures The complex crystallized out with a PF_6 and acetone molecule HL1 and its ruthenium complex are compared from a crystallographic viewpoint It is clearly evident that on complexation HL1 (in which is seen strong H-bonds) undergoes a large rotation to accommodate the ruthenium metal One expects from this evidence that H_2L4 would undergo a similar rotation on complexation

Boron tribromide was used to successfully deprotect all the complexes to their dihydroxy form A general reaction procedure is described for this reaction All the complexes, protected and deprotected were characterized by ^{1}H-NMR and COSY spectra, in many cases, aided peak assignment Deuteriated complexes were also formed and their NMR spectra used for comparison

Absorption and emission spectra of the dimer complexes are introduced The aim of this work was to produce a target complex We have achieved that aim, along with crystal structure formation of ligands, a complex and by-products of the synthesis We have detailed all the products spectrally and outlined experimentally repeatable routes to all the products

3.5 REFERENCES

[1] E A Seddon, K R Seddon, The Chemistry of Ruthenium, Elsevier, Amsterdam, (1984)

[2] K Kalyananasundaram, M Gratzel, E Pelizzetti, *Coord Chem Rev*, **69**, 57, (1986)

[3] J Bolger, Ph D Thesis, Dublin City University, 1993

[4] T Keyes, Ph D Thesis, Dublin City University, 1994

[5] M W Bhatt, S U Kulkarni, *Synthesis*, 249, (1983)

[6] F L Benton, T E Dillon, J Am Chem Soc , 64, 1128, (1942)

[7] J F W McOmie, M L Watts, *Chem Ind (London),* 1658, (1963)

[8] J F W McOmie, M L Watts, D E West, *Tetrahedron*, **24**, 2289, (1968)

[9] C Provent, P Chautemps, G Gillon, J -L Pierre, *Tetrahedron Lett* , **9**, 1393, (1996)

[10] J M Egly, A Pousse, M Brini, *Bull Soc Chim Fr* , 1357, (1972)

[11] H Niwa, T Hida, K Yamada, *Tetrahedron Lett* , **22**, 4239, (1989)

[12] P G Willard, C B Fryhle, *Tetrahedron Lett* , **21**, 3731, (1988)

[13] M Jung, M A Lyster, *J Org Chem* , **42**, 3261, (1977)

[14] M S Newman, V Sankaran, D R Olson, *J Am Chem Soc* , **98**, 3237, (1976)

[15] J R McCarthy, J L Moore, R J Cregge, *Tetrahedron Lett* , 52, 5183, (1978)

[16] I T Harrison, *Chem Comm* , 616, (1969)

[17] R L Burwell, *Chem Rev* , **54**, 615, (1954)

[18] D Landini, F Montanari, F Rolla, *Synthesis*, 771, (1978)

[19] P N Craig, F P Nebenhaver, P M Williams, E Macko, J Toner, *J Am Chem Soc* **74**, 1316, (1952)

[20] H Constable, J Lewis, *Inorg Chim Acta*, **70**, 251, (1983)

[21] P Belser, A von Zelewsky, *Helv Chim Acta*, **57**, 239, (1971)

[22] R Hage, R Prins, J G Haasnoot, J Reedijk, J G Vos, *J Chem Soc Dalton Trans* , 1387, (1987)

[23] B Sc in Applied Chemistry, Year 2 NMR spectroscopy workshop manual, Dublin City University, 1993

[24] R Hage, Ph D Thesis, Leiden University, 1990

[25] A Juris, V Balzani, F Barigelleti, S Campagna, P Belser, A von Zelewsky, *Coord Chem Rev* **84**, 85, (1988)

[26] R A Krause, *Structure and Bonding*, **67**, 1, (1987)

[27] R Hage, J G Haasnoot, J Reedijk, R Wang, E Ryan, J G Vos, A L Spek, A J M Duisenburg, *Inorg Chim Acta*, **174**, 77, (1990)

[28] Md K Nazeeruddin, K Kalayanasudaram, *Inorg Chem* , **23**, 4251, (1989)

[29] J F Ireland, P A H Wyatt, Adv Phys Org Chem , **12**, 131, (1976)

4. Purification and Measurement Methods of Ligands and Complexes

4.1 INTRODUCTION

The synthesis of the ligands and complexes in this thesis often require pre-purification to be carried out on the relevant chemicals and solvents The methods of purification used are often critical in ensuring the purity of the chemicals involved and ultimately the success of the reaction The structures of the ligands and complexes have been elucidated by NMR spectroscopy and X-ray analysis, and confirmed by microanalysis, the specifics of which will also be described The most useful recrystallization methods used will also be described as well as any other relevant useful data to those emulating the work in this thesis

4.1.1 Nuclear Magnetic Resonance Spectroscopy

The proton, ^{13}C and 2-D COSY experiments presented in this thesis were carried out using a Bruker AC400 machine operating at 400 MHz for proton NMR and at 100 MHz for ^{13}C All the solvents used in the NMR experiments were deuterated The most common solvent used in the NMR analysis of the ligands was dimethylsulfoxide-d^6 (DMSO-d^6) while acetonitrile-d^3, acetone-d^6 and dimethylsulfoxide-d^6 were the solvents of choice for the complexes Unless stated otherwise in the text all experiments were carried out at room temperature Where possible acetonitrile-d^3 was the standard solvent used in analysis of complexes but in certain cases a change of solvent often helped to resolve multiplets All the deuterated solvents contained TMS to which all chemical shifts were referenced Deuterated acetic acid proved useful in cases where it was desirable to remove an -OH or -NH peak from the spectrum Since H_2O peaks are prevalent when using dimethylsulfoxide, care was taken at all times to minimise DMSO-d^6 exposure to moisture Where a prevalent water peak is problematic in the spectrum a solvent suppression program[1] was used

Two dimensional COSY experiments were usually carried out in DMSO-d^6 for the ligands and ACN-d^3 for the complexes. In general 256 FID experiments (free induction decays) of 16 (or 32) scans were obtained. The ^{1}H-NMR and ^{13}C spectra were processed using the 1D WIN-NMR program. The multiple display and preview windows have been used to prepare the majority of the NMR's in this work. A subtraction function of the program has also been used in the comparison of complexes to their deuterated bipyridyl analogues.

4.1.2 Absorption and Emission Measurements

A number of absorption and emission experiments of ruthenium complexes were carried out and are described in a chapter four. Absorption bands such as metal-to-ligand charge transfer (MLCT) bands are pointed out as well as an explanation of the appearance and position of these bands with respect to their structure. The luminescence properties of the complexes were also recorded and comparisons drawn between the results. Studies were carried at 298 K and at 77K. The ground and excited state pK_a values were investigated and related to the structure of these molecules. A number of the complexes in this work possess more than one pK value but for the scope of the discussion the pK values solely relating to protonation/deprotonation of the triazole ring are described.

The results and conclusions in this section are described from the perspective of a synthetic chemist and should be regarded as simply a cursory examination or introduction to the physical properties of the ruthenium complexes designed to aid future organic chemists daring to cross the organic-inorganic divide. The UV-vis spectra experiments on the complexes were carried out on a Shimadzu UV-240 spectrophotometer interfaced with a PC equipped with Shimadzu UVPC processing program. The UV, pK_a and extinction coefficient spectra presented are in the form of

this program The emission experiments were carried out on a Perkin Elmer LS 50 luminescence spectrophotometer and processed using Fluorescence Data Manager software An excitation slit width of 5 nm and an emission slit of 10 nm was used unless stated otherwise for room temperature experiments whereas both slits were set to 5 nm for experiments at 77 K Absorption and emission experiments were carried out in general in HPLC grade acetonitrile expect for emission experiments at 77 K in which a glass of ethanol methanol (4 1) was used

Protonation was achieved by addition of a minimum amount of perchloric acid and deprotonation was achieved with diethylamine addition pK_a experiments were carried out in Britton-Robinson buffered solution Ground state pK_as were determined by plotting changes in absorption against pH Excited state pK_as were estimated by charting emission intensity (at a fixed wavelength determined from the isobestic point in the ground state pK_a measurements) against pH pK_as were read from the inflection points of the % change in intensity versus pH plots A Phillips PW9421 pH meter was used to measure pH changes The test solutions were acidified with conc H_2SO_4 and made alkaline with KOH

4.1.3 Purification of Organic Chemicals

Solvents and chemicals described in this have in most cases been purified in-house prior to use unless purchased with a specification sheet indicating purity from a chemical company (in general Aldrich Chemicals) Commonly used purification procedures are described below

4.1.3.1 Chloroform

Chloroform, when exposed to air, may be oxidized to Cl_2 and HCl It often contains a small amount of EtOH (1%) and when constantly used in the lab , contains water To remove EtOH the chloroform was washed with water and

dried with $CaCl_2$ It was then refluxed with phosphorous pentoxide and distilled The pure chloroform was stored over 4A Linde molecular sieves Note On no account should chloroform ever be dried with sodium

4.1.3.2 Tetrahydrofuran (THF)

Impurities such as water, peroxides and others can be removed form THF by refluxing with and distilling from $LiAlH_4$ The dry THF was stored over CaH_2 In cases where a regular supply of dry THF was required a still containing potassium metal and benzophenone indicator (which forms a blue ketyl) was employed

4.1.3.3 Dimethyl Sulphoxide (DMSO)

This liquid is very hygroscopic and has a boiling point of 196° C When heating close to this temperature for a period of time it tends to denature When required dry for recrystallizations of ligands, DMSO which had been stored over 4A Linde Molecular sieves for approximately one month were used Another more awkward method for drying involved refluxing with CaO before drying over CaH_2 and fractionally distilling under greatly reduced pressure

4.1.3.4 *N,N*-Dimethylformamide (DMF)

DMF can in some cases be used as a solvent in the cyclization of acylamidrazones It has a bp of 150° C, at which it, like DMSO, will tend to decompose This introduces impurities of dimethylamine and carbon monoxide The decomposition also occurs if stored over bases such as solid KOH or NaOH or even CaH_2 An efficient method of drying DMF to a degree suitable for most purposes involves stirring with $CaSO_4$ followed by distillation under reduced pressure

4.1.3.5 Dichloromethane (DCM)

DCM found in most laboratories requires careful drying before use In the deprotection reaction of ruthenium complexes involving the use of boron tribromide, DCM is the solvent of choice Rigorous drying of the solvent prior to use is central to the success of the reaction DCM should firstly be shaken with H_2SO_4 in a separatory funnel, then washed with water, dilute Na_2CO_3, then water again The DCM is then stirred with $CaCl_2$ for some time to dry before refluxing with and distilling from CaH_2 The dry DCM should then be stored over 4A Linde molecular sieves, ideally in a darkened glass container Where storing over a period of time, the DCM should be in an inert atmosphere.

4.1.3.6 Ethanol

In the synthesis of amidrazones, hydrazine undergoes reaction with a nitrile in ethanol solvent Though rigorous drying is not required, it is good practise to purify ethanol before use Laboratory ethanol contains water, aldehydes, esters, ketones, longer chain alcohols and very often benzene These traces of benzene can be removed by adding a small amount of water to the ethanol before carrying out a fractional distillation An azeotrope distils at 65 C containing benzene/water/ethanol A second distillation from 4A Linde molecular sieves is then carried out Absolute (99 5%) ethanol can be dehydrate to an acceptable synthetic standard by placing approx 5 g of clean Mg filings in a dry flask with 0 5 g iodine before adding about 30 ml ethanol Gently heating (with an air gun) promotes the reaction and it gradually becomes more vigorous without the aid of heat When the reaction begins to cease heating is again applied until all the Mg is converted to magnesium ethoxide Ethanol can now be added (approx 1 l) and refluxed for one hour before collection by distillation and storage over 4A Linde molecular sieves Dried ethanol is hygroscopic, thus it does not remain dry over long periods of storage

4.1.3.7 Acetone

In general, acetone usually does not contain many organic impurities but usually does contain a troublesome content of water Stirring for approx 24 h with anhydrous $CaSO_4$ followed by distillation from fresh $CaSO_4$ $CaSO_4$ does not promote impurity formation with acetone to the same extent that other drying agents tend to do Acetone dried in this way is suitable for use in the reaction of methyl iodide with phenols, a reaction that requires water impurity elimination in order to proceed

4.1.3.8 Acetonitrile

Much of the acetonitrile used in this work was HPLC grade and used direct from the container In the cases where less pure acetonitrile was required but purification was desirable, it was stirred with $CaSO_4$ for 24 h before storing over 4A Linde molecular sieves

4.1.4 Water Removal from Solid Reactants and Products

4.1.4.1 Dessicator

Drying solids in a vacuum desiccator over an efficient drying agent such as silica gel, $CaSO_4$ or phosphorous pentoxide was the usual procedure

4.1.4.2 Kugelrohr Apparatus

In situations where desiccator drying did not suffice, e g the drying of acylamidrazones and triazoles, a Kugelrohr oven apparatus operated at a suitable temperature under reduced pressure was employed Use of P_2O_5 (preferred) or silica gel as drying agents in the collector made this a very efficient and often used drying method When using P_2O_5 it is important that the solid is partially dried with other agents beforehand, this reduces the risk of vigorous reaction and reduces the amount of P_2O_5 required

4.1.4.3 Freezing and evacuating

In some cases where drying of solvents was required but the other methods were inapplicable, e g for liquids or semi-solid materials a method was used which involved freezing the contents of a large container with liquid nitrogen whilst applying a high vacuum The temperature of the vessel was allowed to equilibrate before freezing again without removing the vacuum This method requires the use of a good vacuum (Schlenk) line equipped with liquid nitrogen traps

4.1.5 Miscellaneous

4.1.5.1 Heating

Up to 200° C Silicone oil baths were used In early heating experiments baths containing 85% orthophosphoric acid metaphosphoric acid 4 1 were used and allowed heating up to approx 250° C Where solids were heated in the absence of solvents, platinum crucibles were used Also a sublimation tube heated in an oil bath under reduced pressure was the method of choice for formation of oxadiazoles.

4.1.5.2 Cooling:

0° C Ice

-5 to -20° C ice/salt mix

~ -70° C Solid CO_2/ethanol

~ -80° C Solid CO_2

~ -90° C liquid N_2/heptane

~ -95° C liquid N_2/toluene, liquid N_2/acetone

~ -100° C liquid N_2/methanol

Note Liquid N_2 that has been exposed to air for a long time must not be mixed with organic solvents as their is a risk of explosion

4.1.5.3 Miscible Solvents:

Acetone and chloroform, ethanol, pet ether, water or ethylene glycol

Dimethyl sulphoxide and acetone, chloroform, diethyl ether, ethanol or water

Ethanol and acetone, diethyl ether, chloroform, toluene or water

Methanol and diethyl ether, chloroform or water

Toluene and pyridine, or diethyl ether

Water and acetone, ethanol, methanol, pyridine or acetic acid

Further information on purification procedures can be found in the text by Perrin and Armerego[2]

4.1.6 Crystallization of Products.

A discussion of the most useful crystallization techniques for acylamidrazones and triazoles can be found in the results and discussion section of chapter one. In general for the bis-acylamidrazones and triazoles, crystallization from ethylene glycol or DMSO resulted in pure compounds being obtained. A bis-triazole crystal suitable for X-ray analysis[3] was grown from ethylene glycol. Mono-triazoles in general showed better dissolution properties and two crystals were grown employing a DCM/pet. ether slow diffusion recrystallization technique. A small amount of the triazole was placed in a thin glass container (which should be clamped to avoid movement) and dissolved in the minimum of DCM. A poor solvent such as petroleum ether was carefully ran into the vial ensuring that the two layers did not mix and the container. Over the next weeks the petroleum ether diffused into the DCM layer causing good crystals to form.

The most useful method for growing crystals of ruthenium complexes employed using solvent mixtures such acetone/toluene, acetone/water or if possible DCM/pet ether. A drop of acetonitrile often helped in the dissolution of complexes. It was found that the rigorous the purification of the complex best trying to grow a crystal, the better the results were. That meant several preparatory recrystallizations were generally carried out along with purification by passage through an alumina column, use of rigorously purified solvents, good drying procedures and patience. Where crystallization is found to be particularly troublesome and only poor quality crystals are being obtained another option may be co-crystallization.

A number of tentative co-crytallization experiments were carried out in the course of this work using triphenylphosine oxide (TPPO)[4] TPPO can itself form complexes using its P=O bond with molecules containing O or N groups Equimolar amounts of TPPO and the compound were dissolved in acetone or acetonitrile then the solvent was allowed to evaporate slowly One should always check (by NMR) crystals obtained using this technique as in many cases the TPPO itself forms fine crystals

4.1.7 Crystallization of Small Amounts

It is common when dealing with ruthenium complexes to require crystallizations of amounts less than 100 mg The procedure used in these cases involves dissolution of the complex in a small amount of solvent in a test tube The solution was filtered by drawing the solution through a plug of cotton wool inserted in the top of a Pasteur pipette This plug effectively removes impurities and is quickly removed when the solution is in the pipette Transferral of the solution to a Craig tube, which is specially designed for this purpose, is the last step The Craig tube has a well fitting glass stopper and when crystal growth occurs in the tube, it fits neatly into a centrifugation tube to allow easy removal of the mother liquor and collection of the crystals The use of a Craig tube minimises the number of transfers of solvents and avoids losses due to filtration

4.2 REFERENCES

---

[1] AS PRESAT AU on Bruker NMR console

[2] D D Perrin, W L F Armarego, Purification of Laboratory Chemicals, 3rd edition, Pergammon, Oxford, 1989

[3] P G Jones, *Chem Br* , **17**, 222, (1971)

[4] M C Mc Etter, P W Baures, *J Am Chem Soc* , **110**, 639, (1988)

Final Remarks

This thesis sets out to form a number of "target" ligands and their ruthenium complexes The four chapters of this work document how this aim was achieved in a clearly defined manner

Chapter one introduced 1,2,4-triazoles and the methods used by our predecessors to form them Reactions were also carried out to form model triazoles which led to the expected unearthing of a hidden gem When forming 2-pyridyl amidrazone the X-ray crystal structures of two by-products of this synthesis were obtained and are presented One of the structures has never before been reported in the literature Chapter one also contains detailed proton NMR and COSY studies on the models

The synthesis, spectroscopic analysis and X-ray crystal structures of the target ligands of the thesis are presented in chapter two The most relevant history of large triazole synthesis is introduced firstly, before describing the new syntheses X-ray crystal structures of three of the four target ligands are presented

Chapter three describes the complexing of the target ligands to ruthenium metal A crystal of one of these complexes yielded a very valuable X-ray structure Since it is these complexes that are hoped to be useful in synthetic applications a cursory examination of their ground and excited state properties was carried out and the results presented

The final chapter of the thesis describes the equipment and methods used in the practical work The purification and preparation of all the chemicals and reagents is described It is hoped the entire work will enable future chemists to easily reproduce all the products described herein

The Future

In the immediate future the electronic and photo-physical properties of the complexes described in this thesis will be investigated in detail The results obtained will be compared to those of previously made complexes The success or failure of this molecule from a photosynthetic application standpoint will become apparent at this stage

Since all the target triazole ligands and their precursor acylamidrazones have never before been synthesized, the screening of these molecules for medicinal use will be carried out Acylamidrazones and triazoles have in general medicinal properties

The question of the metal in the complexes can also be addressed Ruthenium may be substituted for another metal in complex preparation or mixed-metal complexes may be formed and the resultant molecules compared Coordination of the metal through the quinone hydroxyl groups is another synthetic avenue, which should be explored

More sophisticated ligand and complexes may also be formed from those described in this thesis As seen in chapter two the tnazole nitrogens can be used to add on moieties to the existing molecules There also exists a lot of scope for in-depth spectroscopic studies of all these ligands and complexes

Finally, we have succeeded what we set out to achieve in this thesis, the target ligands and complexes have been synthesized and analyzed and all the knowledge needed to recreate the work has been clearly described herein As mentioned at the outset, this work purports to be only a small piece of a large puzzle and exciting times lie ahead Rome wasn't built in a day

APPENDIX 1

Crystal structure data for Bi-2-pyridyl-bis-imidoylhydrazine, $C_{12}H_{12}N_6$ (105)

Table 1. Crystal data and structure refinement for 1.

Identification code	jgvos
Empirical formula	C12 H12 N6
Formula weight	240.28
Temperature	293(2) K
Wavelength	0.71069 A
Crystal system	Orthorhombic
Space group	P c a b
Unit cell dimensions	a = 9.5301(12) A alpha = 90 deg. b = 13.1851(10) A beta = 90 deg. c = 19.840(2) A gamma = 90 deg.
Volume	2493.0(5) A^3
Z	8
Density (calculated)	1.280 Mg/m^3
Absorption coefficient	0.084 mm^-1
F(000)	1008
Crystal size	0.5 x 0.6 x 0.5 mm
Theta range for data collection	2.05 to 24.95 deg.
Index ranges	-9<=h<=9, 0<=k<=15, 0<=l<=20
Reflections collected	3951
Independent reflections	2051 [R(int) = 0.0188]
Refinement method	Full-matrix least-squares on F^2
Data / restraints / parameters	2051 / 0 / 211
Goodness-of-fit on F^2	1.023
Final R indices [I>2sigma(I)]	R1 = 0.0375, wR2 = 0.0920
R indices (all data)	R1 = 0.0654, wR2 = 0.1065
Largest diff. peak and hole	0.218 and -0.214 e.A^-3

Table 2. Atomic coordinates (x 10^4) and equivalent isotropic displacement parameters (A^2 x 10^3) for 1. U(eq) is defined as one third of the trace of the orthogonalized Uij tensor.

	x	y	z	U(eq)
N(1)	-1263(2)	11142(1)	6937(1)	63(1)
N(2)	-1620(2)	9907(1)	5890(1)	63(1)
N(3)	510(1)	9084(1)	6147(1)	43(1)
N(4)	154(1)	8461(1)	5598(1)	42(1)
N(5)	2397(2)	7764(1)	5774(1)	56(1)
N(6)	1760(1)	6330(1)	4830(1)	58(1)
C(1)	-221(2)	10482(1)	6829(1)	44(1)
C(2)	981(2)	10456(1)	7222(1)	51(1)
C(3)	1123(2)	11140(1)	7742(1)	60(1)
C(4)	68(2)	11829(1)	7850(1)	68(1)
C(5)	-1087(2)	11798(1)	7446(1)	76(1)
C(6)	-438(2)	9774(1)	6252(1)	42(1)
C(7)	1163(2)	7834(1)	5446(1)	39(1)
C(8)	913(1)	7138(1)	4871(1)	42(1)
C(9)	-134(2)	7327(1)	4403(1)	55(1)
C(10)	-329(2)	6657(2)	3881(1)	72(1)
C(11)	529(2)	5831(2)	3836(1)	84(1)
C(12)	1550(2)	5697(2)	4311(1)	80(1)

Table 3. Bond lengths [A] and angles [deg] for 1.

N(1)-C(1)	1.338(2)
N(1)-C(5)	1.341(2)
N(2)-C(6)	1.347(2)
N(3)-C(6)	1.299(2)
N(3)-N(4)	1.406(2)
N(4)-C(7)	1.303(2)
N(5)-C(7)	1.348(2)
N(6)-C(8)	1.339(2)
N(6)-C(12)	1.341(2)
C(1)-C(2)	1.386(2)
C(1)-C(6)	1.490(2)
C(2)-C(3)	1.377(2)
C(3)-C(4)	1.372(3)
C(4)-C(5)	1.363(3)
C(7)-C(8)	1.485(2)
C(8)-C(9)	1.385(2)
C(9)-C(10)	1.374(2)
C(10)-C(11)	1.364(3)
C(11)-C(12)	1.366(3)
C(1)-N(1)-C(5)	116.6(2)
C(6)-N(3)-N(4)	111.46(11)
C(7)-N(4)-N(3)	111.82(11)
C(8)-N(6)-C(12)	116.9(2)
N(1)-C(1)-C(2)	122.64(14)
N(1)-C(1)-C(6)	115.27(14)
C(2)-C(1)-C(6)	122.08(13)
C(3)-C(2)-C(1)	119.1(2)
C(4)-C(3)-C(2)	118.6(2)
C(5)-C(4)-C(3)	118.7(2)
N(1)-C(5)-C(4)	124.3(2)
N(3)-C(6)-N(2)	125.89(14)
N(3)-C(6)-C(1)	117.71(13)
N(2)-C(6)-C(1)	116.40(14)
N(4)-C(7)-N(5)	125.16(13)
N(4)-C(7)-C(8)	116.86(13)
N(5)-C(7)-C(8)	117.98(13)
N(6)-C(8)-C(9)	122.49(14)
N(6)-C(8)-C(7)	116.22(13)
C(9)-C(8)-C(7)	121.29(13)
C(10)-C(9)-C(8)	119.1(2)
C(11)-C(10)-C(9)	118.8(2)
C(10)-C(11)-C(12)	119.1(2)
N(6)-C(12)-C(11)	123.7(2)

Symmetry transformations used to generate equivalent atoms:

Table 4 Anisotropic displacement parameters (A^2 x 10^3) for 1.
The anisotropic displacement factor exponent takes the form:
-2 pi^2 [h^2 a*^2 U11 + ... + 2 h k a* b* U12]

	U11	U22	U33	U23	U13	U12
N(1)	54(1)	56(1)	80(1)	-20(1)	4(1)	9(1)
N(2)	52(1)	59(1)	77(1)	-20(1)	-14(1)	19(1)
N(3)	40(1)	39(1)	49(1)	-5(1)	2(1)	1(1)
N(4)	37(1)	40(1)	49(1)	-4(1)	0(1)	0(1)
N(5)	40(1)	61(1)	66(1)	-24(1)	-9(1)	11(1)
N(6)	48(1)	53(1)	75(1)	-23(1)	-6(1)	6(1)
C(1)	42(1)	38(1)	52(1)	-1(1)	9(1)	-2(1)
C(2)	50(1)	49(1)	56(1)	-2(1)	1(1)	-1(1)
C(3)	65(1)	58(1)	56(1)	-4(1)	-2(1)	-13(1)
C(4)	81(2)	61(1)	64(1)	-20(1)	9(1)	-10(1)
C(5)	71(1)	68(1)	88(1)	-32(1)	7(1)	13(1)
C(6)	36(1)	39(1)	50(1)	0(1)	5(1)	-1(1)
C(7)	32(1)	39(1)	45(1)	0(1)	3(1)	-2(1)
C(8)	33(1)	45(1)	47(1)	-3(1)	5(1)	-5(1)
C(9)	49(1)	66(1)	51(1)	-1(1)	-2(1)	2(1)
C(10)	58(1)	97(2)	59(1)	-14(1)	-11(1)	-10(1)
C(11)	73(2)	94(2)	83(1)	-46(1)	-6(1)	-11(1)
C(12)	68(1)	70(1)	100(2)	-42(1)	-11(1)	7(1)

Table 5. Hydrogen coordinates (x 10^4) and isotropic displacement parameters (A^2 x 10^3) for 1.

	x	y	z	U(eq)
H(2N)	-1798(20)	9492(15)	5553(10)	75(6)
H(2N)	-2163(21)	10410(14)	6000(9)	71(6)
H(5N)	2539(17)	8200(12)	6116(9)	57(5)
H(5N)	3031(20)	7335(15)	5642(9)	66(5)
H(2)	1661(18)	9949(13)	7126(8)	60(5)
H(3)	1985(23)	11124(14)	8031(9)	78(6)
H(4)	127(19)	12318(14)	8203(10)	78(6)
H(5)	-1835(22)	12256(15)	7509(10)	90(7)
H(9)	-666(19)	7928(12)	4458(8)	62(5)
H(10)	-1070(24)	6772(14)	3564(11)	89(6)
H(11)	504(23)	5341(16)	3471(11)	108(7)
H(12)	2156(24)	5144(17)	4298(11)	94(7)

Table 6 Observed and calculated structure factors for

Table 6 Observed and calculated structure factors for 1

h	k	l	10Fo	10Fc	10s
1	1	4	491	503	1
2	1	4	499	514	4
3	1	4	326	322	1
4	1	4	90	87	1
5	1	4	107	104	1
6	1	4	257	245	1
7	1	4	64	57	3
8	1	4	203	203	1
9	1	4	162	157	1
0	2	4	1464	1296	9
1	2	4	518	532	5
2	2	4	593	612	2
3	2	4	205	187	1
4	2	4	139	142	1
5	2	4	119	118	1
6	2	4	40	37	11
7	2	4	102	101	2
8	2	4	113	113	1
9	2	4	0	23	1
0	3	4	247	238	2
1	3	4	1100	982	5
2	3	4	1264	1122	17
3	3	4	293	301	2
4	3	4	257	243	1
5	3	4	168	166	5
6	3	4	195	198	1
7	3	4	122	122	1
8	3	4	20	9	14
9	3	4	35	34	5
0	4	4	316	318	2
1	4	4	50	48	1
2	4	4	493	492	2
3	4	4	116	115	1
4	4	4	65	76	1
5	4	4	177	176	1
6	4	4	205	208	1
7	4	4	162	167	1
8	4	4	14	9	14
9	4	4	0	17	1
0	5	4	189	196	1
1	5	4	235	244	2
2	5	4	275	278	2
3	5	4	241	249	1
4	5	4	14	30	13
5	5	4	307	302	2
6	5	4	163	176	4
7	5	4	196	194	1
8	5	4	49	47	3
9	5	4	0	26	1
0	6	4	164	161	1
1	6	4	217	200	2
2	6	4	103	107	1
3	6	4	72	79	1
4	6	4	94	92	1
5	6	4	100	100	1
6	6	4	70	71	1
7	6	4	204	199	2
8	6	4	29	39	29
9	6	4	0	48	1
0	7	4	172	163	1
1	7	4	353	356	2
2	7	4	237	226	1
3	7	4	44	38	1
4	7	4	106	104	1
5	7	4	38	36	12
6	7	4	102	99	1
7	7	4	96	93	1
8	7	4	0	5	1
9	7	4	55	59	3
0	8	4	41	42	2
1	8	4	83	80	1
2	8	4	94	95	1
3	8	4	120	119	1
4	8	4	7	7	7
5	8	4	146	150	1
6	8	4	54	54	2
7	8	4	0	20	1
8	8	4	64	62	2
9	8	4	0	2	1
0	9	4	182	177	1
1	9	4	205	202	1
2	9	4	109	111	1
3	9	4	54	52	1
4	9	4	54	52	1
5	9	4	28	27	4
6	9	4	87	76	1
7	9	4	307	307	2
8	9	4	12	29	11
9	9	4	48	58	15
0	10	4	80	76	1

h	k	l	10Fo	10Fc	10s
1	10	4	128	124	1
2	10	4	0	11	1
3	10	4	0	4	1
4	10	4	28	25	8
5	10	4	109	113	1
6	10	4	0	32	1
7	10	4	141	141	1
8	10	4	98	93	1
0	11	4	112	114	1
1	11	4	142	138	1
2	11	4	115	119	1
3	11	4	16	22	16
4	11	4	144	141	1
5	11	4	0	6	1
6	11	4	0	4	1
7	11	4	0	7	1
0	12	4	329	319	3
1	12	4	90	91	1
2	12	4	78	77	1
3	12	4	0	16	1
4	12	4	99	101	1
5	12	4	23	22	5
6	12	4	44	47	3
0	13	4	70	72	2
1	13	4	13	12	13
2	13	4	71	69	1
3	13	4	46	44	15
4	13	4	53	52	2
5	13	4	57	56	2
0	14	4	0	13	1
1	14	4	72	70	2
2	14	4	28	17	15
3	14	4	45	43	12
4	14	4	38	29	3
0	15	4	44	37	4
1	15	4	0	0	1
2	15	4	0	8	1
2	0	5	77	78	1
4	0	5	648	638	2
6	0	5	111	105	1
8	0	5	25	26	4
1	1	5	33	35	2
2	1	5	727	732	2
3	1	5	201	186	1
4	1	5	53	49	1
5	1	5	216	216	1
6	1	5	166	156	1
7	1	5	76	75	3
8	1	5	0	11	1
9	1	5	156	155	3
1	2	5	114	120	1
2	2	5	41	41	1
3	2	5	117	129	1
4	2	5	321	311	5
5	2	5	391	386	3
6	2	5	92	85	1
7	2	5	187	188	1
8	2	5	61	61	2
9	2	5	34	31	3
1	3	5	233	239	1
2	3	5	96	103	1
3	3	5	166	158	1
4	3	5	525	509	8
5	3	5	75	67	1
6	3	5	106	103	1
7	3	5	48	44	12
8	3	5	61	55	2
9	3	5	120	120	4
1	4	5	315	313	1
2	4	5	114	124	1
3	4	5	197	202	1
4	4	5	80	77	1
5	4	5	76	70	2
6	4	5	113	117	1
7	4	5	78	78	1
8	4	5	23	27	5
9	4	5	61	59	2
1	5	5	293	289	1
2	5	5	397	396	2
3	5	5	127	129	1
4	5	5	76	77	2
5	5	5	0	4	1
6	5	5	44	47	3
7	5	5	80	81	3
8	5	5	67	68	2
9	5	5	26	26	5
1	6	5	61	59	1
2	6	5	161	167	1
3	6	5	87	90	2
4	6	5	59	60	1

h	k	l	10Fo	10Fc	10s
5	6	5	74	77	1
6	6	5	145	139	1
7	6	5	45	36	13
8	6	5	78	80	1
9	6	5	71	74	3
1	7	5	187	196	1
2	7	5	89	88	3
3	7	5	168	168	1
4	7	5	195	191	1
5	7	5	138	147	1
6	7	5	338	347	2
7	7	5	134	136	1
8	7	5	161	166	1
9	7	5	83	78	1
1	8	5	48	45	1
2	8	5	137	137	1
3	8	5	139	138	1
4	8	5	78	74	1
5	8	5	187	188	1
6	8	5	44	46	2
7	8	5	33	22	6
8	8	5	0	5	1
9	8	5	76	77	4
1	9	5	285	284	2
2	9	5	201	200	1
3	9	5	50	45	1
4	9	5	21	24	5
5	9	5	31	26	6
6	9	5	169	174	1
7	9	5	93	81	1
8	9	5	157	157	1
1	10	5	150	149	1
2	10	5	0	15	1
3	10	5	37	37	8
4	10	5	134	131	1
5	10	5	0	20	1
6	10	5	84	88	1
7	10	5	20	19	19
8	10	5	34	28	10
1	11	5	161	163	1
2	11	5	284	287	2
3	11	5	159	162	1
4	11	5	0	18	1
5	11	5	24	9	9
6	11	5	56	54	2
7	11	5	63	64	2
1	12	5	339	334	3
2	12	5	152	153	1
3	12	5	75	76	1
4	12	5	41	46	20
5	12	5	59	55	3
6	12	5	71	70	2
1	13	5	60	58	2
2	13	5	39	41	8
3	13	5	0	20	1
4	13	5	41	43	40
5	13	5	32	27	6
1	14	5	11	11	11
2	14	5	0	20	1
3	14	5	10	15	10
4	14	5	37	30	18
1	15	5	0	7	1
2	15	5	0	13	1
0	0	6	1758	1639	10
2	0	6	31	42	8
4	0	6	227	217	2
6	0	6	17	16	17
8	0	6	156	156	1
0	1	6	229	244	2
1	1	6	164	163	1
2	1	6	280	284	1
3	1	6	145	134	1
4	1	6	254	239	1
5	1	6	90	86	1
6	1	6	31	41	8
7	1	6	63	59	1
8	1	6	153	157	1
9	1	6	31	31	8
0	2	6	112	112	1
1	2	6	155	161	2
2	2	6	203	206	1
3	2	6	87	87	1
4	2	6	695	680	10
5	2	6	224	226	1
6	2	6	0	18	1
7	2	6	86	84	1
8	2	6	199	197	1
9	2	6	0	15	1
0	3	6	640	658	3
1	3	6	116	126	1

h	k	l	10Fo	10Fc	10s
2	3	6	6	23	5
3	3	6	144	134	1
4	3	6	237	225	2
5	3	6	41	42	2
6	3	6	0	2	1
7	3	6	49	49	2
8	3	6	14	19	13
9	3	6	0	17	1
0	4	6	445	433	3
1	4	6	708	733	2
2	4	6	672	698	4
3	4	6	323	336	2
4	4	6	69	54	1
5	4	6	72	71	3
6	4	6	130	129	1
7	4	6	38	38	2
8	4	6	15	8	14
9	4	6	74	69	1
0	5	6	788	775	3
1	5	6	594	575	2
2	5	6	801	805	4
3	5	6	666	658	2
4	5	6	350	348	2
5	5	6	198	203	1
6	5	6	123	126	1
7	5	6	31	32	30
8	5	6	62	64	2
9	5	6	66	66	3
0	6	6	100	95	1
1	6	6	101	97	1
2	6	6	162	162	1
3	6	6	38	29	2
4	6	6	86	86	1
5	6	6	75	75	1
6	6	6	82	88	1
7	6	6	318	315	2
8	6	6	24	28	5
9	6	6	0	4	1
0	7	6	79	75	1
1	7	6	20	23	19
2	7	6	151	164	1
3	7	6	0	19	1
4	7	6	197	192	1
5	7	6	230	225	1
6	7	6	127	132	1
7	7	6	351	354	7
8	7	6	25	35	24
9	7	6	67	71	21
0	8	6	96	97	1
1	8	6	141	143	1
2	8	6	34	38	2
3	8	6	16	6	6
4	8	6	142	141	1
5	8	6	157	154	1
6	8	6	22	23	22
7	8	6	77	77	1
8	8	6	25	41	24
9	8	6	15	27	15
0	9	6	213	213	2
1	9	6	62	68	2
2	9	6	46	38	3
3	9	6	131	132	1
4	9	6	20	28	8
5	9	6	5	2	5
6	9	6	39	47	35
7	9	6	36	35	6
8	9	6	3	2	3
0	10	6	52	51	2
1	10	6	80	84	1
2	10	6	37	42	2
3	10	6	123	121	1
4	10	6	0	3	1
5	10	6	49	46	28
6	10	6	55	61	3
7	10	6	12	9	12
8	10	6	25	23	10
0	11	6	136	137	1
1	11	6	180	183	2
2	11	6	159	160	1
3	11	6	168	161	2
4	11	6	74	74	1
5	11	6	19	10	19
6	11	6	0	28	1
7	11	6	21	30	20
0	12	6	266	269	2
1	12	6	82	85	1
2	12	6	87	89	1
3	12	6	61	59	2
4	12	6	23	26	8
5	12	6	12	2	12

h	k	l	10Fo	10Fc	10s
6	12	6	101	100	1
0	13	6	31	27	5
1	13	6	60	59	3
2	13	6	10	12	10
3	13	6	20	26	10
4	13	6	14	1	13
5	13	6	59	59	2
0	14	6	0	16	1
1	14	6	0	21	1
2	14	6	0	17	1
3	14	6	60	61	2
4	14	6	63	62	2
0	15	6	39	39	5
1	15	6	21	39	20
2	0	7	156	138	1
4	0	7	90	90	1
6	0	7	114	108	1
8	0	7	21	9	6
1	1	7	287	299	4
2	1	7	96	100	1
3	1	7	276	278	2
4	1	7	64	62	1
5	1	7	33	30	5
6	1	7	87	85	1
7	1	7	55	59	1
8	1	7	27	34	27
9	1	7	68	63	2
1	2	7	338	346	1
2	2	7	140	132	1
3	2	7	476	486	2
4	2	7	163	157	1
5	2	7	109	103	1
6	2	7	165	163	1
7	2	7	63	66	1
8	2	7	23	15	5
9	2	7	142	141	1
1	3	7	184	184	2
2	3	7	167	173	1
3	3	7	54	48	1
4	3	7	44	40	1
5	3	7	33	37	12
6	3	7	107	106	1
7	3	7	44	44	3
8	3	7	73	74	1
9	3	7	0	0	1
1	4	7	803	806	2
2	4	7	574	581	2
3	4	7	132	132	1
4	4	7	0	21	1
5	4	7	0	27	1
6	4	7	0	22	1
7	4	7	19	9	11
8	4	7	121	122	1
9	4	7	11	7	11
1	5	7	137	120	1
2	5	7	116	131	1
3	5	7	357	374	2
4	5	7	302	306	2
5	5	7	234	238	1
6	5	7	11	29	11
7	5	7	49	50	4
8	5	7	37	49	11
9	5	7	33	42	16
1	6	7	74	74	1
2	6	7	238	243	1
3	6	7	193	190	1
4	6	7	67	67	1
5	6	7	323	326	2
6	6	7	0	0	1
7	6	7	9	2	8
8	6	7	32	27	4
9	6	7	115	111	1
1	7	7	97	104	1
2	7	7	96	97	1
3	7	7	12	6	11
4	7	7	116	106	1
5	7	7	309	311	2
6	7	7	240	241	1
7	7	7	217	215	2
8	7	7	167	172	1
9	7	7	78	83	2
1	8	7	49	48	1
2	8	7	103	106	1
3	8	7	37	33	2
4	8	7	57	57	1
5	8	7	0	28	1
6	8	7	122	126	1
7	8	7	49	48	2
8	8	7	101	106	1
9	8	7	51	59	13

Table 6 Observed and calculated structure factors for 1

h	k	l	10Fo	10Fc	10s
1	9	7	26	29	3
2	9	7	73	76	2
3	9	7	265	268	1
4	9	7	193	188	1
5	9	7	46	45	4
6	9	7	104	101	2
7	9	7	16	11	15
8	9	7	9	10	9
1	10	7	99	101	1
2	10	7	73	75	1
3	10	7	36	42	10
4	10	7	71	69	1
5	10	7	21	29	20
6	10	7	7	1	7
7	10	7	28	28	7
8	10	7	0	21	1
1	11	7	128	131	1
2	11	7	16	6	16
3	11	7	14	2	15
4	11	7	57	54	2
5	11	7	0	1	1
6	11	7	52	51	2
7	11	7	40	42	3
1	12	7	145	140	1
2	12	7	105	101	1
3	12	7	12	28	11
4	12	7	28	22	6
5	12	7	20	32	20
6	12	7	29	36	28
1	13	7	32	35	6
2	13	7	55	60	2
3	13	7	55	55	2
4	13	7	9	29	8
5	13	7	55	52	4
1	14	7	53	51	3
2	14	7	40	46	3
3	14	7	10	28	9
0	0	8	214	228	2
2	0	8	222	232	1
4	0	8	321	313	2
6	0	8	408	398	2
8	0	8	412	429	4
1	1	8	466	466	3
2	1	8	280	284	1
3	1	8	113	111	1
4	1	8	46	46	1
5	1	8	257	252	2
6	1	8	286	283	2
7	1	8	0	12	8
8	1	8	68	59	8
9	1	8	31	32	4
0	2	8	0	12	1
1	2	8	307	305	2
2	2	8	283	284	1
3	2	8	272	273	1
4	2	8	140	137	2
5	2	8	420	417	2
6	2	8	0	29	1
7	2	8	56	58	3
8	2	8	0	30	1
9	2	8	69	64	2
0	3	8	168	158	1
1	3	8	192	198	1
2	3	8	66	69	2
3	3	8	431	432	2
4	3	8	175	175	1
5	3	8	56	59	1
6	3	8	107	107	1
7	3	8	57	54	2
8	3	8	47	66	16
9	3	8	0	34	1
0	4	8	368	373	2
1	4	8	139	137	1
2	4	8	82	85	1
3	4	8	168	173	1
4	4	8	134	135	1
5	4	8	75	77	1
6	4	8	45	43	2
7	4	8	88	89	1
8	4	8	0	2	1
9	4	8	27	23	26
0	5	8	181	184	1
1	5	8	90	78	6
2	5	8	38	3	9
3	5	8	251	255	1
4	5	8	243	245	1
5	5	8	0	7	1
6	5	8	0	1	1
7	5	8	87	90	1
8	5	8	0	6	1
9	5	8	0	14	1
0	6	8	164	135	1
1	6	8	40	38	2
2	6	8	145	150	1
3	6	8	67	66	1
4	6	8	81	82	1
5	6	8	322	326	2
6	6	8	23	29	23
7	6	8	21	22	7
8	6	8	81	83	1
9	6	8	0	44	1
0	7	8	132	137	1
1	7	8	233	239	1
2	7	8	0	14	1
3	7	8	52	56	18
4	7	8	79	83	1
5	7	8	50	53	10
6	7	8	174	161	1
7	7	8	172	171	2
8	7	8	9	3	8
9	7	8	49	50	3
0	8	8	63	62	2
1	8	8	147	144	1
2	8	8	45	51	2
3	8	8	32	35	19
4	8	8	69	68	1
5	8	8	122	120	1
6	8	8	101	96	1
7	8	8	244	244	1
8	8	8	59	60	35
0	9	8	73	77	1
1	9	8	178	176	1
2	9	8	182	192	1
3	9	8	281	274	1
4	9	8	102	102	1
5	9	8	150	145	1
6	9	8	67	60	2
7	9	8	95	101	2
8	9	8	0	31	1
0	10	8	289	283	2
1	10	8	308	310	2
2	10	8	308	309	2
3	10	8	210	210	2
4	10	8	174	173	1
5	10	8	51	52	2
6	10	8	18	12	10
7	10	8	103	106	1
8	10	8	15	16	15
9	10	8	32	29	3
0	11	8	11	2	11
1	11	8	20	12	11
2	11	8	14	20	13
3	11	8	47	46	3
4	12	8	65	64	3
5	12	8	31	26	5
6	12	8	49	48	5
7	12	8	22	16	5
8	12	8	0	23	1
9	12	8	88	86	1
0	13	8	47	46	3
1	13	8	12	28	12
2	13	8	50	47	11
3	13	8	0	17	1
4	13	8	0	12	1
5	13	8	86	87	2
6	14	8	0	23	1
7	14	8	0	5	1
8	14	8	9	21	9
0	0	9	134	129	1
2	0	9	160	158	1
4	0	9	277	267	4
6	0	9	102	115	1
8	0	9	138	129	2
1	1	9	181	175	2
3	1	9	223	214	2
5	1	9	67	59	1
7	1	9	155	153	4
9	1	9	23	30	4
0	2	9	120	127	1
1	2	9	61	62	2
2	2	9	105	103	1
3	2	9	381	374	5
4	2	9	341	354	1
5	2	9	5	22	5
6	2	9	155	152	1
7	2	9	17	25	9
8	2	9	0	6	1
9	2	9	18	18	17
0	3	9	15	15	14
1	3	9	0	6	1
2	3	9	16	14	14
3	3	9	874	869	3
4	3	9	76	86	1
5	3	9	58	59	2
6	3	9	31	28	2
7	3	9	59	59	1
8	3	9	16	10	16
9	3	9	68	68	1
0	4	9	12	3	11
1	4	9	53	52	2
2	4	9	131	131	1
3	4	9	0	18	1
4	4	9	207	207	1
5	4	9	206	207	2
6	4	9	51	51	1
7	4	9	0	11	1
8	4	9	15	9	14
9	4	9	86	85	1
0	5	9	27	28	5
1	5	9	117	117	1
2	5	9	210	212	1
3	5	9	163	164	1
4	5	9	125	132	1
5	5	9	39	45	2
6	5	9	178	172	1
7	5	9	38	31	3
8	5	9	61	61	2
9	5	9	35	38	1
1	6	9	84	88	1
3	6	9	155	153	1
5	6	9	208	208	1
7	6	9	88	94	1
9	6	9	55	58	2
0	7	9	17	16	17
2	7	9	0	1	1
4	7	9	51	46	2
6	7	9	51	45	3
8	7	9	136	135	1
1	8	9	379	388	2
3	8	9	183	191	1
5	8	9	230	231	1
7	8	9	148	149	1
9	8	9	155	157	1
0	9	9	109	103	1
2	9	9	0	9	1
4	9	9	46	53	2
6	9	9	90	91	1
8	9	9	0	21	1
1	10	9	198	200	1
3	10	9	166	165	1
5	10	9	0	9	1
7	10	9	56	50	2
9	10	9	89	92	1
0	11	9	163	172	1
2	11	9	101	106	1
4	11	9	85	83	1
6	11	9	121	116	1
8	11	9	108	107	2
1	12	9	47	46	3
3	12	9	39	45	3
5	12	9	56	53	2
7	12	9	27	24	21
9	12	9	54	60	2
0	13	9	55	53	32
2	13	9	20	9	19
4	13	9	0	25	1
6	13	9	28	28	5
8	13	9	36	35	5
1	14	9	80	76	4
3	14	9	68	69	2
5	14	9	0	30	1
7	14	9	0	10	1
9	14	9	51	52	2
0	15	9	19	10	7
2	15	9	23	32	7
4	15	9	28	28	7
6	15	9	13	11	13
0	0	10	403	408	3
2	0	10	55	53	1
4	0	10	0	10	1
6	0	10	10	16	9
8	0	10	165	172	2
1	1	10	182	195	1
3	1	10	190	193	1
5	1	10	283	281	2
7	1	10	184	178	1
9	1	10	106	111	1
0	2	10	13	18	12
2	2	10	124	134	1
4	2	10	7	35	6
6	2	10	35	37	3
8	2	10	52	57	14
1	3	10	330	340	3
3	3	10	83	71	1
5	3	10	167	169	1
7	3	10	0	8	1
9	3	10	68	61	1
0	4	10	43	43	24
2	4	10	124	128	1
4	4	10	25	20	11
6	4	10	67	71	1
8	4	10	33	46	32
1	5	10	54	63	1
3	5	10	23	28	5
5	5	10	68	54	1
7	5	10	58	63	4
9	5	10	0	22	1
0	6	10	96	94	1
2	6	10	277	276	1
4	6	10	69	68	2
6	6	10	22	22	12
8	6	10	0	9	1
1	7	10	65	72	1
3	7	10	31	29	4
5	7	10	57	57	2
7	7	10	219	212	2
9	7	10	285	285	2
0	8	10	320	323	2
2	8	10	342	339	1
4	8	10	326	319	1
6	8	10	142	145	1
8	8	10	40	38	5
1	9	10	81	82	1
3	9	10	110	107	1
5	9	10	147	143	2
7	9	10	89	84	1
9	9	10	267	275	1
0	10	10	0	4	1
2	10	10	28	27	25
4	10	10	103	107	1
6	10	10	154	158	2
8	10	10	0	3	1
1	11	10	19	23	19
3	11	10	89	91	1
5	11	10	147	157	1
7	11	10	9	22	8
9	11	10	134	146	2
0	12	10	222	234	1
2	12	10	252	254	1
4	12	10	56	59	2
6	12	10	30	35	4
8	12	10	23	44	23
1	13	10	80	81	1
3	13	10	15	2	11
5	13	10	231	235	1
7	13	10	39	36	2
9	13	10	217	219	1
0	14	10	19	5	19
2	14	10	14	1	13
4	14	10	66	69	6
6	14	10	0	3	1
8	14	10	71	67	2
1	15	10	17	2	11
3	15	10	92	88	1
5	15	10	95	92	4
7	15	10	0	6	1
9	15	10	79	80	1
0	16	10	99	97	1
2	16	10	100	99	2
0	10	10	138	140	1
2	10	10	52	51	2
4	10	10	24	22	14
6	10	10	23	25	9
8	10	10	78	78	1
1	11	10	91	91	2
3	11	10	29	41	5
5	11	10	117	124	1
7	11	10	96	101	2
9	11	10	39	36	4
0	12	10	82	76	1
2	12	10	18	17	18
4	12	10	0	1	1
6	12	10	0	0	1
8	12	10	19	7	19
1	13	10	79	79	2
3	13	10	0	9	1
5	13	10	0	32	1
7	13	10	112	113	1
9	13	10	0	10	1
0	14	10	0	12	1
2	14	10	54	50	2
4	14	10	0	11	1
6	14	10	61	63	3
8	14	10	23	10	22
1	15	10	0	11	1
3	15	10	25	28	3
5	15	10	59	69	3
7	15	10	0	18	1
9	15	10	51	49	3
0	16	10	0	10	1
2	16	10	96	96	1
4	16	10	51	52	1
6	16	10	89	81	1
8	16	10	108	108	1
1	17	10	121	126	1
3	17	10	19	6	12
5	17	10	0	10	1
7	17	10	134	150	1
9	17	10	123	123	1
0	18	11	13	10	8
2	18	11	46	38	1
4	18	11	72	70	1
6	18	11	16	29	15
8	18	11	193	198	3
1	19	11	38	35	4
3	19	11	149	150	4
5	19	11	70	63	1
7	19	11	142	140	1
9	19	11	123	122	1
0	20	11	11	5	10
2	20	11	75	73	1
4	20	11	72	70	1
6	20	11	81	82	1
8	20	11	68	49	2
1	21	11	0	15	1
3	21	11	85	80	1
5	21	11	54	37	2
7	21	11	234	246	2
9	21	11	201	209	2
0	22	11	122	126	1
2	22	11	21	16	6
4	22	11	24	12	8
6	22	11	46	42	10
8	22	11	179	183	1
1	23	11	114	110	1
3	23	11	61	64	2
5	23	11	230	240	4
7	23	11	326	326	4
9	23	11	176	175	1
0	24	11	69	68	19
2	24	11	33	25	5
4	24	11	92	92	1
6	24	11	41	41	2
8	24	11	0	13	1
1	25	11	19	39	18
3	25	11	26	31	6
5	25	11	178	180	1
7	25	11	75	73	3
9	25	11	37	48	7
0	26	11	53	50	2
2	26	11	49	46	3
4	26	11	52	51	1
6	26	11	297	301	2
8	26	11	217	219	1
1	27	11	272	279	2

h

h	k	l	10Fo	10Fc	10s
6	7	11	28	24	27
7	7	11	9	15	9
8	7	11	21	22	21
1	8	11	97	99	1
2	8	11	174	180	1
3	8	11	171	159	1
4	8	11	0	5	1
5	8	11	61	46	3
6	8	11	24	14	11
7	8	11	51	55	3
8	8	11	44	42	33
1	9	11	0	14	1
2	9	11	82	78	1
3	9	11	57	57	2
4	9	11	77	74	1
5	9	11	0	14	1
6	9	11	0	8	1
7	9	11	0	10	1
1	10	11	0	7	1
2	10	11	0	6	1
3	10	11	46	59	46
4	10	11	19	3	9
5	10	11	44	45	3
6	10	11	87	88	3
1	11	11	59	55	4
2	11	11	23	29	23
3	11	11	63	62	2
4	11	11	22	21	21
5	11	11	73	74	2
6	11	11	55	46	2
1	12	11	36	36	13
2	12	11	118	114	1
3	12	11	80	81	2
4	12	11	14	7	15
1	13	11	36	40	12
2	13	11	36	35	13
3	13	11	37	37	2
0	0	12	343	331	3
1	0	12	639	640	3
2	0	12	84	89	2
3	0	12	0	7	1
4	0	12	0	5	1
0	1	12	490	491	4
1	1	12	99	103	3
2	1	12	62	55	2
3	1	12	28	31	3
4	1	12	0	3	1
5	1	12	34	31	3
6	1	12	12	2	11
7	1	12	15	9	14
8	1	12	55	55	2
9	1	12	73	73	2
0	2	12	180	98	1
1	2	12	49	46	2
2	2	12	17	24	16
3	2	12	40	43	2
4	2	12	72	72	2
5	2	12	84	77	3
6	2	12	254	249	3
7	2	12	40	46	3
8	2	12	52	61	3
9	2	12	0	10	1
0	3	12	166	161	1
1	3	12	194	198	2
2	3	12	168	163	1
3	3	12	75	78	1
4	3	12	94	97	1
5	3	12	137	132	1
6	3	12	190	194	1
7	3	12	0	23	1
8	3	12	91	89	2
9	3	12	105	105	3
0	4	12	219	224	2
1	4	12	20	30	14
2	4	12	80	85	10
3	4	12	193	187	1
4	4	12	96	99	1
5	4	12	57	56	2
6	4	12	26	28	6
7	4	12	0	4	1
8	4	12	0	12	1
9	4	12	14	3	13
0	5	12	440	436	3
1	5	12	92	91	1
2	5	12	145	139	1
3	5	12	28	16	13
4	5	12	34	32	15
5	5	12	92	94	2
6	5	12	137	137	1
7	5	12	78	77	1
8	5	12	0	6	1
9	5	12	33	31	7
0	6	12	42	46	3
1	6	12	65	71	1
2	6	12	0	3	1
3	6	12	31	35	1
4	6	12	238	236	3
5	6	12	123	139	1
6	6	12	50	48	2
7	6	12	73	74	3
8	6	12	0	17	1
0	7	12	0	5	1
1	7	12	51	51	2
2	7	12	255	267	1
3	7	12	173	179	1
4	7	12	354	360	2
5	7	12	132	133	2
6	7	12	92	97	1
7	7	12	39	48	12
8	7	12	0	5	1
0	8	12	0	2	1
1	8	12	100	98	1
2	8	12	56	57	2
3	8	12	271	273	1
4	8	12	32	31	11
5	8	12	25	21	6
6	8	12	31	31	2
7	8	12	0	4	1
8	8	12	85	94	2
0	9	12	43	46	1
1	9	12	0	26	1
2	9	12	174	177	1
3	9	12	0	3	1
4	9	12	77	78	1
5	9	12	60	59	2
6	9	12	61	61	2
7	9	12	0	1	1
0	10	12	16	23	12
1	10	12	12	18	12
2	10	12	72	78	1
3	10	12	72	79	1
4	10	12	63	57	6
5	10	12	122	118	1
6	10	12	20	31	9
0	11	12	59	58	2
1	11	12	28	26	20
2	11	12	75	72	1
3	11	12	111	110	1
4	11	12	60	63	13
5	11	12	0	2	1
6	11	12	0	28	1
7	11	12	69	61	2
8	11	12	85	82	1
9	11	12	123	112	2
0	12	12	144	131	1
1	12	12	0	3	1
2	12	12	0	14	1
0	13	12	460	466	2
1	13	12	93	94	14
2	13	12	86	83	3
3	13	12	18	5	18
4	13	12	231	231	1
0	1	13	41	41	13
1	1	13	31	22	5
2	1	13	60	57	1
3	1	13	0	3	1
4	1	13	43	46	2
5	1	13	27	28	6
6	1	13	10	20	10
7	1	13	10	16	10
8	1	13	51	51	1
0	2	13	128	123	1
1	2	13	178	181	1
2	2	13	162	164	1
3	2	13	93	90	2
4	2	13	0	2	1
5	2	13	69	74	2
6	2	13	9	0	8
7	2	13	27	41	10
8	2	13	20	28	20
0	3	13	103	104	1
1	3	13	265	260	5
2	3	13	191	195	1
3	3	13	229	217	1
4	3	13	158	141	1
5	3	13	15	32	15
6	3	13	8	12	7
7	3	13	45	50	9
8	3	13	0	2	1
1	4	13	29	36	10
2	4	13	62	67	2
3	4	13	62	64	1
4	4	13	67	66	1
5	4	13	72	71	1
6	4	13	60	61	2
7	4	13	49	41	20
8	4	13	135	122	1
1	5	13	97	102	1
2	5	13	150	157	1
3	5	13	143	138	1
4	5	13	0	2	1
5	5	13	11	14	10
6	5	13	27	39	27
7	5	13	19	28	17
8	5	13	46	50	9
1	6	13	115	107	1
2	6	13	60	56	1
3	6	13	101	101	1
4	6	13	88	85	2
5	6	13	29	27	8
6	6	13	56	63	3
7	6	13	16	20	15
8	6	13	137	132	1
1	7	13	45	46	9
2	7	13	0	3	1
3	7	13	121	119	1
4	7	13	28	29	6
5	7	13	73	77	4
6	7	13	83	85	2
7	8	13	91	91	1
8	8	13	0	26	1
1	9	13	88	82	1
2	9	13	149	156	1
3	9	13	11	13	10
4	9	13	24	27	8
5	9	13	0	1	1
6	9	13	191	201	1
7	10	13	0	6	1
8	10	13	40	39	16
1	11	13	96	99	2
2	11	13	136	143	1
3	11	13	104	102	1
4	11	13	29	31	7
5	11	13	35	5	14
6	11	13	0	3	1
7	11	13	59	52	5
8	11	13	0	9	1
1	12	13	83	59	2
2	12	13	74	72	1
3	12	13	31	26	4
4	12	13	67	62	1
5	12	13	197	159	1
6	12	13	34	35	15
7	13	13	21	25	9
8	13	13	111	109	1
1	13	13	97	110	1
2	1	14	0	6	8
3	1	14	15	19	8
4	1	14	0	9	1
5	1	14	128	127	1
6	1	14	40	40	11
7	1	14	0	1	1
8	1	14	61	58	6
1	2	14	221	223	2
2	2	14	0	3	1
3	2	14	28	34	4
4	2	14	0	3	1
5	2	14	22	11	6
6	2	14	0	17	1
7	3	14	103	103	1
8	3	14	37	35	2
1	3	14	134	135	1
2	3	14	288	288	1
3	3	14	158	158	1
4	3	14	72	74	1
5	3	14	24	20	8
6	3	14	66	67	2
7	3	14	113	115	1
1	4	14	59	64	1
2	4	14	0	3	1
3	4	14	66	65	2
4	4	14	73	70	1
5	4	14	54	56	2
6	4	14	55	57	3
7	4	14	65	58	5
8	4	14	12	7	11
0	5	14	80	85	1
1	5	14	61	61	3
2	5	14	221	210	7
3	5	14	128	131	1
4	5	14	199	204	1
5	5	14	284	281	2
6	5	14	185	191	2
7	5	14	18	19	17
8	5	14	21	32	20
0	6	14	12	9	12
1	6	14	22	2	21
2	6	14	173	163	2
3	6	14	139	140	1
4	6	14	99	101	1
5	6	14	14	19	13
6	6	14	0	29	1
7	6	14	0	13	1
0	7	14	198	192	1
1	7	14	0	7	1
2	7	14	85	85	1
3	7	16	7	27	0
4	7	16	32	24	3
5	7	16	0	28	1
6	7	16	72	72	1
7	7	16	0	18	1
0	8	16	65	64	2
1	8	16	28	18	19
2	8	16	50	55	2
3	8	16	27	28	2
4	8	16	80	81	3
5	8	16	12	17	12
6	8	16	17	12	17
7	9	16	24	20	23
0	9	16	0	5	1
1	9	16	53	48	4
2	9	16	39	45	4
3	9	16	58	55	4
4	9	16	32	28	4
5	9	16	42	42	5
6	10	16	29	30	5
7	10	16	12	20	12
0	10	16	0	22	1
1	10	16	69	53	1
2	10	16	0	27	1
3	10	16	68	65	6
4	11	16	38	38	6
5	11	16	99	97	1
6	11	16	34	14	15
7	11	16	49	48	2
0	12	16	0	8	1
1	12	16	24	15	24
2	12	16	19	12	9
3	0	15	74	78	1
4	0	15	55	47	2
5	0	15	33	28	5
6	0	15	78	72	1
7	1	15	73	74	1
8	1	15	0	0	1
1	1	15	123	124	1
2	1	15	0	5	1
3	1	15	0	15	1
4	1	15	32	32	5
5	1	15	20	17	7
6	1	15	30	21	30
7	2	15	248	246	1
8	2	15	181	180	1
1	2	15	236	234	2
2	2	15	230	233	1
3	2	15	0	9	1
4	2	15	21	14	6
5	2	15	17	8	17
6	3	15	0	1	1
7	3	15	54	53	15
8	3	15	111	112	1
1	3	15	61	44	2
2	3	15	42	48	8
3	3	15	50	48	2
4	3	15	55	58	2
5	3	15	25	28	25
6	3	15	11	18	11
1	4	15	0	7	1
2	4	15	68	65	1
3	4	15	158	158	1
4	4	15	214	216	1
5	4	15	214	201	1
6	4	15	175	189	1
7	4	15	62	66	2
8	4	15	73	79	2
1	5	15	24	6	6
2	5	15	108	104	2
3	5	15	132	130	1
4	5	15	108	109	1
5	5	15	116	116	1
6	5	15	55	68	4
7	6	15	0	18	1
8	6	15	0	10	1
1	6	15	121	121	1
2	6	15	83	83	3
3	6	15	21	26	10
4	6	15	0	15	1
5	6	15	49	46	17
6	7	15	187	202	2
7	7	15	0	4	1
8	7	15	28	35	14
1	7	15	1	2	1
2	7	15	0	27	1
3	7	15	0	4	1
4	8	15	0	29	1
5	8	15	12	17	11
6	8	15	37	35	13
7	9	15	0	8	1
8	9	15	76	80	1
1	9	15	63	58	4
2	9	15	45	48	3
3	10	15	112	109	2
4	10	15	0	50	12
5	11	15	46	15	1
6	11	15	0	9	1
7	12	15	0	6	1
8	12	15	82	46	21

Table 6. Observed and calculated structure factors for 1

h	k	l	10Fo	10Fc	10s
4	5	16	56	55	2
5	5	16	182	181	2
6	5	16	0	7	1
7	5	16	17	0	17
0	6	16	59	52	2
1	6	16	31	34	7
2	6	16	0	12	1
3	6	16	45	51	2
4	6	16	0	3	1
5	6	16	32	42	11
6	6	16	63	62	2
7	6	16	0	17	1
0	7	16	190	206	1
1	7	16	14	10	13
2	7	16	102	104	1
3	7	16	71	69	1
4	7	16	63	62	2
5	7	16	15	23	15
6	7	16	17	17	13
0	8	16	24	10	24
1	8	16	41	43	2
2	8	16	77	82	2
3	8	16	29	33	9
4	8	16	43	42	4
5	8	16	0	35	1
0	9	16	42	39	4
1	9	16	8	26	8
2	9	16	19	30	7
3	9	16	19	43	18
4	9	16	0	10	1
5	9	16	56	49	2
0	10	16	36	34	5
1	10	16	0	22	1
2	10	16	75	70	2
3	10	16	19	23	15
4	10	16	60	59	2
0	11	16	108	106	2
1	11	16	62	57	2
2	11	16	51	50	5
2	0	17	459	455	2
4	0	17	168	165	1
6	0	17	85	84	2
1	1	17	105	108	1
2	1	17	55	56	2
3	1	17	189	186	1
4	1	17	60	58	5
5	1	17	65	59	1
6	1	17	38	38	3
7	1	17	20	30	20
1	2	17	25	29	11
2	2	17	58	42	29
3	2	17	54	54	2
6	2	17	0	5	1
5	2	17	17	14	16
6	2	17	78	75	1
7	2	17	12	22	12
1	3	17	17	15	12
2	3	17	87	90	1
3	3	17	75	74	5
4	3	17	102	95	1
5	3	17	57	48	2
6	3	17	125	117	1
7	3	17	64	58	2
1	4	17	0	9	1
2	4	17	53	46	2
3	4	17	106	111	1
4	4	17	90	86	2
5	4	17	116	117	1
6	4	17	0	4	1
7	4	17	0	4	1
1	5	17	0	3	1
2	5	17	0	19	1
3	5	17	0	3	1
4	5	17	21	12	9
5	5	17	54	53	2
6	5	17	17	7	17
1	6	17	30	31	29
2	6	17	40	37	2
3	6	17	54	53	2
4	6	17	0	18	1
5	6	17	38	34	11
6	6	17	42	48	3
1	7	17	50	55	2
2	7	17	0	19	1
3	7	17	62	64	2
4	7	17	81	81	1
5	7	17	57	53	3
1	8	17	0	0	1
2	8	17	0	20	1
3	8	17	9	0	8
4	8	17	40	31	5
5	8	17	0	17	1
1	9	17	102	106	1
2	9	17	55	56	2
3	9	17	0	28	1
4	9	17	71	64	2
1	10	17	0	47	1
2	10	17	45	48	19
3	10	17	27	28	27
0	0	18	266	271	2
2	0	18	344	340	2
4	0	18	92	92	1
6	0	18	0	8	1
0	1	18	189	184	1
1	1	18	57	60	2
2	1	18	83	80	1
3	1	18	45	50	4
4	1	18	96	102	2
5	1	18	61	60	2
6	1	18	17	23	16
7	1	18	3	1	2
0	2	18	35	37	4
1	2	18	51	53	2
2	2	18	112	109	1
3	2	18	37	39	24
4	2	18	63	65	1
5	2	18	104	98	3
6	2	18	147	146	1
7	2	18	153	139	1
0	3	18	57	61	2
1	3	18	18	28	11
2	3	18	110	109	1
3	3	18	42	40	3
4	3	18	72	73	3
5	3	18	135	138	1
6	3	18	67	74	2
0	4	18	74	74	2
1	4	18	38	39	16
2	4	18	0	31	1
3	4	18	77	76	1
4	4	18	91	86	3
5	4	18	26	5	7
6	4	18	0	3	1
0	5	18	56	70	3
1	5	18	26	22	25
2	5	18	69	66	1
3	5	18	92	89	1
4	5	18	0	15	1
5	5	18	0	6	1
6	5	18	0	15	1
0	6	18	57	57	2
1	6	18	23	27	5
2	6	18	25	19	24
3	6	18	13	9	13
4	6	18	87	89	3
5	6	18	66	61	3
0	7	18	25	22	7
1	7	18	0	12	1
2	7	18	11	12	11
3	7	18	8	0	8
4	7	18	22	8	9
5	7	18	58	51	5
0	8	18	96	97	2
1	8	18	0	18	1
2	8	18	0	13	1
3	8	18	70	59	2
4	8	18	0	17	1
0	9	18	50	44	3
1	9	18	28	21	21
2	9	18	78	74	1
3	9	18	0	11	1
0	10	18	0	22	1
1	10	18	0	34	1
2	0	19	0	37	1
4	0	19	0	42	1
6	0	19	0	3	1
1	1	19	76	78	1
2	1	19	0	30	1
3	1	19	78	74	2
4	1	19	9	20	8
5	1	19	27	34	5
6	1	19	38	32	18
1	2	19	162	155	1
2	2	19	116	112	2
3	2	19	67	62	1
4	2	19	19	16	12
5	2	19	76	69	1
6	2	19	104	101	1
1	3	19	58	56	2
2	3	19	4	28	3
3	3	19	22	12	22
4	3	19	29	34	29
5	3	19	0	21	1
6	3	19	65	64	3
1	4	19	37	34	4
2	4	19	92	95	1
3	4	19	21	9	9
4	4	19	128	122	2
5	4	19	15	14	14
6	4	19	0	18	1
1	5	19	102	103	1
2	5	19	0	43	1
3	5	19	39	48	9
4	5	19	0	2	1
5	5	19	63	60	3
1	6	19	36	39	4
2	6	19	4	28	3
3	6	19	7	34	7
4	6	19	0	27	1
5	6	19	0	21	1
1	7	19	0	11	1
2	7	19	13	10	12
3	7	19	56	48	2
4	7	19	0	1	1
1	8	19	19	24	8
2	8	19	0	30	1
3	8	19	11	9	10
1	9	19	47	44	2
0	0	20	148	138	1
2	0	20	0	28	1
4	0	20	60	53	2
0	1	20	74	69	2
1	1	20	105	107	1
2	1	20	0	20	1
3	1	20	88	88	3
4	1	20	58	57	2
5	1	20	0	11	1
0	2	20	123	119	1
1	2	20	91	86	1
2	2	20	127	121	1
3	2	20	111	105	3
4	2	20	62	59	2
5	2	20	52	39	2
0	3	20	146	138	1
1	3	20	0	1	1
2	3	20	109	107	2
3	3	20	0	1	1
4	3	20	49	44	2
5	3	20	0	5	1
0	4	20	0	15	1
1	4	20	28	21	6
2	4	20	25	23	25
3	4	20	0	15	1
4	4	20	66	68	2
5	4	20	28	15	28
0	5	20	110	113	1
1	5	20	13	13	12
2	5	20	0	38	1
3	5	20	0	35	1
4	5	20	0	1	1
0	6	20	42	36	4
1	6	20	15	31	14
2	6	20	0	5	1
3	6	20	34	32	2
4	6	20	0	6	1
0	7	20	21	53	20
1	7	20	23	13	8
2	7	20	27	31	7
3	7	20	57	55	2
0	8	20	0	1	1
1	8	20	0	7	1

Appendix 2

Crystal structure data for 3-(2,5-dimethoxyphenyl)-5-pyridinyl-1H-1,2,4-. triazole (HL1).

100 Table 1 Crystal data and structure refinement for 1

Identification code	donal3
Empirical formula	$C_{15}H_{14}N_4O_2$
Formula weight	282 30
Temperature	293(2) K
Wavelength	1 54178 Å
Crystal System	Monoclinic
Space group	$P2_1/n$
Unit cell dimensions	a = 10 664(2) Å alpha = 90° b = 17 689(7) Å beta = 96 96° c = 15 057(3) Å gamma = 90°
Volume, Z	2819 4(14) $Å^3$, 8
Density (calculated)	1 330 Mg/m^3
Absorption coefficient	0 754 mm^{-1}
F(000)	1184
Crystal size	0 85 x 0 19 x 0 12 mm
θ range for data collection	3 87 to 55 03°
Limiting indices	$0 \le h \le 11$, $0 \le k \le 18$, $-15 \le l \le 15$
Reflections collected	3763
Independent reflections	3540 (R_{int} = 0 0549)
Refinement method	Full-matrix least-squares on F^2
Data / restraints / parameters	3540 / 0 / 384
Goodness-of-fit on F^2	1 010
Final R indices [I>2σ(I)]	R1 = 0 0650, wR2 = 0.1599
R indices (all data)	R1 = 0 1103, wR2 = 0 1952
Extinction coefficient	0 0041(4)
Largest diff peak and hole	0 262 and −0 227 $eÅ^{-3}$

Table 2. Atomic coordinates [x 10^4] and equivalent isotropic displacement parameters [$Å^2$ x 10^3] for 1. U(eq) is defined as one third of the trace of the orthogonalized U_{ij} tensor.

	x	y	z	U(eq)
N(1A)	-844(4)	1011(2)	5775(3)	46(1)
C(2A)	-1465(5)	1170(3)	4969(3)	59(2)
C(3A)	-2085(5)	639(3)	4409(4)	61(2)
C(4A)	-2051(4)	-99(3)	4677(3)	50(1)
C(5A)	-1423(4)	-285(3)	5503(3)	44(1)
C(6A)	-826(4)	283(3)	6033(3)	38(1)
C(7A)	-103(4)	120(3)	6908(3)	37(1)
N(8A)	-191(4)	-526(2)	7330(3)	46(1)
N(9A)	666(4)	-438(2)	8068(3)	46(1)
N(10A)	751(3)	616(2)	7317(2)	39(1)
C(11A)	1233(4)	240(2)	8048(3)	39(1)
C(12A)	2268(4)	525(3)	8695(3)	43(1)
C(13A)	3031(5)	1094(3)	8394(3)	52(1)
C(14A)	4053(5)	1379(3)	8950(4)	60(2)
C(15A)	4330(6)	1078(4)	9796(4)	69(2)
C(16A)	3585(5)	528(3)	10111(3)	63(2)
C(17A)	2549(5)	247(3)	9563(3)	48(1)
O(18A)	4835(4)	1938(3)	8720(3)	99(2)
C(19A)	4406(7)	2393(4)	8021(5)	105(2)
O(20A)	1727(4)	-279(2)	9826(2)	66(1)
C(21A)	1943(7)	-569(4)	10720(4)	89(2)
N(1B)	314(4)	-1768(2)	9167(3)	51(1)
C(2B)	-781(5)	-1718(3)	9502(4)	64(2)
C(3B)	-1135(5)	-2191(3)	10144(4)	68(2)
C(4B)	-326(5)	-2755(3)	10465(4)	65(2)
C(5B)	811(5)	-2818(3)	10129(3)	52(1)
C(6B)	1102(4)	-2320(2)	9483(3)	39(1)
C(7B)	2304(4)	-2365(2)	9098(3)	37(1)
N(8B)	3009(4)	-2980(2)	9172(3)	52(1)
N(9B)	3999(4)	-2780(2)	8736(3)	47(1)
N(10B)	2772(3)	-1792(2)	8640(2)	37(1)
C(11B)	3854(4)	-2073(2)	8417(3)	37(1)
C(12B)	4732(4)	-1633(2)	7950(3)	37(1)
C(13B)	4368(4)	-915(3)	7658(3)	42(1)
C(14B)	5152(5)	-459(3)	7225(3)	44(1)
C(15B)	6341(5)	-713(3)	7103(3)	56(1)
C(16B)	6720(5)	-1427(3)	7394(4)	58(2)
C(17B)	5915(5)	-1897(3)	7787(3)	50(1)
O(18B)	4653(4)	225(2)	6936(3)	69(1)
C(19B)	5336(7)	670(4)	6412(5)	107(3)
O(20B)	6216(4)	-2613(2)	8068(3)	82(1)
C(21B)	7211(7)	-2986(4)	7715(5)	104(3)

Table 3 Bond lengths [Å] and angles [°] for 1

N(1A)-C(2A)	1 341(6)	N(1A)-C(6A)	1.344(5)
C(2A)-C(3A)	1.377(7)	C(3A)-C(4A)	1.366(7)
C(4A)-C(5A)	1.378(6)	C(5A)-C(6A)	1 390(6)
C(6A)-C(7A)	1 472(6)	C(7A)-N(8A)	1 316(5)
C(7A)-N(10A)	1 359(5)	N(8A)-N(9A)	1 359(5)
N(9A)-C(11A)	1 345(5)	N(10A)-C(11A)	1 334(5)
C(11A)-C(12A)	1 470(6)	C(12A)-C(17A)	1.395(6)
C(12A)-C(13A)	1.404(6)	C(13A)-C(14A)	1.386(7)
C(14A)-O(18A)	1.366(6)	C(14A)-C(15A)	1 379(7)
C(15A)-C(16A)	1 376(7)	C(16A)-C(17A)	1.388(7)
C(17A)-O(20A)	1 369(6)	O(18A)-C(19A)	1 360(7)
O(20A)-C(21A)	1 433(6)	N(1B)-C(2B)	1 330(6)
N(1B)-C(6B)	1.336(6)	C(2B)-C(3B)	1 366(7)
C(3B)-C(4B)	1.368(7)	C(4B)-C(5B)	1.373(7)
C(5B)-C(6B)	1 377(6)	C(6B)-C(7B)	1 471(6)
C(7B)-N(8B)	1.320(5)	C(7B)-N(10B)	1 356(5)
N(8B)-N(9B)	1 355(5)	N(9B)-C(11B)	1 343(5)
N(10B)-C(11B)	1 335(5)	C(11B)-C(12B)	1.462(6)
C(12B)-C(13B)	1 383(6)	C(12B)-C(17B)	1 394(6)
C(13B)-C(14B)	1.381(6)	C(14B)-O(18B)	1 371(6)
C(14B)-C(15B)	1 379(7)	C(15B)-C(16B)	1 380(7)
C(16B)-C(17B)	1 380(7)	C(17B)-O(20B)	1 361(6)
O(18B)-C(19B)	1 383(6)	O(20B)-C(21B)	1 408(6)

C(2A)-N(1A)-C(6A)	116 8(4)	N(1A)-C(2A)-C(3A)	123.9(5)
C(4A)-C(3A)-C(2A)	118 6(5)	C(3A)-C(4A)-C(5A)	119.1(5)
C(4A)-C(5A)-C(6A)	119.0(5)	N(1A)-C(6A)-C(5A)	122 5(4)
N(1A)-C(6A)-C(7A)	115 8(4)	C(5A)-C(6A)-C(7A)	121 7(4)
N(8A)-C(7A)-N(10A)	115 2(4)	N(8A)-C(7A)-C(6A)	122 9(4)
N(10A)-C(7A)-C(6A)	121 8(4)	C(7A)-N(8A)-N(9A)	102 4(4)
C(11A)-N(9A)-N(8A)	110 1(4)	C(11A)-N(10A)-C(7A)	102 8(4)
N(10A)-C(11A)-N(9A)	109 5(4)	N(10A)-C(11A)-C(12A)	124 0(4)
N(9A)-C(11A)-C(12A)	126 4(4)	C(17A)-C(12A)-C(13A)	119.2(4)
C(17A)-C(12A)-C(11A)	124.0(5)	C(13A)-C(12A)-C(11A)	116 7(4)
C(14A)-C(13A)-C(12A)	120.6(5)	O(18A)-C(14A)-C(15A)	116 4(5)
O(18A)-C(14A)-C(13A)	124 7(5)	C(15A)-C(14A)-C(13A)	118 9(6)
C(16A)-C(15A)-C(14A)	121.5(5)	C(15A)-C(16A)-C(17A)	120 0(5)
O(20A)-C(17A)-C(16A)	124 2(5)	O(20A)-C(17A)-C(12A)	116.0(4)
C(16A)-C(17A)-C(12A)	119 7(5)	C(19A)-O(18A)-C(14A)	117 8(5)
C(17A)-O(20A)-C(21A)	118 6(4)	C(2B)-N(1B)-C(6B)	117 2(4)
N(1B)-C(2B)-C(3B)	123.9(5)	C(2B)-C(3B)-C(4B)	118.7(5)
C(3B)-C(4B)-C(5B)	118 5(5)	C(4B)-C(5B)-C(6B)	119 5(5)
N(1B)-C(6B)-C(5B)	122 2(4)	N(1B)-C(6B)-C(7B)	116.1(4)
C(5B)-C(6B)-C(7B)	121 7(4)	N(8B)-C(7B)-N(10B)	114.7(4)
N(8B)-C(7B)-C(6B)	121 8(4)	N(10B)-C(7B)-C(6B)	123.5(4)
C(7B)-N(8B)-N(9B)	102 3(4)	C(11B)-N(9B)-N(8B)	110.7(4)
C(11B)-N(10B)-C(7B)	103 4(4)	N(10B)-C(11B)-N(9B)	108.8(4)
N(10B)-C(11B)-C(12B)	123 1(4)	N(9B)-C(11B)-C(12B)	128 0(4)
C(13B)-C(12B)-C(17B)	118 5(4)	C(13B)-C(12B)-C(11B)	118 0(4)
C(17B)-C(12B)-C(11B)	123 5(4)	C(12B)-C(13B)-C(14B)	121.5(4)
O(18B)-C(14B)-C(15B)	125.0(4)	O(18B)-C(14B)-C(13B)	115.6(4)
C(15B)-C(14B)-C(13B)	119 4(5)	C(16B)-C(15B)-C(14B)	119.7(5)
C(15B)-C(16B)-C(17B)	121.0(5)	O(20B)-C(17B)-C(16B)	124.0(4)
O(20B)-C(17B)-C(12B)	116 2(4)	C(16B)-C(17B)-C(12B)	119 7(5)
C(14B)-O(18B)-C(19B)	118.2(5)	C(17B)-O(20B)-C(21B)	118 7(4)

Symmetry transformations used to generate equivalent atoms

Table 4. Anisotropic displacement parameters [$Å^2$ x 10^3] for 1
The anisotropic displacement factor exponent takes the form:
$-2\pi^2$ [$(ha^*)^2U_{11}$ + ... + $2hka^*b^*U_{12}$]

	U11	U22	U33	U23	U13	U12
N(1A)	44(2)	42(2)	47(3)	0(2)	-13(2)	0(2)
C(2A)	63(4)	56(3)	54(3)	2(3)	-10(3)	9(3)
C(3A)	51(3)	72(4)	53(3)	-5(3)	-20(3)	7(3)
C(4A)	37(3)	60(4)	51(3)	-14(3)	-5(2)	-9(3)
C(5A)	37(3)	45(3)	49(3)	-9(2)	4(2)	-10(2)
C(6A)	29(2)	40(3)	43(3)	-5(2)	3(2)	-2(2)
C(7A)	33(3)	40(3)	39(3)	-1(2)	7(2)	-6(2)
N(8A)	41(2)	45(2)	51(3)	2(2)	-6(2)	-7(2)
N(9A)	43(2)	44(3)	49(3)	9(2)	-2(2)	-2(2)
N(10A)	38(2)	37(2)	40(2)	1(2)	-3(2)	-6(2)
C(11A)	37(3)	38(3)	41(3)	0(2)	1(2)	5(2)
C(12A)	40(3)	47(3)	39(3)	-1(2)	-5(2)	10(2)
C(13A)	50(3)	53(3)	50(3)	-2(3)	-7(3)	0(3)
C(14A)	46(3)	69(4)	60(4)	-4(3)	-9(3)	-5(3)
C(15A)	60(4)	88(5)	54(4)	-7(3)	-13(3)	0(3)
C(16A)	71(4)	76(4)	37(3)	0(3)	-12(3)	16(3)
C(17A)	52(3)	50(3)	39(3)	1(3)	-1(3)	10(3)
O(18A)	70(3)	116(4)	101(3)	29(3)	-30(3)	-37(3)
C(19A)	107(6)	109(6)	98(6)	14(5)	8(5)	-29(5)
O(20A)	84(3)	68(2)	45(2)	9(2)	2(2)	-4(2)
C(21A)	131(6)	87(5)	48(4)	13(3)	5(4)	1(5)
N(1B)	40(2)	49(3)	66(3)	11(2)	19(2)	6(2)
C(2B)	46(3)	65(4)	86(4)	14(3)	24(3)	12(3)
C(3B)	46(3)	78(4)	87(4)	3(4)	32(3)	1(3)
C(4B)	61(4)	73(4)	66(4)	14(3)	29(3)	-13(3)
C(5B)	57(3)	50(3)	49(3)	13(3)	11(3)	-4(3)
C(6B)	42(3)	34(3)	39(3)	-1(2)	3(2)	-6(2)
C(7B)	31(3)	39(3)	41(3)	4(2)	2(2)	1(2)
N(8B)	43(2)	43(2)	71(3)	9(2)	16(2)	6(2)
N(9B)	37(2)	45(3)	61(3)	7(2)	13(2)	9(2)
N(10B)	31(2)	41(2)	39(2)	6(2)	3(2)	0(2)
C(11B)	38(3)	37(3)	35(3)	2(2)	2(2)	2(2)
C(12B)	30(3)	45(3)	36(3)	0(2)	3(2)	6(2)
C(13B)	36(3)	49(3)	41(3)	0(2)	7(2)	2(2)
C(14B)	44(3)	44(3)	42(3)	2(2)	2(2)	-3(2)
C(15B)	46(3)	67(4)	55(3)	8(3)	8(3)	-11(3)
C(16B)	34(3)	75(4)	68(4)	10(3)	13(3)	6(3)
C(17B)	38(3)	51(3)	60(3)	8(3)	5(2)	9(3)
O(18B)	76(3)	55(2)	80(3)	22(2)	24(2)	8(2)
C(19B)	89(5)	83(5)	152(7)	61(5)	23(5)	-13(4)
O(20B)	57(2)	76(3)	121(4)	37(3)	45(2)	35(2)
C(21B)	94(5)	84(5)	146(7)	33(5)	62(5)	53(4)

Table 5 Hydrogen coordinates (x 10^4) and isotropic displacement parameters ($Å^2$ x 10^3) for 1.

	x	y	z	U(eq)
H(2A)	-1479(5)	1670(3)	4775(3)	71
H(3A)	-2518(5)	779(3)	3860(4)	74
H(4A)	-2445(4)	-472(3)	4307(3)	60
H(5A)	-1400(4)	-783(3)	5702(3)	53
H(9A)	984(4)	-888(2)	8607(3)	55
H(13A)	2848(5)	1282(3)	7816(3)	62
H(15A)	5037(6)	1250(4)	10162(4)	83
H(16A)	3775(5)	345(3)	10691(3)	76
H(19A)	4957(29)	2821(16)	8008(22)	158
H(19B)	3569(21)	2564(24)	8089(19)	158
H(19C)	4390(48)	2115(10)	7472(6)	158
H(21A)	2736(21)	-832(22)	10803(10)	134
H(21B)	1275(24)	-911(20)	10819(10)	134
H(21C)	1962(43)	-158(4)	11138(4)	134
H(2B)	-1339(5)	-1338(3)	9286(4)	77
H(3B)	-1910(5)	-2131(3)	10359(4)	82
H(4B)	-541(5)	-3088(3)	10899(4)	78
H(5B)	1380(5)	-3195(3)	10337(3)	62
H(9B)	4705(4)	-3206(2)	8608(3)	56
H(13B)	3576(4)	-736(3)	7756(3)	50
H(15B)	6885(5)	-406(3)	6827(3)	67
H(16B)	7529(5)	-1593(3)	7324(4)	70
H(19D)	4870(23)	1123(14)	6245(30)	161
H(19E)	5480(42)	397(12)	5884(17)	161
H(19F)	6132(22)	801(25)	6745(13)	161
H(21D)	8003(7)	-2775(21)	7970(26)	156
H(21E)	7119(28)	-2923(26)	7077(6)	156
H(21F)	7189(31)	-3515(6)	7857(32)	156

Appendix 3

Table 1. Crystal data and structure refinement for HL2

Table 1. Crystal data and structure refinement for 1

Identification code	donall
Empirical formula	$C_{14}H_{13}N_5O_2$
Formula weight	283.29
Temperature	293(2) K
Wavelength	1 54178 Å
Crystal System	Monoclinic
Space group	$P2_1$
Unit cell dimensions	a = 3 913(3) Å alpha = 90° b = 14 94(2) Å beta = 94 57° c = 11.215(11) Å gamma = 90°
Volume, Z	653 4(11) $Å^3$, 2
Density (calculated)	1 440 Mg/m^3
Absorption coefficient	0 839 mm^{-1}
F(000)	296
Crystal size	0 67 x 0 21 x 0 13 mm
θ range for data collection	3 95 to 49 95°
Limiting indices	$0 \le h \le 3$, $-14 \le k \le 14$, $-11 \le l \le 11$
Reflections collected	1580
Independent reflections	1335 (R_{int} = 0 0515)
Refinement method	Full-matrix least-squares on F^2
Data / restraints / parameters	1335 / 1 / 190
Goodness-of-fit on F^2	1 054
Final R indices [I>2σ(I)]	R1 = 0.0606, wR2 = 0 1467
R indices (all data)	R1 = 0 0724, wR2 = 0 1571
Absolute structure parameter	0 5(7)
Largest diff. peak and hole	0 204 and −0 327 $eÅ^{-3}$

Table 2 Atomic coordinates [x 10^4] and equivalent isotropic displacement parameters [$Å^2$ x 10^3] for 1 U(eq) is defined as one third of the trace of the orthogonalized U_{ij} tensor.

	x	y	z	U(eq)
N(1)	2880(15)	6938(4)	603(5)	43(2)
C(2)	3630(20)	7806(5)	624(7)	51(2)
C(3)	5593(20)	8195(5)	1548(7)	51(2)
N(4)	6944(16)	7735(4)	2487(5)	52(2)
C(5)	6212(19)	6855(5)	2473(6)	45(2)
C(6)	4246(19)	6460(5)	1540(6)	39(2)
C(7)	3540(16)	5502(4)	1550(5)	33(2)
N(8)	1658(16)	5028(4)	781(5)	48(2)
N(9)	1930(15)	4142(4)	1216(5)	45(2)
C(10)	3935(16)	4167(4)	2187(5)	35(2)
N(11)	5022(11)	5002(3)	2453(3)	16(1)
C(12)	4958(16)	3403(4)	2932(6)	35(2)
C(13)	6847(16)	3475(4)	4052(6)	37(2)
C(14)	7579(18)	2710(5)	4726(6)	42(2)
C(15)	6540(17)	1887(5)	4305(6)	40(2)
C(16)	4757(16)	1806(4)	3184(5)	35(2)
C(17)	3950(16)	2551(4)	2505(6)	36(2)
O(18)	7821(12)	4323(3)	4429(4)	50(1)
C(19)	9661(19)	4396(5)	5582(6)	55(2)
O(20)	3928(12)	940(3)	2842(4)	48(1)
C(21)	2082(21)	802(5)	1696(6)	51(2)

Table 3 Bond lengths [Å] and angles [°] for 1

N(1)-C(2)	1 329(9)	N(1)-C(6)	1 345(8)
C(2)-C(3)	1.369(10)	C(3)-N(4)	1 331(9)
N(4)-C(5)	1.345(9)	C(5)-C(6)	1 381(9)
C(6)-C(7)	1 458(9)	C(7)-N(8)	1 299(8)
C(7)-N(11)	1 351(8)	N(8)-N(9)	1 411(8)
N(9)-C(10)	1 291(8)	C(10)-N(11)	1 344(8)
C(10)-C(12)	1 452(9)	C(12)-C(17)	1 406(8)
C(12)-C(13)	1.410(9)	C(13)-O(18)	1 380(8)
C(13)-C(14)	1 387(9)	C(14)-C(15)	1.367(9)
C(15)-C(16)	1 394(8)	C(16)-C(17)	1 370(9)
C(16)-O(20)	1 381(8)	O(18)-C(19)	1 433(8)
O(20)-C(21)	1 438(8)		

C(2)-N(1)-C(6)	115 5(6)	N(1)-C(2)-C(3)	122 5(7)
N(4)-C(3)-C(2)	123.0(6)	C(3)-N(4)-C(5)	115.1(6)
N(4)-C(5)-C(6)	122 1(7)	N(1)-C(6)-C(5)	121.9(6)
N(1)-C(6)-C(7)	117 6(6)	C(5)-C(6)-C(7)	120 5(6)
N(8)-C(7)-N(11)	112 5(5)	N(8)-C(7)-C(6)	128 9(6)
N(11)-C(7)-C(6)	118 5(6)	C(7)-N(8)-N(9)	105 0(5)
C(10)-N(9)-N(8)	106 8(5)	N(9)-C(10)-N(11)	112.0(5)
N(9)-C(10)-C(12)	125.8(6)	N(11)-C(10)-C(12)	122 3(5)
C(10)-N(11)-C(7)	103.7(4)	C(17)-C(12)-C(13)	119.1(5)
C(17)-C(12)-C(10)	117 3(5)	C(13)-C(12)-C(10)	123.6(6)
O(18)-C(13)-C(14)	123 3(6)	O(18)-C(13)-C(12)	117 1(5)
C(14)-C(13)-C(12)	119 6(6)	C(15)-C(14)-C(13)	120 6(6)
C(14)-C(15)-C(16)	120 2(6)	C(17)-C(16)-O(20)	124 6(5)
C(17)-C(16)-C(15)	120 5(6)	O(20)-C(16)-C(15)	114.9(6)
C(16)-C(17)-C(12)	119.9(6)	C(13)-O(18)-C(19)	116 9(5)
C(16)-O(20)-C(21)	118 2(5)		

Symmetry transformations used to generate equivalent atoms

Table 4. Anisotropic displacement parameters [$Å^2$ x 10^3] for 1
The anisotropic displacement factor exponent takes the form
$-2\pi^2$ [$(ha^*)^2U_{11}$ + . + $2hka^*b^*U_{12}$]

	U11	U22	U33	U23	U13	U12
N(1)	53(4)	32(3)	43(4)	8(3)	-6(3)	0(3)
C(2)	53(5)	48(6)	52(5)	10(4)	2(4)	0(4)
C(3)	69(6)	28(4)	57(5)	11(4)	11(5)	2(4)
N(4)	66(5)	36(4)	54(4)	-2(3)	3(3)	-7(3)
C(5)	56(5)	36(5)	42(5)	-2(4)	2(4)	3(4)
C(6)	45(5)	41(5)	31(4)	-2(4)	2(4)	-1(4)
C(7)	37(5)	31(4)	31(4)	0(3)	-3(4)	-6(3)
N(8)	68(4)	33(3)	40(3)	6(3)	-7(3)	1(3)
N(9)	52(4)	35(4)	46(4)	6(3)	-11(3)	0(3)
C(10)	35(4)	43(5)	28(4)	3(4)	4(3)	7(4)
N(11)	28(3)	10(3)	7(2)	3(2)	-14(2)	-2(2)
C(12)	35(4)	41(5)	29(4)	5(4)	6(3)	2(4)
C(13)	40(4)	32(4)	38(4)	-5(4)	0(4)	3(4)
C(14)	50(5)	48(5)	27(4)	4(4)	-3(3)	4(4)
C(15)	50(5)	29(4)	41(4)	8(4)	0(4)	3(4)
C(16)	39(4)	27(4)	40(4)	-3(4)	0(3)	-1(4)
C(17)	42(4)	29(5)	37(4)	-2(4)	6(3)	-5(3)
O(18)	72(3)	36(3)	38(3)	0(3)	-9(2)	-7(3)
C(19)	67(5)	48(5)	46(4)	-10(4)	-12(4)	-9(4)
O(20)	71(4)	29(3)	43(3)	3(3)	-9(3)	-7(3)
C(21)	62(5)	49(5)	41(4)	-5(4)	-4(4)	-7(4)

Table 5. Hydrogen coordinates (x 10^4) and isotropic displacement parameters ($Å^2$ x 10^3) for 1.

	x	y	z	U(eq)
H(2)	2410(20)	8175(5)	17(7)	61
H(3A)	6027(20)	8827(5)	1524(7)	61
H(5)	7712(19)	6511(5)	3162(6)	54
H(11A)	6414(11)	5187(3)	3083(3)	19
H(14)	8896(18)	2759(5)	5587(6)	50
H(15)	7034(17)	1302(5)	4783(6)	48
H(17)	2501(16)	2526(4)	1612(6)	43
H(19A)	12099(19)	3981(5)	5799(6)	82
H(19B)	7953(19)	4165(5)	6168(6)	82
H(19C)	10140(19)	4989(5)	5783(6)	82
H(21A)	3858(21)	948(5)	1033(6)	77
H(21B)	-53(21)	1156(5)	1417(6)	77
H(21C)	1172(21)	140(5)	1629(6)	77

Appendix 4

Table 1. Crystal data and structure refinement for H_2L3

Table 1. Crystal data and structure refinement for 1.

Identification code	tial
Empirical formula	$C_{22}H_{18}N_8O_2$
Formula weight	426.44
Temperature	153(2) K
Wavelength	0.71073 Å
Crystal System	Monoclinic
Space group	$P2_1/c$
Unit cell dimensions	a = 9.235(3) Å alpha = 90° b = 11.636(3) Å beta = 106.44(2)° c = 10.096(3) Å gamma = 90°
Volume, Z	1040.5(5) $Å^3$, 2
Density (calculated)	1.361 Mg/m^3
Absorption coefficient	0.093 mm^{-1}
F(000)	444
Crystal size	0.76 x 0.21 x 0.30 mm
Θ range for data collection	2.30 to 22.50°
Limiting indices	$-1 \le h \le 9$, $-1 \le k \le 12$, $-10 \le l \le 10$
Reflections collected	1853
Independent reflections	1359 (R_{int} = 0.0528)
Refinement method	Full-matrix least-squares on F^2
Data / restraints / parameters	1359 / 0 / 145
Goodness-of-fit on F^2	1.025
Final R indices [I>2σ(I)]	R1 = 0.0610, wR2 = 0.0991
R indices (all data)	R1 = 0.1398, wR2 = 0.1258
Largest diff. peak and hole	0.244 and −0.252 $eÅ^{-3}$

Table 2 Atomic coordinates [x 10^4] and equivalent isotropic displacement parameters [$Å^2$ x 10^3] for 1 U(eq) is defined as one third of the trace of the orthogonalized U_{ij} tensor

	x	y	z	U(eq)
N(1)	-2947(5)	9709(4)	-3154(4)	40(1)
C(2)	-3419(7)	10629(5)	-3973(6)	51(2)
C(3)	-4262(6)	11516(5)	-3665(5)	40(2)
C(4)	-4621(6)	11470(5)	-2437(5)	38(2)
C(5)	-4169(6)	10535(4)	-1579(5)	28(1)
C(6)	-3318(5)	9678(4)	-1971(5)	23(1)
C(7)	-2719(5)	8688(4)	-1058(4)	23(1)
N(8)	-2796(4)	8651(3)	245(4)	23(1)
N(9)	-2032(4)	7657(3)	724(3)	23(1)
C(10)	-1564(5)	7149(4)	-278(4)	21(1)
N(11)	-2004(4)	7785(3)	-1442(3)	20(1)
C(12)	-747(5)	6055(4)	-131(5)	22(1)
C(13)	-998(5)	5318(4)	-1266(5)	20(1)
C(14)	263(5)	5740(4)	1142(5)	23(1)
O(15)	482(4)	6536(3)	2173(3)	32(1)
C(16)	1358(6)	6191(5)	3532(4)	43(2)

Table 3 Bond lengths [Å] and angles [°] for 1

N(1)-C(6)	1.333(5)	N(1)-C(2)	1 348(6)
C(2)-C(3)	1 380(7)	C(3)-C(4)	1 372(7)
C(4)-C(5)	1 380(7)	C(5)-C(6)	1.395(6)
C(6)-C(7)	1 480(6)	C(7)-N(8)	1.338(5)
C(7)-N(11)	1.356(6)	N(8)-N(9)	1 369(5)
N(9)-C(10)	1 344(5)	C(10)-N(11)	1 350(5)
C(10)-C(12)	1 466(6)	C(12)-C(13)	1.397(6)
C(12)-C(14)	1 406(6)	C(13)-C(14)#1	1 394(6)
C(14)-O(15)	1.365(5)	C(14)-C(13)#1	1 394(6)
O(15)-C(16)	1 439(5)		

C(6)-N(1)-C(2)	116 8(5)	N(1)-C(2)-C(3)	124 1(5)
C(4)-C(3)-C(2)	118 0(5)	C(3)-C(4)-C(5)	119.4(5)
C(4)-C(5)-C(6)	118 7(4)	N(1)-C(6)-C(5)	122 9(4)
N(1)-C(6)-C(7)	115 7(4)	C(5)-C(6)-C(7)	121 4(4)
N(8)-C(7)-N(11)	115 0(4)	N(8)-C(7)-C(6)	121 5(4)
N(11)-C(7)-C(6)	123 5(4)	C(7)-N(8)-N(9)	102 1(4)
C(10)-N(9)-N(8)	110 4(3)	N(9)-C(10)-N(11)	109 4(4)
N(9)-C(10)-C(12)	124 8(4)	N(11)-C(10)-C(12)	125.7(4)
C(10)-N(11)-C(7)	103 1(3)	C(13)-C(12)-C(14)	120.2(4)
C(13)-C(12)-C(10)	119 2(4)	C(14)-C(12)-C(10)	120 6(4)
C(14)#1-C(13)-C(12)	120 3(4)	O(15)-C(14)-C(13)#1	124.6(4)
O(15)-C(14)-C(12)	115 9(4)	C(13)#1-C(14)-C(12)	119 5(4)
C(14)-O(15)-C(16)	117 4(4)		

Symmetry transformations used to generate equivalent atoms

#1 -x,-y+1,-z

Table 4 Anisotropic displacement parameters [$Å^2 \times 10^3$] for 1

The anisotropic displacement factor exponent takes the form

$-2\pi^2 [(ha^*)^2 U_{11} + . \quad + 2hka^*b^* U_{12}]$

	U11	U22	U33	U23	U13	U12
N(1)	54(3)	37(3)	37(3)	10(2)	26(2)	13(3)
C(2)	72(5)	49(4)	41(4)	25(3)	28(3)	26(4)
C(3)	49(4)	32(3)	38(3)	13(3)	10(3)	16(3)
C(4)	44(4)	29(3)	40(3)	2(3)	11(3)	6(3)
C(5)	35(4)	25(3)	26(3)	0(2)	10(3)	8(3)
C(6)	22(3)	25(3)	20(3)	1(2)	3(2)	5(3)
C(7)	26(3)	26(3)	18(3)	0(3)	7(2)	-2(3)
N(8)	27(3)	20(2)	23(2)	0(2)	7(2)	3(2)
N(9)	31(3)	21(2)	18(2)	2(2)	9(2)	8(2)
C(10)	24(3)	20(3)	21(3)	-1(2)	8(2)	-1(3)
N(11)	31(3)	16(2)	17(2)	-2(2)	12(2)	0(2)
C(12)	25(3)	21(3)	22(3)	-1(2)	12(2)	0(3)
C(13)	25(3)	18(3)	16(3)	5(2)	3(2)	4(3)
C(14)	30(3)	22(3)	18(3)	-3(2)	8(3)	-5(3)
O(15)	42(2)	25(2)	23(2)	-5(2)	1(2)	12(2)
C(16)	53(4)	42(4)	26(3)	-10(3)	-5(3)	15(3)

Table 5 Hydrogen coordinates (x 10^4) and isotropic displacement parameters ($Å^2$ x 10^3) for 1

	x	y	z	U(eq)
H(2)	-3186(7)	10611(5)	-4972(6)	61
H(3)	-4476(6)	12183(5)	-4381(5)	48
H(4)	-5113(6)	12170(5)	-2169(5)	45
H(5)	-4254(6)	10396(4)	-564(5)	34
H(9)	-1888(4)	7422(3)	1830(3)	28
H(13)	-1862(5)	5590(4)	-2264(5)	24
H(16A)	2498(6)	6019(5)	3457(4)	52
H(16B)	681(6)	5417(5)	3802(4)	52
H(16C)	1396(6)	7015(5)	4086(4)	52

Appendix 5

Table 1. Crystal data and structure refinement for $[Ru(bpy)_2L1](PF_6).2H_2O$

Table 1 Crystal data and structure refinement for 1

Identification code	donal2
Empirical formula	$C_{35}H_{30}F_6N_9O_5PRu$
Formula weight	902 72
Temperature	293(2) K
Wavelength	1 54178 Å
Crystal System	Triclinic
Space group	P-1 (or P1bar)
Unit cell dimensions	a = 11 704(7) Å alpha = 69 920(10)° b = 12 915(7) Å beta = 88 60° c = 15 631(9) Å gamma = 63 140(10)°
Volume, Z	1956(2) $Å^3$, 2
Density (calculated)	1 533 Mg/m^3
Absorption coefficient	4 358 mm^{-1}
F(000)	912
Crystal size	0 32 x 0 11 x 0 15 mm
θ range for data collection	3 05 to 54 99°
Limiting indices	$0 \le h \le 12$, $-12 \le k \le 13$, $-16 \le l \le 16$
Reflections collected	7006
Independent reflections	4917 (R_{int} = 0.0501)
Refinement method	Full-matrix least-squares on F^2
Data / restraints / parameters	4917 / 0 / 488
Goodness-of-fit on F^2	1.489
Final R indices [I>2σ(I)]	R1 = 0 0716, wR2 = 0.2009
R indices (all data)	R1 = 0 0824, wR2 = 0.2090
Largest diff peak and hole	0 808 and -1 087 $eÅ^{-3}$

Table 2. Atomic coordinates [x 10^4] and equivalent isotropic displacement parameters [$Å^2$ x 10^3] for 1. U(eq) is defined as one third of the trace of the orthogonalized U_{ij} tensor.

	x	y	z	U(eq)
Ru(1)	1479(1)	3641(1)	2543(1)	30(1)
N(1)	1612(6)	2806(6)	1615(5)	36(2)
C(2)	1696(9)	1669(8)	1796(6)	45(2)
C(3)	1916(10)	1137(9)	1134(7)	52(2)
C(4)	2020(10)	1780(9)	246(7)	55(3)
C(5)	1883(9)	2987(9)	33(6)	47(2)
C(6)	1692(8)	3451(7)	736(6)	35(2)
C(7)	1522(8)	4722(7)	589(5)	34(2)
C(8)	1581(9)	5521(9)	-257(6)	47(2)
C(9)	1405(9)	6692(8)	-346(7)	51(2)
C(10)	1153(9)	7035(8)	427(6)	50(2)
C(11)	1078(8)	6200(7)	1248(6)	42(2)
N(12)	1281(6)	5039(6)	1348(4)	35(2)
N(13)	1516(7)	4561(6)	3377(4)	37(2)
C(14)	443(10)	5306(8)	3667(6)	48(2)
C(15)	566(11)	5903(9)	4221(7)	56(3)
C(16)	1786(12)	5717(9)	4510(6)	57(3)
C(17)	2869(11)	4957(9)	4227(6)	55(3)
C(18)	2670(9)	4409(7)	3648(5)	37(2)
C(19)	3758(8)	3645(7)	3247(6)	37(2)
C(20)	5020(9)	3466(9)	3393(7)	52(3)
C(21)	5938(10)	2790(9)	2951(7)	56(3)
C(22)	5593(9)	2321(9)	2391(7)	55(3)
C(23)	4339(8)	2498(8)	2298(6)	44(2)
N(24)	3404(6)	3185(6)	2699(4)	34(2)
N(25)	1645(7)	2148(6)	3726(5)	37(2)
C(26)	2767(9)	1171(8)	4237(6)	46(2)
C(27)	2799(10)	260(9)	5059(7)	57(3)
C(28)	1642(10)	343(8)	5341(6)	53(3)
C(29)	451(10)	1338(8)	4797(6)	52(3)
C(30)	508(8)	2204(7)	4012(6)	38(2)
C(31)	-628(8)	3314(7)	3374(6)	35(2)
N(32)	-431(6)	4056(6)	2625(4)	30(2)
N(33)	-1625(7)	5043(6)	2203(5)	37(2)
C(34)	-2443(8)	4791(7)	2741(5)	34(2)
N(35)	-1882(7)	3721(6)	3492(5)	38(2)
C(36)	-3855(8)	5679(8)	2606(6)	40(2)
C(37)	-4350(8)	5895(8)	3382(6)	43(2)
C(38)	-5644(9)	6756(9)	3309(7)	46(2)
C(39)	-6467(9)	7354(10)	2497(8)	58(3)
C(40)	-5994(9)	7123(10)	1715(7)	59(3)
C(41)	-4679(9)	6270(9)	1773(6)	53(3)
O(42)	-6011(7)	6899(7)	4122(5)	69(2)
C(43)	-7136(11)	8018(11)	4070(9)	78(4)
O(44)	-4140(7)	6000(8)	1039(5)	75(2)
C(45)	-5011(14)	6582(19)	153(9)	133(7)
P(1)	-837(3)	9612(2)	1922(2)	61(1)
F(11)	-1845(28)	10463(27)	1025(19)	174(11)
F(12)	-1031(20)	10794(18)	2163(12)	110(6)
F(13)	-32(22)	9859(21)	1121(15)	120(7)
F(14)	104(19)	8631(17)	2899(13)	115(6)
F(15)	-860(20)	8437(19)	1853(14)	113(6)

F(16)	-2039(15)	9748(14)	2471(10)	74(4)
F(11')	-1904(17)	10905(17)	1239(12)	97(5)
F(12')	-201(22)	10232(19)	2344(13)	126(6)
F(13')	431(24)	9328(23)	1464(17)	135(9)
F(14')	311(19)	8270(18)	2471(14)	121(6)
F(15')	-1260(16)	8911(16)	1443(12)	87(5)
F(16')	-1602(24)	9389(22)	2787(16)	126(8)
N(2)	-4254(17)	8915(16)	2900(12)	141(5)
O(21)	-5116(17)	9594(15)	3226(11)	185(6)
O(22)	-3080(16)	7820(16)	3656(11)	186(6)
O(23)	-4300(16)	9080(16)	1927(11)	190(6)

Table 3. Bond lengths [Å] and angles [°] for 1.

Ru(1)-N(12)	2.033(7)	Ru(1)-N(1)	2.051(7)
Ru(1)-N(13)	2.056(7)	Ru(1)-N(24)	2.052(7)
Ru(1)-N(32)	2.062(7)	Ru(1)-N(25)	2.098(7)
N(1)-C(2)	1.352(10)	N(1)-C(6)	1.367(10)
C(2)-C(3)	1.388(13)	C(3)-C(4)	1.386(14)
C(4)-C(5)	1.410(13)	C(5)-C(6)	1.392(12)
C(6)-C(7)	1.495(11)	C(7)-N(12)	1.366(10)
C(7)-C(8)	1.393(12)	C(8)-C(9)	1.388(12)
C(9)-C(10)	1.405(13)	C(10)-C(11)	1.396(12)
C(11)-N(12)	1.359(10)	N(13)-C(18)	1.331(11)
N(13)-C(14)	1.375(11)	C(14)-C(15)	1.389(13)
C(15)-C(16)	1.40(2)	C(16)-C(17)	1.382(14)
C(17)-C(18)	1.404(12)	C(18)-C(19)	1.496(12)
C(19)-N(24)	1.360(10)	C(19)-C(20)	1.399(12)
C(20)-C(21)	1.388(14)	C(21)-C(22)	1.378(14)
C(22)-C(23)	1.383(13)	C(23)-N(24)	1.360(11)
N(25)-C(26)	1.348(11)	N(25)-C(30)	1.373(11)
C(26)-C(27)	1.401(13)	C(27)-C(28)	1.383(14)
C(28)-C(29)	1.416(14)	C(29)-C(30)	1.372(12)
C(30)-C(31)	1.476(11)	C(31)-N(32)	1.326(10)
C(31)-N(35)	1.349(10)	N(32)-N(33)	1.368(9)
N(33)-C(34)	1.335(10)	C(34)-N(35)	1.350(10)
C(34)-C(36)	1.493(11)	C(36)-C(37)	1.390(12)
C(36)-C(41)	1.386(12)	C(37)-C(38)	1.394(12)
C(38)-C(39)	1.360(14)	C(38)-O(42)	1.378(11)
C(39)-C(40)	1.399(14)	C(40)-C(41)	1.413(13)
C(41)-O(44)	1.370(11)	O(42)-C(43)	1.426(12)
O(44)-C(45)	1.479(14)	P(1)-F(11)	1.55(3)
P(1)-F(11')	1.56(2)	P(1)-F(14')	1.57(2)
P(1)-F(15')	1.58(2)	P(1)-F(13)	1.58(2)
P(1)-F(16)	1.60(2)	P(1)-F(15)	1.57(2)
P(1)-F(12')	1.60(2)	P(1)-F(13')	1.58(2)
P(1)-F(14)	1.63(2)	P(1)-F(12)	1.61(2)
P(1)-F(16')	1.62(2)	F(13')-F(14')	1.75(3)
N(2)-O(21)	1.24(2)	N(2)-O(23)	1.46(2)
N(2)-O(22)	1.57(2)		

N(12)-Ru(1)-N(1)	79.5(3)	N(12)-Ru(1)-N(13)	94.8(3)
N(1)-Ru(1)-N(13)	172.1(3)	N(12)-Ru(1)-N(24)	86.1(3)
N(1)-Ru(1)-N(24)	95.2(3)	N(13)-Ru(1)-N(24)	78.8(3)
N(12)-Ru(1)-N(32)	100.9(2)	N(1)-Ru(1)-N(32)	93.0(2)
N(13)-Ru(1)-N(32)	93.5(3)	N(24)-Ru(1)-N(32)	170.1(2)
N(12)-Ru(1)-N(25)	176.3(2)	N(1)-Ru(1)-N(25)	97.1(3)
N(13)-Ru(1)-N(25)	88.8(3)	N(24)-Ru(1)-N(25)	95.6(3)
N(32)-Ru(1)-N(25)	77.8(2)	C(2)-N(1)-C(6)	117.6(7)
C(2)-N(1)-Ru(1)	126.8(6)	C(6)-N(1)-Ru(1)	115.5(5)
N(1)-C(2)-C(3)	122.0(9)	C(4)-C(3)-C(2)	120.5(9)
C(3)-C(4)-C(5)	118.4(9)	C(6)-C(5)-C(4)	117.9(9)
N(1)-C(6)-C(5)	123.4(8)	N(1)-C(6)-C(7)	113.8(7)
C(5)-C(6)-C(7)	122.7(8)	N(12)-C(7)-C(8)	123.1(8)
N(12)-C(7)-C(6)	114.3(7)	C(8)-C(7)-C(6)	122.6(8)
C(9)-C(8)-C(7)	119.4(8)	C(8)-C(9)-C(10)	118.3(8)
C(11)-C(10)-C(9)	119.3(8)	N(12)-C(11)-C(10)	122.8(8)
C(11)-N(12)-C(7)	117.0(7)	C(11)-N(12)-Ru(1)	126.8(6)
C(7)-N(12)-Ru(1)	115.7(5)	C(18)-N(13)-C(14)	118.9(8)
C(18)-N(13)-Ru(1)	116.6(6)	C(14)-N(13)-Ru(1)	124.5(6)
N(13)-C(14)-C(15)	120.1(9)	C(14)-C(15)-C(16)	120.1(9)
C(17)-C(16)-C(15)	119.8(9)	C(16)-C(17)-C(18)	117.1(10)
N(13)-C(18)-C(17)	123.9(8)	N(13)-C(18)-C(19)	114.4(7)

C(17)-C(18)-C(19)	121 6(8)	N(24)-C(19)-C(20)	123 0(8)
N(24)-C(19)-C(18)	114 3(7)	C(20)-C(19)-C(18)	122.7(8)
C(21)-C(20)-C(19)	117 8(9)	C(22)-C(21)-C(20)	120 0(9)
C(21)-C(22)-C(23)	119 4(9)	N(24)-C(23)-C(22)	122.2(9)
C(19)-N(24)-C(23)	117.6(7)	C(19)-N(24)-Ru(1)	115.8(5)
C(23)-N(24)-Ru(1)	126.7(6)	C(26)-N(25)-C(30)	117.9(7)
C(26)-N(25)-Ru(1)	125 5(6)	C(30)-N(25)-Ru(1)	116 5(5)
N(25)-C(26)-C(27)	122 1(9)	C(28)-C(27)-C(26)	119 0(9)
C(27)-C(28)-C(29)	119 8(9)	C(30)-C(29)-C(28)	117.4(9)
C(29)-C(30)-N(25)	123.7(8)	C(29)-C(30)-C(31)	125 0(8)
N(25)-C(30)-C(31)	111.3(7)	N(32)-C(31)-N(35)	114.4(7)
N(32)-C(31)-C(30)	118 6(7)	N(35)-C(31)-C(30)	126.9(8)
C(31)-N(32)-N(33)	106.2(6)	C(31)-N(32)-Ru(1)	115 4(5)
N(33)-N(32)-Ru(1)	137 1(5)	C(34)-N(33)-N(32)	104.3(6)
N(33)-C(34)-N(35)	115 1(7)	N(33)-C(34)-C(36)	123 6(7)
N(35)-C(34)-C(36)	120.9(7)	C(31)-N(35)-C(34)	100 0(7)
C(37)-C(36)-C(41)	119.4(8)	C(37)-C(36)-C(34)	116.4(7)
C(41)-C(36)-C(34)	124.2(8)	C(36)-C(37)-C(38)	120.3(9)
C(39)-C(38)-O(42)	124 0(9)	C(39)-C(38)-C(37)	121 3(9)
O(42)-C(38)-C(37)	114 7(8)	C(38)-C(39)-C(40)	119 2(9)
C(41)-C(40)-C(39)	120 2(9)	O(44)-C(41)-C(36)	116 6(8)
O(44)-C(41)-C(40)	123 8(8)	C(36)-C(41)-C(40)	119.6(9)
C(38)-O(42)-C(43)	118.1(9)	C(41)-O(44)-C(45)	117 5(9)
F(11')-P(1)-F(14')	171.1(10)	F(11')-P(1)-F(15')	90.5(9)
F(14')-P(1)-F(15')	84 5(10)	F(11)-P(1)-F(13)	74 2(12)
F(11)-P(1)-F(16)	87 3(12)	F(13)-P(1)-F(16)	160.8(10)
F(11)-P(1)-F(15)	89 9(13)	F(13)-P(1)-F(15)	98 9(11)
F(16)-P(1)-F(15)	85.7(9)	F(11')-P(1)-F(12')	93.2(10)
F(14')-P(1)-F(12')	90.8(11)	F(15')-P(1)-F(12')	171 0(10)
F(11')-P(1)-F(13')	105.7(11)	F(14')-P(1)-F(13')	67.3(11)
F(15')-P(1)-F(13')	92.2(10)	F(12')-P(1)-F(13')	78.9(11)
F(11)-P(1)-F(14)	172 6(13)	F(13)-P(1)-F(14)	111 6(11)
F(16)-P(1)-F(14)	87.3(9)	F(15)-P(1)-F(14)	84 7(10)
F(11)-P(1)-F(12)	92 4(13)	F(13)-P(1)-F(12)	94 0(10)
F(16)-P(1)-F(12)	81 6(8)	F(15)-P(1)-F(12)	166.9(10)
F(14)-P(1)-F(12)	91.7(10)	F(11')-P(1)-F(16')	100.4(11)
F(14')-P(1)-F(16')	87 3(11)	F(15')-P(1)-F(16')	95 1(10)
F(12')-P(1)-F(16')	92.4(11)	F(13')-P(1)-F(16')	152 8(13)
P(1)-F(13')-F(14')	56 3(10)	P(1)-F(14')-F(13')	56 4(10)
O(21)-N(2)-O(23)	125(2)	O(21)-N(2)-O(22)	112(2)
O(23)-N(2)-O(22)	123(2)		

Symmetry transformations used to generate equivalent atoms

C(17)-C(18)-C(19)	121 6(8)	N(24)-C(19)-C(20)	123 0(8)
N(24)-C(19)-C(18)	114 3(7)	C(20)-C(19)-C(18)	122 7(8)
C(21)-C(20)-C(19)	117 8(9)	C(22)-C(21)-C(20)	120.0(9)
C(21)-C(22)-C(23)	119 4(9)	N(24)-C(23)-C(22)	122.2(9)
C(19)-N(24)-C(23)	117 6(7)	C(19)-N(24)-Ru(1)	115.8(5)
C(23)-N(24)-Ru(1)	126 7(6)	C(26)-N(25)-C(30)	117 9(7)
C(26)-N(25)-Ru(1)	125.5(6)	C(30)-N(25)-Ru(1)	116 5(5)
N(25)-C(26)-C(27)	122 1(9)	C(28)-C(27)-C(26)	119 0(9)
C(27)-C(28)-C(29)	119 8(9)	C(30)-C(29)-C(28)	117 4(9)
C(29)-C(30)-N(25)	123 7(8)	C(29)-C(30)-C(31)	125 0(8)
N(25)-C(30)-C(31)	111 3(7)	N(32)-C(31)-N(35)	114.4(7)
N(32)-C(31)-C(30)	118 6(7)	N(35)-C(31)-C(30)	126.9(8)
C(31)-N(32)-N(33)	106 2(6)	C(31)-N(32)-Ru(1)	115 4(5)
N(33)-N(32)-Ru(1)	137 1(5)	C(34)-N(33)-N(32)	104 3(6)
N(33)-C(34)-N(35)	115 1(7)	N(33)-C(34)-C(36)	123 6(7)
N(35)-C(34)-C(36)	120 9(7)	C(31)-N(35)-C(34)	100.0(7)
C(37)-C(36)-C(41)	119 4(8)	C(37)-C(36)-C(34)	116.4(7)
C(41)-C(36)-C(34)	124 2(8)	C(36)-C(37)-C(38)	120 3(9)
C(39)-C(38)-O(42)	124 0(9)	C(39)-C(38)-C(37)	121.3(9)
O(42)-C(38)-C(37)	114 7(8)	C(38)-C(39)-C(40)	119 2(9)
C(41)-C(40)-C(39)	120 2(9)	O(44)-C(41)-C(36)	116 6(8)
O(44)-C(41)-C(40)	123 8(8)	C(36)-C(41)-C(40)	119.6(9)
C(38)-O(42)-C(43)	118 1(9)	C(41)-O(44)-C(45)	117 5(9)
F(11')-P(1)-F(14')	171 1(10)	F(11')-P(1)-F(15')	90.5(9)
F(14')-P(1)-F(15')	84 5(10)	F(11)-P(1)-F(13)	74.2(12)
F(11)-P(1)-F(16)	87 3(12)	F(13)-P(1)-F(16)	160 8(10)
F(11)-P(1)-F(15)	89 9(13)	F(13)-P(1)-F(15)	98 9(11)
F(16)-P(1)-F(15)	85.7(9)	F(11')-P(1)-F(12')	93.2(10)
F(14')-P(1)-F(12')	90.8(11)	F(15')-P(1)-F(12')	171 0(10)
F(11')-P(1)-F(13')	105 7(11)	F(14')-P(1)-F(13')	67 3(11)
F(15')-P(1)-F(13')	92 2(10)	F(12')-P(1)-F(13')	78 9(11)
F(11)-P(1)-F(14)	172 6(13)	F(13)-P(1)-F(14)	111 6(11)
F(16)-P(1)-F(14)	87.3(9)	F(15)-P(1)-F(14)	84 7(10)
F(11)-P(1)-F(12)	92 4(13)	F(13)-P(1)-F(12)	94 0(10)
F(16)-P(1)-F(12)	81 6(8)	F(15)-P(1)-F(12)	166 9(10)
F(14)-P(1)-F(12)	91 7(10)	F(11')-P(1)-F(16')	100 4(11)
F(14')-P(1)-F(16')	87 3(11)	F(15')-P(1)-F(16')	95 1(10)
F(12')-P(1)-F(16')	92 4(11)	F(13')-P(1)-F(16')	152 8(13)
P(1)-F(13')-F(14')	56 3(10)	P(1)-F(14')-F(13')	56 4(10)
O(21)-N(2)-O(23)	125(2)	O(21)-N(2)-O(22)	112(2)
O(23)-N(2)-O(22)	123(2)		

Symmetry transformations used to generate equivalent atoms

Table 4 Anisotropic displacement parameters [$Å^2$ x 10^3] for 1

The anisotropic displacement factor exponent takes the form

$-2\pi^2$ [$(ha^*)^2U_{11}$ + + $2hka^*b^*U_{12}$]

	U11	U22	U33	U23	U13	U12
Ru(1)	27(1)	27(1)	35(1)	-13(1)	7(1)	-11(1)
N(1)	30(4)	34(4)	44(4)	-15(3)	4(3)	-14(3)
C(2)	44(6)	31(5)	61(6)	-18(4)	1(5)	-18(4)
C(3)	58(7)	45(5)	56(6)	-23(5)	7(5)	-25(5)
C(4)	52(6)	49(6)	73(7)	-36(5)	9(5)	-23(5)
C(5)	43(6)	50(6)	52(5)	-28(5)	9(4)	-19(5)
C(6)	27(5)	35(5)	42(5)	-14(4)	10(4)	-14(4)
C(7)	28(5)	34(5)	38(5)	-10(4)	4(4)	-16(4)
C(8)	44(6)	52(6)	41(5)	-13(4)	9(4)	-25(5)
C(9)	52(6)	35(5)	56(6)	-8(4)	11(5)	-20(5)
C(10)	53(6)	44(5)	49(6)	-8(5)	6(5)	-27(5)
C(11)	38(5)	28(5)	54(5)	-15(4)	1(4)	-10(4)
N(12)	32(4)	32(4)	41(4)	-16(3)	7(3)	-14(3)
N(13)	41(5)	31(4)	35(4)	-10(3)	4(3)	-14(3)
C(14)	62(7)	34(5)	44(5)	-20(4)	17(5)	-16(5)
C(15)	78(8)	48(6)	55(6)	-31(5)	23(6)	-32(6)
C(16)	90(9)	48(6)	40(5)	-18(5)	10(5)	-36(6)
C(17)	74(8)	51(6)	46(5)	-17(5)	12(5)	-37(6)
C(18)	44(6)	33(5)	27(4)	-6(4)	-2(4)	-16(4)
C(19)	35(5)	29(4)	43(5)	-5(4)	0(4)	-17(4)
C(20)	35(6)	43(5)	73(7)	-14(5)	5(5)	-19(5)
C(21)	45(6)	46(6)	71(7)	-4(5)	-1(5)	-28(5)
C(22)	30(5)	37(5)	78(7)	-8(5)	11(5)	-9(4)
C(23)	29(5)	36(5)	45(5)	-8(4)	2(4)	-4(4)
N(24)	35(4)	27(3)	34(4)	-7(3)	6(3)	-12(3)
N(25)	32(4)	33(4)	42(4)	-13(3)	6(3)	-13(3)
C(26)	43(6)	31(5)	48(5)	-10(4)	-5(4)	-6(4)
C(27)	56(7)	39(6)	60(6)	-11(5)	-1(5)	-14(5)
C(28)	66(7)	38(5)	46(5)	-9(4)	12(5)	-22(5)
C(29)	61(7)	40(5)	49(6)	-10(5)	16(5)	-24(5)
C(30)	35(5)	32(5)	46(5)	-16(4)	8(4)	-14(4)
C(31)	28(5)	33(5)	45(5)	-20(4)	9(4)	-11(4)
N(32)	35(4)	23(3)	29(3)	-8(3)	0(3)	-11(3)
N(33)	32(4)	38(4)	43(4)	-19(3)	9(3)	-15(4)
C(34)	31(5)	37(5)	38(5)	-19(4)	12(4)	-15(4)
N(35)	32(4)	37(4)	40(4)	-11(3)	12(3)	-14(3)
C(36)	30(5)	45(5)	45(5)	-16(4)	11(4)	-19(4)
C(37)	36(5)	46(5)	58(6)	-28(5)	21(4)	-22(4)
C(38)	38(6)	53(6)	62(6)	-33(5)	22(5)	-25(5)
C(39)	28(5)	60(7)	80(8)	-25(6)	8(5)	-17(5)
C(40)	31(6)	68(7)	64(7)	-19(6)	1(5)	-14(5)
C(41)	36(6)	68(7)	48(6)	-18(5)	6(5)	-21(5)
O(42)	47(4)	90(5)	82(5)	-57(5)	25(4)	-26(4)
C(43)	58(7)	67(7)	101(9)	-53(7)	27(7)	-8(6)
O(44)	44(4)	111(6)	55(4)	-38(4)	9(4)	-20(4)
C(45)	71(10)	226(20)	70(9)	-75(11)	-5(7)	-30(11)
P(1)	56(2)	47(2)	78(2)	-20(1)	21(2)	-25(1)